

https://dspace.org/

Synthesis and characterization of bis-(salicylaldiminato) chromium and cobalt complexes and their catalytic evaluation for the coupling of CO2/CS2 with propylene oxide

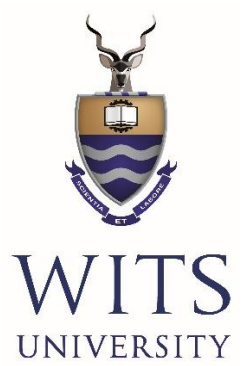
Tumeli, Ts'epo Richard

2021

https://hdl.handle.net/10539/33066

Downloaded from a DSpace repository. https://dspace.org/

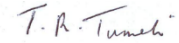
Molecular Science Institute, School of Chemistry
University of the Witwatersrand



Synthesis and characterization of bis-(salicylaldiminato) chromium and cobalt complexes and their catalytic evaluation for the coupling of CO_2/CS_2 with propylene oxide.

By: Ts'epo Richard Tumeli
1413908

A thesis submitted to the Faculty of Science, University of the Witwatersrand, in partial fulfillment of the requirement for the degree, Doctor of Philosophy (PhD) in Chemistry

Signature:	Student:	Date:
	Mr T. R. Tumeli	07/10/2020
Signature:	Supervisor:	Date:
	Dr J. L. van Wyk	07/10/2020

ABSTRACT

The coupling reaction of carbon dioxide (CO_2) and epoxides has attracted much attention from researchers. This reaction utilizes CO_2, as feedstock, which is relatively non-toxic, cheap, and abundant, to produce biodegradable cyclic compounds or co-polymers. Carbon disulfide (CS_2) a more reactive CO_2 analogue, can also be utilized in the process to prepare sulfur derivatives which are also commercially relevant. In this investigation, metal complexes prepared from salicylaldimine ligands were prepared and evaluated as catalysts for the coupling of CO_2 or CS_2 with propylene oxide (PO). The synthesis and characterization of several salicylaldimine ligands, both neutral and ionic functionalized is described. In addition the synthesis and characterization of neutral and ionic functionalized metal complexes containing Cr(II), Cr(III) and Co(II) metal centers prepared from $CrCl_2$, $CrCl_3(THF)_3$ and $Co(OAc)_2 \cdot 4H_2O$ respectively is also reported. Analytical techniques such as FT-IR, UV-Vis and NMR spectroscopy, mass spectrometry, and elemental analysis, where appropriate, were employed as characterization methods for the synthesized ligands and metal complexes. Catalytic evaluation of the synthesized neutral complexes, Cr(II) (**1**-**4**), Cr(III) (**7**-**10**) and Co(II) (**13**-**16**) as catalysts for the coupling of CS_2 and PO in neat (solventless) reactions resulted in the production of only cyclic products, confirmed with ^{1}HNMR spectroscopy. Preliminary reactions showed that the complexes are not active for the coupling reaction on their own and required the presence of a co-catalyst. Complexes **2** and **8**, were the best performing Cr(II) and Cr(III) complexes in the presence of [PPN]Cl as a co-catalyst while the corresponding Co(II) complexes, **14**, performed better in the presence of DMAP. The synthesized metal complexes were evaluated in the presence of organic solvents. Significantly better substrate conversions were obtained when the coupling reactions were performed in methanol (MeOH). However, in these reactions different cyclic products were produced compared to products obtained in neat reactions. No clear trend in performance was observed when comparing the Cr(II) and Cr(III) complexes, however it was observed that the Cr(II) complexes performed better than their corresponding Co(II) complexes for reactions performed neat and in MeOH. Product selectivity was observed to be influenced by the nature of the metal when comparing Co(II) and Cr(II) complexes and by the oxidation state when comparing the Cr(II) and Cr(III) complexes. The ionic functionalized complexes, Cr(II) (**19** and **20**) Cr(III) (**21** and **22** and Co(II) (**23** and **24**) were also evaluated as catalysts for the coupling of CS_2 and PO. These

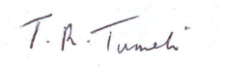
complexes were also active producing the same cyclic product observed when reactions are performed neat and in MeOH as solvent. However, in the presence of [PPN]Cl a decrease in product selectivity was observed compared to when the complexes were used on their own. The nature of the metal and oxidation state was also observed to have an effect on catalytic performance. All complexes, both neutral and ionic functionalized, were finally evaluated as catalysts for the coupling of CO_2 and PO. All reactions carried out produced only propylene carbonate, confirmed with ^{1}HNMR spectroscopy. The complexes showed an increase in PO conversions when the reactions were performed at 80 ^oC compared to room temperature. When the reaction was performed at 5 MPa CO_2 pressure, lower conversions of PO was obtained compared to when the reactions was performed at 1 MPa CO_2 pressure.

Key words: salicylaldimine, chromium, cobalt, complexes, propylene oxide, carbon dioxide carbon disulfide, coupling

DECLARATION

I declare that the thesis "S*ynthesis and characterization of bis-(salicylaldiminato) chromium and cobalt complexes and their catalytic evaluation for the coupling of CO_2/CS_2 with propylene oxide*." is my own work, that it has not been submitted before for any degree in any other university, and that any sources used or quoted have been indicated and acknowledged as complete references.

Signature: Date:



07/10/2021

Student: Mr T. R. Tumeli

1413908

ACKNOWLEDGEMENTS

I would like to express my sincere gratitude to Dr J.L. van Wyk under whose guidance this research project was completed. I would also like to thank the School of Chemistry, University of the Witwatersrand, for giving me an opportunity to further my studies. Many thanks also go to Dr I. Kotzé and post-graduate students in the School for their advice throughout this project. Financial support from the NRF is also highly appreciated. Most importantly I would like to thank God Almighty for spiritual guidance and protection throughout this research work. Finally, I would like to thank my family, my late father, mother, brothers and sister for their constant support and encouragement throughout the completion of all my degrees including this one.

TABLE OF CONTENTS

Abstract…….....ii
Declaration……..iv
Acknowledgements…….....v
List of figures……vii
List of schemes…….....xiii
List of tables…….....xiv
Abbreviations……...xvi

Chapter 1: *Literature Review: Transition Metal Complexes as Catalysts for Carbon dioxide and Carbon disulfide coupling reactions with epoxides*

Chapter 2: *Synthesis and characterization of neutral and ionic functionalized ligands*

Chapter 3: *Synthesis and characterization of bis-(salicylaldiminato) chromium and cobalt complexes*

Chapter 4: *Catalytic performance of bis(salicylaldiminato) chromium and cobalt complexes in the coupling of CS_2 with propylene oxide in neat reaction condition*

Chapter 5: *Catalytic performance of bis(salicylaldiminato) Cr(II), Co(II) and Cr(III) complexes in the coupling of CS_2 with propylene oxide in the presence of organic solvents solvent*

Chapter 6: *Catalytic evaluation of ionic functionalized Cr(II), Co(II) and Cr(III) salicylaldiminato complexes as catalysts for the coupling of CS_2 with PO*

Chapter 7: *Catalytic evaluation of neutral and multifunctional Cr(II), Co(II) and Cr(III) complexes as catalysts for the coupling of CO_2 with PO*

Chapter 8 *Summary*

LIST OF FIGURES

Chapter 1

Figure 1.1: Zinc phenoxide complexes reported by Darensbourg and his co-workers…….14
Figure 1.2: Zinc phenoxide derivative complexes for CO_2/CHO coupling…….…….14
Figure 1.3: Diimine quinoxaline zinc alkoxide complex for CO_2/CHO coupling…….....15
Figure 1.4: Binuclear zinc β-diiminate complexes for CO_2/CHO co-polymerization process…….16
Figure 1.5: Zinc β-diiminate complexes with modified ligand architecture……..16
Figure 1.6: New Zinc β-diiminate complexes with CN substituent on the para position……..17
Figure 1.7: Aluminum and manganese porphyrins complexes for CO_2 and epoxide co-polymerization (R = alkyl, oligomer of PPO)……...18
Figure 1.8: Chromium (III) porphyrin complexes……19
Figure 1.9: Jacobsen salen catalyst system……..……....20
Figure 1.10: Modified Jacobsen salen catalyst system reported by Rieger and co-workers ……...……...21
Figure 1.11: Co-salen catalyst system reported by Coates and coworkers ……...22
Figure 1.12: (Salen) Cr(III) complex that was utilized for conversion of PO to PC…….....22
Figure 1.13: First salen-like complex for CO_2/CHO coupling…….....23
Figure 1.14: Complexes reported as catalysts for CS_2 and PO coupling reaction…….25
Figure 1.15: Bimetallic (salen) Al (III) complex reported for CS_2 and PO coupling .……...26
Figure 1.16: Bifunctional ionic liquid grafted Zn porphyrin complex reported by Chen and coworkers……...……..27
Figure 1.17: Ionic liquid functionalized Zinc porphyrin complexes…….....29
Figure 1.18: Bifunctional Alumminium porphyrin complexes reported by Wu and his coworkers..31
Figure 1.19: An ionic liquid grafted cobalt porphyrin system reported by Wu and his coworkers…32
Figure 1.20: Neutral (**61**) and ionic liquid functionalized Co(III) salen (**62**) complexes……..33
Figure 1.21: A highly active and recyclable bifunctional cobalt salen complex reported as a catalyst for CO_2 and propylene oxide coupling reaction by Lee and his coworkers…….34

Chapter 2:

Figure 2.1: Salicylaldimine, **a**, and salen, **b**, Schiff base ligands reported by Hugo Schiff……...…….43

Figure 2.2: a) Ionic functionalized imidazolium ligand prepared by Kumar [11], b) ionic functionalized imidazolium ligand prepared by Chen……..43

Figure 2.3: ^{1}HNMR spectrum for ligand **HL_1**……..47

Figure 2.4: COSY NMR spectrum for ligand **HL_1** obtained in $CDCl_3$, 25 ^{o}C…….48

Figure 2.5: ^{13}CNMR spectrum for ligand **HL_1** obtained in $CDCl_3$ at 25 ^{o}C…….53

Figure 2.6: HSQC NMR spectrum for ligand **HL_1** obtained in $CDCl_3$ at 25 ^{o}C……..54

Figure 2.7: DEPT NMR spectrum for ligand **HL_1** obtained in $CDCl_3$ at 25 ^{o}C……..55

Figure 2.8: HMBC NMR spectrum for ligand **HL_1** obtained in $CDCl_3$ at 25 ^{o}C…….56

Figure 2.9: Hydrogen bonding interaction within the salicylaldimine ligand……..59

Figure 2.10: FTIR spectrum for ligand **HL_1**……...…..60

Figure 2.11: Stacked ^{1}HNMR spectra for ligand **HL_5** and **HL_7**……....63

Figure 2.12: Stacked ^{1}HNMR spectra ($CDCl_3$) for ligands **HL_7** and **HL_8**……...64

Figure 2.13: ^{19}FNMR spectrum for ligand **HL_7**……...66

Figure 2.14: ^{31}PNMR spectrum for **HL_7**…….....67

Figure 2.15: ^{13}CNMR spectra for ligand **HL_7** ($CDCl_3$)……68

Figure 2.16: ^{1}HNMR spectrum for ligand **HL_{10}** , a) $CDCl_3$ and b) DMSO……. ……....71

Figure 2.17: Stacked ^{1}HNMR spectra (DMSO) for ligand **HL_{10}** and **HL_{11}**……...72

Figure 2.18: Stacked ^{191}FNMR spectra ($CDCl_3$) for ligand **HL_{12}**…….73

Figure 2.19: ^{11}BNMR spectrum ($CDCl_3$) for ligand **HL_{12}**……..…....74

Figure 2.20: Stacked ^{1}HNMR spectra for ligand **HL_3** and **HL_{13} (b**, Scheme **2.5**)…….77

Figure 2.21: ^{1}HNMR spectra for ligand compound ‘b’ Scheme **2.6**……..…78

Figure 2.22: ^{1}HNMR spectrum for ligand **HL_{14}**…….....80

Chapter 3:

Figure 3.1: Pentacoordinate Cr(III) (**a**) [7] and Co(III) (**b**) [8] complexes derived from salicylaldimine ligands…….....86

Figure 3.2: Ionic functionalized Mn(III) complexes reported by Ceng and co-workers……..87

Figure 3.3: Overlayed FTIR spectra for ligand HL_1, Cr(II) complex **1** and Cr(III) complex **7**……90

Figure 3.4: Overlayed Uv-vis spectra of ligand **HL_1**, complex **1** and **7** recorded in DMSO (c = 0.1 mM)……...……...92

Figure 3.5: Overplayed uv-vis spectra of ligand HL_1, complex **1** and **7** recorded in DMSO (c = 10 mM)……...……...93

Figure 3.6: Overlayed Uv-vis spectra of ligand and Co(II) complexes recorded in DCM (c = 0.1 mM)……..……....94

Figure 3.7: Overlayed CV voltammogram for 0.5 mM solution of complexes **3** and **9** in DMSO (0.1 M TBAP)…….....96

Figure 3.8: ESI mass spectrum obtained for complex **1**……98

Figure 3.9: Isotopologue pattern for complex **1**……98

Figure 3.10: ESI mass spectrum obtained for complex **7**…….....99

Figure 3.11: Isotopologue pattern for complex **7**……..99

Figure 3.12: Isotopologue pattern for complex **13**…….…….100

Figure 3.13: Ortep structure for Co(II) complex **15**……106

Figure 3.14: Stacked FT-IR spectrum for **HL_1**, complex **15** and products **a** and **b** of attempted Co(III) reactions…….108

Figure 3.15: Stacked FT-IR spectrum for **HL_1**, complex **13** and products **a** and **b** of attempted Co(III) reactions…….109

Figure 3.16: Overlayed FTIR spectra for ligand HL_7, Cr(II) complex **19** and Cr(III) complex **21**111

Chapter 4:

Figure 4.1: Metal complexes used by Wang and workers for the coupling of CS_2 and epoxides..123

Figure 4.2: Bis(salicylaldiminato) Cr(II) and Cr(III) complexes investigated as catalyst precursors in this study…….……124

Figure 4.3: ^{1}HNMR spectrum of the products for the CS_2 and PO coupling reaction (Table **4.1**, entry **3**) $CDCl_3$, 25 ^oC, products 1, 3 and 4 are shown on Scheme **4.1**…….……126

Figure 4.4: Mass spectrum of the reaction residue obtained for coupling reaction products (Table 4.1, entry 3)……...……..127
Figure 4.5: Comparison of the activity of complex **8** in the presence of different co-catalysts for CS_2/PO coupling…….…..…….129
Figure 4.6: Comparison of the activity of Cr (III) complexes **7 - 10** towards CS_2/propylene oxide coupling……..……....130
Figure 4.7: ^{1}H-NMR spectrum of the product obtained for entry **2**, Table **4.2**, products **1**, **3** and **4** are shown on Scheme **4.1**…….....131
Figure 4.8: Comparison of the activity of complex **2** in the presence of different co-catalysts for CS_2/PO coupling……..……...133
Figure 4.9: Comparison of the activity of different bis-salicylaldimine Cr (II) complexes towards CS_2/PO coupling…….…….…..134
Figure 4.10: Comparison of the activity of bis-(salicylaldiminato) Cr (II) and Cr (III) complexes for CS_2/PO coupling in the presence of [PPN]Cl……135
Figure 4.11: ^{1}HNMR spectrum of the products for the coupling CS_2 and PO reaction using complex **14** and [PPNCl], entry **2** table **4.3**…….…….137
Figure 4.12: Comparison of the activity of different co-catalysts in the presence of complex **14** towardsCS_2/epoxide……...……138
Figure 4.13: Comparison of the activity of different Co (II) complexes towards CS_2/epoxide coupling..……...……..…….139
Figure 4.14: Comparison of the activity of Co(II) and Cr(II) complexes towards CS_2/PO coupling……...……...140

Chapter 5:

Figure 5.1: Effect of solvent on the coupling of CS_2 and PO when complex was used as catalyst at 24 ^{o}C and atmospheric pressure…….……....149
Figure 5.2: ^{1}HNMR spectrum for the product obtained when MeOH was used as a solvent for the coupling creaction……..……..……..……...150
Figure 5.3: Staked spectrum for the spectra that was obtained when the coupling reaction was performed in MeOH and neat……...…….……151

Figure 5.4: COSY spectrum for the product obtained when MeOH was used as a solvent for the coupling reaction……...….152
Figure 5.5: ^{13}CNMR and **b)** 135 DEPT spectrum when MeOH was used as a solvent for the coupling reaction……...……..……153
Figure 5.6: HMBC NMR spectrum for a product formed when the coupling reaction was performed in MeOH……..……..……154
Figure 5.7: FT-IR spectrum of the coupling product when the reaction was performed in MeOH……..……..…..155
Figure 5.8: Mass spectrum for CS_2, MeOH and coupling product…….....156
Figure 5.9: Effect of monomer ratio on the coupling of CS_2 and PO catalytic reaction, catalyst: complex **8**, co-catalyst: [PPN]Cl……159
Figure 5.10: Stacked ^{1}HNMR spectrum for CS_2/PO coupling reaction at 22 (a), and 40 ^{o}C (b)..160
Figure 5.11: Effect of time on the coupling of CS_2 and PO catalytic reaction……161
Figure 5.12: Stacked ^{1}HNMR spectra for the coupling of CS_2 and PO reaction product……162
Figure 5.13: Effect of ligand architecture around Cr(III) complexes (7 – 10) on the coupling of CS_2 and PO catalytic reaction……164
Figure 5.14: Effect of ligand architecture around Cr(II) complexes (**1** – **4**) on the coupling of CS_2 and PO catalytic reaction……165
Figure 5.15: Effect of ligand architecture around Co(II) complexes, **13** – **16**, on the coupling of CS_2 and PO catalytic reaction……166
Figure 5.16: Effect of Cr metal oxidation state on the coupling of CS_2 and PO catalytic reaction at 22 ^{o}C……..…….167
Figure 5.17: Effect of Cr metal oxidation state on the coupling of CS_2 and PO catalytic reaction at 40 ^{o}C……..…….168
Figure 5.18: Effect of metal center on the coupling of CS_2 and PO catalytic reaction at 22 ^{o}C.....169
Figure 5.19: Effect of metal center on the coupling of CS_2 and PO catalytic reaction at 40 ^{o}C….169

Chapter 6:

Figure 6.1: Asymmetric single functional, 6a [9], and bifunctional, 6b, salenCrN_3 [8] reported by Darensbourg and co-workers for the coupling of CPO and CO_2……175

Figure 6.2: Co(III) complexes that were used as catalysts for the coupling of CO_2 and PO by He and his co-workers……...…….176
Figure 6.3: Ionic functionalized complexes used as catalysts for the coupling of CS_2 and PO…...177
Figure 6.4: ^{1}HNMR spectrum of product that was obtained when complex **19** was used as catalysts for CS_2 and PO coupling reaction (entry 1, Table **6.1**)……178
Figure 6.5: ^{1}HNMR spectrum of the products for the CS_2 and PO coupling reaction in the presence of MeOH as a solvent (Table **6.3**, entry **1**) $CDCl_3$, 25 ^{o}C……183

Chapter 7:

Figure 7.1: SalenCr(III) and Co(III) complexes reported by Darensbourg as catalysts for the coupling of CO_2 and cyclohexene oxide…….191
Figure 7.2: Aminebisphenolato cobalt(II) complexes reported by Saunders as catalysts for the coupling of PO and CO_2……..192
Figure 7.3: Bis-(salicylaldiminato) Zn(II) complexes reported by Darensbourg and co-workers...193
Figure 7.4: Single functional, a, and bifunctional salen Co(III) metal complexes reported by Darensbourg as catalysts for the coupling of CO_2 and PO……..194
Figure 7.5: Neutral complexes used as catalysts for the coupling of CS_2 and PO……..195
Figure 7.6: Ionic functionalized complexes used as catalysts for the coupling of CS_2 and PO…..196
Figure 7.7: ^{1}HNMR spectrum for the product obtained at 80 ^{o}C, Table **7.1**, entry **5**……..197
Figure 7.8: Comparison of the activity of Cr(II), Cr(III) and Co(II) complexes derived from the same ligand for CO_2 and PO coupling…….201
Figure 7.9: Comparison of the effect of oxidation state of Cr complexes for CO_2 and PO coupling reaction……...202
Figure 7.10: Influence of metal center between Cr(II) and Co(II) complexes for CO_2 and PO coupling reaction……...…….…...….203

LIST OF SCHEMES

Chapter 1:

Scheme 1.1: The proposed catalytic cycle for a CO_2/epoxide coupling reaction …..……4

Scheme 1.2: Mechanism for metal bound carbonate depolymerization ……...…....5

Scheme 1.3: Mechanism for metal bound carbonate depolymerization ……..…...5

Scheme 1.4 Coupling of carbon disulfide and propylene oxide …..…….....6

Scheme 1.5: Proposed mechanism for scrambling in the coupling of cyclopentane oxide and CS_2……...……...7

Scheme 1.6: Proposed mechanisms for the initiation process in CO_2/CHO coupling reaction…….10

Scheme 1.7: Coupling of CO_2 with propylene oxide and cyclohexene oxide..…….……11

Scheme 1.8: Coupling of CS_2 and propylene oxide to produce cyclic products .....……....24

Chapter 2:

Scheme 2.1: General synthetic route for Schiff base ligands……42

Scheme 2.2: General procedure for the synthesis of salicylaldimine ligands **HL_1 – HL_6**…….....45

Scheme 2.3: Tautomerization and hydrogen bonding in salicylaldimine ligands…….46

Scheme 2.4: Synthetic procedure for the preparation of IL functionalized ligands **HL_7**, **HL_8** and **HL_9**……..…….62

Scheme 2.5: Synthetic procedure for the preparation of ligands **HL_{10}**, **HL_{11}** and **HL_{12}**……...70

Scheme 2.6: Synthetic procedure for the preparation of IL functionalized ligands **HL_{13}**……76

Scheme 2.7: Synthetic procedure for the preparation of intermediates '**a**' and '**b**' in the preparation of **HL_{14}**……..…….……..78

Scheme 2.8: Synthetic procedure for the preparation of IL functionalized ligands **HL_{14}**……79

Chapter 3:

Scheme 3.1: General procedure for the synthesis of bis-(salicylaldiminato) Cr(II), Cr(III) and Co(II) complexes **1** – **18** ……89

Scheme 3.2: General procedure for the synthesis of bis-(salicylaldiminato) Cr(II), Cr(III) and Co(II) complexes **19** – **24**……..……110

Chapter 4:

Scheme 4.1: Coupling of CS_2 and propylene oxide with the X groups indicating that scrambling of the oxygen and sulfur atoms are observed for this process…….122

Scheme 4.2: Coupling of CS_2 and epoxides to produce cyclic carbonate……..125

Scheme 4.3: Proposed mechanism of the CS_2 and PO coupling reaction to produce cyclic products……..……142

Chapter 5:

Scheme5.1: Coupling of CS_2 and propylene oxide in the presence of organic solvents……..…….151

Scheme5.2: Proposed reaction pathway for the coupling of CS_2 and PO in the presence of MeOH as solvent and Cr(II), Cr(III), and Co(II) as catalysts…….……..…..157

Chapter 6:

Scheme 6.1: Coupling of CS_2 and epoxides to produce cyclic carbonates…….179

Scheme 6.2: Coupling of CS_2 and PO using ionic functionalized complexes as catalysts in the presence of MeOH as solvent…….182

Chapter 7:

Scheme 7.1: Coupling of CO_2 and propylene oxide……195

LIST OF TABLES

Chapter 2

Table 2.1: ^{1}HNMR data for ligands **HL_1** – **HL_3**..…….....50

Table 2.2: ^{13}CNMR data for ligands **HL_1** – **HL_3**..…….57

Table 2.3: FTIR spectroscopy, mass spectrometry and elemental data for ligands **HL_1** – **HL_2**……61

Table 2.4: ^{1}HNMR data for ligands **HL_7 – HL_8**..…….65

Table 2.5: ^{13}CNMR data for ligands **HL_7** and **HL_8**…….....69

Table 2.6: Yield, mass spectrometry, FT-IR and elemental analysis data for ionic functionalized ligands ……..75

Chapter 3:

Table 3.1: Uv-Vs and FTIR spectroscopy data for complexes **1 – 18**.……95

Table 3.2: Oxidation values for Co(II) complexes DCM (0.1 M TBAP), Ag/AgCl…….....97

Table 3.3: Mass spectrometry and elemental analysis data for bis-(salicylaldiminato) Cr(II) and Cr(III) complexes **1 – 12**..……..……101

Table 3.4: Mass spectrometry and elemental analysis data for bis-(salicylaldiminato) Co(II) complexes **13 - 18**..…….....102

Table 3.5: Magnetic moment data and number of unpaired electrons for neutral bis-(salicylaldiminato)Co(II), Cr(II) and Cr(III) complexes **1 – 12**..……104

Table 3.6: Magnetic moment data and number of unpaired electrons for neutral bis-(salicylaldiminato)Co(II) complexes **13 – 18**.……105

Table 3.7: Selected bond distances and bond angles for complex **15**…….106

Table 3.8: Uv-vis and FTIR spectroscopy data for ionic liquid functionalized bis-(salicylaldiminato)Co(II), Cr(II), Cr(III) complexes **13 – 24**.. ……..112

Table 3.9: Mass spectrometry and elemental analysis data for ionic liquid functionalized bis-(salicylaldiminato)Co(II), Cr(II) and Cr(III) complexes **19** – **24**..…….113

Chapter 4:

Table 4.1: CS_2/epoxide coupling using Cr (III) complexes **7** – **8** as catalysts…..……..125

Table 4.2: CS_2/epoxide coupling reactions using Cr (II) complexes **1** – **4** as catalyst precursors...132

Table 4.3: CS_2/epoxide coupling using Co (II) complexes **13** – **16** as catalysts……...136

Chapter 5:

Table 5.1: Effect of monomer ratio, CS_2: PO, on the coupling reaction…….157

Chapter 6:

Table 6.1: Evaluation of ionic functionalized complexes for CS_2 and PO catalytic activity in absence of a co-catalyst……..……..179

Table 6.2: Evaluation of ionic functionalized complexes for CS_2 and PO catalytic activity in the presence of [PPN]Cl as a co-catalyst……..181

Table 6.3: Evaluation of ionic functionalized complexes for CS_2 and PO catalytic activity in the absence of [PPN]Cl as a co-catalyst and in the presence of MeOH a s a solvent……....185

Chapter 7:

Table 7.1: CO_2/epoxide coupling using bis-salicylaldiminato complex **8** as catalysts[a] ……..198

Table 7.2: CO_2/epoxide coupling using neutral bis-salicylaldiminato Cr (**1** – **4** and **6** – **10**) and Co (**13** – **16**) complexes as catalysts[a]……200

Table 7.3: CO_2/epoxide co-polymerization using ionic functionalized bis-salicylaldiminato Cr (**19** – **22**) and Co (**23** – **24**) complexes as catalysts[a] ……..….....205

ABBREVIATIONS

Br	Broad
Calc	Calculated
Δ	chemical shift
°C	degrees Celsius
D	Doublet
Dd	doublet of doublets
DMAP	4-dimetylaminopyridin
ESI-MS	electrospray ionization mass spectrometry
FT-IR	Fourier transform infrared spectroscopy
g	gram (s)
h	hour (s)
Hz	Hertz
i-Pr	Isopropyl
J	coupling constant
M	Multiplet
Melm	*N*-methylimidazol
Mp	melting point
m/z	mass to charge ratio
MHz	Megahertz
Min	minute (s)
NMR	nuclear magnetic resonance
Nd	not determined
PC	propylene carbonate
PO	propylene oxide
Ppm	parts per million
Psi	pounds per square inch
[PPN]Cl	bis-(triphenylphosphine)imium chloride
‘s’	Singlet

‘t’	Triplet
TBAC	tetrabutylammonium chloride
TOF	Turnover frequency
UV-Vis	Ultraviolet-visible

Chapter 1

Literature review: Transition metal complexes as catalysts for the coupling reactions of carbon dioxide or carbon disulfide with epoxides

Contents

1.1. Introduction 2
1.2. Overview of carbon dioxide and epoxide coupling 3
1.2.1. Mechanistic aspects of carbon dioxide and epoxide coupling 3
1.2.2. Using carbon disulfide for the coupling reaction 6
1.2.3. Effect of the co-catalysts on the coupling of CO_2 or CS_2 and epoxides 8
1.2.4. Scope of epoxide substrates that can be used for coupling 11
1.2.5. Application of coupling products 12
1.3. Transition metal catalyst for carbon dioxide and epoxide coupling 13
1.3.1. Single site zinc(II) β-diiminate complexes 14
1.3.2. Transition metal complexes based on porphyrin ligands 17
1.3.3. Transition metal complexes based on salen ligands 19
1.3.4. Transition metal complexes investigated for CS_2 coupling with epoxides 23
1.4. Ionic functionalized transition metal catalysts for epoxides coupling with CO_2/CS_2 26
1.4.1. Ionic functionalized complexes based on porphyrin ligands 27
1.4.2. Ionic functionalized complexes derived from salen ligands 32
1.5. Problem statement 34
1.6. References 35

1.1. Introduction

Carbon dioxide is an abundant, renewable, and nontoxic source of carbon feedstock and its utilization to produce chemicals and materials has added value to carbon dioxide capture. To achieve this, a successful commercial process in the production of methanol was reported by Carbon Recycling International. They applied waste CO_2 and H_2 produced by electrolysis of water [1]. Another example is the application of pure CO_2 to produce materials such as poly(ether carbonate) [2, 3]. This process is a result of the copolymerization of CO_2 and epoxides. This coupling process has attracted so much attention because it produces biodegradable products which are either polycarbonates or cyclic products.

The transformation of CO_2 into useful products is however considered very challenging because it is thermodynamically stable with the standard formation enthalpy of -393.5 KJ/mol [4, 5]. The use of catalysts has however made the transformation of CO_2 into useful products achievable with relative ease. Catalysts are used to reduce the activation energy of reactions in which CO_2 is involved. Metal complexes have proved to be good homogeneous catalyst for the transformation of CO_2.

Carbon disulfide, CS_2, on the other hand is a more reactive CO_2 analogue. It is therefore used to develop model reactions that can later be used in the transformation of CO_2. It is not produced in vast quantities as a waste product like CO_2. Its study has also attracted attention because it is easier to work with because it is a liquid therefore simple glassware chemistry can be applied. It also just like CO_2 results in biodegradable products, either cyclic products or copolymers when it is coupled with epoxides. The study of the coupling of CS_2 and epoxide is however challenging due to atom exchange between oxygen and sulphur which results in multiple products [6].

The coupling of CO_2/CS_2 and epoxide catalytic reactions either produce cyclic products or polycarbonates depending on several reaction conditions such as solvent, temperature, catalyst nature, reaction time, pressure etc. These conditions influence the catalytic reactions in many ways. For instance, they can influence the type of product produced between cyclic products or copolymers. In the case where copolymers are produced, these conditions can influence the characteristics, such as molar mass and polydispersity index etc., of the polymer chain. The objective of this chapter is to give a brief survey of the work that has been achieved in the development of the catalytic coupling reactions of CO_2 or CS_2 with epoxides.

1.2. Overview of carbon dioxide and epoxide coupling

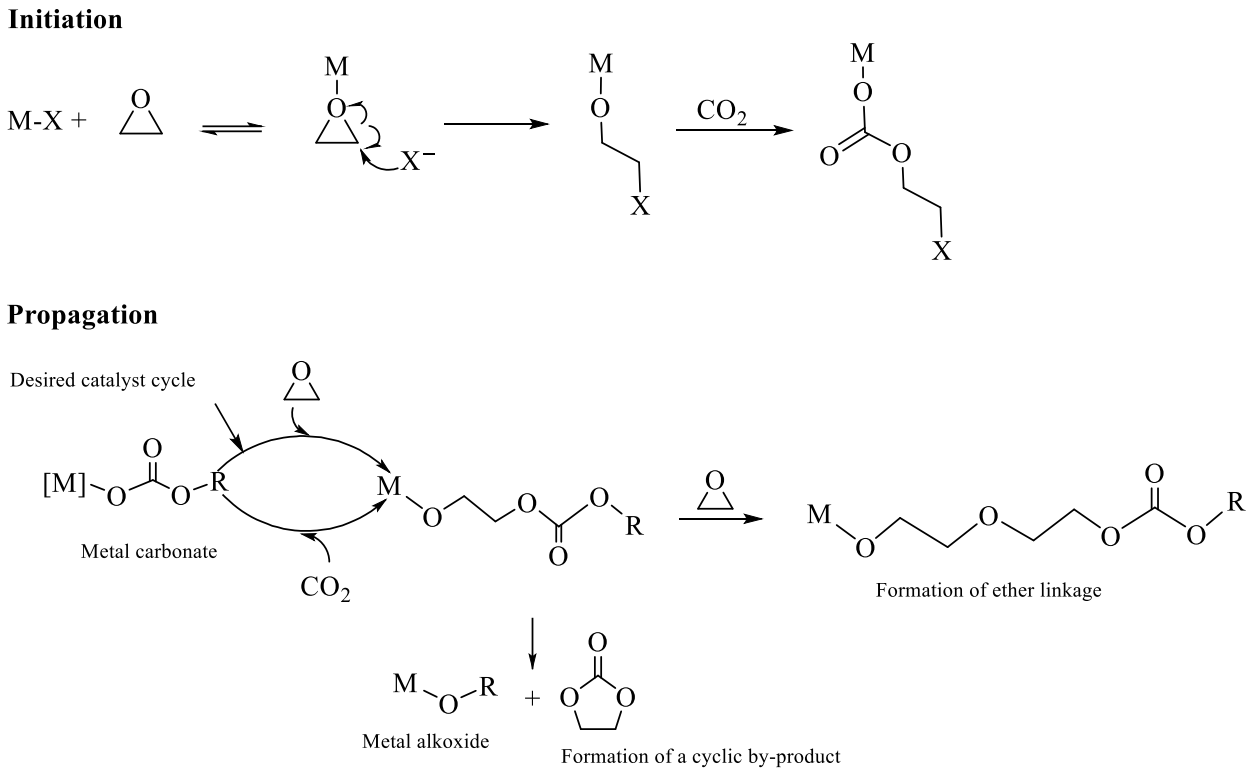
The coupling reaction of CO_2 and epoxides was first reported by Inoue and co-workers in the late 1960s [7]. A 1:1 mixture of $ZnEt_2$ and water was utilized as a catalyst system for the coupling of propylene oxide and CO_2. This catalytic reaction produced a polymer with very low molecular weight and small TOF of 0.12 h^{-1}. This discovery led to developments in the 1970s and 1980s where $ZnEt_2$ and alcohols was used as a catalyst system and the TOF improved to 1 h^{-1}. A big challenge however, with this catalyst systems was that it was very difficult to define the active site. This made structure/activity relationship, and therefore catalyst design very difficult. These including high polydisperse polymer produced and low CO_2 incorporation led to the development of well-defined homogeneous catalysts as transition metal complexes [8].

1.2.1. Mechanistic aspects of carbon dioxide and epoxide coupling

Carbon dioxide and epoxide coupling reaction when catalyzed by metal complexes is proposed to occur through a coordination-insertion mechanism [9, 10] as shown in Scheme **1.1**. The mechanism comprises of several steps which are initiation, propagation and a chain transfer may also be possible. The initiation step involves coordination of the epoxide to the metal center, followed by an attack of the nucleophilic group (**X** = axial ligand of the metal and can be halide, carboxylate) which results in ring opening of the epoxide and formation of a metal bound alkoxide (Scheme **1.1**). This is followed by CO_2 insertion resulting in the formation of a metal carbonate. In cases where the **X** group is an alkoxide/aryloxide, Scheme **1.1**, the initiation step is CO_2 insertion.

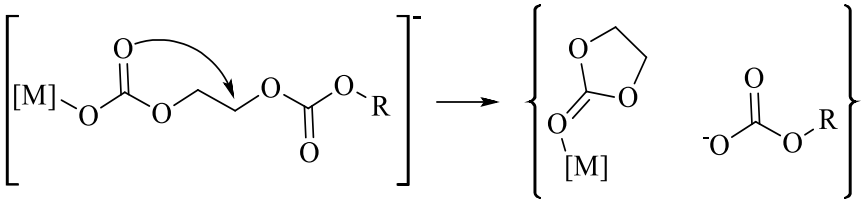
The propagation step results in polycarbonate formation which occurs as result of successive coordination and insertion of the epoxide substrate and carbon dioxide. After formation of the metal carbonate, propagation occurs when the nucleophilic attack of the metal bound carbonate on a coordinated epoxide molecule takes place, producing a metal alkoxide followed by CO_2 insertion. Repetitive alternating series of these reactions leads to the formation of the polycarbonate co-polymer. The basic assumption is that co-polymer with only carbonate linkages is formed (100% carbonate) but some catalysts can also homopolymerize epoxide to some extent or undergo decarbonation reaction and form ether linkages in the copolymer backbone [11].

In the coupling reaction, the nucleophilic attack occurs predominantly on the less sterically hindered carbon atom since this is the most easily accessible carbon atom in the epoxide ring. This facilitates the ring opening at the less sterically hindered C-O bond. In the coupling of CO_2 and alicyclic epoxides the C-O bond cleavage occurs with inversion of configuration at the site of attack (S_N2-type mechanism) to result in the formation of the trans ring-opened product [12]. Chain transfer reactions (Scheme **1.1**) are some of the termination steps. They occur once the reaction mixture is exposed to protic solvents such as water, amines, or alcohols [13, 14, 15]. In the presence of protic reagents, they form free hydroxy terminated polymer chains and metal alkoxides. They usually occur faster than the propagation step [11].



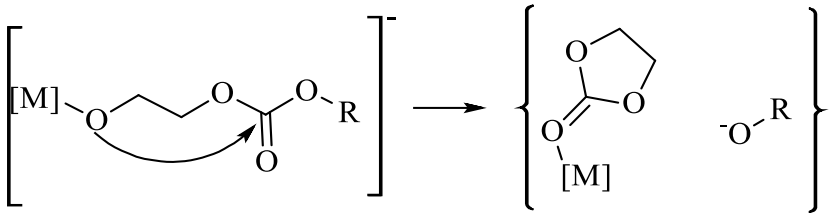
Scheme 1.1 *The proposed catalytic cycle for a CO_2/epoxide coupling reaction* [11]

The coupling of epoxides and CO_2 can sometimes result in the mixture of co-polymers and cyclic products. Cyclic products can also be produced as main products of the coupling process. Cyclic carbonates form because of backbiting or depolymerization which is the degradation of the growing copolymer chain [16]. There are two ways in which backbiting occurs to form cyclic products. One is metal-bound carbonate backbiting in the presence of CO_2, Scheme **1.2** (ΔG = 79 – 104 KJ mol^{-1}). It is expected to occur through the free C=O oxygen atom [17]. Carbonate backbiting leads to a metal bound cyclic carbonates which can be displaced by epoxide or a polymeric alkoxide, enabling further coupling.



Scheme 1.2: *Mechanism for metal bound carbonate depolymerization*

Alkoxide backbiting has a much lower free energy barrier (Scheme **1.3**, ΔG = 38 -59 KJ mol^{-1}). In the presence of transition metal catalysts, the energy barrier for these backbiting reactions increases and the backbiting reactions are retarded. The metal complex is believed to cap the carbonate or the alkoxide such that it does not go through the lower-energy metal degradation reaction. A major concern has been that these cyclic carbonates may sometimes competitively bind to the catalyst, poisoning it [18].

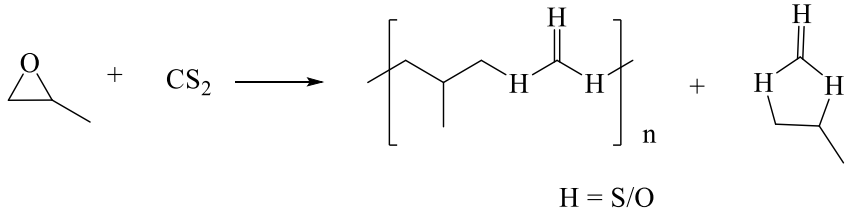


Scheme 1.3: *Mechanism for metal bound carbonate depolymerization*

Most catalyst systems favor cyclic products because they are relatively more thermodynamically stable than the polycarbonates [19]. The coupling process can be tailored to favor cyclic products or polycarbonate by changing the process conditions such as the catalyst, additives, temperature, CO_2 pressure and epoxide concentration. The stability of cyclic carbonates makes it difficult for them to undergo any ring opening polymerization. Darensbourg and his coworker in their computational studies showed that the coupling of epoxide and CO_2 to produce co-polymer is generally exothermic by 21 – 23 Kcal mol^{-1} whereas the coupling of CO_2 and epoxide to form cyclic carbonates is much less (14 – 15 Kcal mol^{-1}) and this makes them more favorable as entropic products [20].

1.2.2. Using carbon disulfide for the coupling reaction

Carbon disulfide (CS_2) is an isoelectronic molecule to CO_2 and can be used as substrate to couple with epoxides resulting in the incorporation of sulphur in the co-polymer or cyclic products of coupling reactions, Scheme **1.4**. As a result, this changes the properties of the products produced. For instance, the co-polymers produced possess very high optical and thermal properties, and excellent chemical resistance [21 – 24]. Cyclic products can also be used in various applications and that will be discussed in some sections that follow. Sulphur can be introduced through the replacement of CO_2 with CS_2 in the coupling reaction.

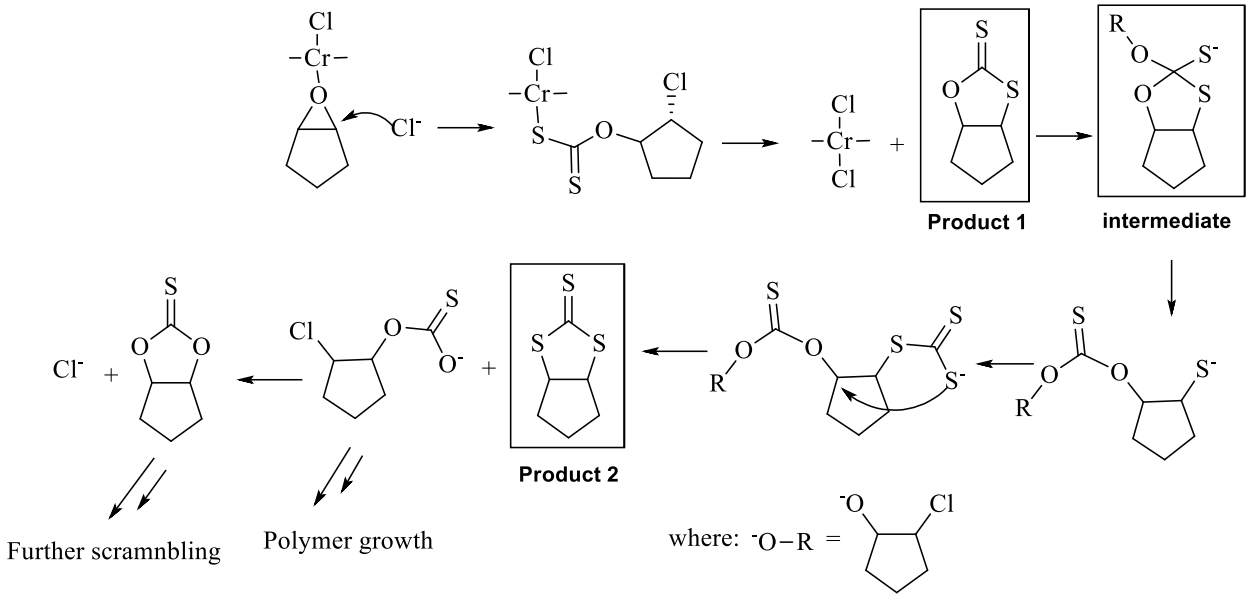


Scheme 1.4: *Coupling of carbon disulfide and propylene oxide*

CS_2 is more reactive than CO_2, therefore this makes the incorporation of sulphur into the coupling reaction products using CS_2 as monomer much easier. The coupling of CS_2 and PO is however complicated by the scrambling of sulphur and oxygen atoms in either the polythiocarbonate or the

cyclic products. Expectation is that the coupling of propylene oxide (PO) and CS_2 should result in a polymer and/or cyclic product with a repeating -O-(C=S)-S-, however more linkages such as -O-(C=O)-S- and -S-(C=S)-S- were observed because of the sulphur and oxygen atoms scrambling process [25].

There are few reports in literature on the scrambling mechanism. Darensbourg and coworkers proposed that the insertion of CS_2, COS, and CO_2 is reversible, and it is this reversibility that brings about the scrambling [26]. The same was observed by North [27] and Endo [28]. In both cases, when aluminum and titanium-based complexes were used as catalysts multiple cyclic products were formed. It is postulated that the catalysts do not only catalyze the coupling reaction but also provide exchange sites for scrambling in the reaction. As shown in Scheme **1.5** below, the catalyst is required to activate, and ring open the epoxide. Then CS_2 inserts to form product **1**, Scheme **1.5**. The alkoxide that results as a byproduct can attack product **1** resulting in an intermediate.which undergoes ring opening followed by nucleophilic attacks on CS_2 and the ring closes to form a new cyclic product **2**, Scheme **1.5**. The repeated alkoxide attack on the cyclic products can result in multiple cyclic products being formed.



Scheme 1.5: *Proposed mechanism for scrambling in the coupling of cyclopentane oxide and CS_2* [26]

1.2.3. Effect of the co-catalysts on the coupling of CO_2 or CS_2 and epoxides

CO-catalysts are quaternary ammonium salts (PPN^+X^-, TBA^+X^-, where X is usually a halogen) or heterocyclic nitrogen Lewis bases (*N*-methylimidazole, (dimethylamino)pyridine) that are added to the catalytic reactions to enhance the performance of the catalysts. The presence of co-catalysts in the catalytic reactions have a very significant effect. They are confirmed to bind to the metal center at the vacant sites therefore activating them. They then participate in the initiation step of the copolymerization process.

1-Methylimidazol (Melm) was utilized as a co-catalyst to activate the coupling of CO_2 and PO which did not occur when an aluminum porphyrin complex was used as catalyst alone. When the same porphyrin complex was used in the presence of ammonium and phosphonium salts for CO_2/CHO (cyclohexene oxide) coupling an increase in the activity of the catalyst to produce a copolymer was observed. A drastic increase in the carbonate linkage (>99 %) was also observed after the addition of the co-catalysts [29].

Quaternary ammonium salts nBu_4NX (X = Cl, Br, I) and neutral organic compounds pyridine, and Melm have been utilized as co-catalysts in the synthesis of ethylene carbonate in the presence of a (salen) Al (III) complex as a catalyst. The co-catalysts were reported to enhance the rate of coupling by a factor of five. When nBu_4NBr was utilized as a co-catalyst at 110 °C and 150 atm CO_2 pressure, ethylene oxide was converted to a cyclic product, ethylene carbonate, with TOF of 2220 h^{-1} [30].

A mixture of copolymer, TOF of 103 h^{-1}, and cyclic product was obtained when DMAP was used as a co-catalyst in the presence of a chromium porphyrin complex reported by Kruper and Della for CO_2/CHO at 95 °C and 50 atm. The same co-catalyst was utilized by Nguyen and his coworkers in the presence of (salen)Cr(III) complex for the coupling of terminal aliphatic epoxides including PO, styrene oxide (SO), butadiene monoepoxide and epichlorohydrin [31]. In this case the catalytic process was more selective for cyclic products. It was observed that the activity of the catalyst depended on the amount of DMAP that was added with the increase in activity observed when the concentration of DMAP was increased from one to two equivalents. Beyond this concentration the activity of the catalyst dropped significantly [32].

Darensbourg and his co-workers also reported [PPN]Cl as a very active co-catalyst in the presence of (salen)Cr(III) complex for CO_2/CHO coupling reaction. The same complex and [PPN]Cl were applied for CS_2/PO coupling to prepare polythiopropylene carbonate. The kinetic study that was conducted by Darensbourg and his coworkers showed that amongst all the Lewis bases or quaternary salts, $[PPN]^+X^-$ derivatives were rated as the best co-catalysts [33].

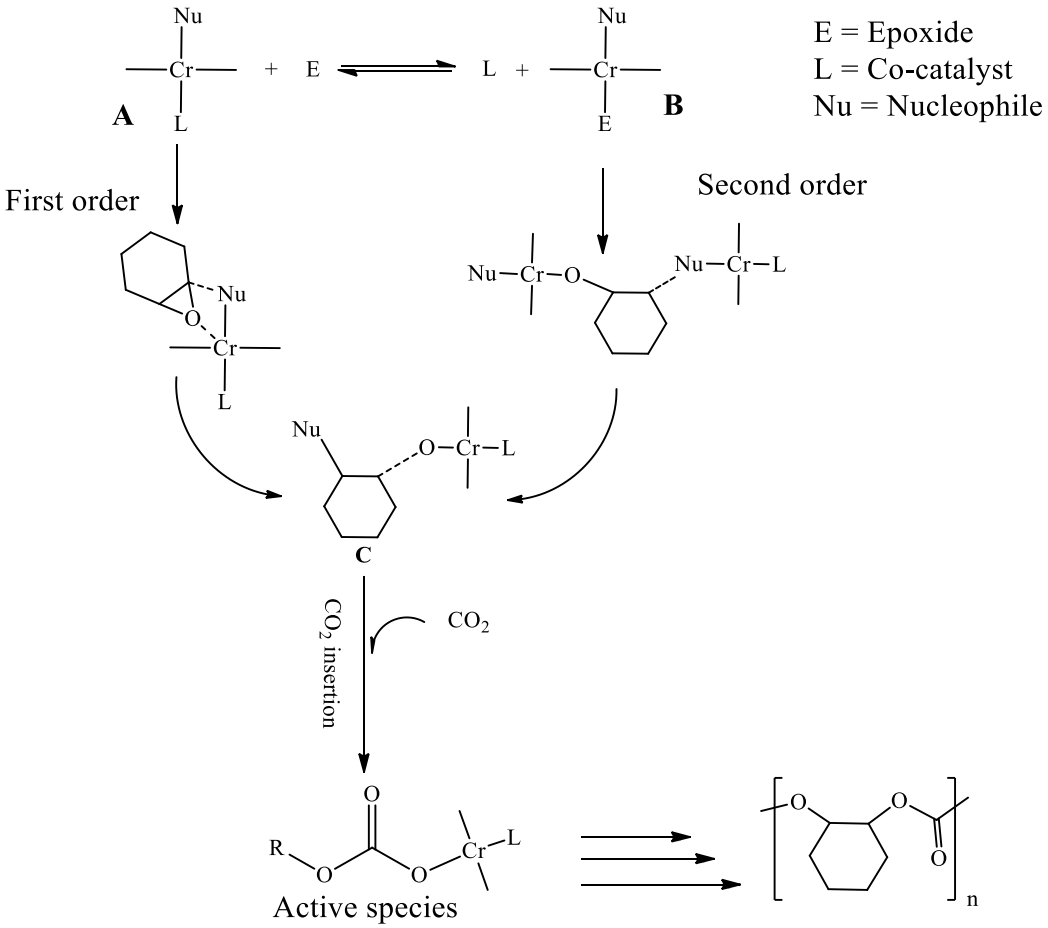
In their study they found that the (triphenylphosphorylidine)ammonium (PPN) cation is none interacting even when used in weak coordinating solvents such as epoxide. This characteristic of the PPN cations is mostly required for a better co-catalyst. When [PPN]Cl is used as a co-catalyst the initiation time is effectively reduced to almost zero resulting in a significant gain in turnover frequency. Tetra-n-butylammonium chloride (TBAC) is also believed to have a very low initiation time which makes it almost active as a co-catalyst to [PPN]Cl [33, 34].

One of the major differences in co-catalysts is their affinity with water. PPN salts are very hydrophobic and thus they are easily recrystallized from water and isolated in high purity. This was found not to be the case with hydrophilic salts such as ammonium and phosphonium salts which must be recrystallized several times and might still contain significant amounts of water. The presence of water can cause detrimental effects in the anionic coupling reactions including low catalytic activity, low molecular weight copolymer and high PDI [33].

Co-catalysts act as a catalyst activator and their role in coupling reactions is to initiate the coupling reaction. They do this by opening the epoxide ring to allow for CO_2 insertion. Most of the co-catalysts are Lewis bases and they are electron donors. Their ability to donate electrons allows them to form coordinate bonds with metal complexes and such metal complexes become activated. Depending on the nature of the co-catalyst there are two ways in which the epoxide ring can be opened, either through a first order or second order reaction mechanism as shown in Scheme 1.6.

When a strongly donating co-catalyst is present the metal nucleophile bond weakens, and this allows coordination of concerted epoxide rings. Once the epoxide ring is attached to the metal a nucleophilic attack by the nucleophile coordinated to the metal occurs at the most electrophilic and less sterically hindered carbon of the epoxide and this results in the ring opening of the epoxide through a first order reaction mechanism.

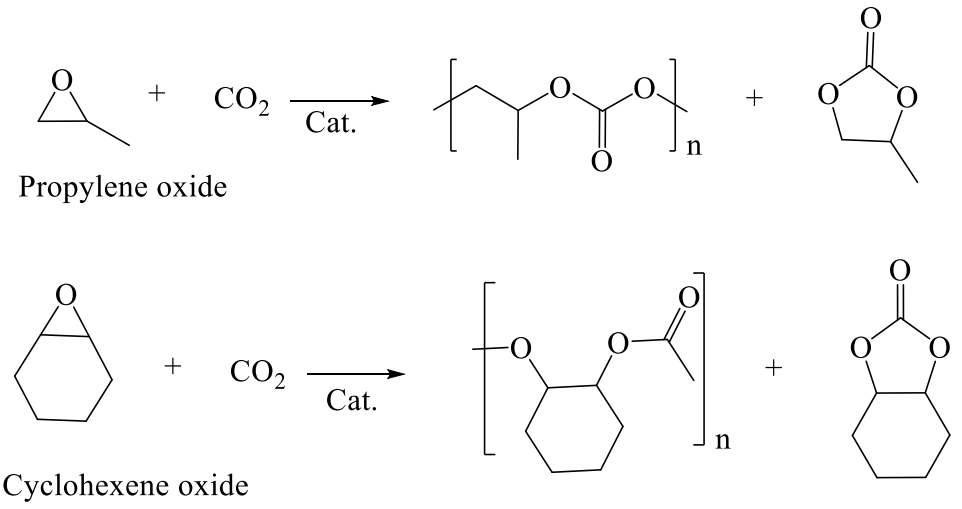
When a weak co-catalyst is coordinated to the metal this does not labialize the metal nucleophile bond enough hence it becomes very difficult for the epoxide ring to coordinate to the metal. In this case the epoxide ring opening goes through a dinuclear transition state. The epoxide coordinates to the inactivated metal and then its electrophilic and less sterically hindered carbon gets attacked by a nucleophilic from a co-catalyst coordinated to another catalyst and this results in the ring opening of the epoxide through a second order reaction mechanism. In this pathway adequate concentrations of **A** and **B** (Scheme **1.6**) are required for initiation. The initiation time increases with the increase in the concentration of the co-catalyst [35].



Scheme 1.6: *Proposed mechanisms for the initiation process in CO_2/CHO coupling reaction* [35].

1.2.4. Scope of epoxide substrates that can be used for coupling

There are many epoxides that have been utilized as starting material in the coupling of CO_2 to produce either cyclic products or co-polymers but the mostly studied ones are propylene oxide and cyclohexene oxide (Scheme **1.7**) [11]. Cyclohexene oxide (CHO) is a convenient comonomer because it is cheap and produce linear polycarbonates with high tensile strength with relatively high T_g value of 116 ^oC [36] and good thermal stability. However, copolymers prepared from CHO are brittle and have low biodegradability. On the other hand, polycarbonates produced from the coupling of PO and CO_2 have good biodegradability and toughness however they have low glass transition temperature. It is therefore obvious that the epoxide can be chosen as a monomer depending on the target properties of the product.



Scheme 1.7: *Coupling of CO_2 with propylene oxide and cyclohexene oxide.*

Epoxide monomers are also chosen depending on their reactivity. In a study that was performed by Rieger and coworkers, they found that some epoxides favor formation of cyclic products while others favor formation of copolymers. When the compared ethylene oxide (EO), CHO and PO based on enthalpic point of view they discovered that cyclic carbonates of EO and PO are about 12 $KJmol^{-1}$ less stable than their corresponding copolymers. The cyclic carbonate formed from PO was found 5 $KJmol^{-1}$ more stable than the corresponding copolymer [37].

1.2.5. Application of coupling products

The products of the coupling reactions of CO_2 and PO have a lot of potential applications. Five-membered cyclic carbonates on one hand were commercialized in the mid-1950s [38] because they attracted a growing interest due to their outstanding physical properties which include low odor, high boiling and flash points and low toxicity compared to ordinary organic solvents [39]. In addition, they are biodegradable and have relatively high solvency. These cyclic carbonates are utilized as aprotic polar solvents in degreasing, paint stripping, and cleaning. Additionally, cyclic carbonates are regarded as very useful intermediates in organic synthesis which can be used for the protection of 1,2- and 1,3-diols and construction of structurally complex organic molecules [38]. Cyclic carbonates are also an important feedstock material in the production of modern lithium batteries [40].

Cyclic products prepared from the coupling of CS_2 and PO have biological activity. dithiocarbonate products, **1** and **2**, Scheme **1.8**, have radioprotective activity therefore they have been used in polymer syntheses [41, 42]. Cyclic product **3** has been incorporated into compounds which possess fungicidal and antibacterial properties. The trithiocarbonate product, **4**, has been found to possess radioactive and insecticidal activity [27].

On the other hand, aliphatic polycarbonates prepared from CO_2 and PO have attracted a lot of interest for biomedical applications specifically in tissue engineering and drug delivery systems because of their biodegradable and biocompatible nature [43, 44, 45]. They also have attracted attention in the application as packaging materials [46]. Their use as packaging material can help in minimizing pollution because of non-biodegradable polymers that are now in use. Co-polymers can also be used as ceramic binders, adhesives, and coatings. They also have very promising application as chemically stable ion exchange membranes for electromembrane processes, and a proton conducting electrolytes.

The introduction of sulphur atom into the polymer chain can be achieved through the coupling of CS_2 and epoxides. The presence of sulphur into the polymer chain improves mechanical, optical, and electrical properties. They have potential to be applied as optical, optoelectronic, and photochemical materials [46]. They also have features such as heavy metal recognition as well as

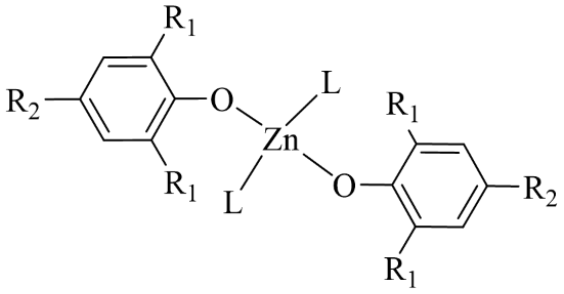
good adhesion to metals, resistance to radiation, chemical and bacteria. Sulphur containing polymers therefore have potential in application as high-performance plastic.

1.3. Transition metal catalyst for carbon dioxide and epoxide coupling

In 1968 Inoue and coworkers discovered a heterogeneous equimolar reaction mixture of $ZnEt_2$ and H_2O for CO_2/propylene co-polymerization [47]. This discovery resulted in the production of low molecular weight poly(propylene carbonate) with a turn over frequency (TOF) of 0.12 h^{-1} at 20-50 atm CO_2 and 80 °C. This led to a development, in the 1970s and 1980s, of a variety of catalysts to enhance this result and a mixture of either $ZnEt_2$ or ZnO and alcohol and a TOF increase to 1 h^{-1} were discovered.

The first highly active well-defined zinc bis-phenoxide complex (Figure **1.1**) was developed by Darensbourg [18]. When Zn complex **1** was used as catalyst for the coupling of cyclohexene oxide and CO_2 at 800 psi CO_2 pressure, 80 ^oC and 69 hours, the reaction resulted in the formation of high molecular weight copolymer. On the other hand, when complex **1** was used as catalyst for the coupling of propylene oxide and CO_2 at the same reaction conditions, a cyclic product was predominantly formed as major product. Discrete zinc catalysts prepared from phenolic derivatives and $Zn[N(SiMe_3)_2]_2$ were also reported to catalyze CO_2/CHO to produce a copolymer with high carbonate linkage (90%) and molar mass 38 kg mol^{-1} with TOF of 2.4 and 9.6 h^{-1} respectively.

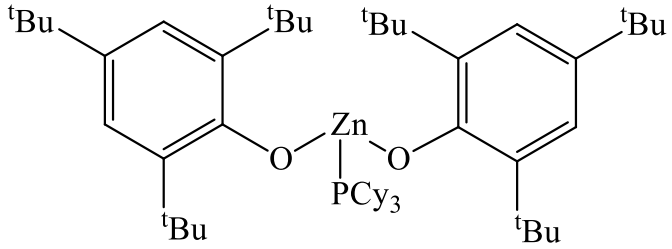
These catalyst systems have potential to produced polymers with very high polydispersity indices, however in some cases high proportions of ether linkages were produced as a result of catalyst activity towards epoxide homopolymerisation [48]. When complex **2** was used as catalyst in the coupling of cyclohexene oxide and CO_2, homopolymerisation of cyclohexene oxide occurred even before CO_2 was added. This condition occurs mostly when the cyclohexene oxide/catalyst ratio is increased. It is clear from these observations that the product produced by the coupling in the presence of these zinc complexes does not only depend on reaction conditions such as temperature and pressure but also on the nature of the monomer used.



1) R_1 = Ph, R_2 = H, L = Et_2O
2) R_1 = R_2 = Me, L = THF

Fig. 1.1: *Zinc phenoxide complexes reported by Darensbourg and his co-workers* [48]

More zinc phenoxide derivatives (Figure **1.2**) were developed which could afford 100 % carbonate linkage of the polymer prepared from a CO_2/CHO coupling reaction [49]. After these derivatives no further, catalytic performance improvements were achieved with the zinc phenoxide derivatives.



3

Fig. 1.2: *Zinc phenoxide derivative complexes for CO_2/CHO coupling* [49].

1.3.1. Single site zinc(II) β-diiminate complexes

Quinoxaline zinc alkoxide complexes (Figure **1.3**) which are believed to be the ancestors for BDI (β-diiminate) catalysts were first reported in 2002 [50]. These complexes displayed very poor performance towards CHO/CO_2 coupling.

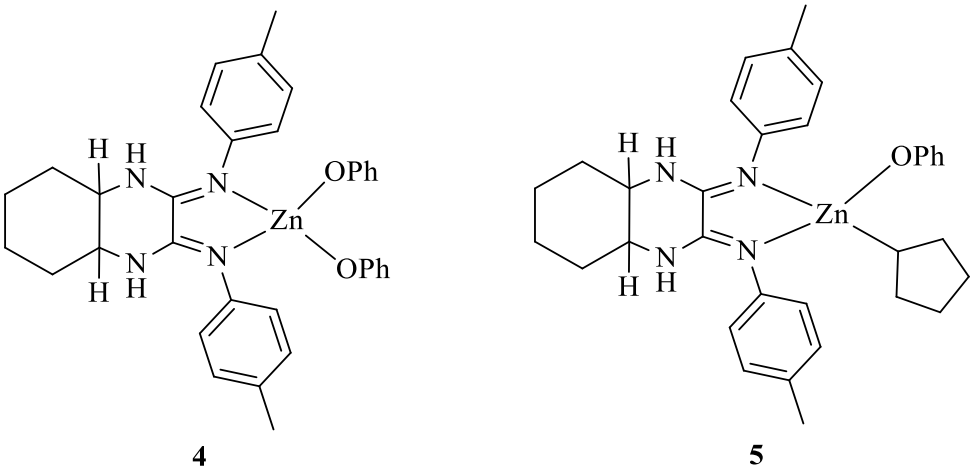
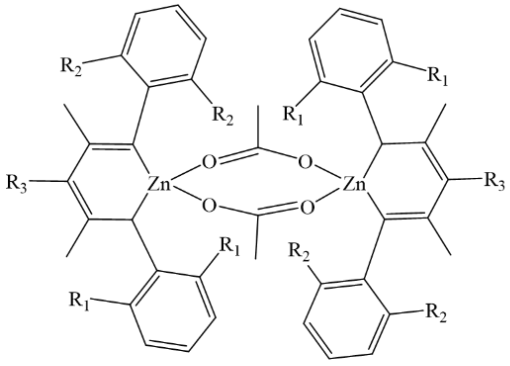


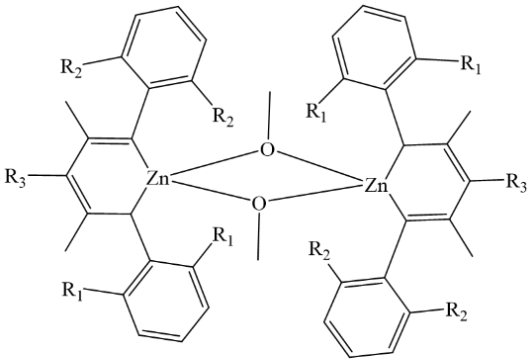
Fig. 1.3: *Diimine quinoxaline zinc alkoxide complex for CO_2/CHO coupling.*

From the knowledge of these quinoxaline zinc complexes Coates and coworkers reported a series of zinc β-diiminate complexes with greater activity for CO_2/epoxide co-polymerization [51, 52, 53]. They reported bulkier binuclear zinc β-diiminate complexes which showed very high activity for the CO_2/CHO coupling s process. In a detailed dynamic solution study, it was discovered that these complexes exist in three forms – a monomeric and tightly bounded dimeric form, which are inactive for coupling reactions, and a greatly active poorly bound dimeric form [54].

Temperature, concentration, and steric effects of the substituents are the conditions that influence the equilibrium of these three forms of complexes. The electronic and steric properties of the substituents were observed to influence the rate of polymerization. For example, a less sterically hindered complex (**6**, Figure **1.4**) was reported to be inactive in CO_2/CHO coupling while bulkier ethyl and isopropyl groups (**7, 8** Figure **1.4**) showed TOF of 431 and 360 h^{-1} respectively. The highest activity was obtained with unsymmetrical complex (**9**, Figure **1.4**) and with a complex with electron withdrawing cyano substituent in the R_3 position (**10**, Figure **1.4**).



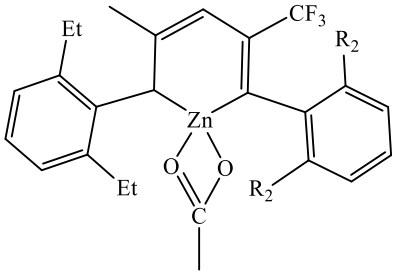
6) R_1, R_2 = Me, R_3 = H
7) R_1, R_2 = Et, R_3 = H
8) R_1, R_2 = iPr, R_3 = H
9) R_1 = Et, R_2 = iPr, R_3 = H
10) R_1, R_2 = Et, R_3 = CN



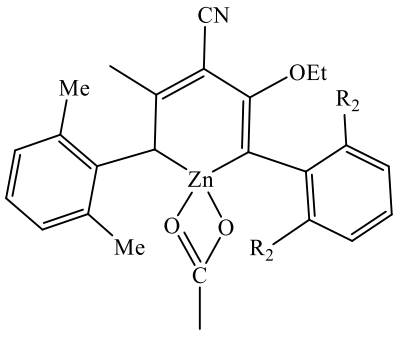
11) R_1, R_2 = Et, R_3 = H
12) R_1, R_2 = iPr, R_3 = H
13) R_1 = Et, R_2 = iPr, R_3 = CN
14) R_1, R_2 = Et, R_3 = CN

Fig. 1.4: *Binuclear zinc β-diiminate complexes for CO_2/CHO co-polymerization process [54]*

Alkoxy zinc complexes were also reported active as catalysts for CO_2/CHO co-polymerization with TOFs ranging from 239 to 224 h^{-1} for complexes **11** and **12** (Figure **1.4**) respectively [52]. Even in this case where alkoxy zinc complexes were used as catalysts a higher catalytic activity was observed when R_3 was a cyano substituent [53]. Complexes **13** and **14** (Figure **1.4**) displayed activities of 2170 and 1690 h^{-1} respectively. This led to the development of new complexes **15** [55] and **16** (Figure **1.5**) [56] with CF_3 or CN and OEt as substituents. Complex **15** (Figure **1.5**) displayed quite good activity for CO_2/PO coupling producing PPC with TOFs of 234 h^{-1} while complex **16** (Figure **1.5**) displayed good activity for CO_2/CHO with a TOF of 210 h^{-1} but the carbonate linkage of only 88 % was obtained.



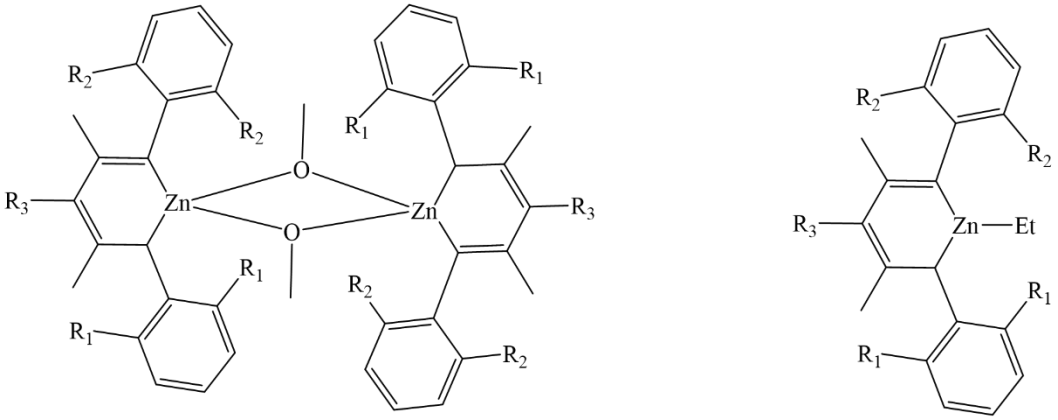
15)



16)

Fig. 1.5: *Zinc β-diiminate complexes with modified ligand architecture* [56, 55].

Three new catalysts with varying degree of bulkiness having CN substituent in the para position of the aryl ring (**17** – **20**, Figure **1.6**) have been recently reported as very highly active catalysts for CO_2/CHO coupling reaction [57]. The percentage of carbonate linkage of the polymer produced was obtained in the range 80 – 93 %.



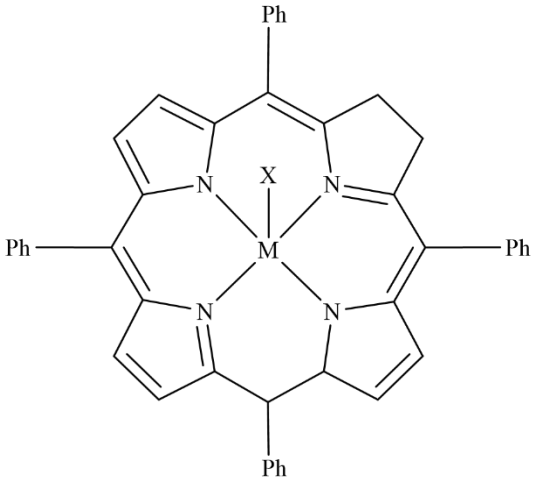
17) R_1 = Et, R_2 = iPr, R_3 = H
18) R_1 = Me, R_2 = iPr, R_3 = H
19) R_1 = Et, R_2 = Et, R_3 = CN

20)

Fig. 1.6: *New zinc β-diiminate complexes with CN substituent on the para position* [57].

1.3.2. Transition metal complexes based on porphyrin ligands

In 1978, Inoue discovered a single-site (homogeneous) catalyst for CO_2/epoxide copolymerization based on a tetraphenylporphyrin ligand framework (Figure **1.7**) [14]. Aluminum (**21** – **24** Figure **1.7**) complexes specifically were active for co-polymerization of both cyclohexene oxide and propylene oxide and copolymers with molecular weights between 3500 and 6000 kg mol^{-1} were produced with polydispersity indices (PDI) below 1.1 and 30 – 40 % of carbonate unit in polymer; however, the reaction took roughly thirteen days to reach completion [8]. When ammonium and phosphonium salts were added as co-catalysts the carbonate linkage of the polycarbonates increased (> 99%) but the reaction time remained approximately the same as when the co-catalysts were not used. The coupling reaction in the presence of these aluminum porphyrin complexes resulted in the formation of cyclic products as by-products.



21) M = Al, X = Cl
22) M = Al, X = OMe
23) M = Al, X = Me
24) M = Al, X = OR
25) M = Mn, X = OAc

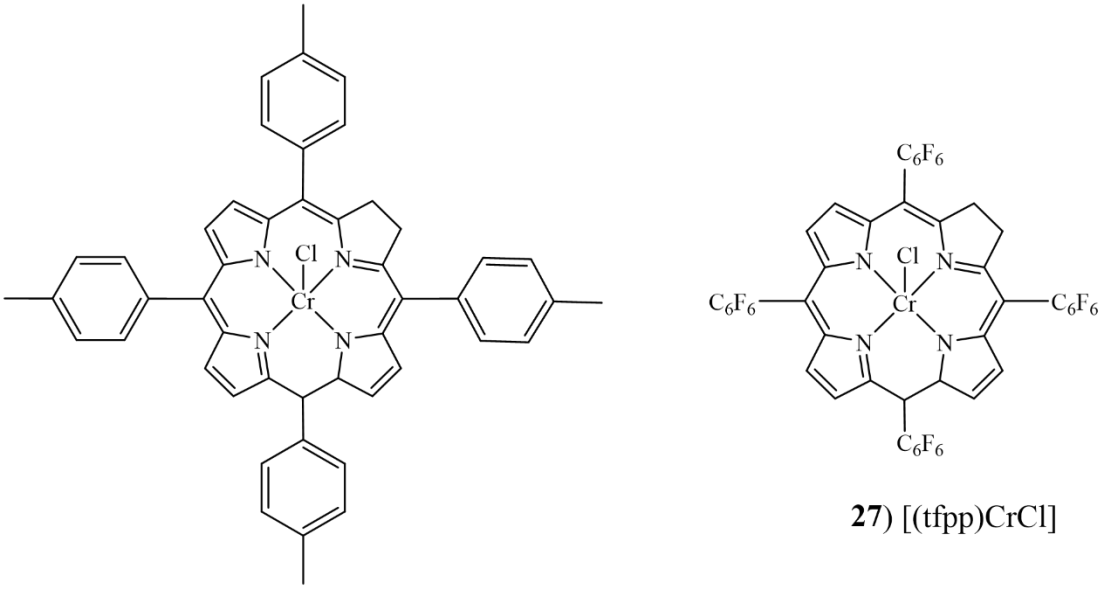
Fig. 1.7: *Aluminum and manganese porphyrins complexes for CO_2 and epoxide co-polymerization (R = alkyl, oligomer of PPO)* [14].

A porphyrin system utilizing manganese as an active metal center (**25**, Figure **1.7**) was developed by Inoue and coworkers in 2003. This catalyst system facilitated cyclohexene oxide (CHO) and CO_2 co-polymerization at 80 °C and 50 atm CO_2 to yield a copolymer with 99% carbonate linkage with moderate TOF of 16.3 h^{-1}. In the case of propylene oxide and CO_2 co-polymerization, a polycarbonate was produced with no poly(propylene carbonate) but the formation of a one-to-one cyclic adduct between CO_2 and propylene oxide [58].

A cobalt porphyrin system was also reported to display some activity towards polycarbonate preparation in the presence of some Schiff bases. Narrow polymer dispersity and 100 % polymer selectivity were obtained when this porphyrin complex was utilized as a catalyst for CO_2/CHO coupling. When DMAP and pyridine were added as co-catalysts a polymer with TOF of 21 h^{-1}, Mn = 14 – 20 kg mol^{-1} and with 99 % carbonate unit of the polymer.

Kruper and Dellar also reported a porphyrin system utilizing chromium as an active metal center (**26**, Figure **1.8**). When these complexes were evaluated for activity towards CO_2 and epoxides (PO, CHO and CPO) coupling reactions in the presence of 4 -10 equivalents of a co-catalyst (such as DMAP or Melm) cyclic products were formed as major products with moderate activity [59]. Following this, Holmas and co-workers developed (**27**, Figure **1.8**) catalyst which showed activities of up to 173 h^{-1} for the alternating copolymerization of CHO and CO_2 at 225 atm CO_2

and 110 °C [60]. The copolymer was only produced when this complex was used in the presence of DMAP as a co-catalyst.



26) [(tpp)CrCl]

27) [(tfpp)CrCl]

Fig. 1.8: *Chromium (III) porphyrin complexes* [59, 60]

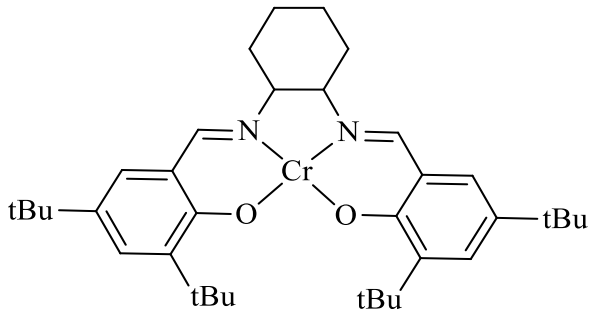
1.3.3. Transition metal complexes based on salen ligands

Recently, metal complexes based on Schiff base ligands, which were named after Hugo Schiff, have proved very active for CO_2/epoxide co-polymerization. A Schiff base ligand class, salen, which is generally used to describe a [O,N,N,O] tetradentate bis-Schiff ligand is the one specifically reported for these metal complexes [61]. Complexes of salen ligands have attracted much attention since salen ligands are easily and effectively synthesized compared to porphyrin ligands which yield about 20% in their synthesis [62]. Due to the ease of synthesis, a tailoring of catalyst steric and electronic properties is readily achieved [63, 64, 65].

Schiff base ligands which are also known as privileged ligands [66] are prepared by a condensation reaction between aldehydes and amines. Condensation of salicylaldehyde or salicylaldehyde derivatives with 1, 2-diamines results in a formation of salen ligands [61]. Schiff base ligands use imino nitrogen and the phenoxy oxygen atom to coordinate with the metal. Metal salen complexes [salenMX], where M= Co, Cr, and Al, alone or in conjunction with Lewis base, onium salt, or

ionic liquid as co-catalyst have been of great interest because they are easy to synthesis, they have good stability against moisture and air, and high selectivity of polycarbonates over cyclic carbonates [67].

The first highly active chromium-salen catalyst system was reported by Jacobsen and coworkers for asymmetric ring opening of epoxide (**28**, Figure **1.9**) [68, 69]. From this development by Jacobsen, Darensbourg and Yarbrough investigated whether the same catalyst is capable to repetitively ring open epoxide accompanied by CO_2 insertion [70]. When the complex was evaluated for catalytic activity for CHO and CO_2 coupling at 80 °C and 60 atm of CO_2, a polycarbonate was produced with moderate TOF of 10.4 h^{-1}. Nearly 100 % carbonate linkage, a M_n of 8900 g/mol^{-1} and M_w/M_n of 1.2 were observed when the polycarbonate was analyzed. This catalyst reported by Darensbourg showed an increase in activity when it was used together with Melm as co-catalyst, such that 5 equivalents of Melm tripled the coupling rate to 32 h^{-1}. A cyclic product was produced in very small quantities in this case.



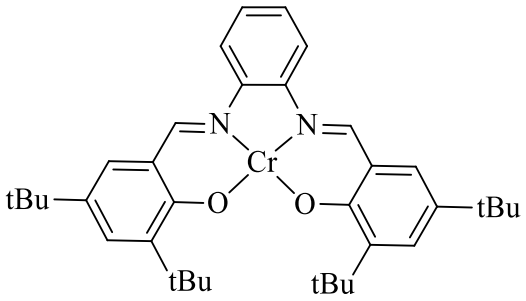
28

Fig. 1.9: *Jacobsen salen catalyst system*

Rieger and co-workers reported a modified Jacobson's (salen) Cr(III) complex in which the ethyl substituent on the imino nitrogens was replaced with a phenyl substituent (**29**, Figure **1.10**) [71]. This complex was found inactive in the absence of a co-catalyst. It showed very high activity in the presence of DMAP as a co-catalyst. When the coupling reaction was performed at 75 °C and 35 bar CO_2 with 1 equivalent of DMAP a co-polymer was formed with TOF of 160 h^{-1} while a cyclic product was formed with a TOF of 66 h^{-1}. The overall conversion of PO was recorded at 60%. In this case the effect of pressure on the coupling product was observed, where the overall

conversion of PO to the cyclic product was recorded at 68% when CO_2 pressure was reduced to 13 bar. This is slightly higher than when 35 bar of CO_2 pressure was used.

The ratio of DMAP to the complex was reported to have very significant influence on the product distribution. When two equivalents of DMAP were used at 13 bar CO_2 pressure, the coupling process formed a cyclic product instead of a copolymer. The smallest conversion was observed when 0.5 equivalents of DMAP was used. In this case the coupling reaction formed a mixture of products; cyclic product and a copolymer and the copolymer was formed as a major product. A reaction where DMAP was used as a co-catalyst did not result in the formation of any coupling product. It is therefore clear that the depolymerization towards formation of cyclic products in the presence of **29** is effective at high DMAP concentration.



29

Fig. 1.10: Modified *Jacobsen salen catalyst system reported by Rieger and co-workers*

Cobalt complexes were also used as catalysts for CO_2/PO coupling reactions. Soga and co-workers utilized $Co(OAc)_2$ as a catalyst for the CO_2/PO coupling reaction and a copolymer was obtained with a very low TOF of 0.06 h^{-1}. An improvement in the catalytic activity of cobalt complexes was observed from a (salen)Co(III) complex that was recently reported by the Coates' group (Figure **1.11**). The complex exhibited moderate activity of around 81 h^{-1} for the coupling of PO and CO_2 to produce a copolymer [72, 73]. The catalyst system (**30**, Figure **1.11**) produced a polycarbonate with no observable cyclic products, 95% carbonate linkages, a M_n of 15 300 g mol^{-1}, and a polydispersity (M_w)/M_n of 1.22. The co-polymerization process was carried out at 25 °C and 55 atm CO_2. A pressure of 55 atm was reported as essential as lower pressures (40 atm) significantly hinder the co-polymerization process.

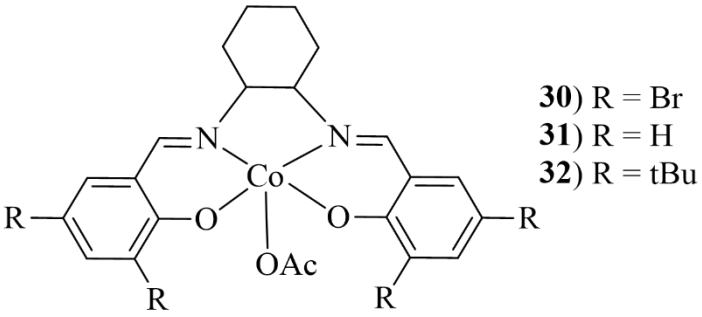
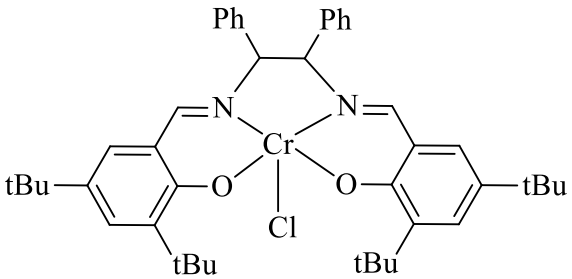


Fig. 1.11: *Co-salen catalyst system reported by Coates and coworkers* [71]

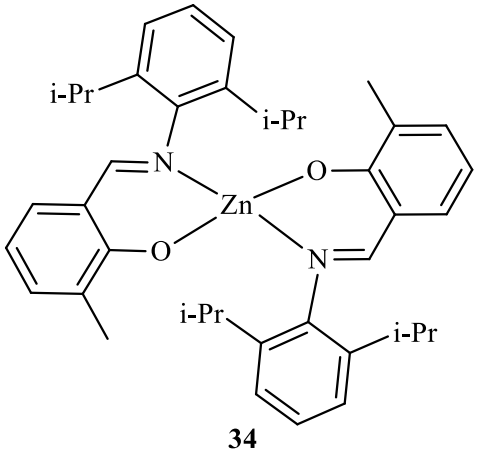
Nguyen utilized a binary catalyst system consisting of (salen)Cr (III) complex (**33**, Figure **1.12**) and DMAP for the preparation of propylene carbonate from PO and CO_2. PO was quantitatively converted to PC at 75 °C and 0.34 MPa CO_2. When the temperature and pressure were raised to 100 °C and 0.69 MPa respectively the conversion of PO to cyclic product also increased with a TOF of 916 h^{-1}. This catalytic process was found to be highly selective (100 %) for cyclic carbonates than a co-polymer at these reaction conditions [62].



33

Fig. 1.12: *(Salen) Cr(III) complex that was utilized for conversion of PO to PC*

Darensbourg reported for the first time a coupling reaction where salen-like complexes were utilized as catalysts for CO_2/CHO coupling reaction. The bis-(salicylaldiminato)zn(II) complexes were prepared by reacting $Zn[N(SiMe_3)_2]_2$ and two equivalents of a salicyaldimine ligand [74]. Most activity was observed when complex **34** (Figure **1.13**) was used as a catalyst for CO_2/CHO coupling reaction and a copolymer with 99 % carbonate unit, Mn = 41 kg mol^{-1} and TOF = 15 h^{-1} was obtained.



34

Fig. 1.13: *First salen-like complex for CO_2/CHO coupling*

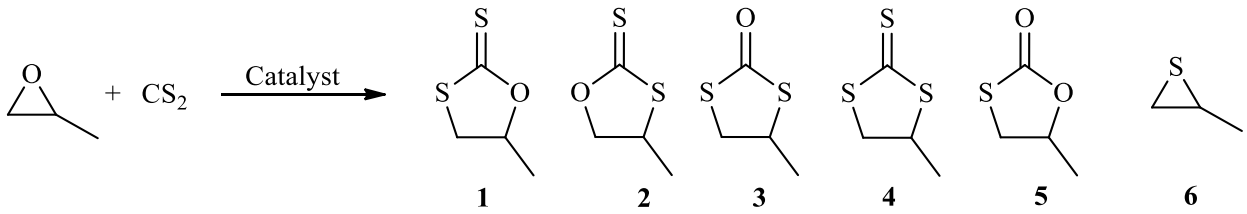
1.3.4. Transition metal complexes investigated for CS_2 coupling with epoxides

Adachi and his coworkers reported a synthetic procedure where carbonyl disulfide (CS_2) was directly coupled with propylene oxide. Diethyl zinc and various electron donors (such as water, alcohol, primary or secondary and tertiary amines) were used as catalyst. Tertiary amines such as tertiary phosphines and hexamehylphosphoric triamide were the effective donors while $ZnEt_2$-water, alcohol, and primary or secondary amine were not effective for the coupling of CS_2 and PO. However, very long reaction times were required. The reaction resulted in very low molecular weight polymers and 1,3-oxathioran-4-methyl-2-thion [75].

Darensbourg utilized (salen)Cr(III) catalyst reported by Jacobsen for CS_2/CHO coupling [76]. The complex was evaluated for activity towards this coupling reaction in the presence of [PPN]Cl as a co-catalyst at different temperatures. It was observed that the reaction proceeded with high selectivity for poly(thiocarbonate) at temperatures equal to or below 50 °C. Scrambling of the oxygen and sulphur atoms was observed at all temperature.

Lu and his coworkers utilized several binary aluminum salen complexes (Figure **1.14**) [77] as catalysts and PPNCl, $PPNN_2$, $^nBu_4NCl$, $^nBu_4NBr$ and $^nBu_4NI$ as co-catalysts for the coupling of PO and CS_2 (Scheme **1.8**). The complexes together with the quaternary ions were soluble in the starting material therefore no organic solvents were used. The coupling reaction depended on the temperature. When complex **36** (Figure **1.14**), was used as catalyst at room temperature no

coupling product was obtained but when the same reaction was performed at 100 ^{o}C gave different cyclic products with 94% yield.



Scheme 1.8: *Coupling of CS_2 and propylene oxide to produce cyclic products.*

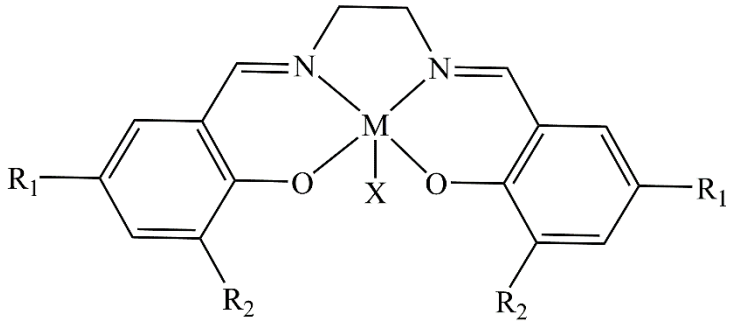
The effect of substituents on the catalytic activity of the complexes was also investigated. The catalysts were found to have different activity towards the coupling of CS_2 and PO. The bulk substituents on the salen ligand seem to have a negative effect on the activity of the complexes. For example, when there was no bulky substituents on the salen ligand, **36** Figure **1.14**, the complex had greater activity than when the ligand had the bulky tert-butyl group on the salen ligand, **38**. The order of activity in the complexes was observed as in the order **40** > **36** > **39** > **37** > **38**.

The axial ligand, X, on the aluminium metal also seem to have some effect on the catalytic activity of the metal complexes. When the axial ligand was a chlorine, **40**, the catalytic activity was found greater than when the axial ligand was used as 'Et', **36**. This could be as a result of the effect the two ligands have on the electronic properties of the central metal. Chlorine is a halogen, and it is electron withdrawing while 'Et' is electron donating. The electron density around the aluminum metal will therefore be different as a result of this difference in electronic properties of the ligands. Electron withdrawing groups on the central metal lower electron density of the metal therefore making it more electrophilic and this increases chances of the epoxide coordinating to the metal for the ring opening process.

The quaternary ammonium salts also showed difference in activity as co-catalysts in the binary catalyst system for the coupling of CS_2 and PO. The experimental results show that the activity of the salts is in the order PPNCl, $PPNN_2$, $^{n}Bu_4NCl$ > $^{n}Bu_4NBr$ >> $^{n}Bu_4NI$. The anion of the quaternary salt also influenced product selectivity. $^{n}Bu_4NBr$ preferred to form cyclic product **1**

(Scheme **1.8**) while $^{n}Bu_4NCl$ preferred the formation of cyclic product **3** (Scheme **1.8**). This could suggest that the mechanism of action in the presence of these two salts could be different. This occurred when complex **30** (Figure **1.14**) was used as a catalyst in both cases.

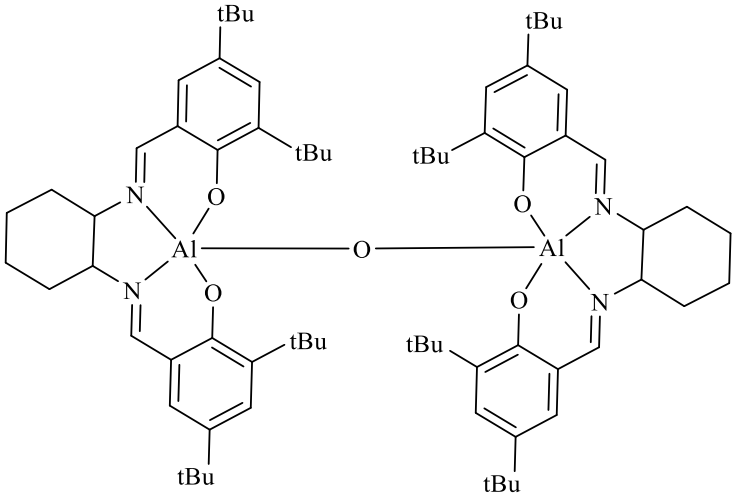
The influence of the metal center was also investigated, and it was observed that metal center of the complex influences the coupling process. When complex **38** bearing Al as a central metal was used as catalyst cyclic products were obtained. On the other hand, when a corresponding cobalt complex **42** was used as a catalyst no coupling products were obtained. It was assumed that the presence of the Sulphur atom in the starting material poisoned the cobalt complex catalyst. Very low catalytic conversions of PO to cyclic products were observed when complex **41** was used as a catalyst.



36) M = Al, X = Et, $R_1 = R_2 = H$;
37) M = Al, X = Et, $R_1 = t_{Bu}$, $R_2 = H$;
38) M = Al, X = Et, $R_1 = R_2 = t_{Bu}$;
39) M = Al, X = Et, R_1 = Br, $R_2 = H$;
40) M = Al, X = Cl, $R_1 = R_2 = H$;
41) M = Cr, X = Cl, $R_1 = R_2 = t_{Bu}$;
42) M = Co, X = Cl, $R_1 = R_2 = t_{Bu}$;

Fig. 1.14: *Complexes reported as catalysts for CS_2 and PO coupling reaction [77].*

North and coworkers reported a catalytic process where they utilized CS_2 and PO for the preparation of cyclic thiocarbonates (Scheme **1.8**). In this process a bimetallic (salen)Al(III) complex **43** (Figure **1.15**) was used as a catalyst in the presence of tetrabutylammonium bromide as a co-catalyst. This system has proven to be a highly active catalyst for the preparation of cyclic thiocabonates both in academia and industrial environments. The reaction resulted in the formation of two cyclic products, and this is a result of the scrambling of the oxygen and sulphur atoms [27, 78]



43

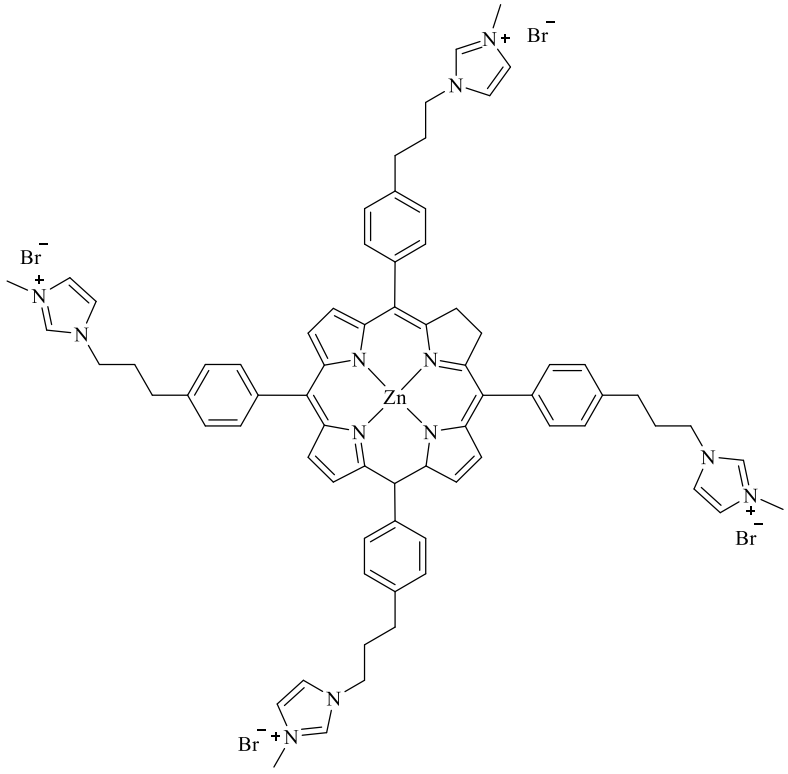
Fig. 1.15: *Bimetallic (salen) Al (III) complex reported for CS_2 and PO coupling*

1.4. Ionic functionalized transition metal catalysts for epoxides coupling with CO_2/CS_2

Ionic liquids have also been incorporated into metal complexes for various reasons which include: 1) to enhance the catalytic performance of the metal complexes. Lu and Wang incorporated a quaternary ammonium salt into the salen ligand framework of a Co(III) complex. When this complex was evaluated as a catalyst for the coupling of CO_2 and CHO catalytic, activity of the complex was increased to 170 h^- TOF compared to 87 h^- TOF that was obtained when a Co(III) salen complex without the quaternary ammonium salt was used [79]. The inclusion of ionic functionalities into the metal complex backbone introduces the nucleophilic group that would be provided by the co-catalyst. This nucleophilic group is needed for ring opening of the epoxide as shown in the coupling reaction mechanism. 2) To improve catalyst separation from the reaction products. Ionic functionalities on the metal complexes increase their solubility into the ionic liquids therefore the leaching of the catalysts into the product/organic phase is unfavorable when they are used in the biphasic systems.

1.4.1. Ionic functionalized complexes based on porphyrin ligands

Chen and his coworkers used a bifunctional ionic liquid functionalized zinc porphyrin (IL-ZnTPP) complex (**44,** Figure **1.16**) as an active catalyst for the coupling of CO_2 with epoxides [80]. The complex was prepared by grafting quaternary imidazolium-based IL moieties onto the para position of each phenyl ring in the zinc porphyrin framework through a highly stable covalent linkage. This complex catalyzed CO_2 and epoxide coupling reaction to yield a cyclic product (propylene carbonate). The catalyst possessed an excellent catalytic performance due to the cooperative effect between the Lewis acidic metal center (Zn) and the flexible nucleophile (Br^-) in one molecule at low catalyst loading under solvent and additive-free conditions.



44

Fig. 1.16: *Bifunctional ionic liquid grafted Zn porphyrin complex reported by Chen and coworkers* [80]

Ionic liquid-based catalysts possess special solubility. Considering this and the concept of "one-phase catalysis and the biphasic catalyst separation", catalyst **44** (Figure **1.16**) can be conveniently reused more than ten times while still maintaining good catalytic activity and selectivity. From this it was concluded that this catalyst is very stable. Therefore, this new bifunctional catalyst reported

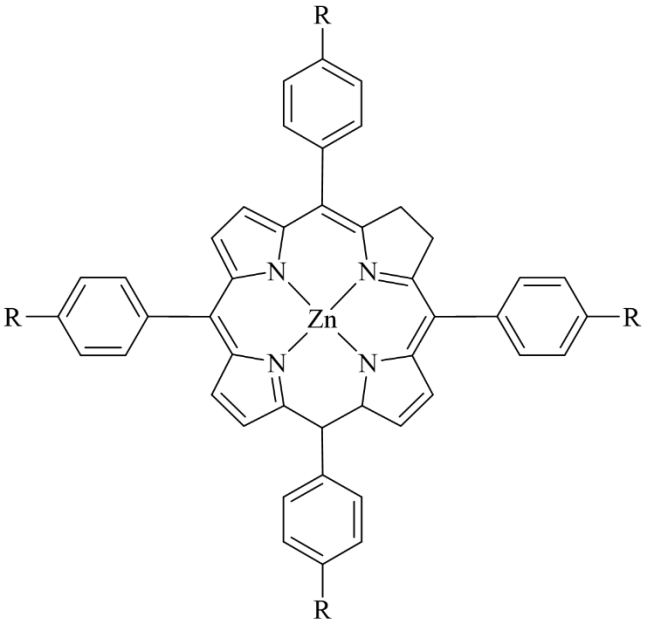
by Chen and his coworkers provide a candidate for the catalytic coupling of CO_2 and epoxides under mild conditions, simultaneously resolving the inevitable problem of the difficulty in recycling the homogeneous catalyst.

Jiang and his coworkers also reported a series of ionic liquid functionalized Zinc porphyrin complexes as catalysts for the coupling of CO_2 and epoxides to form cyclic products [81]. Catalytic activity of these complexes was reported to depend on reaction temperature just like it was observed with neutral complexes. When complex **47** (Figure **1.17**) was evaluated at 40 and 120 ^oC yields of 5.7 and 99.99% were observed, respectively. It was further observed that the reaction time could be reduced while increasing the reaction temperature from 120 to 140 ^oC.

Counter ions were also reported to have a significant effect on the catalytic activity of the complexes. The study on the effect of the halogen ions (X^-) on the catalytic activity showed that complex **47** (Figure **1.17**) had the best catalytic activity comparatively and the order of activities was observed to be **47** > **48**> **45** > **46** (Br^-, I^-, F^-, Cl^-) (Figure **1.17**). Nucleophilicity and leaving group ability were reported to have a drastic impact on the catalytic activity of the catalysts.

Steric hinderance which results from the position of the ionic liquid functionality of the complexes also was reported to have a significant effect on the catalytic activity of the complexes. Three complexes **47, 49** and **50** (Figure **1.17**) were investigated and it was observed that catalyst **49** (Figure **1.17**) which bares the ionic liquid functionality on the meta position showed the highest activity (99.9 % yield). It was followed by the complex bearing the ionic liquid functionality at the ortho position (**50**, Figure **1.17**, 90.5 % yield) while the one bearing this functionality at the para position showed relatively lower activity (**47**, Figure **1.17**, 79.4 % yield). These results were obtained when these catalysts were evaluated within 5 hours, however when the time was increased to 6 h the catalytic activity of the complexes was the same with 99.9 % yield.

To clarify the advantage of ionic liquid functionalized catalysts, DPP-Zn (**51**, Figure **1.17**) which is a neutral corresponding complex was synthesized and applied in the coupling reaction of CO_2 and epoxide at the same reaction conditions. When DPP-Zn was applied alone as a catalyst yield of 0.1 % was obtained which is fairly very low comparing the yields that were obtained with ionic liquid functionalized catalysts. A binary catalyst system of DPP-Zn/TBAB was also evaluated and the ionic liquid functionalized catalysts still out-performed it. This phenomenon is attributed to the proximity effect generated by the increased local concentration of ammonium species.



45) R = *p*-$O(CH_2)_4N^+Bu_3F^-$
46) R = *p*-$O(CH_2)_4N^+Bu_3Cl^-$
47) R = *p*-$O(CH_2)_4N^+Bu_3Br^-$
48) R = *p*-$O(CH_2)_4N^+Bu_3I^-$
49) R = *m*-$O(CH_2)_4N^+Bu_3Br^-$
50) R = *o*-$O(CH_2)_4N^+Bu_3Br^-$
51) R = none (DPP-Zn)

Fig. 1.17: *Ionic liquid functionalized zinc porphyrin complexes* [81].

Bifunctional Aluminum porphyrin complexes were reported by Wu and his coworkers as catalysts for the coupling of CO_2 and PO to produce polycarbonate [82]. Complex **53** (Figure **1.18**) was employed as catalyst and the influence of reaction conditions such as CO_2 pressure, reaction temperature etc., on the coupling reaction were investigated. It was observed that when CO_2 pressure was increased from 2.0 to 3.0 MPa there was an increase in the TOF from 286 to 305 h^{-1}, however further increase in pressure to 4.0 MPa resulted in a decrease in the TOF to 292 h^{-1}. This is attributed to the dilution effect of the reaction mixture by the high CO_2 pressure hence reduction in activity of the catalyst.

The effect of reaction temperature was also studied utilizing complex **53** (Figure **1.18**) as a catalyst and CO_2 pressure was maintained at 3.0 MPa and [PO]/[CO_2] ratio at 5000. It was observed that at 25 ^oC a copolymer was obtained with TOF 20 h^{-1} and 5 % cyclic carbonate. TOF of the copolymer increased to 305 h^{-1} at 70 ^oC whereas the polymer selectivity reduced to 88 %. Further increase in TOF to 985 h^{-1} was observed at 90 ^oC and even at this temperature a decrease in polymer selectivity was obtained. This phenomenon is anticipated to be due to the acceleration of back-biting reaction leading to the degradation of the copolymer. To produce a copolymer Wu and his

coworkers performed all copolymerization studies at optimum conditions obtained which are 3.0 MPa CO_2 pressure and 70 ^oC reaction temperature.

The effect of the axial ligand and quaternary ammonium anion were studied for complexes **52**, **53**, **54**, and **55** (Figure **1.18**). When these complexes were utilized as catalysts a decrease in catalytic activity was observed in the order **52** > **53** > **54** was observed but an increase in copolymer selectivity was observed. This is consistent with what was reported in literature by Lee and his coworkers that where anion in a quaternary ammonium salt has poorer leaving ability a higher copolymer selectivity is expected. In the case of complex **55** large TOF of 330 h^{-1} was obtained however the generated copolymer had only 75 % carbonate linkage. This suggested that PO and CO_2 insertion in to the growing alkoxide may have been too competitive in this case. It was then concluded that coupling of CO_2 and PO is highly affected by the quaternary ammonium anion and the axial ligand of the bifunctional aluminum porphyrin complex.

The activity of homogeneous catalysts was reported on literature to be dependent on the coordination environment around the central metal [83]. This concept was also studied for bifunctional Al porphyrin complexes **52**, **53**, **56**, **57**, **58**, and **59** (Figure **1.18**). Complexes (**56**, **57**) bearing fluorine-functionalized aryl substituent displayed increased copolymerization rate (TOF 466 and 392 h^{-1} respectively) in comparison to the unsubstituted catalysts **52**, **53** (Figure **1.18**) which only showed TOF of 422 and 306 h^{-1} respectively. Therefore, introducing an electron withdrawing group in the complex backbone was beneficial to improve the catalytic activity of unsubstituted complexes. Complexes **58** and **59** (Figure **1.18**) bearing a tertiary butyl-functionalized aryl substituent on the backbone also showed improved catalytic activity with relatively high polymer selectivity especially for complex **56** (Figure**1.18**) with TOF of 449 h^{-1} and polycarbonate selectivity of 92 % were obtained. Therefore, when an electron donating group is incorporated in the backbone of the complex a relatively high activity than when an electro withdrawing group was incorporated in the complex backbone was obtained.

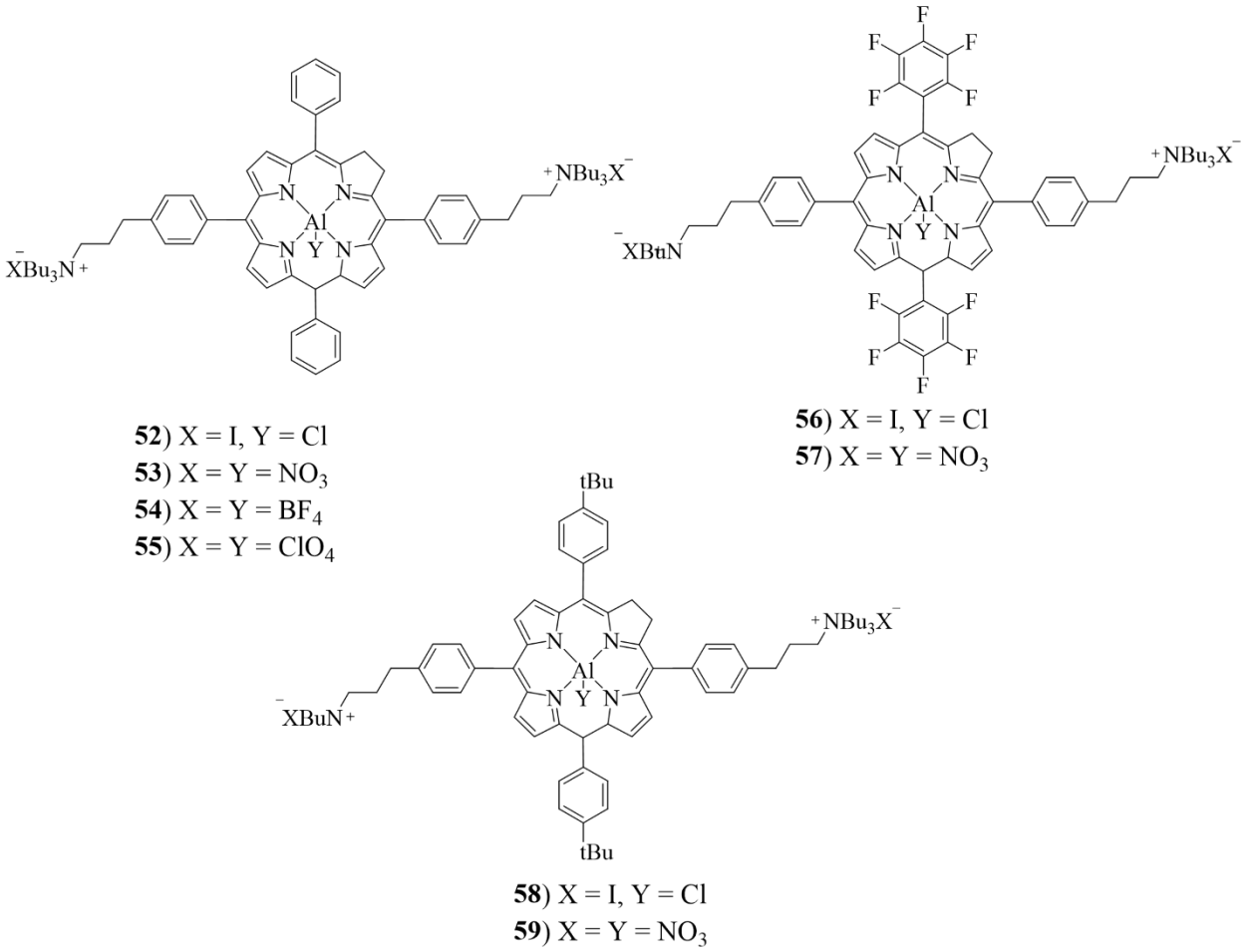
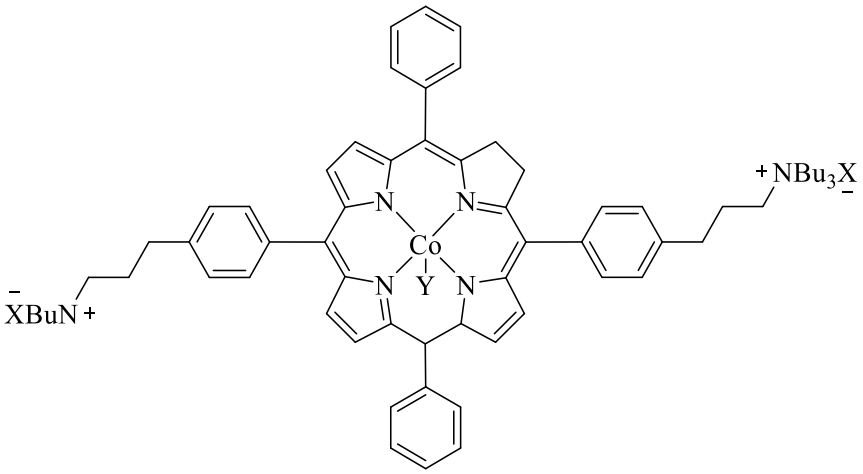


Fig. 1.18: *Bifunctional alumminium porphyrin complexes reported by Wu and his coworkers* [82]

Wu and his coworkers also reported an ionic liquid grafted cobalt porphyrin system (**60**, Figure 1.19) for CO_2 and propylene oxide coupling reaction [84]. When this complex was applied as catalyst for this process in neat PO it was observed that its catalytic activity depended on factors like CO_2 pressure and reaction temperature just like with the bifunctional Al porphyrin complex. When the coupling reaction was performed at 25 ^oC and 1 atm CO_2 pressure a copolymer was obtained with 25 % yield over 24 hours with 75 % cyclic carbonate. When the CO_2 pressure was increased to 40 atm a significant increase in catalytic activity was observed with TOF of 120 h^{-1} and cyclic carbonate yield degreased to 5 %. When the temperature was increased to 50 ^oC and CO_2 pressure kept at 40 atm an increase in catalytic activity was observed producing a copolymer with TOF of 495 h^{-1}.



X = NO_3, Y = Cl

60

Fig. 1.19: *An ionic liquid grafted cobalt porphyrin system reported by Wu and his coworkers* [84]

1.4.2. Ionic functionalized complexes derived from salen ligands

A functionalized ionic liquid Co(III) salen complex (**62**, Figure 1.20) was reported by Lu and his coworkers for the coupling of CO_2 and cyclohexene oxide (CHO) [85]. This complex was utilized as a catalyst in the absence of a solvent because it was together with the co-catalysts found soluble in CHO. Initial studies showed that complex **62** (Figure 1.20) could efficiently catalyze CHO/CO_2 coupling reaction to afford selectively a copolymer with 99 % carbonate linkage at [CHO]/[catalyst] molar ratio of 200 under a CO_2 pressure of 1.5 MPa and at ambient temperature. It was observed that the catalyst activity of complex **62** (Figure 1.20) was about double that of the neutral corresponding Co(III) salen complex (**61**, Figure 1.20) with activities of 170 and 87 h^{-1} TOF respectively.

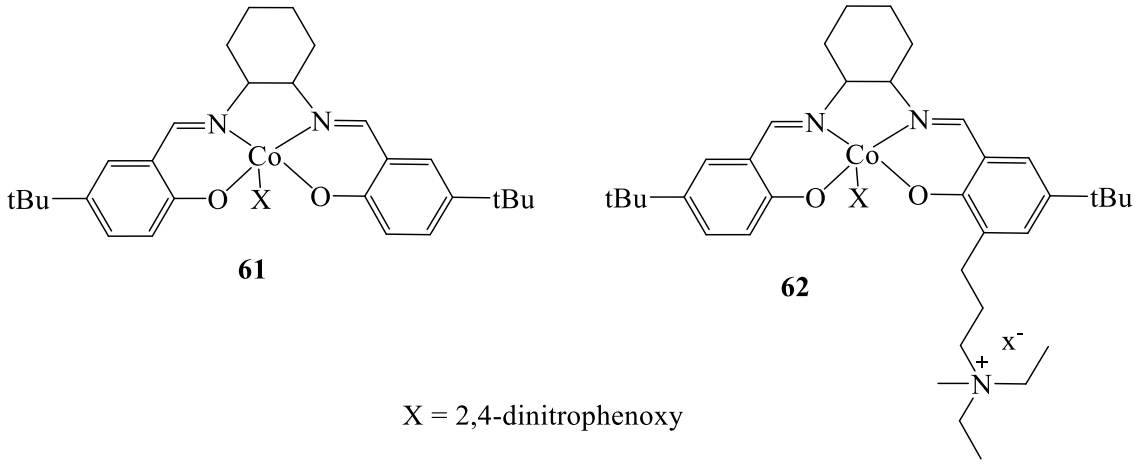


Fig. 1.20: *Neutral (**61**) and ionic liquid functionalized Co(III) salen (**62**) complexes* [85].

A highly active and recyclable bifunctional cobalt salen complex, **64** Figure **1.21**, was reported as a catalyst for CO_2 and propylene oxide coupling reaction by Lee and his coworkers [86]. This catalyst was screened under the following conditions: 80 ^{o}C, 2.0 – 1.7 MPa CO_2 pressure and [PO]/[catalyst] = 25 000. The coupling reaction was terminated before 25 % conversion was obtained because after this time the reaction mixture became highly viscous thus making stirring and diffusion very difficult. When the tetra butyl group in this complex was replaced with a methyl group, **65** Figure **1.21**, this behavior was not observed and an increase in TOF was observed.

A significant increase in the catalytic activity was obtained when more ammonium salt units were attached (**67**, Figure **1.21**). With this complex 25 % conversion was obtained in 15 min and this catalyst showed more selectivity for a copolymer formation over a cyclic product (>99 %). When a neutral system was used only a cyclic carbonate was obtained. Easy separation of the catalysts from the reaction products was achieved with ease for all complexes except for the neutral complex (**63**, Figure **1.21**).

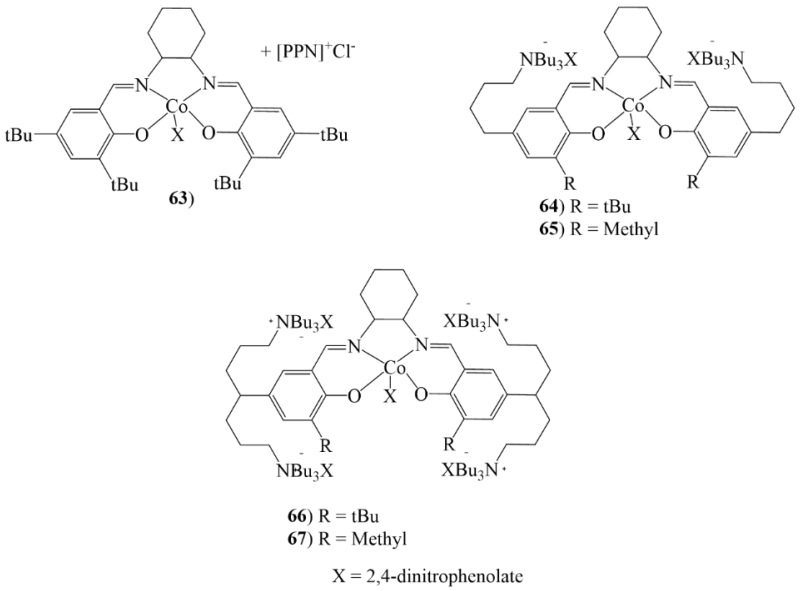


Fig. 1.21: *A highly active and recyclable bifunctional cobalt salen complex reported as a catalyst for CO_2 and propylene oxide coupling reaction by Lee and his coworkers [86]*

1.5. Problem statement

The increasing concentrations of carbon dioxide continues to be an issue of concern due to its long-term impact on the environment. In recent years research focus by industry and academia has been directed towards the use of CO_2 as feedstock. Its use as a feedstock brings major advantages to the synthetic processes because it is renewable, abundant, and nontoxic. The coupling of CO_2 and epoxides provides a means of utilizing carbon dioxide as feedstock in the production of biodegradable products such as cyclic carbonates and/or polycarbonates.

The use of CO_2 as C-1 feedstock is however limited by the fact that it is highly thermodynamically stable. To use CO_2 in synthetic processes to produce biodegradable materials, suitable catalyst technology and process methodology must be developed. CS_2, which is a more reactive carbon dioxide analogue, has been used to develop catalysts and catalytic processes that can be used later in the transformation of CO_2 to useful products.

Metals, such as Cr and Co, complexes based on a salen ligands framework, which are tetradentate Schiff base ligands, have been reported as active catalysts for CS_2/CO_2 and epoxide coupling reactions. These ligands are easy to prepare compared to usually used ligands such as porphyrins. Salicylaldimine ligands, which are bidentate Schiff base ligands, are even more easily prepared.

Therefore, they can be easily tailored to tune both their electronic and steric properties. Metal complexes based on salicylaldimine ligands have not been extensively applied in these coupling reactions. Their ease in preparation also makes it simple to incorporate ionic functionalities in the ligand backbone.

The catalytic coupling of CS_2/CO_2 and epoxides is homogeneous in nature. Homogeneous catalysis is limited by difficulty to recycle and reuse the catalysts after the reaction and difficulty to remove the metal catalyst from the reaction product [87, 88]. These limitations have a very negative impact from both economic and environmental point of view. This has brought most of the synthetic researchers all around the world to one thinking, that is, how to deal with these problems associated with homogeneous catalysis. The use of ionic liquids has attracted attention in developing economic catalytic synthetic processes.

Metal complexes can activate CO_2/ CS_2 and epoxides coupling reactions, by simply lowering their activation energy, to produce either copolymers or cyclic products. The properties of these metal complexes such as oxidation state, nature of the metal (Cr and Co e.t.c.) and ligand architecture (electron withdrawing and donating groups and steric bulkiness) do influence the catalytic reaction. Therefore, the aims of this study were: (i) synthesize a range of salicylaldimine ligands bearing different substituents (ii) prepare bis-(salicylaldiminato) Co(II), Cr(II) and Cr(III) complexes from the synthesized ligands and characterize these complexes with analytical techniques. (iii) evaluate the catalytic activity of the complexes in the coupling reactions of CO_2 and CS_2 with propylene oxide. In pursuit of these aims, bis-(salicylaldiminato) Co(II), Cr(II) and Cr(III) complexes were to be synthesized. The successfully prepared complexes were to be evaluated for the coupling reactions of CS_2 and CO_2 with propylene oxide and the reaction products were to be analyzed with ^{1}HNMR spectroscopy and mass spectrometry.

1.6. References

[1] G. A. Olah, *Angew. Chem., Int. Ed.,* vol. 52, pp. 104 - 107, 2013.

[2] N. von der Assen, P. Voll, M. Peters and A. Bardow, *Chem. Soc. Rev.,* vol. 43, pp. 7982 - 7994, 2014.

[3] J. Langanke, A. Wof, J. Hofmann, K. Bohm, M. A. Subhani, T. E. Muller and W. G. C. Leitner, *Green Chem.,* vol. 16, pp. 1865 - 1870, 2014.

[4] J. A. Ibers, *Chem. Soc. Rev.,* vol. 11, p. 57, 1982.

[5] A. Alvarez, M. Borges, J. J. Corral-Perez, G. J. Olcina, L. Hu, D. Cornu, R. Huang, D. Stoian and A. Urakawa, *ChemPhysChem,* vol. 18, p. 3135 3141, 2017.

[6] M. Luo, H. X. Zhang and J. D. Darensbourg, *Macromolecules,* vol. 48, pp. 5526 - 5532, 2015.

[7] S. Inoue and H. Koinuma, *J.Poly.Sci.BPolym.Lett,* vol. 7, pp. 287-292, 1969.

[8] M. R. Kember, A. Buchard and C. K. Williams, *Chem. Commu.,* vol. 47, pp. 141-163, 2011.

[9] M. R. Kember, A. Buchard and C. K. Williams, *Chem.Commu,* vol. 47, pp. 141-163, 2011.

[10] S. Paul, Y. Zhu, C. Romain, P. Sain, R. Brooks and C. Williams, *Chem.Commun,* vol. 51, pp. 6459-6479, 2005.

[11] G. Trott, K. P. Saini and C. Williams, *Phil. Trans. R. Soc,* pp. 1 - 19, 2015.

[12] W. Kuran and T. Listos, *Macromol. Chem. Phys.,* vol. 195, pp. 977-984, 1994.

[13] H. Li and Y. Niu, *Polym. J.,* vol. 43, pp. 121 - 125, 2011.

[14] S. Inoue, *J. Polym. Sci. Part A: Polym. Chem,* vol. 38, pp. 2861-2871, 2000.

[15] A. Cyriac, J. V. S. Lee, E. Park, J. Park and B. Lee, *Macromolecules,* vol. 43, pp. 7398 - 7401, 2010.

[16] P. Gorecki and W. Kuran, *J. Polym. Sci: Pol. Letters Edition,* vol. 23, pp. 299-304, 1985.

[17] D. Adhikari, T. S. Nguyen and H. M. Baik, *Chem. Commun,* vol. 50, p. 2676, 2014.

[18] J. D. Darensbourg, W. M. Holtcamp, E. G. Struck, S. M. Zimmer, A. S. Niezgoda, P. Rainey, B. J. Robertson, D. J. Draper and H. J. Reibenspies, *J. Am. Chem. Soc,* vol. 121, pp. 107 - 116, 1999.

[19] D. Darensbourg and M. Holtcamp, *Coordination Chemistry Reviews,* vol. 153, pp. 155-174, 1996.

[20] J. D. Darensbourg and D. A. Yeung, *Polym. Chem.,* vol. 6, p. 1103, 2015.

[21] H.-X. Zhang, F. Liu, K.-X. Sun, S. Chen, Y.-B. Du, R.-G. Qi and M. K. Wan, *Macromolecules* , vol. 41, pp. 1587 - 1590, 2008.

[22] K. Nakano, G. Tatsumi and K. Nozaki, *J. AM. Chem. Soc.* , vol. 129, pp. 15116 - 15117, 2007.

[23] B. Ochiai, K. Yoshii, D. Nagai and T. Endo, *Macromolecules,* vol. 37, pp. 2329 - 2331, 2004.

[24] E. Marianucci, C. Berti, F. Pilati and P. Manaresi, *Polym. J.,* vol. 35, pp. 1564 - 1566, 1994.

[25] J. Diebler, H. Komber, L. HauBler, A. Lederer and T. Werner, *Macromolecules,* vol. 49, pp. 4723 - 4731, 2016.

[26] D. J. Darensbourg, S. J. Wilson and A. D. Yeung, *Macromolecules,* vol. 46, pp. 8102 - 8110, 2013.

[27] W. Clegg, W. R. Harrington, M. North and P. Villuendas, *J. Org. Chem.,* vol. 75, pp. 6201 - 6207, 2010.

[28] S. Motokucho, D. Takeuchi, F. Sanda and T. Endo, *Tetrahedron,* vol. 57, p. 7149 7152, 2001.

[29] T. Aida and S. Inoue, *Macromolecules,* vol. 14, pp. 1166 - 1169, 1981.

[30] B. X. Lu, R. He and X. C. Bai, *J. Mol. Catal. A,* vol. 186, pp. 1 - 11, 2002.

[31] J. D. Darensbourg, C. J. Yarbrough, C. Ortiz and C. C. Fang, *J. Am. Chem. Soc.,* vol. 125, pp. 7586 - 7591, 2003.

[32] W. G. Coates and R. D. Moore, *Angew. Chem. Int. Ed.,* vol. 43, pp. 6618 - 6639, 2004.

[33] J. D. Darensbourg and R. M. Mackiewicz, *J. Am. Chem. Soc.,* vol. 127, pp. 14026 - 14038, 2005.

[34] J. D. Darensbourg, R. M. Mackiewicz, J. L. Rodgers and A. L. Phelps, *Inorg. Chem.,* vol. 43, pp. 1831 - 1833, 2004.

[35] J. D. Darensbourg, M. R. Mackiewicz, L. J. Rodgers and L. A. Phelps, *Inorg. Chem.,* vol. 43, pp. 1831 - 1833, 2004.

[36] C. Koning, J. Wildeson, R. Parton, B. Plum, P. Steeman and D. Darensbourg, *Polymer,* vol. 42, pp. 3995 - 4004, 2001.

[37] W. M. Lehenmeier, C. Bruckmeier, S. Klaus, E. J. Dengler, P. Deglmann, A.-K. Ott and B. Rieger, *Chem. Eur. J.,* vol. 17, pp. 8858 - 8869, 2011.

[38] H. J. Clements, *Ind. Eng. Chem. Res.,* vol. 42, pp. 663 - 674, 2003.

[39] M. Yoshida and M. Ihara, *Chem. Eur. J.,* vol. 10, pp. 2886 - 2893, 2004.

[40] I. A. Adeleye, D. Patel, D. Niyogi and B. Saha, *Ind. Eng. Chem. Res.,* vol. 53, pp. 18647 - 18657, 2014.

[41] W. Choi, F. Sanda and T. Endo, *Macromolecules,* vol. 31, pp. 2454 - 2460, 1998.

[42] W. Choi, F. Sanda and T. Endo, *Heterocycles,* vol. 52, pp. 125 - 128, 2000.

[43] A. Hasan, A. Memic, N. Annabi, M. Hossain, A. Paul, R. Dokmeci, F. Dehghani and A. Khademhosseini, *Acta Biometerialia,* vol. 10, pp. 11-25, 2004.

[44] A. Welle, M. Kroger, M. Doring, K. Niederer, E. Pindel and S. I. Chronakis, *Biomaterials,* vol. 28, pp. 2211-2219, 2007.

[45] J. Feng, R. Zhuo and X. Zhang, *Progress in Polymer Science,* vol. 37, pp. 211-236, 2012.

[46] B.-X. Lu and J. D. Darensbourg, *Chem. Soc. Rev.,* vol. 41, pp. 1462 - 1484, 2012.

[47] S. Inoue, H. Koinuma and T. Tsruta, *J. Poly. Sci. B Polym. Lett,* vol. 7, pp. 287-292, 1966.

[48] J. Darensbourg and W. Holtcamp, *Macromolecules,* vol. 28, pp. 7577-7579, 1995.

[49] D. J. Darensbourg, M. S. Zimmer, P. Rainey and D. L. Larkins, *Inorg. Chem.,* vol. 39, pp. 1578 - 1585, 2000.

[50] O. Hampel, C. Rode, D. Walther, R. Beckert, H. Gorls and Z. Naturforsch, *B: Chem. Sci.,* vol. 57, pp. 946 - 956, 2002.

[51] M. Cheng, B. Lobkovsky and W. Coates, *J. Am. Chem. Soc,* vol. 120, pp. 11018-11019, 1998.

[52] M. Cheng, D. Moore, J. Reczek, B. Chamberlain, E. Lobkovsky and G. Coates, *J. Am. Chem. Soc.,* vol. 123, pp. 8738-8749, 2001.

[53] D. Moore, M. Cheng, E. Lobkovsky and G. Coates, *Angew. Chem. Int. Ed.,* vol. 41, no. 14, pp. 2599-2602, 2002.

[54] R. D. Moore, M. Cheng, B. E. Lobkovsky and W. G. Coates, *J. AM. CHEM. SOC,* vol. 125, pp. 1191-11924, 2003.

[55] S. Allen, D. Moore, E. Lobkovsky and G. Coates, *J. AM. Chem. Soc.*, pp. 14284-14285, 2002.

[56] M. Kroger, C. Folli, O. Walter and M. Doring, *Advanced Synthesis and Catalysis,* vol. 347, pp. 1325 - 1328, 2005.

[57] N. M. Rajendran, A. Haleel and N. D. Reddy, *Organometallics,* vol. 33, pp. 217 - 224, 2014.

[58] H. Sugimoto, H. Ohshima and S. Inoue, *J. Pol. Sci: Part A: Pol. Chem,* vol. 41, pp. 3549-3555, 2003.

[59] J. W. Kruper and V. D. Dellar, *J. Org. Chem.,* vol. 60, pp. 725 - 727, 1995.

[60] S. Mang, I. A. Cooper, E. M. Colclough, N. Chauhan and B. A. Holmes, *Macromol.*, vol. 33, pp. 303 - 308, 2000.

[61] G. Cozzi, *Chem. Soc. Rev,* vol. 33, pp. 410-421, 2004.

[62] L. Paddock and T. Nguyen, *J. Am. Chem. Soc,* vol. 123, pp. 11498-11499, 2001.

[63] R. Luo, X. Zhou, S. Chen, Y. Li, L. Zhou and H. J, *Green Chem.,* vol. 16, pp. 1496-1506, 2014.

[64] Q.-H. Xia, H.-Q. Ge, C.-P. Ye, Z.-M. Liu and K.-X. Su, *Chem. Rev,* vol. 105, pp. 1603-1662, 2005.

[65] A. Yaul, C. PETHE and A. ASWAR, *Rev. Roum. Chim.,* vol. 59, no. 1, pp. 15-26, 2014.

[66] N. E. Jacobsen and P. T. Yoon, *Science,* vol. 299, pp. 1691-1693, 2003.

[67] B. Liu, Y. Gao, X. Zhao, W. Yan and X. Wang, *Journal of Polymeer Science: Part A: Polymer Chemistry,* vol. 48, pp. 359-365, 2010.

[68] N. Jacobsen, *Acc. Chem. Res,* vol. 33, pp. 421-431, 2000.

[69] B. Hansen, L. Leighton and N. Jacobsen, *J. Am. Chem. Soc,* vol. 118, pp. 10924-10925, 1996.

[70] J. D. Darensbourg and C. J. Yarbrough, *J. Am. Chem. Soc,* vol. 124, pp. 6335 - 6342, 2002.

[71] R. Eberhardt, M. Allmendinger and B. Rieger, *Macromol. Rapid Commun.,* vol. 24, pp. 194 - 196, 2003.

[72] R. Moore and W. Coates, *Angew. Chem. Int. Ed,* vol. 43, pp. 6618-6639, 2004.

[73] Z. Qin, M. Thomas, S. Lee and W. Coates, *Angew. Chem. Int. Ed,* vol. 42, pp. 5484-5487, 2003.

[74] J. D. Darensbourg, P. Rainey and J. Yarbrough, *Inorg. Chem.,* vol. 40, pp. 986 - 993, 2001.

[75] N. Adachi, Y. Kida and K. Shikata, *J. Polym. Sci.,* vol. 15, pp. 937 - 944, 1977.

[76] D. J. Darensbourg, J. R. Andreatta, M. J. Jungman and J. H. Reibenspies, *Dalton Trans.,* pp. 8891 - 8899, 2009.

[77] M.-Y. Wang, B. Li, H. Wang, C.-Z. Zhang and B.-X. Lu, *Appl. Organometal. Chem.,* vol. 26, p. 614 618, 2012.

[78] M. North and P. Villuendas, *Advanced online publication,* vol. 4, pp. 623 - 627, 2010.

[79] W.-M. Ren, Z. X., Y. Liu, J.-F. Li, H. Wang and X.-B. Lu, *Macromolecules,* vol. 43, pp. 1396 - 1402, 2010.

[80] Y. Chen, R. Luo, Z. Yang, X. Zhou and H. Ji, *Sustainable Energy Fuels,* vol. 2, pp. 125 - 132, 2018.

[81] X. Jiang, F. Gou, X. Fu and H. Jing, *J. Carbon dioxide utilizing,* vol. 16, pp. 264 - 271, 2016.

[82] W. Wu, X. Sheng, Y. Qin, L. Qiao, Y. Miao, X. Wang and F. Wang, *J. Polym. Sci. A,* vol. 52, pp. 2346 - 2355, 2014.

[83] C. Chatterjee and H. M. Chisholm, *Inorg. Chem.,* vol. 50, pp. 4481 - 4492, 2011.

[84] W. Wu, Y. Qin, X. Wang and F. Wang, *J. Polym. Sci. A,* vol. 51, pp. 493 - 498, 2013.

[85] M. W. Ren, X. Zhang, Y. Liu, F. J. Li, H. Wang and B. X. Lu, *Macromolecules,* vol. 43, pp. 1396 - 1402, 2010.

[86] S. Sujith, K. J. Min, E. J. Seong, J. S. Na and Y. B. Lee, *Angew. Chem. Int. Ed,* vol. 47, pp. 7306 - 7309, 2008.

[87] H. Clavier, N. Audic, C. Guillemni and M. Mauduit, *J. Organomet. Chem.,* vol. 690, pp. 3585-3599, 2005.

[88] P. Cserjesi, K. Belafi-Bako, N. Nemestothy and L. Gubiza, *Hung. j. ind. chem. (Online),* vol. 36, pp. 27-34, 2008.

Chapter 2

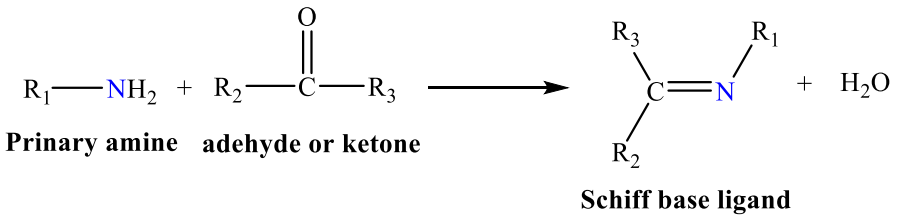
Synthesis and characterization of neutral and ionic liquid functionalized bidentate salicylaldimine ligands

Contents

2.1. Introduction 42
2.2. Results and discussion 44
2.2.1. Synthesis and characterization of neutral salicylaldimine ligands 44
2.2.2 Synthesis and characterization of ionic functionalized Schiff base ligands 62
2.3 Conclusion 80
2.4 Experimental 81
2.4.1 Material and instrumentation 81
2.4.2 Preparation of salicylaldimine ligands **HL_1** – **HL_5** 81
2.4.3 Preparation of salicylaldimine ligands **HL_6** 81
2.4.4 Preparation of the salicylaldimine ligand **HL_7** 82
2.4.5 Preparation of the salicylaldimine ligand **HL_8** 82
2.4.6 Preparation of salicylaldimine ligand **HL_{10}** 82
2.4.7 Preparation of salicylaldimine ligand **HL_{11}** 82
2.4.8 Preparation of salicylaldimine ligand **HL_{12}** 83
2.5 References 83

2.1. Introduction

Schiff ligands have attracted increasing attention in research due their ease of preparation and ability to stabilize metals in various oxidation states. These compounds are prepared through a simple condensation reaction between a carbonyl compound (aldehyde or ketones) and primary amine (Scheme **2.1**). Typically, this reaction occurs in the presence of an acid or a base as catalyst or upon heating in the presence of suitable polar or non-polar solvent. The ease in preparation enables simple tailoring/tuning of the steric and electronic properties of these ligands [1, 2, 3]. Generally, modifications to change the ligand architecture can be done on three positions and those are 'R_1', 'R_2' and 'R_3' (Scheme **2.1**). Aromatic Schiff base ligands are the most stable while alkyl ligands easily polymerize [4].



Scheme 2.1: *General synthetic route for Schiff base ligands* [5]

Schiff base ligands can be obtained as polydentate and that is determined by the nature of the primary amine. For example, if the primary amine constitutes one heteroatom a bidentate ligand can be prepared and if it contains two heteroatoms a tetradentate ligand can be prepared. Bidentate ligands are referred to as salicylaldimines (Figure **2.1**, (**a)**) while tetradentate ligands are referred to as salens (Figure **2.1**, **b**) [6]. Salicylaldime ligands are more interesting because they offer more room to play around with the substituents both on the phenoxy moiety (R_1 group, Scheme **2.1**) and the substituent on the amino nitrogen (R_2 group, Scheme **2.1**) while for the tetradentate ligands the variation of the substituents on the amino nitrogen is not as simple as for the salicylaldimines. There are different substituents that can be part of the ligand backbone and practically the 'R' group on Figure **2.1**, **a** can be an alkyl or an aryl ring.

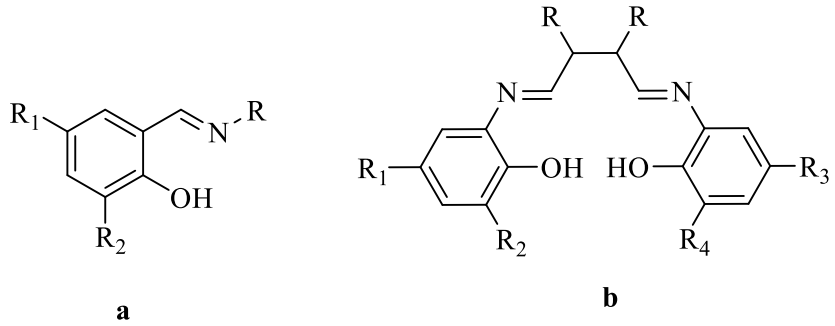
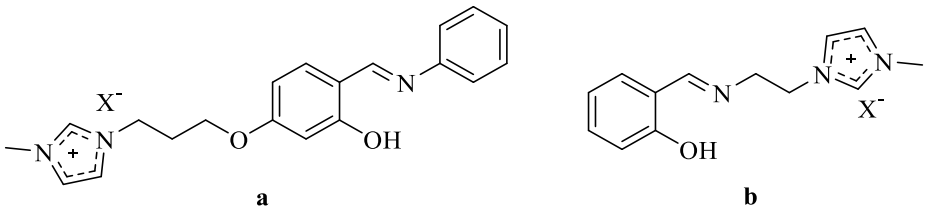


Fig. 2.1: *Salicylaldimine, **a**, and salen, **b**, Schiff base ligands reported by Hugo Schiff* [6].

The ease in preparation of the bidentate Schiff base ligands allows facile incorporation of ionic functionalities onto the ligand backbone. Ionic functionalities can easily be incorporated on the ligand architecture utilizing functional groups such as hydroxyl (-OH) [7, 8] and amino and imidazole moiety [9, 10, 11], which can be transformed into ionic functionalities. Depending on the targeted steric and electronic properties, the ionic functionalities can be incorporated either on the phenolic moiety (Figure **2.2 a**) or on the imino nitrogen substituent group (Figure **2.2 b**) of the salicylaldimine ligands. The counter ions of the ligands are chosen depending on the targeted properties of the ligand. For example, to increase affinity of the ligands for specific ionic liquids bearing PF_6^- as a counter-ions the ligands counter ions can also be chosen as PF_6^- [12].



X = halogen, PF_6^-, BF_4^-

Fig. 2.2: *a) Ionic functionalized imidazolium ligand prepared by Kumar* [8], *b) ionic functionalized imidazolium ligand prepared by Chen* [10, 11]

In this chapter studies performed toward the development of a suitable synthetic protocol that allows for facile preparation of ionic tagged salicylaldimine ligands is reported. The approach

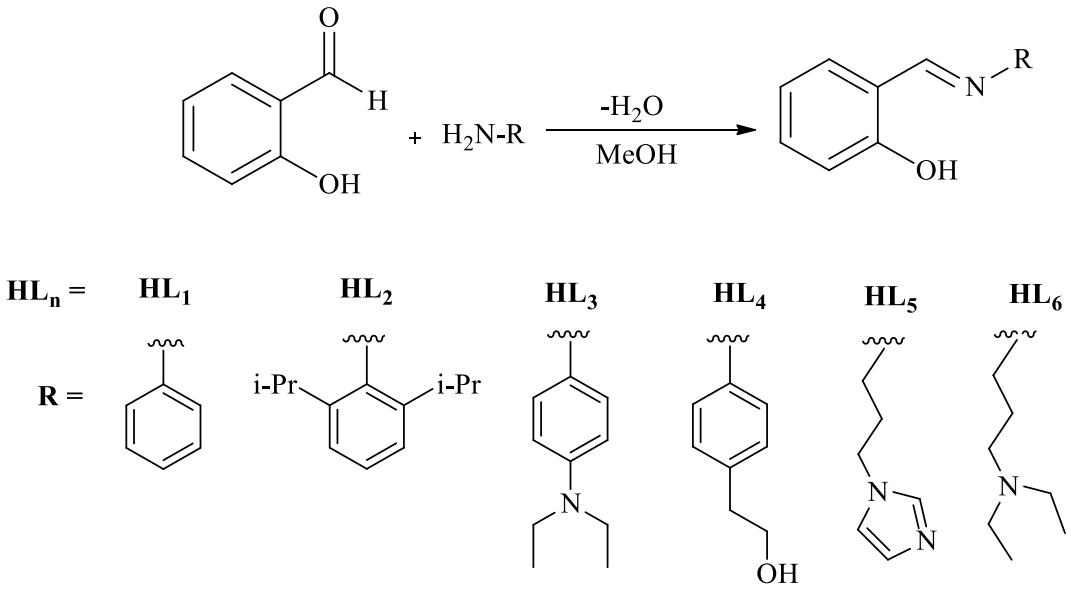
investigated involves the synthesis of neutral ligands that contain a suitable functional group on the ligand backbone that can easily be transformed into an ionic functionality. Various synthetic methodologies were investigated to transform the different functional groups into ionic functionalities. The successfully prepared ligands were all fully characterized using several analytical techniques.

2.2. Results and discussion

2.2.1. Synthesis and characterization of neutral salicylaldimine ligands

The Schiff base ligands were synthesized via a condensation reaction of salicylaldehyde with an appropriate amine as shown in Scheme **2.2**. The choice of the substituents on the ligands backbones was motivated by both electronic and steric properties. Ligand **HL_2** for example contain sterically demanding iso-propyl groups in the ortho positions of the phenyl ring of the imino nitrogen substituent while ligand **HL_1** does not and is not as sterically hindered as **HL_2**.

In addition, groups that can be transformed into ionic functionalities are also targeted. For instance, the nitrogen atom of the imidazolium ring of **HL_5** can be easily transformed into an ionic functionality by alkylation of the imidazolium group [10, 11]. **HL_3** and **HL_6** were also included in the ligands selection and contain an amine which can be transformed into ionic groups by alkylating the nitrogen of the tertiary amine. Ligand **HL_4** contain an ethylhydroxy group which can be utilized to incorporate an ionic functionality on the ligand backbone as well [7].



Scheme 2.2: *General procedure for the synthesis of salicylaldimine ligands (**HL$_1$ – HL$_6$**)*

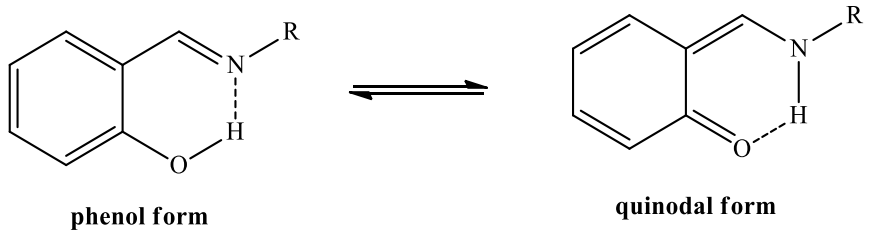
In the synthesis of ligands **HL$_1$** – **HL$_5$** a catalytic amount of formic acid was added, however in the case of ligand **HL$_6$** the addition of formic acid resulted in the reaction not going to completion. It was observed that omitting formic acid from the reaction yielded better results and thus the acid catalyst was not added in order to obtain efficient results. The ligands were obtained in relatively high yields of 69 – 94 % as yellow solids except for **HL$_6$** which was obtained as a yellow oil. These ligands are stable when stored at room temperature even for a prolonged time. Ligands **HL$_2$** and **HL$_3$** were found sparingly soluble in methanol and other alcohols at room temperature with all other ligands easily dissolved in methanol and other alcohols. When ligands **HL$_1$**, **HL$_4$** and **HL$_5$** were concentrated and put in the freezer at around 3 ^{o}C they could recrystallize with time and this was used as a purification method. All ligands were found readily soluble in solvents such as dichloromethane, acetone, and acetonitrile. They were found not soluble in all nonpolar solvents like hexane and diethyl ether except ligand **HL$_6$** which dissolved in these solvents.

2.2.1.1. Characterization of salicylaldimine ligands with ^{1}HNMR and COSY NMR

All ligands were fully characterized with ^{1}HNMR and COSY NMR spectroscopy. The assignments of the proton resonances for the ligands are summarized in Table **2.1**. ^{1}HNMR spectrum that was obtained for the ligand **HL$_1$** (Figure **2.3**) is shown as an example of the spectra that were obtained

for the ligands. The resonance of the azomethine proton -CH=N- is characteristic of these ligands and indicates successful condensation of the amine and aldehyde. This proton signal is observed at 8.46 ppm for **HL_1** and the OH proton signal for the phenoxy group is observed at 13.17 ppm. In the COSY NMR spectrum (Figure **2.4**) the imino proton (-CH=N-) and the phenoxy (-OH) protons do not have any protons to couple to three bonds away therefore the COSY NMR spectrum does not show any correlations for the specific peaks assigned to these two protons.

Hydrogen bonding and valence tautomerization are characteristic in Schiff base ligands as shown in Scheme **2.3**. Valence tautomerization is the intramolecular electron transfer process. These two features can affect the peak shape and position of the proton resonance of the OH functionality in the NMR spectrum. For instance, a free hydroxyl proton is usually observed at 6.10 – 9.53 ppm however for **HL_1** this peak is observed at 13.17 ppm. This downfield shift indicates strong intramolecular hydrogen bonding between the imine group (-CH=N-) and the hydroxy group (-OH) [13]. The azomethine proton peak appears as a singlet. The multiplicity of the peak indicates that the ligand exists in a phenol form not a quinodal form [14], therefore there is no tautomerization occurring for **HL_1**.



Scheme 2.3: *Tautomerization and hydrogen bonding in salicylaldimine ligands* [14]

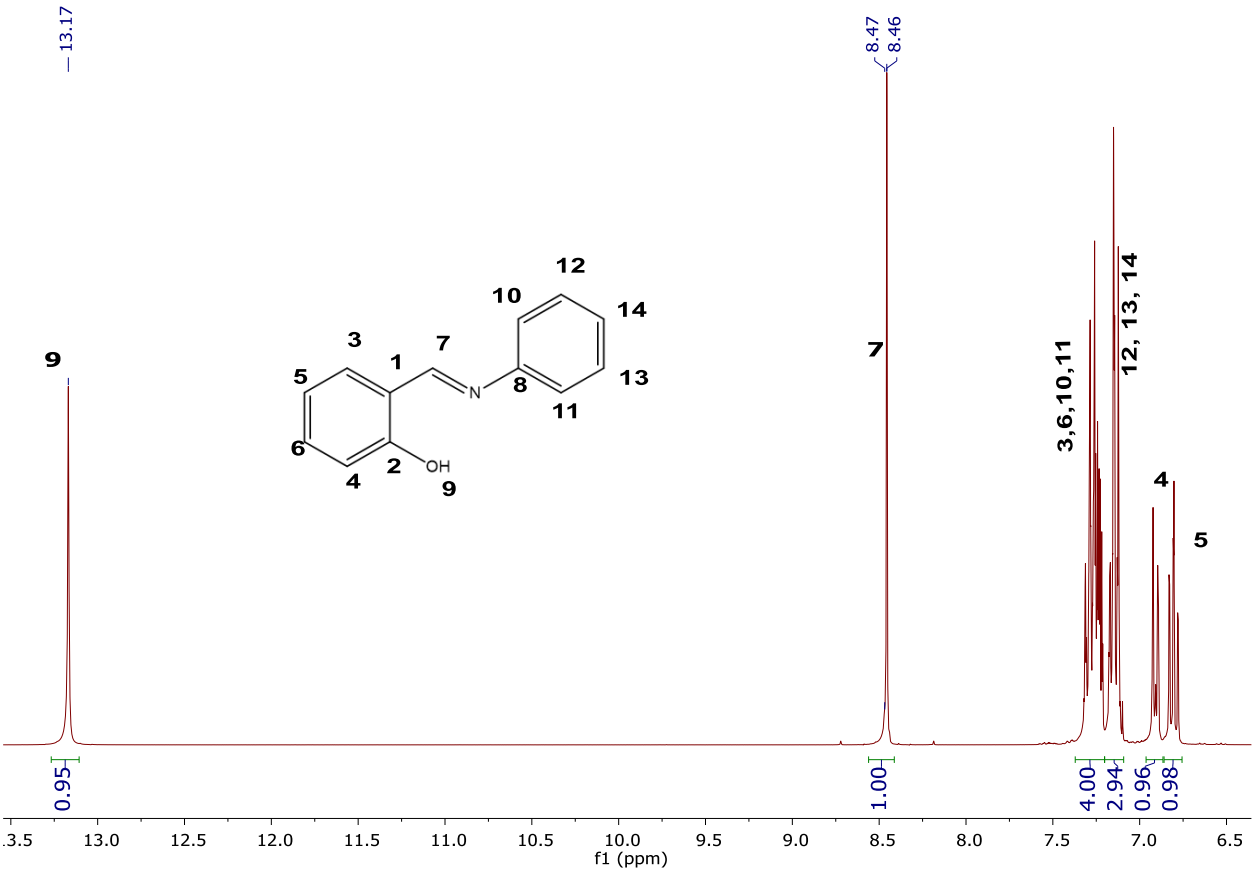


Fig. 2.3: *[1]HNMR spectrum for ligand* ***HL₁***

The resonances for the aromatic protons of **HL_1** are observed in the range 7.33 – 7.22 ppm. The COSY NMR spectrum shows correlation in the aromatic region where it can be observed that proton **5** and proton **6** in the aromatic region correlate meaning that they are three bonds away from each other. The spectrum also shows that there is correlation between protons **4** and **6**. For protons **10**, **11**, **12**, **13** and **14** it is difficult to tell if there is some correlation because their peaks appear as overlapping multiplets.

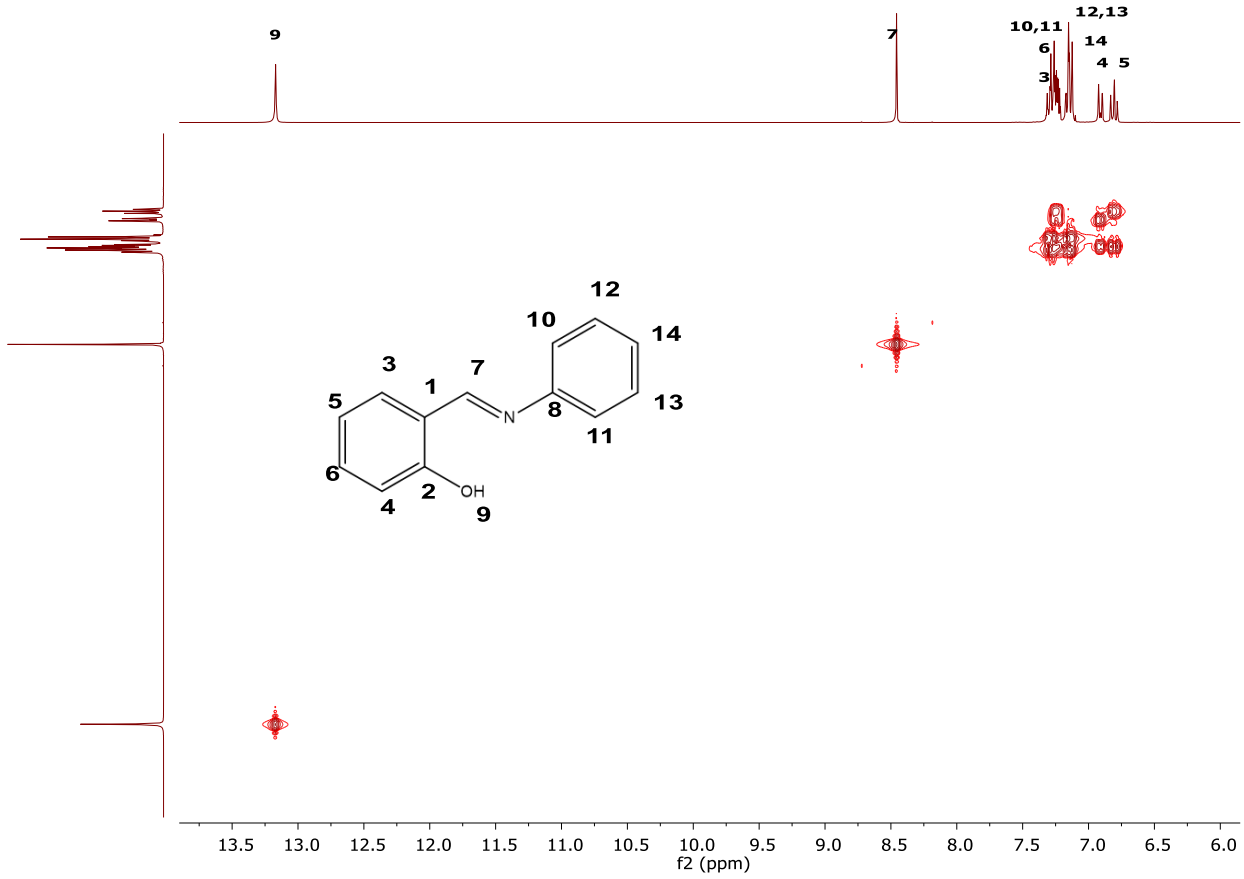


Fig. 2.4: *COSY NMR spectrum for ligand* ***HL₁*** *obtained in* $CDCl_3$, *25* ^oC

The spectra of these ligands generally exhibit similar features. The imino proton (-CH=N-) signal is observed at 8.33, 8.62, 8.61 and 8.30, 8.35 ppm for **HL_2**, **HL_3**, **HL_4**, **HL_5**, **and HL_6**, respectively. It can be observed that when an alkyl group is directly attached to the imino nitrogen, e.g. **HL_5 and HL_6**, the peak appears at 8.30 and 8.35 ppm respectively and when a phenyl group is directly attached this peak is observed at 8.46, **HL_1**. This could mean that the substituents have an influence on the electronic properties of the ligand around the imino functionality. A slight increase in the imino nitrogen peak position was observed when some electron donating groups were incorporated on the para position of the phenyl group, e.g **HL_3** and **HL_4**, where the peak appears at higher chemical shift 8.61 and 8.62 ppm respectively compared to all ligands and due to resonance, this could mean that electron density around this proton is low.

The -OH proton resonances is observed at 13.86, 13.86, 13.26, 13.13, and 13.62 ppm for **HL_2**, **HL_3**, **HL_4**, **HL_5**, **and HL_6** respectively. No clear trend was also observed on the position of the -

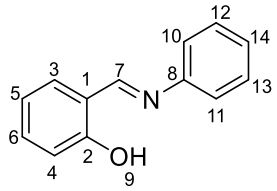
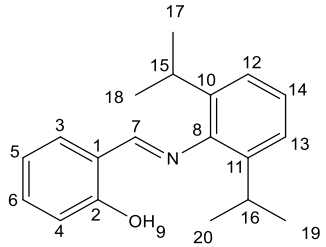
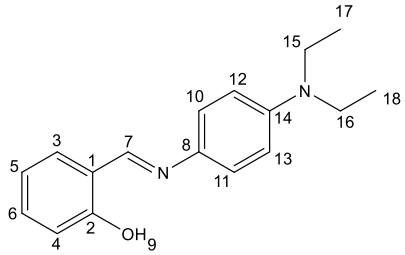
OH group on the synthesized ligands. There are many factors that can affect the position of these two peaks on the ligands and one of them is hydrogen bonding which can occur between the -OH proton and the imino nitrogen.

Ligands **HL_1** – **HL_4** contain aromatic substituents on the imino nitrogen. The proton signals for the phenyl rings are observed in the range 6.71 – 7.29 ppm. The isopropyl protons ($CH(CH_3)_3$) of ligand **HL_2** are observed as a doublet at 1.22 ppm (-C<u>H</u>$_3$,) and a multiplet at 3.08 ppm (-C<u>H</u>). The proton signals for the ethyl group of the diethyl amine substituent of ligand **HL_3** are observed as a triplet at 1.21 ppm (-C<u>H</u>$_3$) and a quartet at 3.39 ppm (-C<u>H</u>$_2$,). The ethyl alcohol protons of ligand **HL_4** are observed at as two triplets at 2.91 (Ar-C<u>H</u>$_2$) and 3.90 ppm (-C<u>H</u>$_2$OH) respectively. The proton signal for the ethyl alcohol group (-CH_2C<u>H</u>$_2$OH) is observed as a broad singlet at 1.57 ppm.

All COSY NMR spectra for ligands **HL_1** – **HL_4** show that no proton correlates to the imine proton (-C<u>H</u>=N-) labeled **8**. This is expected as there are no protons that are 2 or 3 bonds away from this imine proton. The same principle applies to the -OH proton labeled **9**. Aromatic protons of the salicylaldehyde backbone labelled **5** correlates by a three-bond H-H coupling constant to protons **3** and **6**. Proton **6** also correlates to proton **4** and this is observed for all the ligands. Aromatic Protons **10** and **11** of the phenyl group on the imine moiety for ligands **HL_1** – **HL_4** correlates to protons **12** and **13,** respectively.

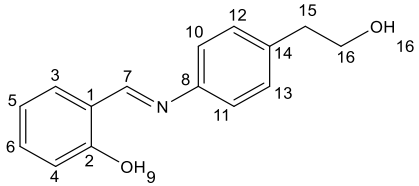
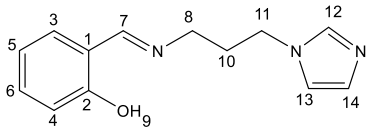
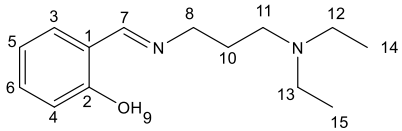
Ligands **HL_5** and **HL_6** contain a propyl chain on the imino nitrogen. For ligand **HL_5** these protons are assigned to signals at 2.15, 3.53 and 4.05 ppm while for ligand **HL_6** these protons are observed at 1.85, 2.55 and 3.64 ppm. The ethyl chain protons for ligand **HL_5** are observed at 1.05 and 2.55 ppm while the protons of the imidazole group attached to the propyl chain of ligand **HL_6** are observed at δ 6.91, 7.06 and 7.45 ppm. The assignment of these protons is shown in Table **2.1**. Ligand **HL_5** and **HL_6** contain a propyl chain on the imine moiety and protons on **8** correlates to those at **10** and those at **11** also correlate to those at **10** and so on. COSY NMR spectra for other ligands are provided in the appendix section.

Table 2.1: ^{1}HNMR data for ligands (**HL_1 – HL_6**)

Ligand structure	-O<u>H</u>	-C<u>H</u>=N-	Phenolic moiety	Imino nitrogen substituent
 **HL_1**	13.17 (br, 1H)	8.46 (s, 1H)	**5**: 6.80 (td, 1H, J_{HH} = 7.3) **4**: 6.96 (dd, 1H, J_{HH} = 8.6) **3** & **6**: 7.27 – 7.31 (m, 2H)	**12**, **13** & **14**: 7.12 – 7.17 (m, 3H) **10** & **11**: 7.21 – 7.25 (m, 2H)
 **HL_2**	13.86 (br, 1H)	8.33 (s, 1H)	**5**: 6.99 (td, 1H, J_{HH} = 7.4) **4**: 7.11 (dd, 1H, J_{HH} = 8.3) **3**: 7.40 (dd, 1H, J_{HH} = 7.4) **6**: 7.47 (td, 1H, J_{HH} = 8.3)	**17**, **18**, **19**, **20:** 1.22 (d, 12H, J_{HH} = 6.9) **15**, **16:** 3.08 (m, 2H) **12**, **13** & **14:** 7.21 (m, 3H)
 **HL_3**	13.86 (br, 1H)	8.62 (s, 1H)	**5:** 6.92 (td, 1H, J_{HH} = 7.4) **4:** 7.02 (d, 1H, J_{HH} = 8.2) **3** & **6:** 7.33 - 7.37 (m, 2H)	**17** & **18:** 1.21 (t, 6H, J_{HH} = 7.1) **15** & **16:** 3.39 (q, 4H, J_{HH} = 7.1) **12** & **13:** 6.71 (dd, 2H, J_{HH} = 8.9) **10** & **11** 7.29 (d, 2H, J_{HH} = 8.1)

br: broad, s: singlet, d: doublet, dd: doublet of doublets, t: triplet, td: triplet of doublets, q: quintet, J_{HH}: coupling constant

Table 2.1 (Cont.): ^{1}HNMR data for ligands (**HL_1 – HL_6**)

Ligand structure	OH	-C<u>H</u>=N-	Phenolic moiety	Imino nitrogen substituent
 **HL_4**	13.26 (br, s, 1H)	8.61 (s, 1H)	**5:** 6.94 (tb, 1H, J_{HH} = 7.4) **4:** 7.04 (dd, 1H, J_{HH} = 8.2) **3** & **6:** 7.35 – 7.41 (m, 2H)	**17** 1.57 (br s, 1H) **15** 2.91 (t, 2H, J_{HH} = 6.5) **16** 3.90 (t, 2H, J_{HH} = 6.5) **11**, **12**, **13** & **14:** 7.23 – 7.31 (m, 4H)
 **HL_5**	13.13 (br s, 1H)	8.30 (s, 1H)	**5:** 6.87 (td, 3H, J_{HH} = 7.4) **4:** 6.95 (dd, 1H, J_{HH} = 8.2) **3&6:**7.25 – 7.31 (m, 2H,)	**10:** 2.15 (q, 2H, J_{HH} = 6.8) **8:** 3.53 (t, 2H, J_{HH} = 6.4) **11:** 4.05 (t, 2H, J_{HH} = 6.9) **13:** 6.91 (br s, 1H) **14:** 7.06 (br s, 1H) **12:** 7.45 (s, 1H)
 **HL_6**	13.62 (br s, 1H)	8.35 (s, 1H)	**5:** 6.88 (td, 3H, J_{HH} = 7.4) **4:** 7.00 (dd, 1H, J_{HH} = 8.2) **3&6:** 7.23 - 7.27 (m, 2H)	**14** & **15:** 1.05 (t, 6H, J_{HH} = 7.2) **10:** 1.85 (q, 2H, J_{HH} = 6.9) **11**, **12** & **13:** 2.55 (q, 6H, J_{HH} = 7.0) **8:** 3.64 (t, 2H, J_{HH} = 6.7)

br: broad, s: singlet, d: doublet, dd: doublet of doublets, t: triplet, td: triplet of doublets, J_{HH}: coupling constant in Hz

2.2.1.2. Characterization of salicylaldimine ligands with ^{13}CNMR spectroscopy

All the ligands were further characterized with ^{13}CNMR spectroscopy and 2D NMR spectroscopy was used for conclusive assignment of the carbon resonances. The ^{13}CNMR spectral data and relevant assignments for all the ligands are provided in Table **2.2**. The ^{13}CNMR spectrum for ligand **HL_1** is shown in Figure **2.5** as an example of a typical spectra obtained for the synthesized ligands. The signal at δ 162.78 ppm is assigned to the imine (H<u>C</u>=N) carbon of **HL_1**. This peak was observed at δ 162.78, 166.74, 160.89, 162.19, 166.08, 164.25 ppm for ligands **HL_1**, **to HL_6** respectively. The chemical shift is in the order **HL_3 < HL_1=HL_4<HL_6<HL_2<HL_5**. What is interesting is the fact that this order is different from that which was observed for the imine proton on ^{1}HNMR. One example is, in the ^{1}HNMR, the chemical shift of the imine proton of **HL_1**>**HL_2** but in the ^{13}CNMR, the imine carbon follows a different trend **HL_2**>**HL_1**. The behaviors can also be observed between **HL_5** and **HL_6** also between **HL_3** and **HL_4**. This could be due to magnetic anisotropy effect.

The peak at 160.10 ppm on **HL_1** spectrum is assigned to the aromatic carbon, labelled **2**, attached to the -OH group. For ligands **HL_2 - HL_6** this peak was observed at are observed in the range δ 160.89 – 161.40 ppm. Other aromatic carbons of the ligand are observed in the range 116.21 – 132.09 ppm for ligand **HL_1**. For ligands **HL_2** – **HL_6** other aromatic carbon peaks are observed at δ 116.86 - 161.40 ppm.

Ligands **HL_1** – **HL_4** contain a phenyl group on the imine moiety which has some substituents for ligands **HL_2** and **HL_4**. The aromatic carbons **8**, **10**, **11**, **12**, **13**, and **14** of this phenyl groups are observed at δ 112.13 – 148.50 ppm. The isopropyl substituent carbons for ligand **HL_2** are observed at δ 23.69 and 28.7 ppm which are assigned to CH(<u>C</u>H_3)$_2$ and <u>C</u>H(CH_3)$_2$ carbons, respectively.

The ethyl amine substituent carbons for ligand **HL_3** are observed at δ 23.69 and 28.27 ppm which are assigned to the ethyl chain <u>C</u>H_3 and <u>C</u>H_2 carbons respectively and the ethyl chain substituent carbons of ligand **HL_4** are observed at δ 38.72 and 63.57 ppm and are assigned to CH_2 directly attached to the benzene ring and the one bonded to the OH group, respectively. For ligand **HL_5** and **HL_6** a propyl chain is attached to the imine moiety and carbons of these propyl chains are observed at δ 28.26 – 55.86 ppm.

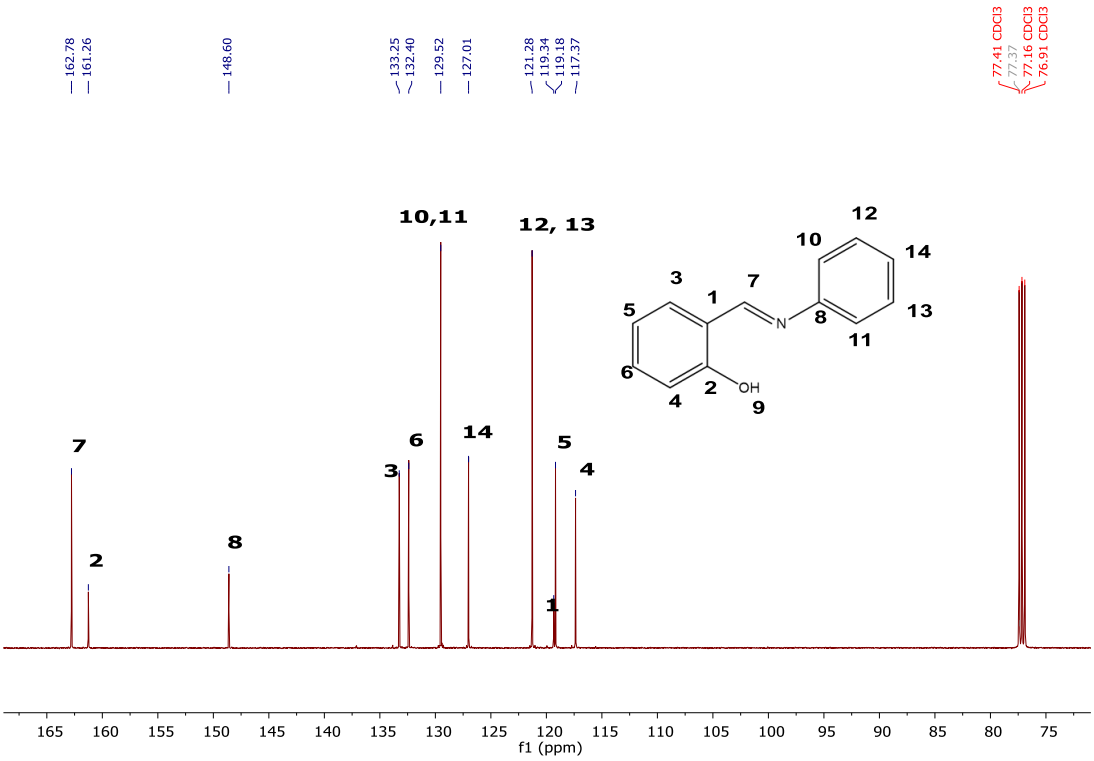


Fig. 2.5: *^{13}CNMR spectrum for ligand **HL$_1$** obtained in $CDCl_3$ at 25 ^{o}C*

The HSQC NMR spectra show the hydrogen signals to which each carbon signals is correlated by one-bond coupling (C-H). A typical HSQC spectrum for **HL$_1$** ligand is shown in Figure **2.8** as an example of the spectra that were obtained for the ligands. Carbons and protons at positions **3**, **4**, **5**, **6**, **10**, **11**, **12**, **13**, and **14** are correlated by one bond coupling constant for ligand **HL$_1$**. The imine bond proton and carbon at position **7** are also correlated by one-bond C-H coupling. From the assignments made in Table **2.1** and **2.2**, it can be deduced from the HSQC spectra of all the ligands that the protons and carbons in the same position are correlate by one bond coupling.

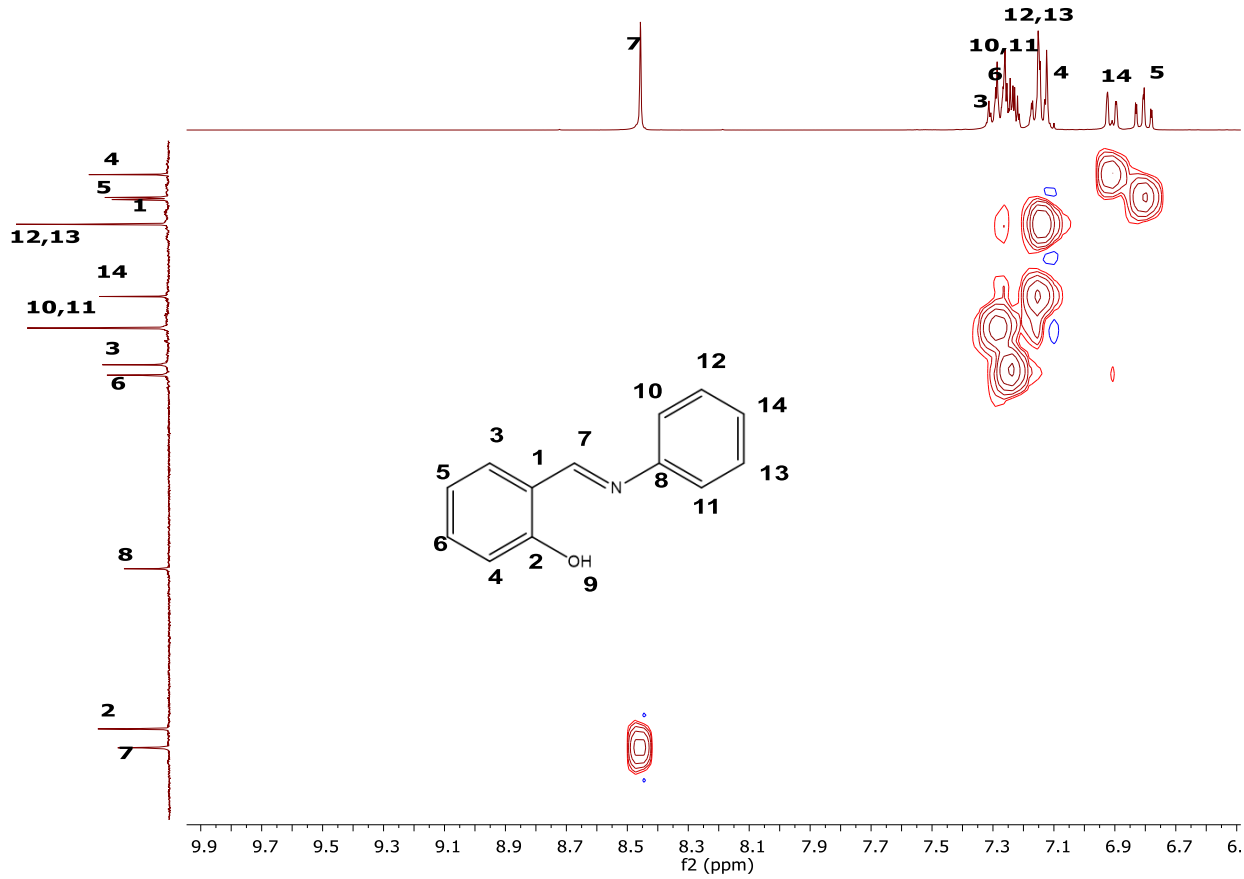


Fig. 2.6: *HSQC NMR spectrum for ligand* ***HL₁*** *obtained in* $CDCl_3$ *at 25* ^oC

Quaternary carbons were confirmed with DEPT NMR spectroscopy. From Figure **2.7** it can be observed that the peaks that were observed at 118.17, 147.44, and 160.10 ppm on the ^{13}CNMR spectrum does not appear on the DEPT NMR spectrum and this suggest that these carbons are quaternary.

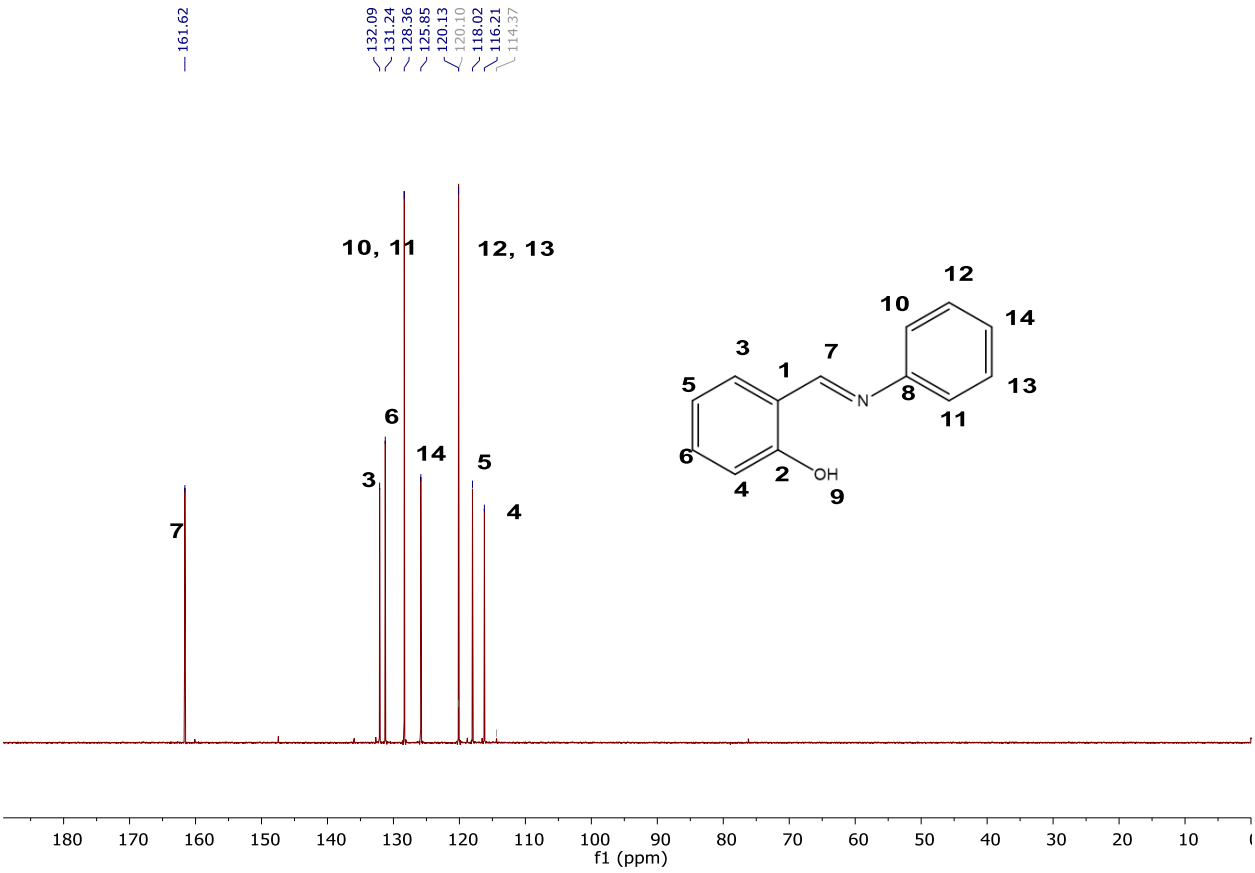


Fig. 2.7: *DEPT NMR spectrum for ligand* ***HL₁*** *obtained in* $CDCl_3$ *at 25 °C*

The quaternary carbons **1**, **2** and **8** were assigned using HMBC NMR spectroscopy. HMBC shows correlation between protons and carbons that are about 3 bonds away. Figure 2.8 is a spectrum that was obtained for **HL₁** and it is used as an example of how the spectra for all the ligands was analyzed to confirm quaternary carbons. Proton **4** shows correlation to a carbon signal 161.19 ppm. The intensity is very low which suggests that the distance between the proton and the carbon is short and with this information the carbon resonance at 161.19 ppm was assigned to carbon **2**. The same analogy was used to assign the carbon signal at 148.50 ppm to carbon **8**. For the carbon resonance at 118.02 ppm there is a low intensity peak that shows correlation to proton **7** and because carbon **1** is 2 bonds away and could result in this low intensity peak this carbon signal was assigned to carbon **1**.

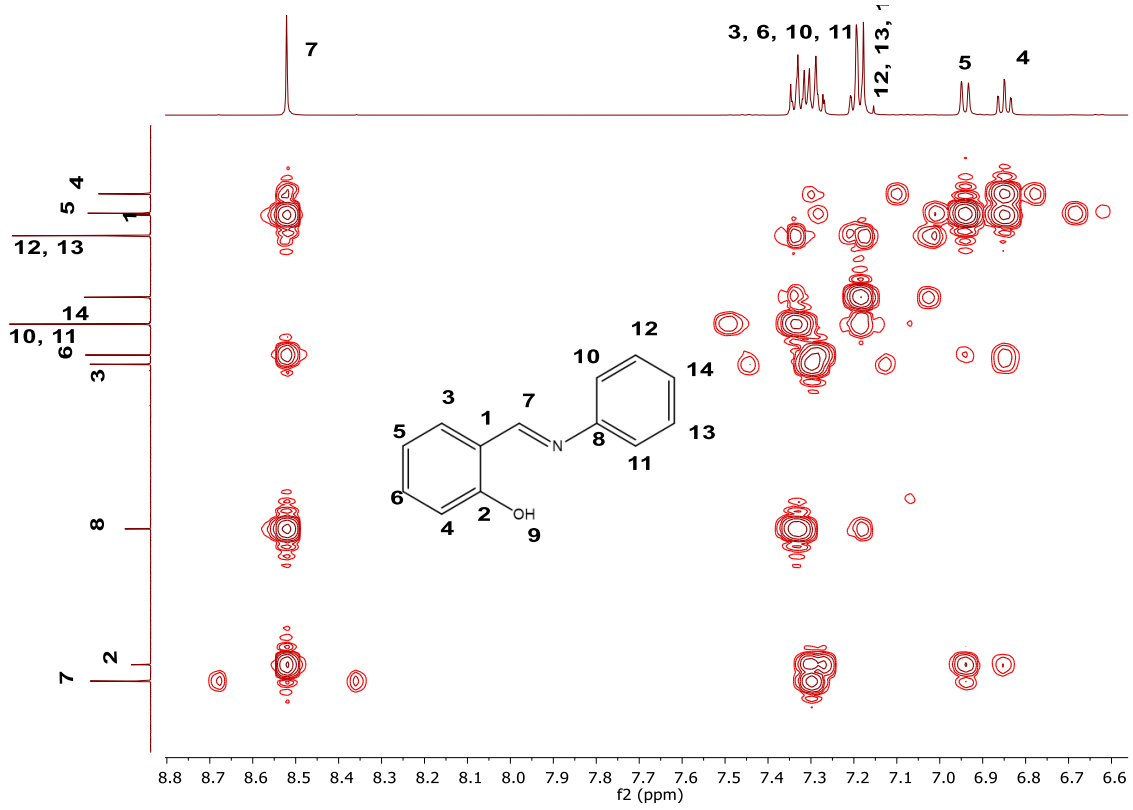


Fig. 2.8: *HMBC NMR spectrum for ligand* ***HL$_1$*** *obtained in $CDCl_3$ at 25 ^oC*

Table 2.2: ^{13}CNMR data for ligands (**HL_1 – HL_6**)

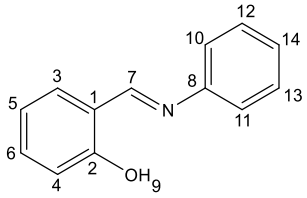
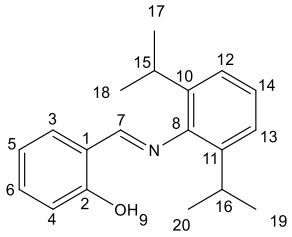
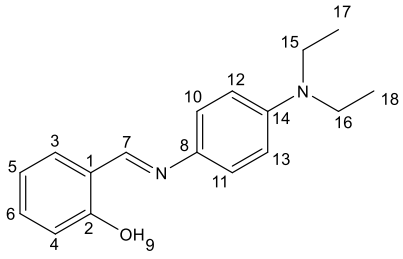
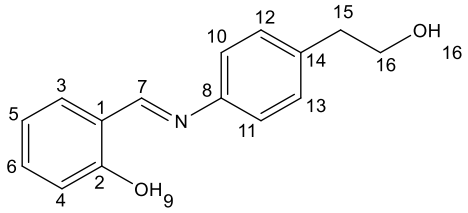
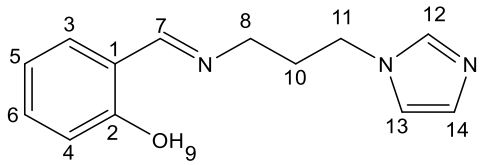
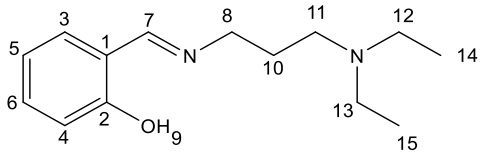
Ligand structure	-CH=N-	phenolic moiety	Imino nitrogen substituent
 **HL_1**	**7:** 162.78	**4**: 117.37, **5:** 119.18, **1:** 119.34, **6:** 132.40, **3:** 133.25, **2:** 161.26	**12** &**13:** 121.28, **14**, 122.01, **8:** 148.0, **10** & **11:** 129.54
 **HL_2**	**7:** 166.74	**4:** 117.50, **1:** 118.85, **5:** 119.19, **6:** 132.38, **3:** 133.40, **2:** 161.40	**17**, **18**, **19**, **20:** 23.69, **15** & **16** 28.27, **12** & **13:** 123.41, **10** & **11:** 138.84, **8:** 146.29
 **HL_3**	**7:** 160.89	**4:** 117.09, **5:** 118.86, **1:** 119.97, **3:** 131.50, **6:** 131.92, **2:** 156.93	**17** &**18:** 12.73, **15:** 16 44.67, **12** & **13:** 112.13, **10** & **11:** 122.56, **14:** 136.15, **8:** 147.37

Table 2.2 (cont.): ^{13}CNMR data for ligands (**HL_4 – HL_6**)

Ligand structure	-CH=N-	Phenolic moiety	Imino nitrogen substituent
 **HL_4**	**7:** 162.19	**4:** 117.23, **5:** 119.06, **1:** 119.24, **3:** 132.21, **6:** 133.07, **2:** 161.10	**15:** 38.72, **16:** 63.57, **12** & **13:** 121.32, **10** &**11:** 130.02, **14:** 137.52, **8:** 146.86
 **HL_5**	**7:** 166.08	**4:** 116.96, **5:** 118.55, **1:** 118.71, **3:** 131.41, **6:** 132.55, **2:** 160.89	**10:** 31.79, **8:** 44.30, **11:** 55.86, **13:** 118.84, **14:** 129.78, **12:** 137.12
 **HL_6**	**7:** 164.25	**5:** 116.86, **1:** 118.26, **4:** 118.70, **3:** 131.00, **6:** 131.89, **2:** 161.25	**14** & **15:** 116.96, **10:** 28.26, **12** & **13:** 46.80, **11:** 50.11, **8:** 57.39,

2.2.1.3.Characterization of the salicylaldimine ligands with Infrared spectroscopy, mass spectrometry and elemental analysis

The characterization data for the ligands obtained with FT-IR spectroscopy is summarized in Table **2.3** for all the ligands. The O-H stretching frequency of these ligands is expected in the range 3300 – 3800 cm^{-1} but it can however sometimes be observed in the range 2840 - 2960 cm^{-1} due to hydrogen bonding as shown in Figure **2.9** [15]. In the case of ligands **HL_1** – **HL_6** the band due to the ν(O-H) stretching frequency was not observed which is attributed to strong intramolecular hydrogen bonding within the ligand [16].

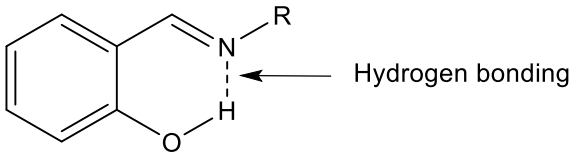


Fig. 2.9: *Hydrogen bonding interaction within the salicylaldimine ligand* [17]

The imine ν(C=N) stretching frequencies of this ligand class are reported generally in the range 1595 – 1640 cm^{-1} [18, 19] and for the synthesized ligands it is observed in the region 1614 - 1632 cm^{-1} confirming the presence of the imine functionality. The position of the stretching frequency depends on structural features of the molecule such as electron delocalization, the electronic effect of neighboring substituents and hydrogen bonding. As it can be observed from Table **2.3**, this peak is observed at a higher wavenumber in the ligands that have an alkyl chain substituent on the imino nitrogen, **HL_5** and **HL_6**. The delocalization of electrons and the mesomeric effect in **HL_1** – **HL_4** result in lower double bond character and this results in lower ν(C=N) stretching frequency in these ligands. The decrease in double bond character for these ligands follow the order, **HL_6=HL_5>HL_2>HL_4=HL_3=HL_1**.

The phenolic ν(C-O) stretching frequency is reported to generally appear in the range 1290 – 1340 cm^{-1} [13, 20] and for the synthesized ligands it is observed in the region 1266 -1282 cm^{-1}. There is no clear trend that is observed in the position of the phenolic ν(C-O) stretching frequency in different ligands. A typical FT-IR spectrum for ligand **HL_1** is shown in Figure **2.10** as an example of the spectra that were obtained for all the ligands.

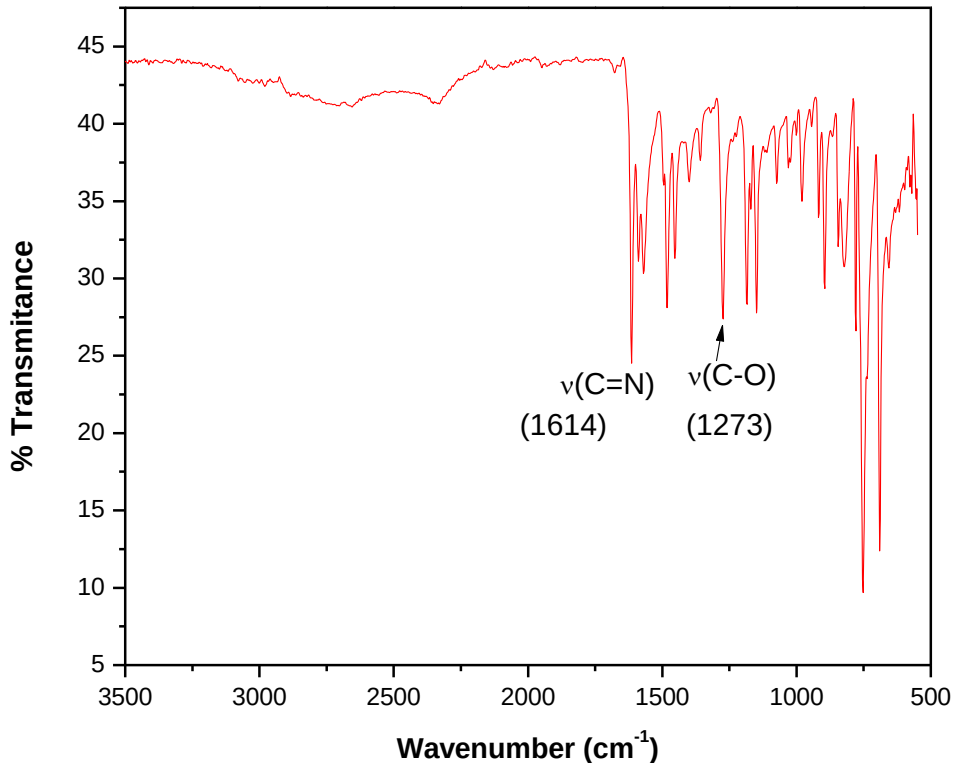


Fig. 2.10: *FTIR spectrum for ligand* ***HL₁***

The elemental analysis data obtained for the ligands agreed with the proposed structures and this data is summarized in Table **2.3**. In the mass spectrometry spectra the molecular ion for the ligands are all observed as $[M + H]^+$ and this data is also summarized in Table **2.3**.

Table 2.3: FTIR spectroscopy Elemental analysis and mass spectrometry data for ligands (**HL_1 – HL_6**)

Ligand	Yield (%)	M.P (°C)	Formula	ESI MS $[M+H]^+$	FT-IR (cm^{-1})		Analytical Found (Calc.)		
				Found (Calc.)	ν (C=N)	ν (C-O)	C	H	N
HL_1	79.6	50.1 – 50.8	$C_{13}H_{11}NO$	198.1 (198.3)	1614	1274	79.00 (79.17)	5.29 (5.62)	7.01 (7.10)
HL_2	89.7	63.5 – 64.1	$C_{19}H_{23}NO$	282.2 (282.4)	1623	1277	80.94 (81.10)	7.86 (8.21)	5.13 (4.98)
HL_3	87.1	100.6 – 101.4	$C_{17}H_{20}N_2O$	269.2 (269.4)	1614	1267	76.15 (76.09)	7.11 (7.51)	10.64 (10.44)
HL_4	93.2	92.9 – 93.7	$C_{15}H_{15}NO_2$	242.1 (242.3)	1618	1282	74.53 (74.67)	6.06 (6.27)	5.51 (5.81)
HL_5	68.5	85.4 – 86.8	$C_{13}H_{15}N_3O$	230.2 (230.3)	1631	1279	67.74 (68.10)	6.21 (6.59)	18.56 (18.33)
*__HL_6__	93.5	-	$C_{14}H_{22}N_2O$	235.2 (235.3)	1632	1277	71.33 (71.79)	9.11 (9.46)	11.45(11.95)

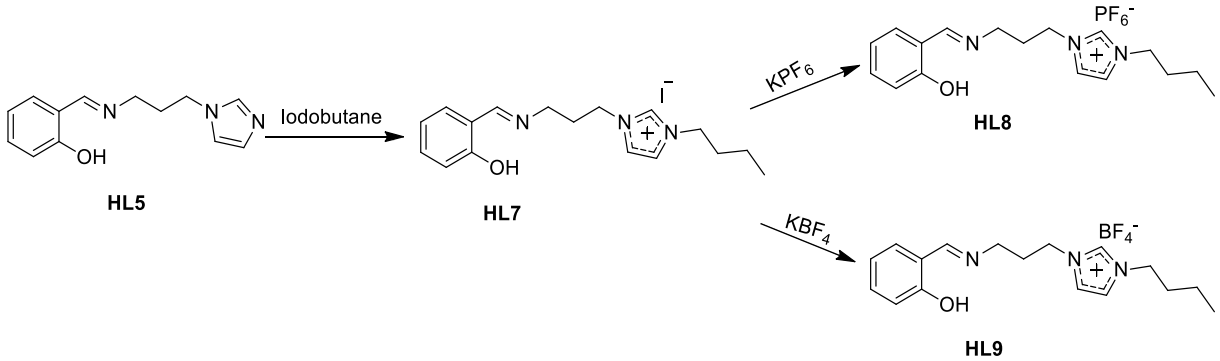
*Obtained as a yellow oil

2.2.2 Synthesis and characterization of ionic functionalized Schiff base ligands

The synthesis and characterization of salicylaldimine ligands that contain groups that can be transformed into ionic functionalities (**HL_3** – **HL_6**) was achieved and reported in the previous section. Ligands **HL_3**, **HL_5** and **HL_6** contain an amine group which can be transformed to an ionic functional group through quaternization of the nitrogen atom in the amine group. On the other hand, **HL_4** contain an -OH group in the para position of the azomethine phenyl substituent which can be utilized for functionalization. In this section, the development of synthetic protocols for the transformation of these neutral ligands to ionic functionalized ligands is reported.

2.2.2.1 Preparation of ionic liquid functionalized ligands HL_7 – HL_9

Schiff base ligand **HL_7**, was synthesized through alkylation of ligand **HL_5** as shown in Scheme **2.3**. Two attempts were made in the synthesis of **HL_7**. In the first attempt the reaction was performed following a literature procedure where a solventless reaction condition was used [21]. The ^{1}HNMR spectrum of this first attempt show peaks which could not be assigned to the targeted product. This method was modified and in the second attempt the reaction was performed in the presence of acetonitrile as a solvent. ^{1}HNMR spectroscopy confirmed that the product produced was the targeted one and this method was the best one to prepare ligand **HL_7**.



Scheme 2.4: *Synthetic procedure for the preparation of IL functionalized ligands **HL_7**, **HL_8** and **HL_9***

An ion exchange reaction was performed with ligand **HL_7** where I^- counter ion was exchanged for the PF_6^- counter ion to produce ligand **HL_8**. In this reaction, ligand **HL_7** was dissolved in ethanol and KPF_6 was added after which the reaction was refluxed overnight. The ligands were obtained

in relatively good yields, 81% and 94 % for **HL$_7$** and **HL$_8$** respectively as yellowish-brown viscous oils. These ligands are stable when stored at room temperature even for prolonged time. The assignments of the proton resonances for **HL$_7$** and **HL$_8$** is summarized in Table **2.4**. The alkylation of ligand **HL$_5$** to produce ligand **HL$_7$** was confirmed by the appearance of additional peaks, **18**, **17**, **16** and **15**, to those of **HL$_5$**, upfield in the aliphatic region. These peaks are characteristic of the protons of the butyl chain attached to the imidazolium group, Figure **2.11,** on ligand **HL$_7$**.

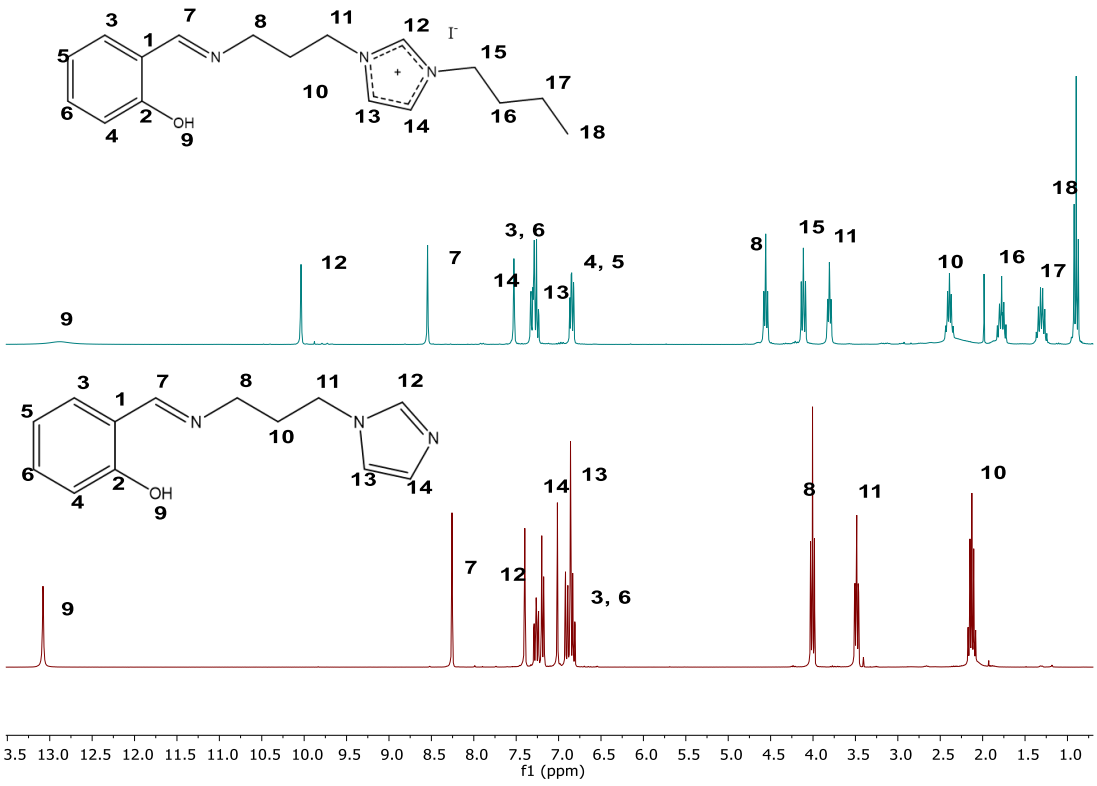


Fig. 2.11: *Stacked ^{1}HNMR spectra for ligand **HL$_5$** and **HL$_7$***

The quaternization of the imidazole nitrogen of **HL$_5$** results in the change in the electronic environment around the imidazole ring. This concept is also very vital in confirming that the neutral ligand, **HL$_5$,** was alkylated. The proton assigned **12** (Figure **2.11**) shifts to a higher chemical shift from 7.45 (s) ppm, in the spectrum of **HL$_5$** (Figure **2.11**) to 10.04 (s) ppm in the spectrum of **HL$_7$**. A major shift is also observed in the peaks assigned to protons **13** and **14**. These peaks shift from 6.91(s) and 7.06 (s) ppm respectively in the spectrum of **HL$_5$** to 7.29 (s) and 7.53

(s) ppm (Figure **2.9**) in the spectrum of **HL**$_7$, respectively. Conclusive assignment of the ^{1}HNMR spectra of this ligand was made using COSY NMR spectroscopy shown in the appendix section.

Successful exchange from I^- to PF_6^- results in the change of the electronic environment of the imidazolium ring. The proton resonances **12**, **13** and **14** of **HL**$_7$, shifted slightly upfield in the ^{1}HNMR spectrum of ligand **HL**$_8$ as seen in Figure **2.12**. When the exchange reaction was done for I^- to BF_4^-, ligand **HL**$_9$, the reaction did not occur, and this was confirmed with NMR. The ^{1}HNMR spectrum did not show any expected shift in the peaks **12**, **13**, and **14** of **HL**$_7$. On the other hand, ^{19}FNMR did not show any peak that could be assigned to a fluorine nucleus from BF_4^-.

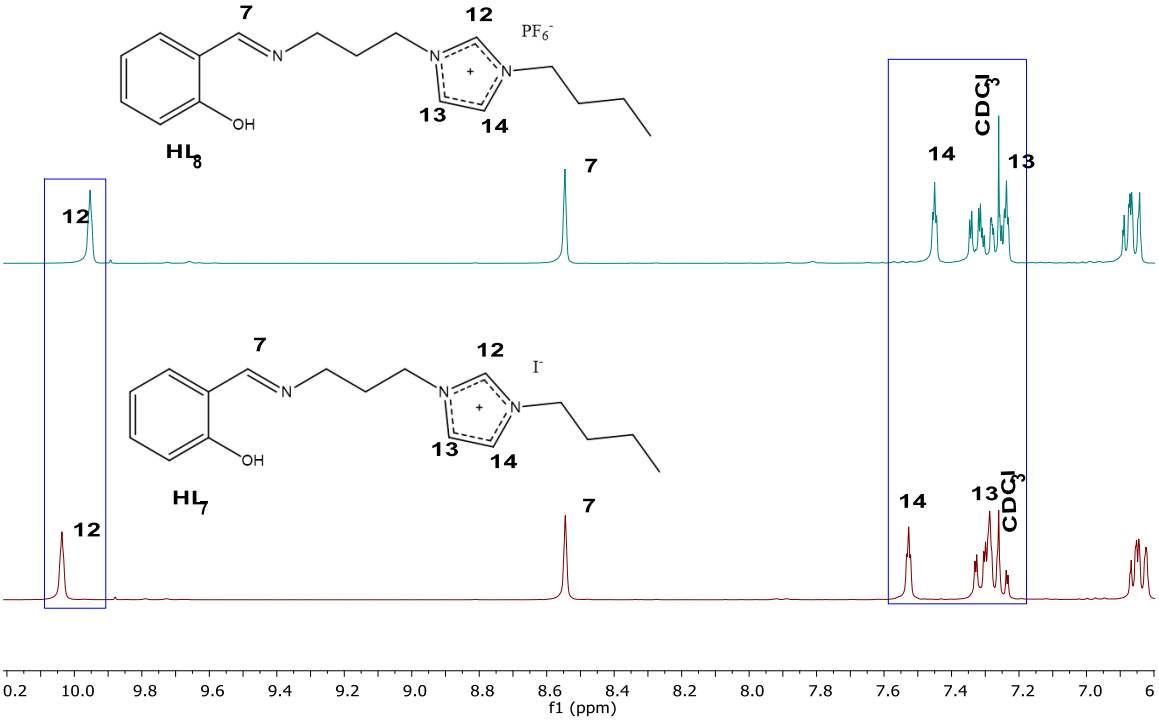
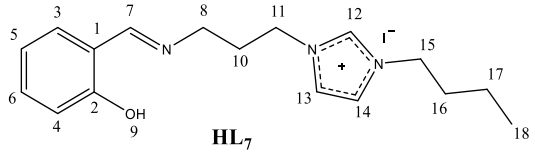
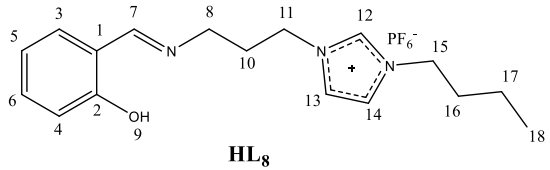


Fig. 2.12: *Stacked ^{1}HNMR spectra ($CDCl_3$) for ligands* ***HL***$_7$ and ***HL***$_8$

Table 2.4: *^{1}HNMR data for ligands (**HL_7 – HL_8**)*

Ligand structure	-O<u>H</u>	-C<u>H</u>=N-	Phenolic moiety	Imino nitrogen substituent
 **HL_7**	12.07 (br, s, 1H)	8.54 (s, 1H)	**4** & **5**: 6.84 (m, 2H) **3** & **6**: 7.23 - 7.33 (m, 2H)	**8**: 4.56 (t, 2H, J_{HH} = 6.4) **10**: 2.39 (q, 2H, J_{HH} = 6.8) **11**: 3.81 (t, 2H, J_{HH} = 6.9) **12**: 10.04 (s, 1H), **13**: 7.29 (s, 1H), **14**: 7.53 (s, 1H) **15**: 4.11 (t, 2H, J_{HH} = 7.02) **16**: 1.78 (q, 2H, J_{HH} = 7.7) **17**: 1.32 (septet, 2H, J_{HH} = 8.2) **18**: 0.90 (t, 2H, J_{HH} = 7.4)
 **HL_8**	12.91(br, s, 1H)	8.55 (s, 1H)	**4 & 5:** 7.45 (m, 2H) **3 & 6:** 7.35 (m, 2H)	**8**: 4.55 (t, 2H, J_{HH} = 6.4) **10**: 2.40 (q, 2H, J_{HH} = 6.8) **11**: 3.82 (t, 2H, J_{HH} = 6.9) **12**: 9.95 (s, 1H), **13**: 7.24 (s, 1H), **14**: 7.46 (s, 1H) **15**: 4.10 (t, 2H, J_{HH} = 7.02) **16**: 1.78 (q, 2H, J_{HH} = 7.7) **17**: 1.33 (septet, 2H, J_{HH} = 8.2) **18**: 0.91 (t, 2H, J_{HH} = 7.02)

br: broad, s: singlet, d: doublet, dd: doublet of doublets, t: triplet, td: triplet of doublets, q quintet, J_{HH}: coupling constant in Hz

The presence of fluorine in PF_6^- which is a counter ion of ligand **HL$_8$** was confirmed with ^{19}FNMR spectroscopy and the spectrum is shown in Figure **2.13**. One peak is observed, and this was expected because fluorine atoms in the ligand are all in the same environment. The peak is observed as a doublet due to coupling to one phosphorus atom which is NMR active.

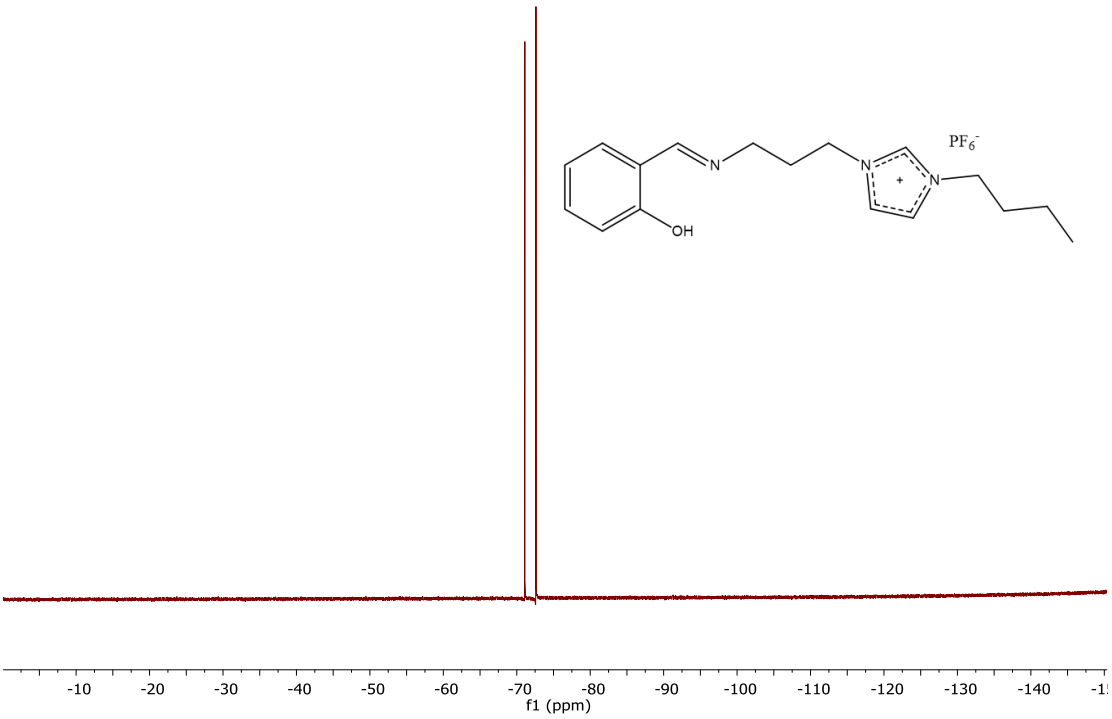


Fig. 2.13: *^{19}FNMR spectrum for ligand **HL$_8$***

The presence of PF_6^- as a counter ion in ligands **HL$_8$** was also confirmed with ^{31}PNMR spectroscopy. The spectrum confirmed the presence of phosphorus atom and ^{31}PNMR spectrum is shown in Figure **2.14**. The spectrum shows one peak. The peak is observed as a septet due to the coupling of phosphorus to six fluorine atoms which are NMR active.

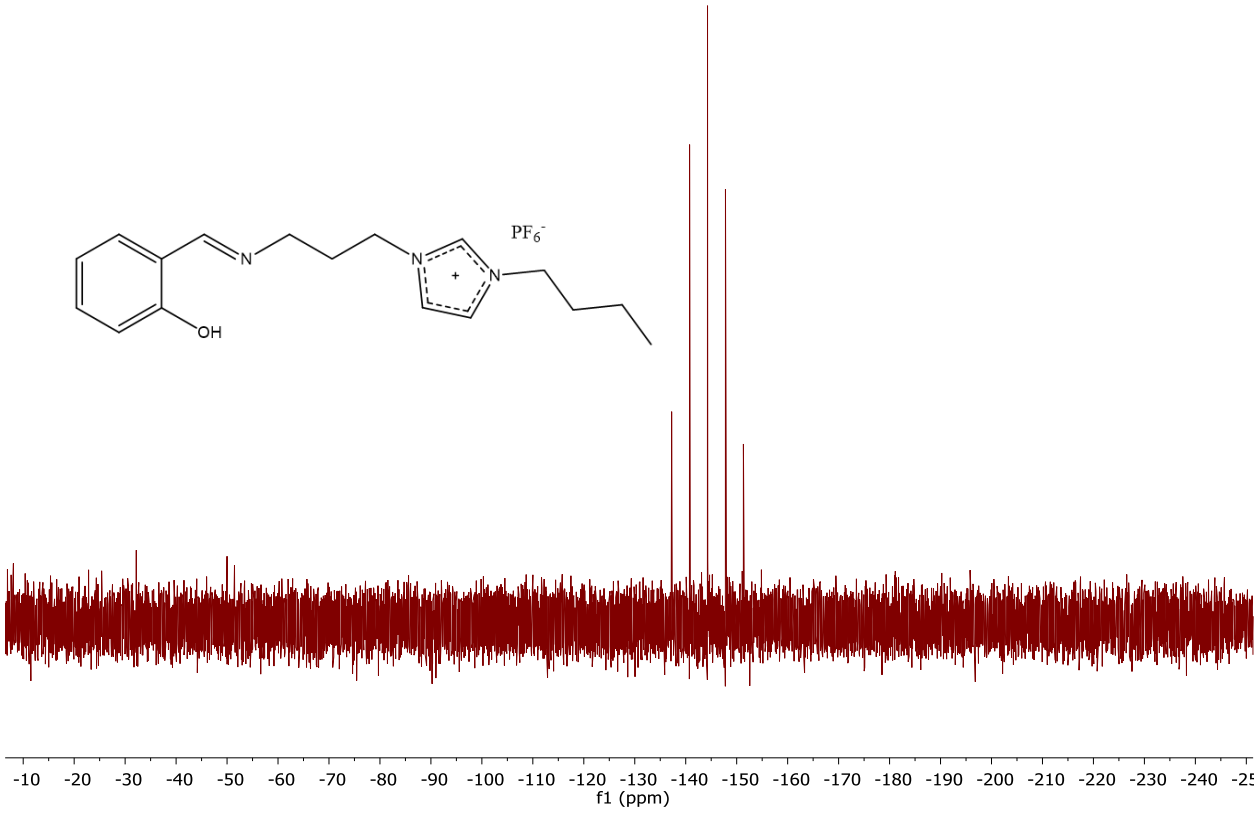


Fig. 2.14: *^{31}PNMR spectrum for* ***HL$_8$***

HL$_7$ and **HL$_8$** were further characterized with ^{13}CNMR and HSQC NMR spectroscopy. Figure **2.13** shows the ^{13}CNMR spectrum of **HL$_7$** with full assignment of the ^{13}C resonances. What is very important to note here is the presence of signals that are assigned to carbons of the butyl chain at 13.21, 19.17, 31.60, and 49.57 ppm, which confirms that **HL$_5$** was successfully alkylated. From HSQC NMR spectra carbons and protons at positions **3** to **7** and **10** to **18** are correlated by one bond coupling constant. Table **2.5** summarizes the peaks that were obtained for ligands **HL$_7$** and **HL$_8$**. There is no significant change in the peak position of the aliphatic carbons between **HL$_7$** and **HL$_8$**. There is a slight shift in the peak position of the five membered ring imidazolium carbon. Carbons at position **12, 13** and **14** appears at 135.65, 122.10 and 122.42 ppm for ligand **HL$_7$** but at 135.15, 121.97 and 122.19 ppm for **HL$_8$**, respectively**.**

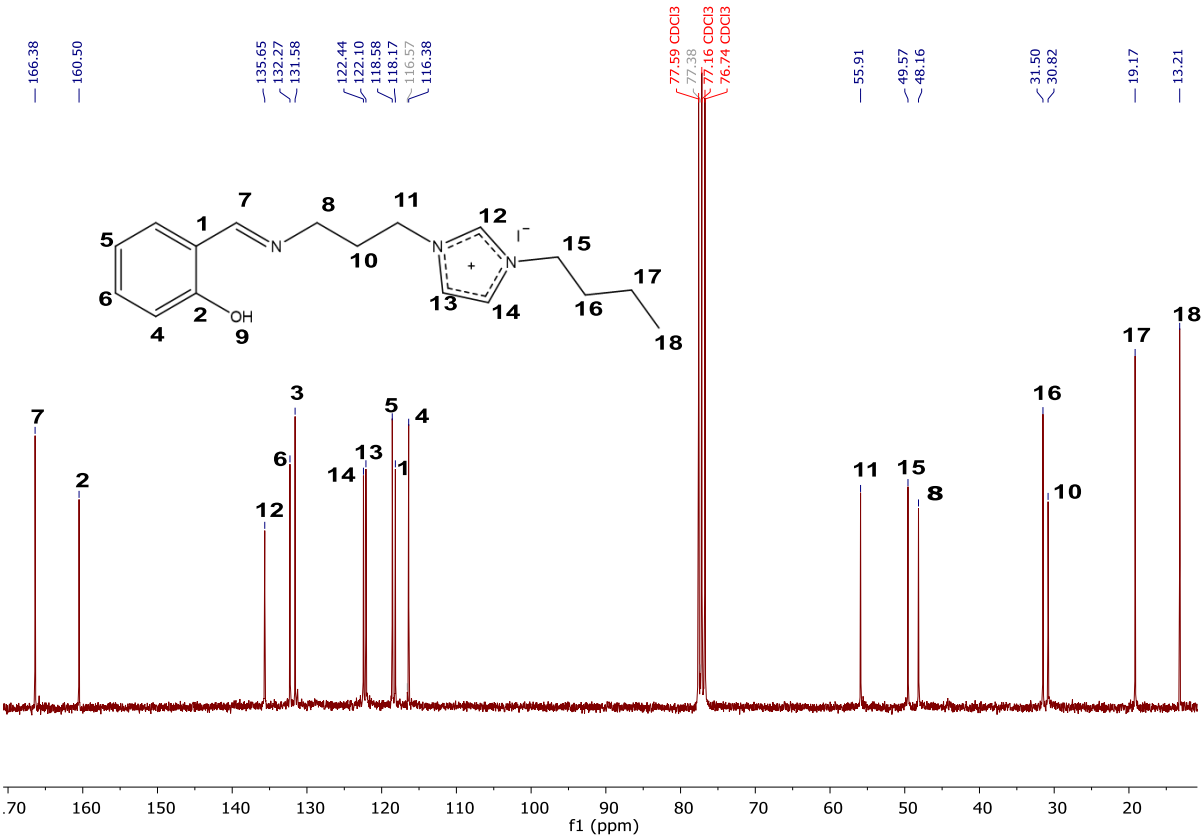
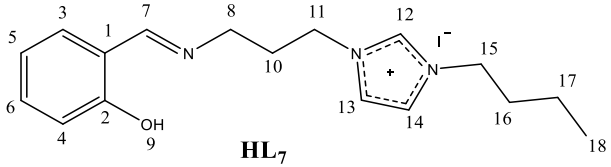
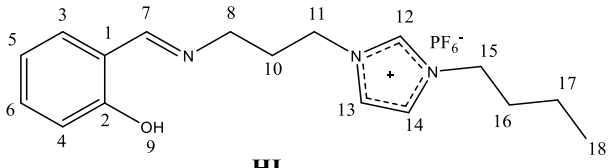


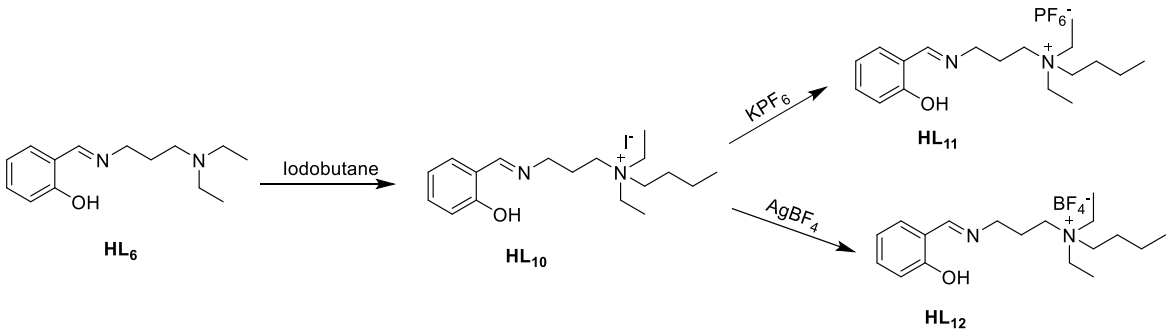
Fig. 2.15: *^{13}CNMR spectra for ligand **HL$_7$** ($CDCl_3$)*

Table 2.5: *^{13}CNMR data for ligands (**HL_7** and **HL_8**)*

Ligand structure	-C<u>H</u>=N-	Phenolic moiety	Imino nitrogen substituent
 **HL_7**	**7:** 166.38	**4:** 116.38, **5:** 118.58, **1:** 118.17, **3:** 131.58, **6:** 132.27, **2:** 160.50	**18**: 13.21 **17**: 19.17, **10:** 30.82, **16:** 31.60, **15:** 49.57, **11:** 55.91, **8:** 48.16, **12:** 135.65 **13**: 122.10, **14:** 122.42
 **HL_8**	**7:** 166.14	**4:** 116.38, **5:** 118.34, **1:** 117.96, **3:** 131.35, **6:** 132.05, **2:** 160.28	**18**: 13.21 **17**: 19.17, **10:** 30.82, **16:** 31.60, **15:** 49.57, **11:** 55.91, **8:** 48.16, **12:** 135.15 **13**: 121.97, **14:** 122.19

2.2.2.2 Preparation of ionic liquid functionalized ligands $HL_{10} - HL_{12}$

The tertiary amino nitrogen of **HL_6** was successfully quarternized by reacting the ligand with iodobutane, Scheme **2.5**. The reaction was carried out neat and in acetonitrile as a solvent. Both reactions gave the same results as evidenced by ^{1}HNMR spectroscopy. The first method was adopted as the best method because it was easy to work up the reaction where the excess iodobutane could just be removed by washing with a non-polar solvent, either hexane or diethyl ether. These solvents were also used to remove any unreacted neutral ligand as it dissolved in them while the ionic functionalized ligand did not.



Scheme 2.5: *Synthetic procedure for the preparation of ligands **HL_{10}**, **HL_{11}** and **HL_{12}***

The quaternization of ligand **HL_6** was performed in a neat reaction and the product obtained was analyzed with ^{1}HNMR spectroscopy in $CDCl_3$. In this case quaternization was only confirmed by the appearance of more peaks in the aliphatic region, Figure **2.16**. Addition of the butyl chain increases aliphatic groups of the ligand, therefore there are so many overlapping peaks as a result of the aliphatic protons on the ^{1}HNMR spectrum, and it is very difficult to clearly assign the peaks of the attached butyl chain.

In the ^{1}H-NMR spectrum obtained in $CDCl_3$ (Figure **2.16)**, the imine proton for **HL_6** is observed as two singlets at 8.47 (s) and 8.56 (s) ppm. These peaks combined intergrade for one proton. This therefore suggests that there could be some tautomerization occurring in solution when the ligand is dissolved in chloroform.

When ligand **HL$_6$** was analyzed with ^{1}HNMR spectroscopy in DMSO a slightly different spectrum was obtained, Figure **2.16**. The two peaks that were observed at 8.47 (s) and 8.56 (s) ppm in the $CDCl_3$ spectrum now appears as one peak at 8.62 (s) ppm and still intergrade for one proton. However, for the spectrum obtained in DMSO the -OH proton signal is observed as two broad singlets at 13.14 (s, b) and 13.22 (s, b) ppm which combined intergrade for one proton. Tautomerization is affected by the nature of the solvent used [14] and this could suggest that a different behavior takes place in the presence of DMSO.

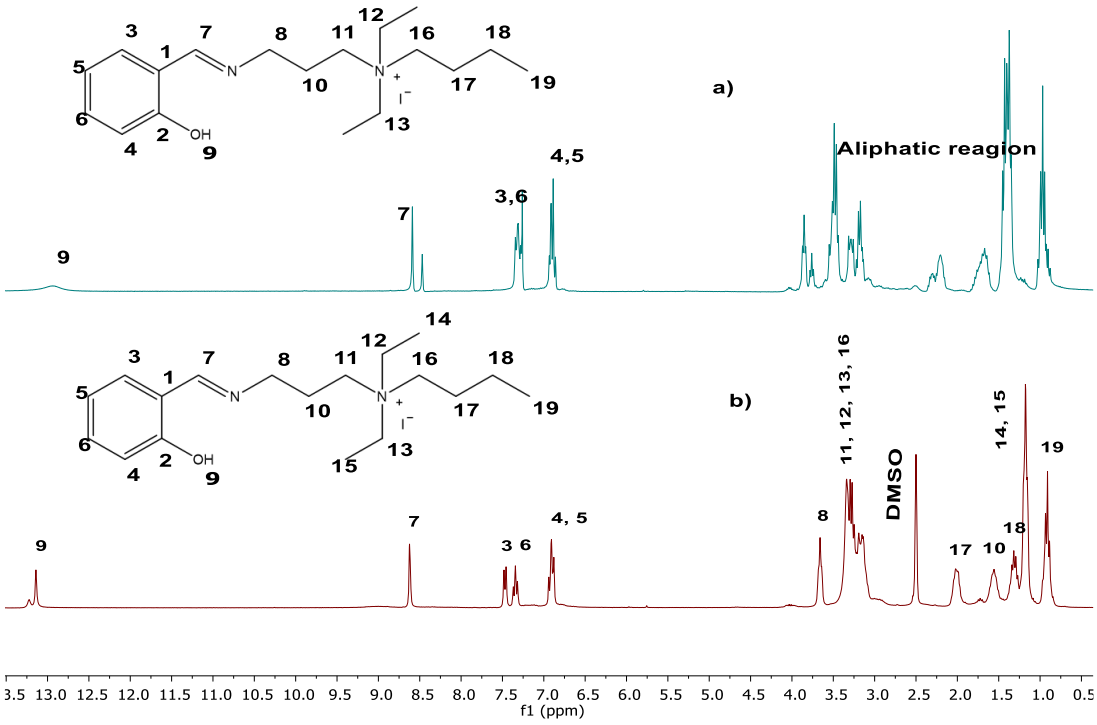


Fig. 2.16: *^{1}HNMR spectrum for ligand **HL$_{10}$** , a) $CDCl_3$ and b) DMSO*

Ion exchange reaction was also performed with ligand **HL$_{10}$** where I^- was exchanged for PF_6^- to produce ligand **HL$_{11}$** using KPF_6. Ligands **HL$_{10}$** and **HL$_{11}$** were obtained in relatively good yields of 81 to 94 % respectively as yellowish-brown viscous oil. These ligands are stable when stored at room temperature even for prolonged time. When ion exchange from I^- to BF_4^- to produce **HL$_{12}$** was attempted using KBF_4 as a salt, the ^{19}FNMR did not show peak that could be assigned to a fluorine signal. The fluorine peak was observed in the ^{19}FNMR spectrum only when $AgBF_4$ was used as a salt to perform the ion exchange to produce **HL$_{12}$**.

It was found very difficult to confirm ion exchange, I^- to PF_6^-, for ligand **HL$_{10}$** to **HL$_{11}$**, using ^{1}HNMR. There are no observable shifts in the peak positions, especially in the aliphatic region for protons signals **11**, **12**, **13**, and **16**, Figure **2.17**. An example of the spectrum that was obtained for the exchange of I^- to PF_6^- is shown in Figure **2.17**.

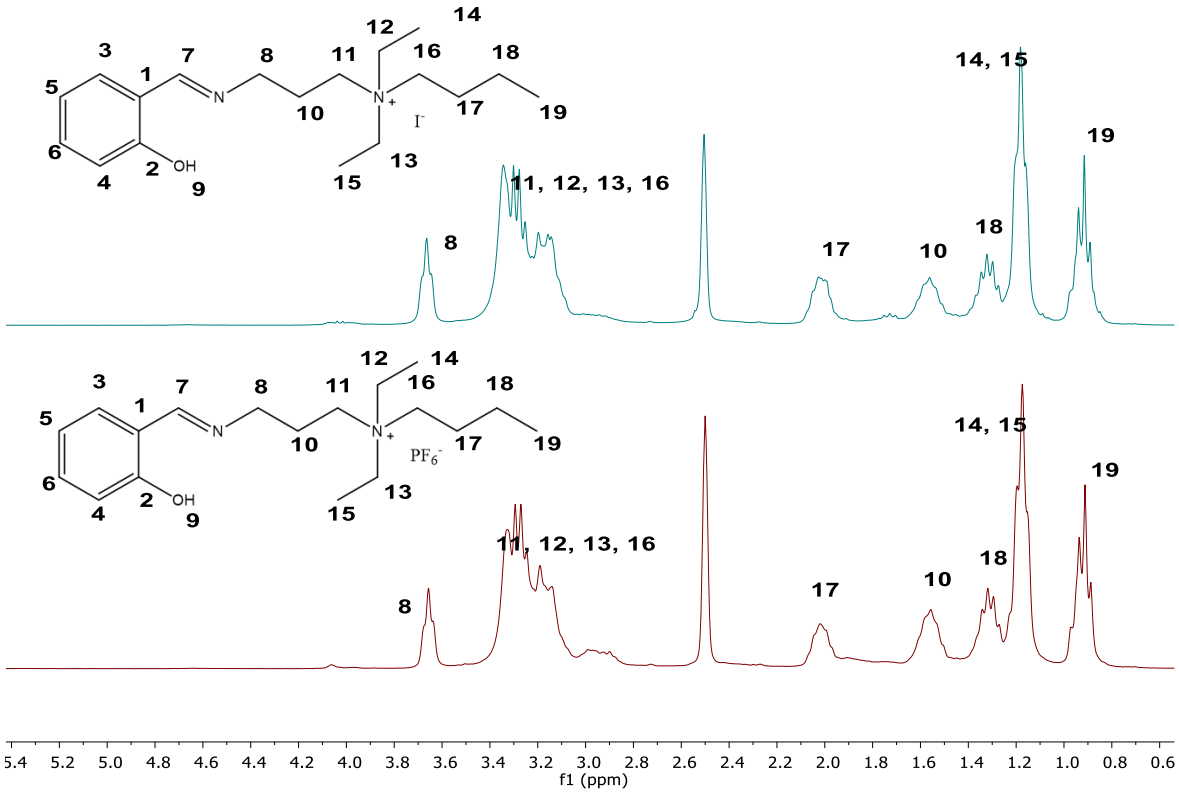


Fig. 2.17: *Stacked ^{1}HNMR spectra (DMSO) for ligand **HL$_{10}$** and **HL$_{11}$***

The presence of PF_6^- as a counter ion was conformed with ^{19}FNMR spectroscopy. A ^{19}FNMR spectrum like the one that was obtained for **HL$_8$**, Figure **2.11**, was obtained. One doublet peak was observed at 70.1 ppm, and this was expected because fluorine atoms in the ligands are all in the same environment. The peak is observed as a doublet due to coupling to the phosphorus atom which is NMR active. The ^{19}FNMR spectrum (Figure **2.18**) that was obtained for ligand **HL$_{12}$** is a bit different from that was obtained for products **HL$_{11}$** and **HL$_8$**. The spectrum shows a singlet peak a 150 ppm together with a low intensity peak which is a result of isotopologues. This was expected because the fluorine atom is not coupling with any NMR active nuclei about 3 bonds

away. The chemical environment is also different due to the difference in the interacting nuclei as the fluorine is bonded to boron instead of phosphorus like in ligands **HL_8** and **HL_{11}**.

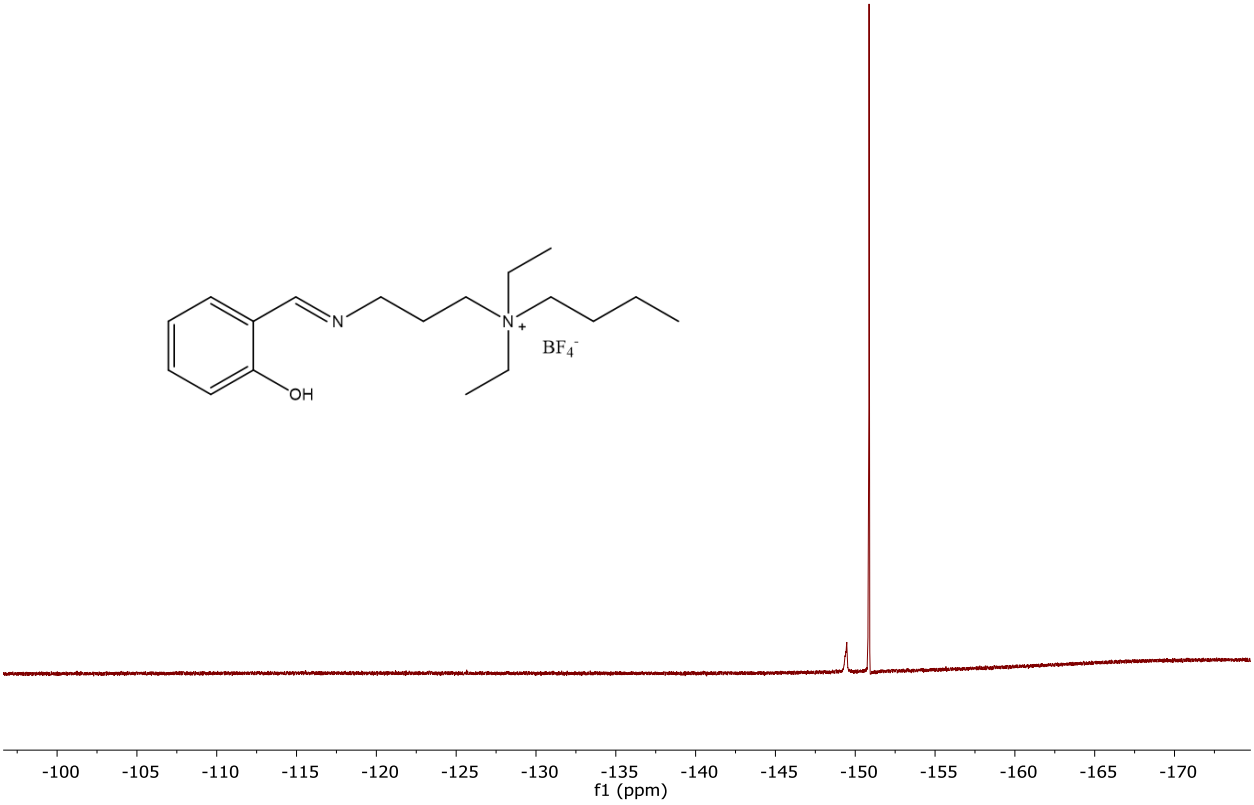


Fig. 2.18: *^{19}FNMR spectra ($CDCl_3$) for ligand **HL_{12}***

The presence of BF_4^- as a counter ion was confirmed with boron NMR spectroscopy. A boron peak was clearly observed around zero ppm, Figure **2.19**. The spectrum also shows a broad peak on the background and this peak can be assigned to the boron in the NMR tube which is normally made of borosilicate glass. The sharp singlet can be assigned to ^{11}B nuclide of the boron atom in BF_4^-. ^{11}BNMR is more sensitive and yield more sharper signals than ^{10}BNMR. This peak is usually observed as a singlet because the coupling between boron and the fluorine atoms produces negative and positive components that cancel out.

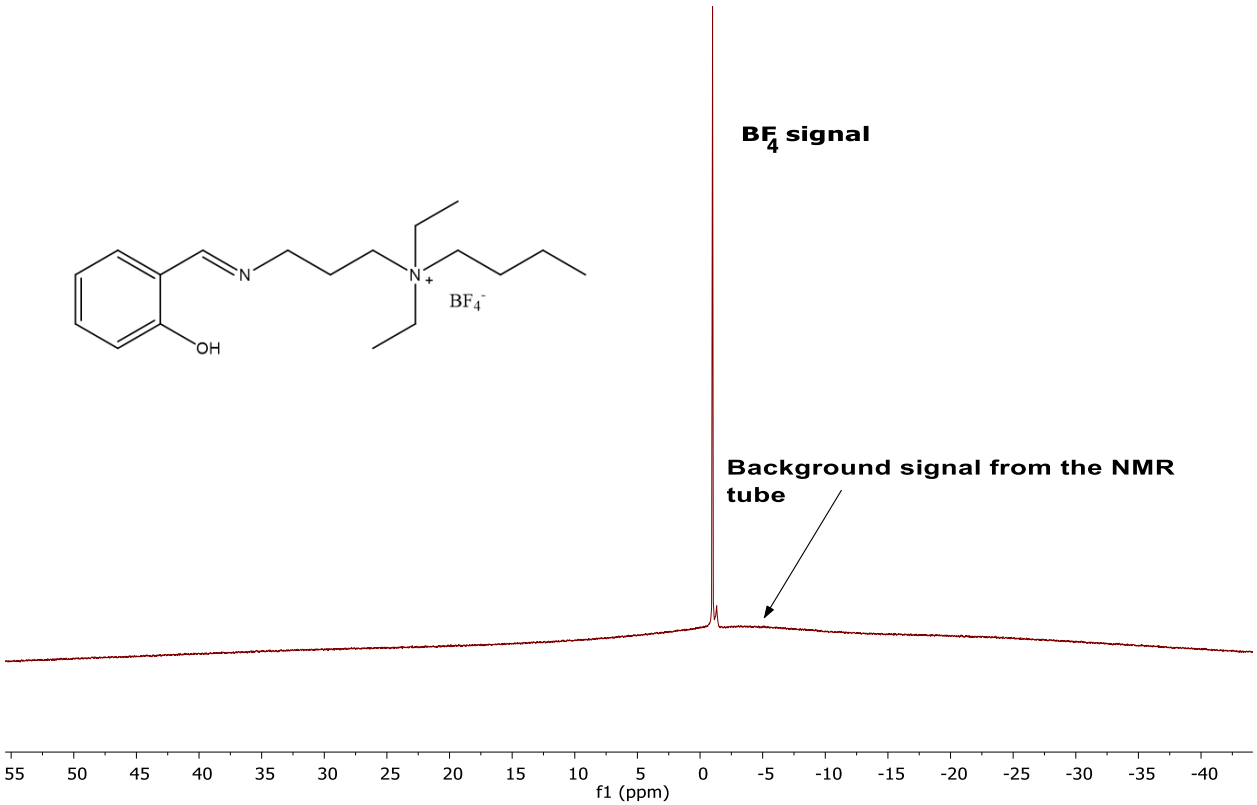


Fig. 2.19: *^{11}BNMR spectrum ($CDCl_3$) for ligand* ***HL_{12}***

The ionic functionalized ligands were also characterized with FTIR spectroscopy. These ligands also contain the characteristic imine (HC=N-) and phenolic (C-O) functionalities. Bands due to imine bond stretching frequency are observed at 1628, 1630, 1630 and 1629 cm^{-1} for ligands **HL_7**, **HL_8**, **HL_{10}**, and **HL_{11}** respectively. The phenolic (C-O) band stretching frequency for these ligands was observed at 1277, 1277, 1278, 1278 cm^{-1} respectively.

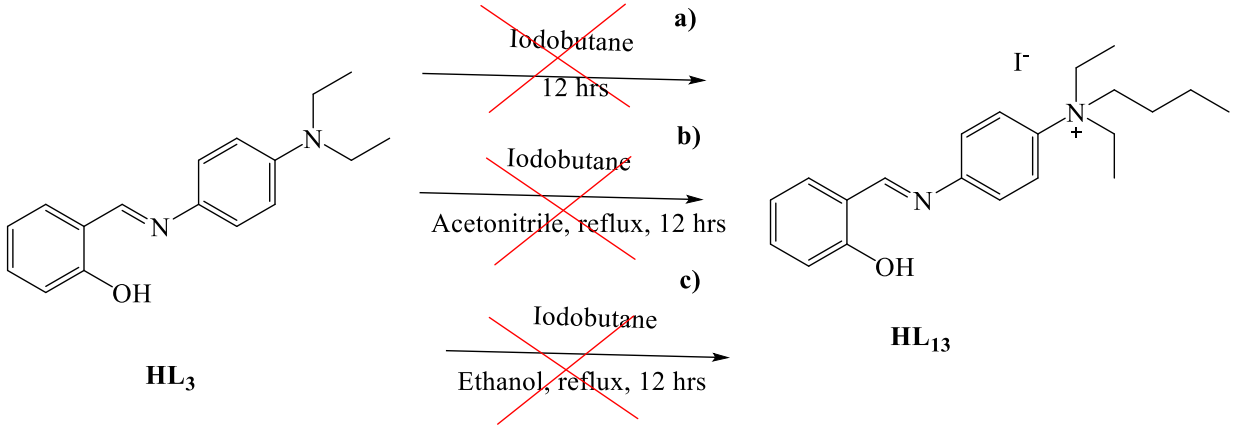
The elemental analysis data obtained for the IL functionalized ligands **HL_7**, **HL_8** and **HL_{10}** agreed with the proposed structures and this data is summarized in Table **2.6**. The positive mode mass spectrometry data confirms that the ligands were obtained as $[M - X]^+$ where 'X' represent either I^-, PF_6^- and BF_4^- for ligands **HL_7**, **HL_8**, **HL_{10}**, **HL_{11}** and the data is summarized in Table **2.6**. The negative mode mass spectrometry data confirms the presence of the counter ions I^- for ligands **HL_7** and **HL_{10}**. It also confirms the presence of PF_6^- for ligands **HL_8** and **HL_{11}**.

Table 2.6: Yield, mass spectrometry, FT-IR and elemental analysis data for ionic functionalized ligands

Ligand	Yield (%)	Formula	ESI MS $[M+H]^+$	ESI MS $[M]^-$	FT-IR (cm^{-1})		Found (Calc)		
			Found (Calc)	Found (Calc)	ν (C=N)	ν (C-O)	C	H	N
HL_7	98.2	$C_{17}H_{24}IN_3O$	286.1919 (286.1906)	126.9048(126.9050)	1628	1277	48.94 (49.16)	5.98(6.31)	9.66(10.12)
HL_8	98.7	$C_{17}H_{24}F_6N_3OP$	286.1919 (286.1914)	144.9749(144.9647)	1630	1277	46.86(46.38)	6.24(6.14)	9.53(9.55)
HL_{10}	94.0	$C_{18}H_{31}IN_2O\cdot 1(1/2)H_2O$	291.2434 (291.2436)	126.9051(126.9050)	1630	1276	48.93(48.50)	7.79(7.69)	6.53(6.29)
HL_{11}	92.1	$C_{18}H_{31}F_6N_2OP\cdot H_2O$	291.2431 (291.2436)	144.9651(144.9647)	1629	1276	47.7(47.57)	7.6(7.32)	5.8(6.16)

2.2.2.3 Preparation of ionic liquid functionalized ligands HL_{13}

Several attempts were made to prepare ligand **HL_{13}** from **HL_3** as shown in Scheme **2.6**. In the first method the reaction was performed neat and in the second case the reaction was performed in the presence of a solvent, acetonitrile. These methods were adopted from the procedure that was used to alkylate **HL_5**. A third method was attempted, and this method was adopted from literature where solvent was changed to a protic solvent, ethanol [9].



Scheme 2.6: *Synthetic procedure for the preparation of IL functionalized ligands* ***HL_{13}***

These three methods all failed to produce the target ligand, **HL_{13}**. The failure was conformed with ^{1}HNMR spectroscopy. The spectra of the reaction residue obtained after work up of the reactions looked the same as that of ligand **HL_3** for all three experiments performed. The ^{1}HNMR spectrum of the experiment of **HL_3** and iodobutane in acetonitrile is shown in Figure **2.20**. These results indicated that there was no reaction that occurred between the neutral ligand, **HL_3** and iodobutane.

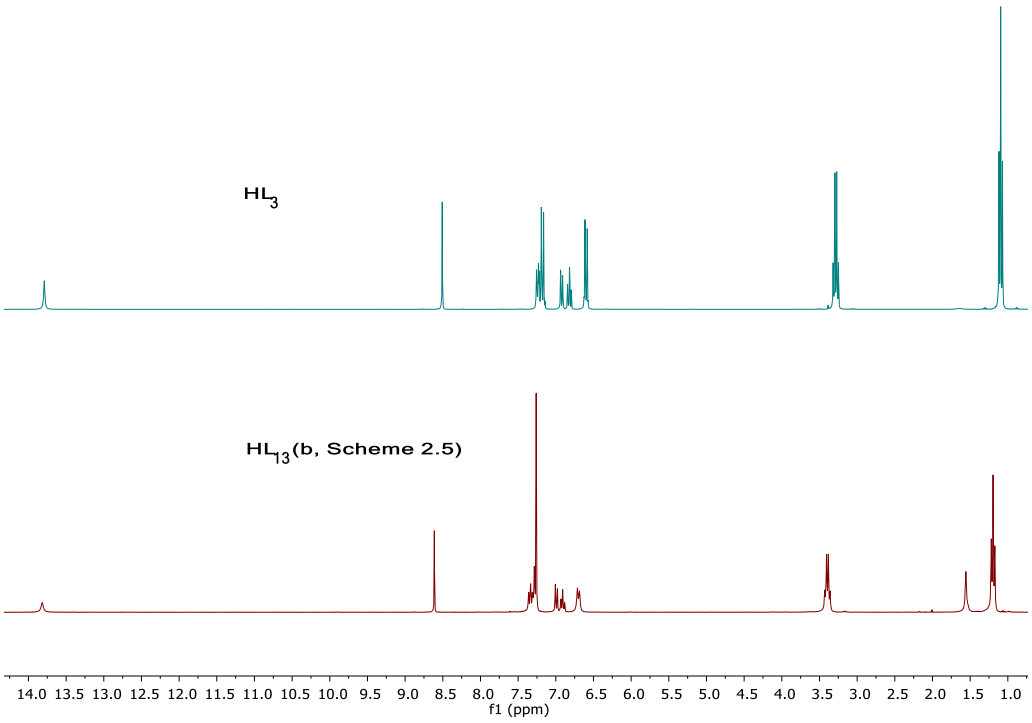
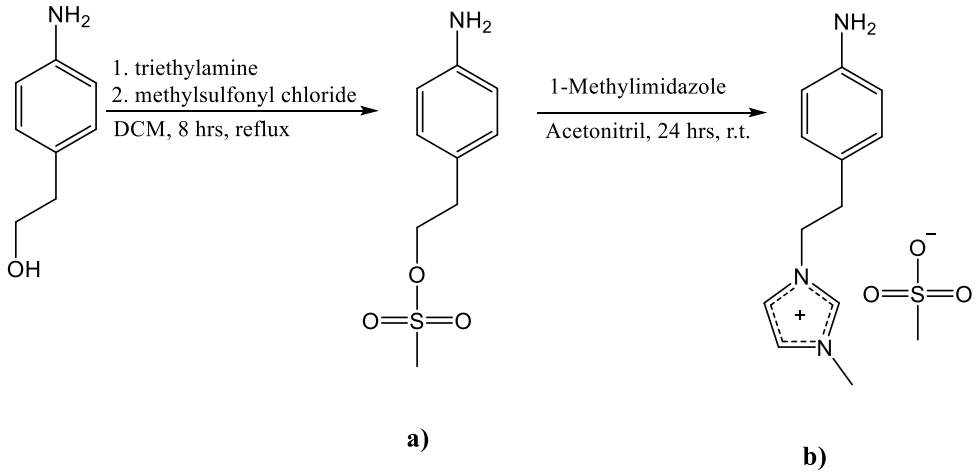


Fig. 2.20: *Stacked [1]HNMR spectra for ligand* ***HL₃*** *and* ***HL₁₃*** ***(b****, Scheme* ***2.5)***

2.2.2.4 Preparation of ionic liquid functionalized ligands HL_{14}

Ligand **HL_4** has two -OH groups which potentially could make it difficult to selectively add an ionic functionality to its backbone. A literature procedure [7] was therefore followed for the synthesis of **HL_{14}**, where the -OH group of 4-aminophenylethyl alcohol was transformed into an imidazolium group as shown in Scheme **2.7**. The sulfonated aniline derivative (**a**)was prepared and confirmed with ^{1}HNMR spectroscopy (appendix section, Figure **S-10)**. Successful alkylation of 1-methylimidazole using the sulfonated aniline to produce the imidazolium ionic liquid (**b**) was confirmed with ^{1}HNMR spectroscopy (Figure **2.21**). Product **b** was found unstable in the open atmosphere where it decomposed back to the starting materials and this was confirmed with ^{1}HNMR spectroscopy. It was therefore stored under inert atmosphere.



Scheme 2.7: *Synthetic procedure for the preparation of intermediates '**a**' and '**b**' in the preparation of* ***HL₁₄***

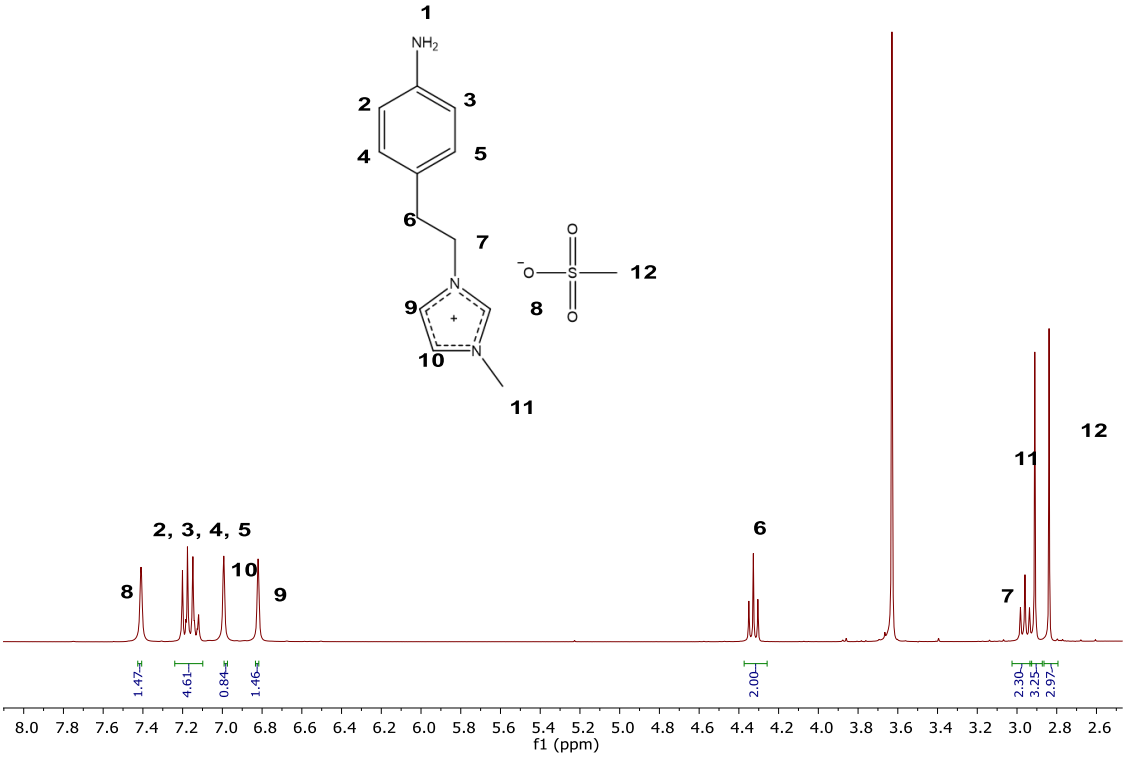
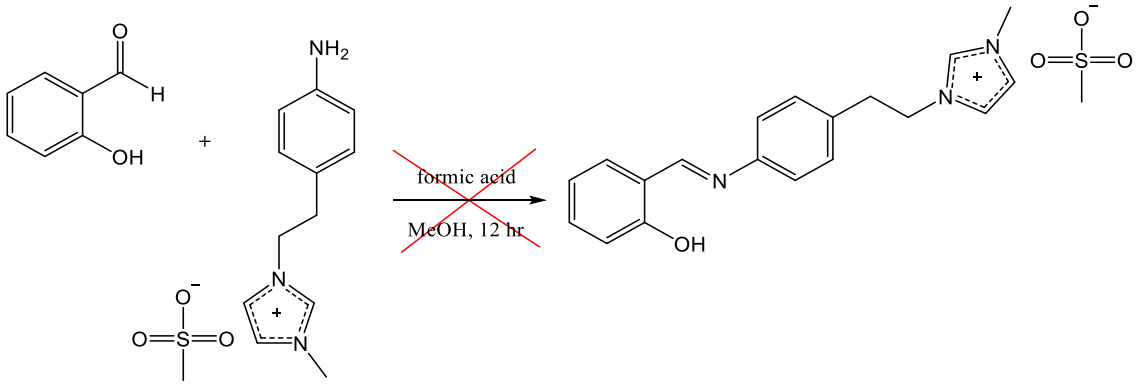


Fig. 2.21: *[1]HNMR spectra for ligand compound 'b' Scheme* ***2.6***

An attempt was made to prepare an ionic functionalized salicylaldimine ligand in a reaction between the ionic functionalized amine and salicylaldehyde, Scheme **2.8**. The reaction product was analyzed with ^{1}HNMR spectroscopy and the spectrum confirms multiple products, Figure **2.22**. Firstly, there is a confirmation of the presence of starting materials, amine, and the aldehyde. The aldehyde is confirmed with the presence of the peak at 9.91 ppm. The other peaks could be assigned to the newly formed product. The most visible peak that could be assigned to the newly formed product is the one at 8.40 ppm. This peak could be from the desired product as the condensation product forms an imine bond (HC=N) which its proton appears around this region.



Scheme 2.8: *Synthetic procedure for the preparation of IL functionalized ligands* ***HL₁₄***

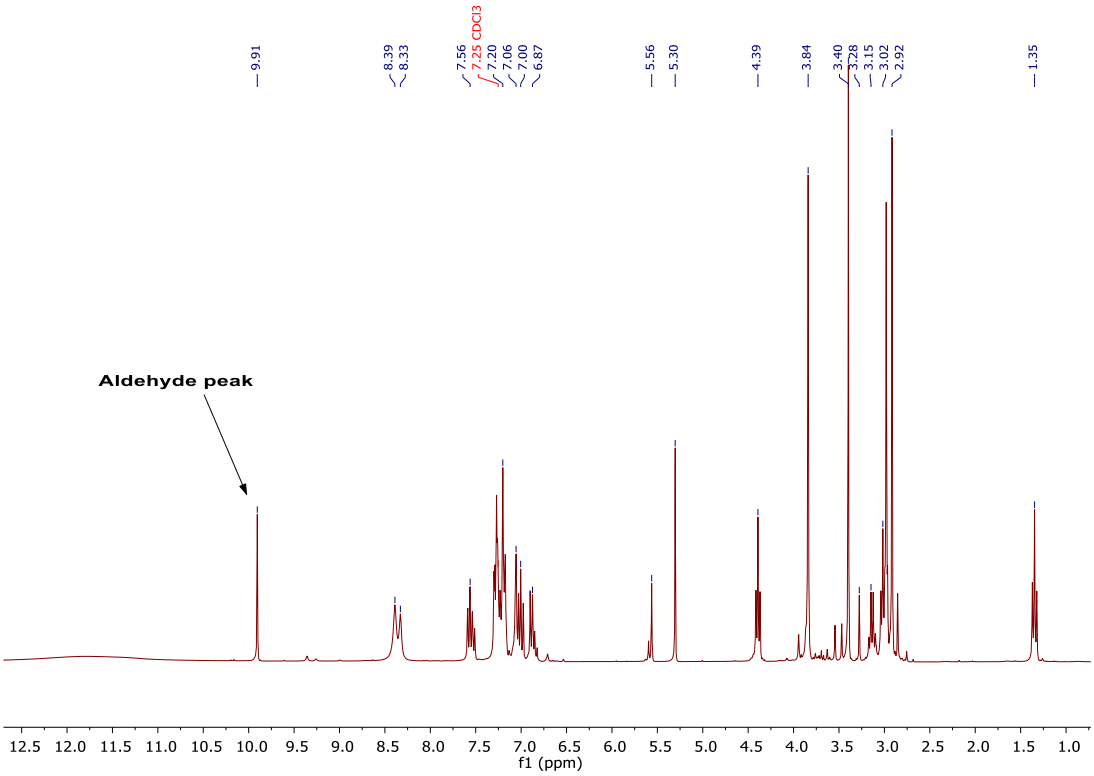


Fig. 2.22: *^{1}HNMR spectrum for ligand* ***HL$_{14}$***

2.3 Conclusion

Neutral ligands (**HL$_1$** – **HL$_6$**) were successfully synthesized and characterized with analytical techniques such as NMR and FT-IR spectroscopy, mass spectrometry and elemental analysis. All these techniques confirmed that the desired neutral ligands were successfully prepared with moderate to good yields ranging 69 – 94 %. Ligands **HL$_1$** – **HL$_5$** were obtained as yellow solids while ligand **HL$_6$** was obtained as a yellow viscous oil.

Ionic functionalized ligand **HL$_7$** was successfully prepared and characterized with analytical techniques with a yield of 84 %. This ligand was obtained as viscous yellow oil. Ion exchange of HL7 with KPF6 to produce **HL$_8$** as a yellow viscous oil with yield of 94 % was successful, however ion exchange of HL7 with BF4 did not produce **HL$_9$** as expected. Confirmation of the ion exchange experiments was achieved with NMR spectroscopy.

Preparation of ligand **HL$_{10}$** was achieved by quaternization of the amino nitrogen with iodobutane. Successful synthesis of this ligand was confirmed with mass spectrometry. The ^{1}H-NMR spectra

of this ligand in $CDCl_3$ and DMSO exhibited two signals for the HC=N and OH proton signals respectively indicating that there may be a solvent effect resulting in different ligand conformations. Attempts to prepare ligands **HL_{13}** and **HL_{14}** were unsuccessful as confirmed with ^{1}H-NMR spectroscopy.

2.4 Experimental

2.4.1 Material and instrumentation

All chemical reactions and manipulations were performed on a dual vacuum/nitrogen line using standard Schlenk techniques unless otherwise stated. Reagent grade chemicals were obtained from Sigma Aldrich and used as received. All solvents were dried under appropriate drying reagent and distilled prior to use. ^{1}HNMR (300, 400 and 500), ^{13}CNMR (75), ^{31}P (202.45 MHz) ^{19}F (376.46 Mhz) and ^{11}BNMR (128.38) NMR spectra were recorded on a Varian spectrometer using tetramethylsilane as an internal standard. Chemical shifts are reported in (ppm) and referenced to residual proton in $CDCl_3$ and DMSO NMR solvent. FTIR spectra were recorded on Bruker TENSOR 27 spectrometer using ATR. Mass spectra of the ligands were recorded on Advion Expressional L compact mass spectrometer while those of the complexes were recorded on a Bruker Compact Ultimate 3000 HR-MS. Elemental analysis were performed in the micro analytical laboratory of the University of Johannesburg and the University of Cape Town. Melting points of the ligands were recorded using a Suart SMP30 melting point apparatus.

2.4.2 Preparation of salicylaldimine ligands HL_1 – HL_5

The synthesis of ligands is described using conditions for **HL_1** as an example. To a methanol solution (15 mL) of salicylaldehyde (1.279 g, 12 mmol) in a Schlenk tube was added formic acid (0.5 mL) followed by aniline (1.49 g, 16 mmol). The resulting reaction mixture was stirred at room temperature for approximately 15 h after which a yellow solid was formed. The solid was filtered and recrystallized from hot methanol. The recrystallized product was then dried under vacuum.

2.4.3 Preparation of salicylaldimine ligand HL_6

To a methanol solution (15 mL) of salicylaldehyde (1.279 g, 12 mmol) in a Schlenk tube was added 3-(diethylamin) propylamine (1.563 g, 12 mmol). The resulting reaction mixture was stirred at room temperature for approximately 15 h. After this time, the solvent was removed by rotary

evaporator and the resulting yellow oil was further dried under reduced pressure. There was no further purification performed for this ligand.

2.4.4 Preparation of the salicylaldimine ligand HL_7

Ligand **HL_5** (0.9 g, 3.934 mmol) was dissolved in acetonitrile (15 ml) and iodobutane (3.934 mmol, 0.45 ml) was added to the resulting solution. The mixture was stirred under reflux for 12 h. Solvent of the reaction mixture was removed using a rotary evaporator resulting in a yellow oil. The oil was washed with diethyl ether 3 times to remove any unreacted iodobutane. Then the oil was further dried under reduced pressure.

2.4.5 Preparation of the salicylaldimine ligand HL_8

Ligand **HL_7** was dissolved in ethanol (0.2809 g, 0.681 mmol) and to the resulting ethanol solution was added KPF_6 (0.1254 g, 0.681 mmol). The resulting reaction mixture was stirred under reflux for 10 hours. After this time the solvent of the reaction mixture was removed resulting in a mixture of a white solid and a yellow oil. The mixture was dissolved in dichloromethane (10 ml) and the suspended white solid was isolated by vacuum filtration. The solvent of the filtrate was removed resulting in a yellow oil.

2.4.6 Preparation of salicylaldimine ligand HL_{10}

Ligand **HL_6** (0.2025 g, 0.864 mmol) was dissolved in iodobutane (2 ml) and the resulting solution was stirred at 70 ^oC for 12 hours. During this time, a sticky very viscous oil deposits on the walls of the round bottom flask. The solution was decanted, and the oil was washed several times with diethyl ether (5 ml). The oil was then dried under reduced pressure.

2.4.7 Preparation of salicylaldimine ligand HL_{11}

Ligand **HL_{10}** (31.9 mg, 0.1094 mmol) was dissolved in ethanol and to the resulting ethanol solution was added KPF_6 (20.2 mg, 0.1094 mmol). The resulting reaction mixture was stirred under reflux for 10 hours. After this time, the solvent of the reaction mixture was removed resulting in a mixture of a white solid and a yellow oil. The mixture was dissolved in dichloromethane (10 ml) and the suspended white solid was isolated by vacuum filtration. The solvent was removed from the filtrate resulting in a yellow oil.

2.4.8 Preparation of salicylaldimine ligand HL_{12}

Ligand **HL_{10}** (31.9 mg, 0.0763 mmol) was dissolved in methanol and to the resulting solution was added $AgBF_4$ (14.9 mg, 0.0763 mmol). The resulting reaction mixture was stirred at room temperature for 10 min and a cream white solid formed. After this time, the solvent was removed resulting in a mixture of a white solid and a yellow oil. The mixture was dissolved in dichloromethane (10 ml) and the suspended white solid was isolated by vacuum filtration. The solvent was removed from the filtrate resulting in a dark brown oil.

2.5 References

[1] A. Majumder, M. G. Rosair, A. Mallick, N. Chattopadhyay and S. Mitra, *Polyhedron,* vol. 25, pp. 1753-1762, 2006.

[2] N. E. Jacobsen, W. Zhang and L. M. Guler, *J. Am. Chem. Soc.,* vol. 113, pp. 6703 - 6704, 1991.

[3] M. Palucki, S. N. Finney, J. P. Pospisil, L. M. Guler, T. Ishida and N. E. Jacobsen, *J. Am. Chem. Soc.,* vol. 120, pp. 948 - 954, 1998.

[4] A. W. Zoubi, *Spectrochim. Acta,* vol. 132, pp. 854 - 870, 2014.

[5] A. W. Zoubi and G. Y. Ko, *J. Organomet. Chem.,* vol. 822, pp. 173 - 188, 2016.

[6] G. Cozzi, *Chem. Soc. Rev,* vol. 33, pp. 410-421, 2004.

[7] R. Kagit, O. Dayan and N. Ozdemir, *Polyhedron,* vol. 117, pp. 504 - 412, 2016.

[8] P. Nehra, B. Khungar, K. Pericherla, C. S. Sivasubramania and A. Kumar, *Green Chem,* vol. 16, pp. 4266 - 4271, 2014.

[9] K. Kuca, M. Kivala and V. Dohnal, *J. Appl. Biomed.,* vol. 2, pp. 195 - 198, 2004.

[10] Y. Peng, Y. Cai, G. Song and J. Chen, George Thieme Verlag Stuttgart, New York, 2005.

[11] S. Saha, G. Basak and B. Sinha, *J. Chem. Sci.,* vol. 130:9, pp. 1 - 9, 2018.

[12] B. Khungar, S. M. Rao, K. Pericherla, P. Nehra, N. Jain, J. Panwar and A. Kumar, *C. R. Chimie,* vol. 15, pp. 669 - 674, 2012.

[13] C. G. Percy and D. A. Theornton, *J. Inorg. Nucl. Chem,* vol. 34, pp. 3357 - 3367, 1972.

[14] G. O. Dudek and E. P. Dudek, *Chem. Commun.,* vol. 2, pp. 464 - 466, 1965.

[15] K. Ueno and E. Martell, *J. Phys. Chem.,* vol. 60, pp. 1270 - 1275, 1955.

[16] N. E. Jacobsen and P. T. Yoon, *Science,* vol. 299, pp. 1691-1693, 2003.

[17] A. Carreno, M. Gacitua, D. Paez-Hernandez, R. Polanco, M. Preite, A. J. Fuentes, C. G. Mora, I. Chavez and R. Arratia-Perez, *New J. Chem.,* vol. 39, pp. 7822 - 7831, 2015.

[18] A. Vogt, S. Wolowiec, L. R. Prasas, A. Gupta and J. Skarzeviski, *Polyhedron,* vol. 17, p. 1231, 1998.

[19] R. J. Zamian and R. E. Dockal, *Transition Met. Chem.,* vol. 21, p. 370, 1996.

[20] K. Ueno and E. A. Martel, *J. Phys. Chem. ,* vol. 60, p. 1270, 1956.

[21] A. Ouadi, B. Gadenne, P. Hesemann, E. J. J. Moreau, I. Billard, C. Gillard, S. Mekki and G. Moutiers, *Chem. Eur. J.,* vol. 12, pp. 3074 - 3081, 2006.

[22] R. Kannappan, S. Tanasae, I. Mutikainen, U. Turpeinen and J. Reedijk, *Polyhedron,* vol. 25, pp. 1646-1654, 2006.

[23] H. Schiff, *Ann. Chem. Suppl.,* vol. 3, pp. 343 - 349, 1864.

Chapter 3

Synthesis and characterization of bis-(salicylaldiminato) Co(II), Cr(II) and Cr(III) complexes

Contents

3.1 Introduction 86

3.2 Results and discussions 88

3.2.1 Synthesis and characterization of neutral chromium and cobalt complexes **1** - **18** 88

3.2.2 Synthesis and characterization of ionic functionalized bis-(salicylaldiminato)Cr(II), Cr(III) and Co(II) complexes 109

3.3 Conclusion 114

3.3.1 Neutral bis-(salicylaldiminato) complexes 114

3.3.2 Ionic functionalized bis-(salicylaldiminato) Cr(II), Co(II) and Cr(III) 114

3.4 Experimental 115

3.4.1 Material and instrumentation 115

3.4.2 Preparation of the sodium salt of salicylaldimine ligands (**HL_1** - **HL_6**) for preparation of chromium complexes 115

3.4.3 Preparation of the sodium salt of salicylaldimine ligands (**HL_1** - **HL_6**) for the preparation of cobalt complexes 116

3.4.4 Preparation of Cr(II) complexes **1** - **6** 116

3.4.5 Preparation of Cr(III) complexes **7** - **12** 116

3.4.6 Preparation of Co(II) complexes **13** – **18** 117

3.4.7 Preparation of ionic functionalized Cr(II) complexes **19** and **20** 117

3.4.8 Preparation of ionic functionalized Cr(III) complexes **21** and **22** 117

3.4.9 Preparation of ionic functionalized bis-(salicylaldiminato)Co(II) complexes (**23** and **24**)……..118

3.5 References 118

3.1 Introduction

Several reports have been made in literature on the synthesis of Cr(III) and Co(III) [1, 2] complexes derived from tetradentate, salen, Schiff base ligands. These complexes are of interest as catalysts in the coupling of CS_2 or CO_2 with epoxides and have been shown to produce catalyst systems with high activity [3, 4, 5]. Schiff base ligands have also attracted attention because of their ease in preparation which brings flexibility in varying the architecture around the metal center of the complex. This is important because different substituent groups, that are electron donating or electron withdrawing can be incorporated on the ligand structure or groups which have different steric properties. The nature of the different substituent groups on the ligand backbone can affect the metal complexes and therefore its catalytic activity [6].

Bidentate Schiff base ligands, such as salicylaldimines, have already been reported to provide even more flexibility in substituent variation on the ligands backbone, however there are few reports on the preparation of Cr(III) or Co(III) complexes derived from salicylaldimine ligands with a pentacoordinate geometry similar to the salen complexes which have been shown to be active for CS_2/CO_2 coupling with epoxides.

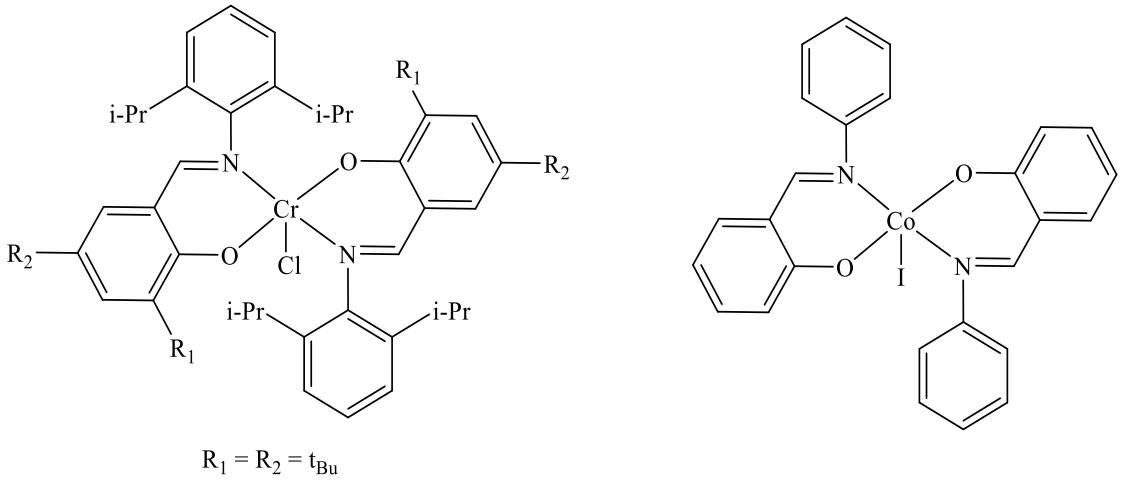


Fig. 3.1: *Pentacoordinate Cr(III) (**a**) [7] and Co(III) (**b**) [8] complexes derived from salicylaldimine ligands.*

An example of a Cr(III) complexes derived from salicylaldimine ligands with a pentacoordinate coordination sphere similar to Cr(III) salen complexes are those prepared by Gibson et al. as shown in Figure **3.1 (a).** These complexes were synthesized by treatment of the $CrCl_3(THF)_3$ adduct with 2 moles of a corresponding salicylaldimine ligand. Trans-O, O and cis-N, N dispositions were observed for the two N, O chelate ligands [7]. There are also currently no reports on the synthesis of Cr(II) complexes derived from salicylaldimine ligands to our knowledge.

Likewise, Co(III) complexes with a pentacoordinate geometry similar to Co(III) salen complexes, Figure **3.1 (b)**, are just as rare. The only example that could be found was the complexes prepared by Sibauih et al. The complexes were prepared by oxidizing the metal center using iodine. These complexes were studied for the coupling of CO_2 with epoxides and were observed to exhibit good activity [8]. In contrast, the preparation of tetracoordinate bis-(salicylaldiminato)Co(II) complexes have been explored by many researchers such as Chandran and coworkers [9] for other application but not for the coupling of CS_2/ CO_2 with epoxide.

One of the objectives of this study is the preparation and characterization of Cr(III) and Co(III) complexes which have a similar coordination sphere as complexes derived from salen ligands and study the catalytic performance of these complexes for CS_2/CO_2 coupling with propylene oxide. In this investigation, salicylaldimines are targeted as ligands due to their synthetic flexibility which allow for easy tailoring of the ligand architecture and metal complex properties. In this regard ligands containing ionic functionalities such as the manganese complex shown in Figure **3.2** are also targeted due recent reports which demonstrated that complexes with ionic groups exhibit activity for the targeted coupling reaction without requirement of a co-catalyst [11, 12]. In addition, the metal complexes in the 2+ oxidation state are also of interest to investigate the influence of the oxidation state of the metal on the catalytic performance. This chapter reports on the synthesis and characterization of both chromium and cobalt complexes derived from salicylaldimines.

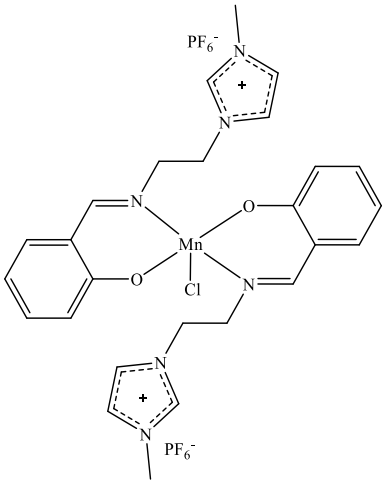


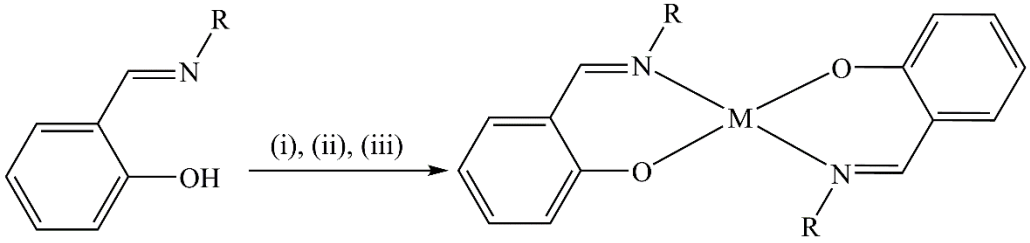
Fig. 3.2: *Ionic functionalized Mn(III) complexes reported by Ceng and co-workers [10]*

3.2 Results and discussions

In chapter 2 the synthesis and characterization of two classes of salicylaldimine ligands, neutral (**HL_1- HL_6)** and ionic tagged (**HL_7-HL_{12}**) were reported. These ligands were utilized to synthesis chromium and cobalt complexes. This section is focused on discussing the synthesize methodologies that were investigated as well as the characterization of the successfully prepared metal complexes.

3.2.1 Synthesis and characterization of neutral chromium and cobalt complexes 1 - 18

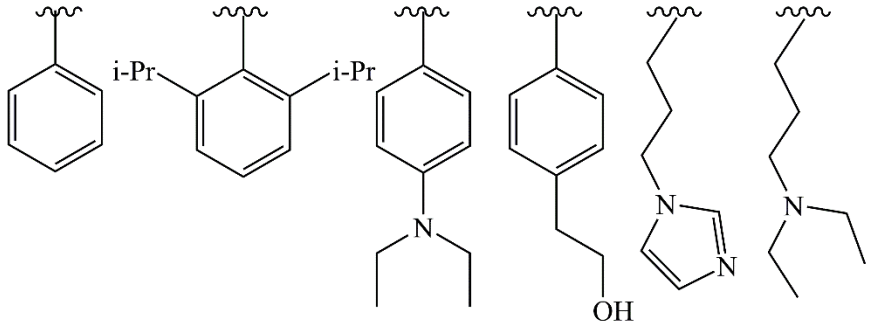
Mononuclear tetra-coordinate neutral chromium (II) complexes **1** – **6** and cobalt (II) complexes **13 – 18** were quite readily synthesized via a 2:1 reaction of the sodium salt of the ligands with anhydrous $CrCl_2$ and $Co(OAc)_2{\cdot}4H_2O$ respectively as shown in Scheme **3.1**. Initial attempts to synthesize Cr (III) complexes by using a literature procedure where $CrCl_3{\cdot}6H_2O$ was reacted with the sodium salt of the ligand prepared with NaOH [13] was unsuccessful. No reaction between the metal salt and sodium salt of the ligands was observed. The metal salt was replaced $Cr(OAc)_2OH$ and NaOH as well as NaH investigated as base to deprotonate the ligand, however these attempts also did not result in complexation. These unsuccessful attempts were confirmed using FT-IR spectroscopy that showed the ligand did not coordinate to the metal.



(i): NaH, $CrCl_2$, THF
(ii): NaH, $CrCl_3$(THF), THF
(iii): NaOH, $Co(OAc)_2 4H_2O$, MeOH

M= Cr (II):	**1**	**2**	**3**	**4**	**5**	**6**
Cr (III)Cl:	**7**	**8**	**9**	**10**	**11**	**12**
Co (II):	**13**	**14**	**15**	**16**	**17**	**18**

R =



Scheme 3.1: *General procedure for the synthesis of bis-(salicylaldiminato) Cr (II), Cr (III) and Co(II) complexes **1** – **18***

Successful complexation was only observed when one equivalent of $CrCl_3(THF)_3$ [14] was reacted with two equivalents of the sodium salt of the ligands producing the mononuclear penta-coordinate complexes **7** – **12** (Scheme **3.1**). All complexes exhibit good solubility in polar organic solvents such as methanol, DMSO and DMF except for complexes **5**, **6**, **11**, **12, 17** and **18** which were only sparingly soluble in DMSO and water. All chromium complexes were found to be highly hygroscopic when exposed to air, with some complexes immediately transforming from a powder to a sticky solid after a prolonged exposure to air. These complexes however did not seem to decompose because when they were dried again and analyzed with FT-IR spectroscopy the spectra obtained were just like those obtained initially.

3.2.1.1 Characterization of neutral Schiff base complexes 1 - 18 with FT-IR and UV-Vis spectroscopy

Complexes **1** - **18** are all paramagnetic and thus NMR spectroscopy could not be used for their characterization. FT-IR spectroscopy was used as preliminary characterization technique to confirm coordination between the metal and the ligands. Comparison of the FT-IR spectra of the metal complex with that of the free ligand indicates that coordination occurs via the azomethine nitrogen and the deprotonated phenolic oxygen as depicted in Scheme **3.3**. The FT-IR spectra obtained for ligand **HL_1**, complex **1** and complex **7** are shown in Figure **3.3** as an example of spectra typically obtained for these Schiff base ligands and metal complexes.

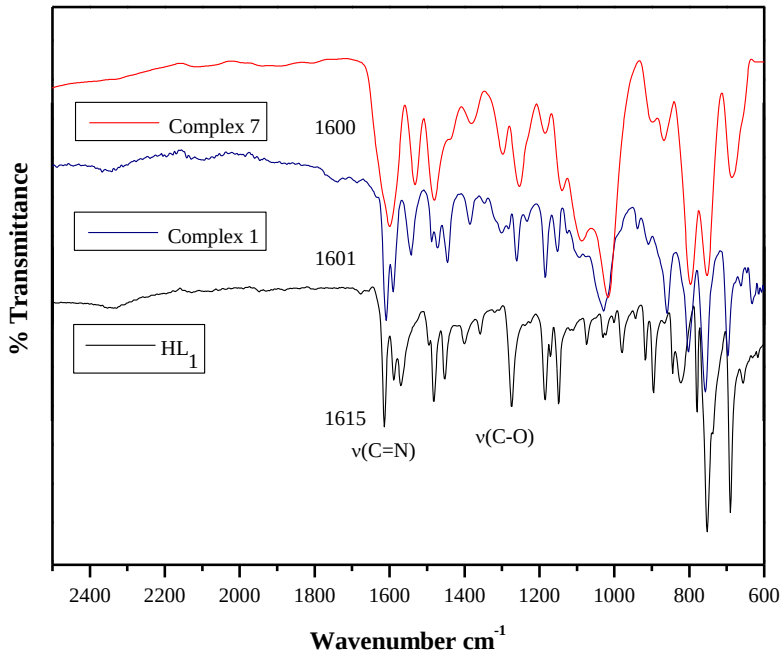


Fig. 3.3: *Overlayed FTIR spectra for ligand **HL_1**, Cr(II) complex **1** and Cr(III) complex **7**.*

It can be observed from Figure **3.3** that the peak assigned to the ν(C=N) stretching frequency shifts to a lower wavenumber upon coordination to Cr(II) and Cr(III) metals. The ν(C=N) stretching frequency is usually shifted to lower frequency upon coordination of the metal to the imino nitrogen resulting in a decrease in the C=N bond order [15]. On the other hand, the peak of ν(C-

O) shifts to a higher wavenumber upon coordination to the metals. This peak usually appears with low intensity upon coordination to the metal [15, 16]. Therefore, these two changes confirm coordination to the azomethine nitrogen and phenolic oxygen atoms.

The FTIR data for all complexes is summarized in Table **3.1**. The imine stretching frequency ν(C=N) is observed in the range 1601-1613 and 1601-1616 cm^{-1} for Cr (II) complexes (**1** - **6**) and Cr (III) complexes (**7** -**12**) respectively. This peak has shifted from 1614-1632 cm^{-1} in the spectrum of the ligand. The phenoxy ν(C-O) stretching frequency has shifted from 1267-1282 cm^{-1} in the spectra of the ligands to 1300 -1321 cm^{-1} and 1286-1332 cm^{-1} for Cr (II) and Cr (III) complexes respectively upon complexation.

The FT-IR spectra of Co(II) complexes (**13 – 18**) exhibited similar changes when to those observed for the Cr(II) and Cr(III) complexes when compared to the ligand spectra. As it can be observed from Table **2.4** the (C=N) in observed in the range 1601 - 1619 cm^{-1} for Co(II) complexes and (C-O) is observed in the range 1291 – 1322 cm^{-1}. This observation was also reported by van Wyk and coworkers [17].

The Uv-vis spectra of the ligands and chromium complexes were recorded in DMSO. The spectra of **HL_1**, complex **1** (Cr (II)) and complex **7** (Cr(III)) are shown in Figure **3.4** as an illustrative example of the spectra that were obtained for the ligands and their corresponding complexes. It can be observed from Figure **3.4** that the spectrum of the ligand exhibits a peak at 340 nm which is assigned to the $\pi - \pi^*$ transition of the ν(C=N) chromophore. This band is normally observed between 270 and 300 nm [18, 19] and the major shift in this band is attributed to conjugation [20]. The spectra of all the ligands exhibit a $\pi - \pi^*$ transition of the ν(C=N) chromophore band between 329 – 411 nm.

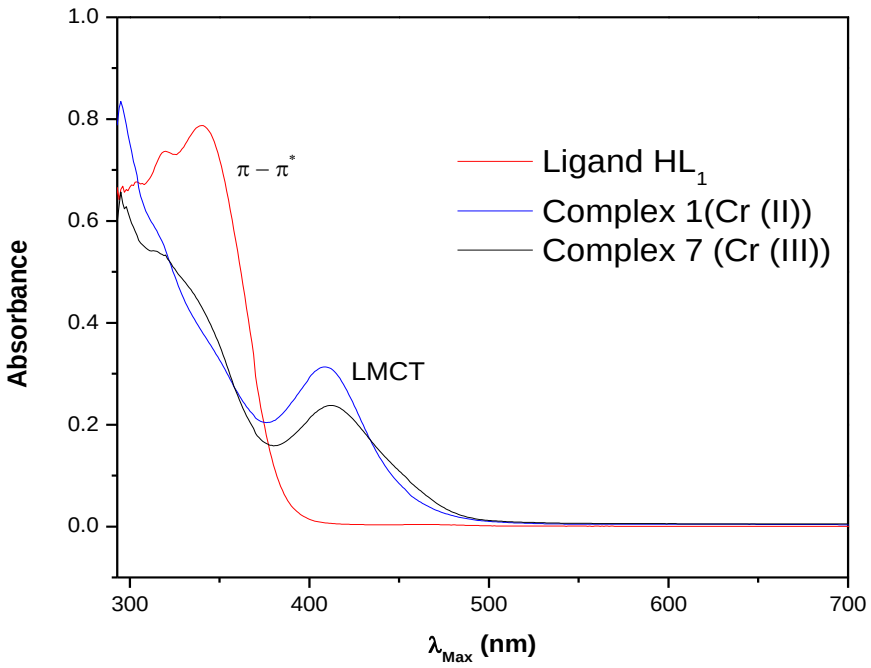


Fig. 3.4: *Overlayed Uv-vis spectra of ligand **HL$_1$**, complex **1** and **7** recorded in DMSO (c = 0.1 mM)*

The π – π* transition band is not observed in the UV-Vis spectra of the complexes due to the formation of the metal–nitrogen bond in the complex which stabilizes the electron pair on the nitrogen atom [21]. It can be observed in some complexes but shifted and that depends on the nature of the substituents of the ligand. This instance is observed in the spectrum for complex **8,** Figure **S-12** appendix section. There are strong bands observed at 411 and 409 nm in the spectra for Cr (II) and Cr (III) complexes **1** and **7** respectively. These bands are attributed to ligand to metal charge transfer transition (LMCT). These charge transfer transitions are probably due to the transfer of an electron from the π-orbitals of the ligand to the d-orbital of chromium and it is not observed in the free ligands. For all the complexes this band is observed in the range 390 – 415 and 394 – 419 nm for Cr(II) and Cr(III) complexes respectively, as summarized in Table **3.1**.

In the visible region of the UV-Vis spectra of complex **1** and complex **7**, a broad low intensity band at 591 to 626 nm is observed for the respective complexes (Figure **3.5)**. This band is attributed to the d – d transition of the chromium metal. This band is of low molar absorptivity and Laporte forbidden and thus observed in relatively low intensity [22]. It can be deduced from the data in Table **3.1** that the d – d transitions bands of Cr (III) complex are shifted to a higher wavelength

with respect to those of the Cr (II) complexes and this is due to the requirement of a lower splitting energy for the d – d transition in the Cr (III) complex compared to the Cr (II) complex. The d-d transition bands of both bis-(salicylaldiminato)Cr(II) and Cr(III) complexes show two overlapped bands, Figure **3.6**, which could be due to Jahn Teller effect which is the distortions in the geometries of the metal complexes. This band is observed in all Cr (II) and Cr (III) complexes at 567 – 626 and 594 – 690 nm (Table **3.1**) respectively.

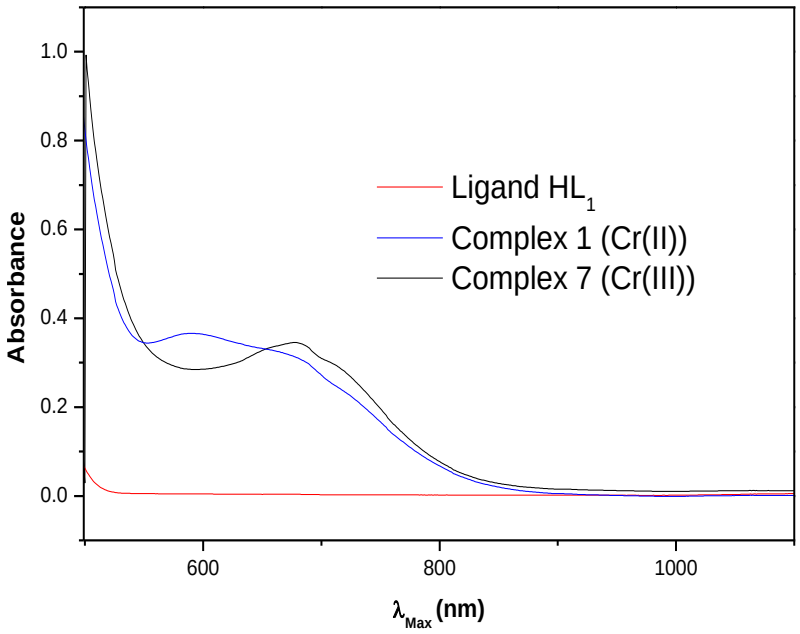


Fig. 3.5: *Overplayed uv-vis spectra of ligand HL_1, complex **1** and **7** recorded in DMSO (c = 10 mM)*

The UV-Vis spectra of Co(II) complexes (**13** – **18**) were recorded in DCM. A different solvent from the Cr complexes was used because complex **14** and **15** did not dissolve completely in DMSO. In Figure **3.6** the overlayed ligand and complex spectra are shown for the Co(II) complexes. In the spectrum of **HL_1** and complex **13,** a $\pi - \pi^*$ transition of the C=N chromophore band at 341 nm [23] is observed for the ligand and not observed for the complex. In the spectrum of complex **13** there is a peak at 390 nm that is not observed in the spectrum of the ligand. This peak can be attributed to $n - \pi^*$ LMCD from the filled p–π orbital of the phenolic oxygen to the empty d orbital of the Co(II) ions [24]. This confirms complexation of the Co(II) metal to the nitrogen and oxygen atoms of the ligand respectively. Similar behavior was observed for complex **16**, Table **3.1**.

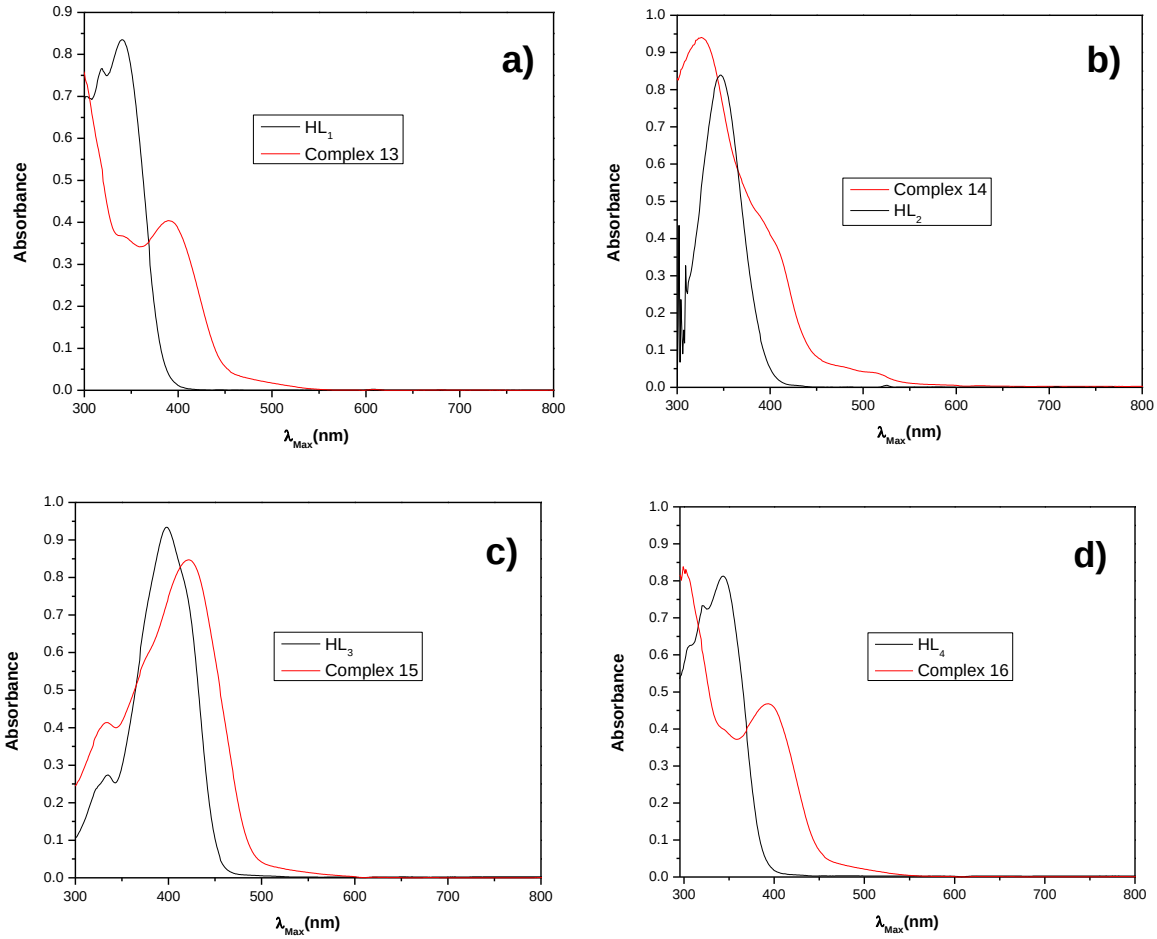


Fig. 3.6: *Overlayed UV-Vis spectra of ligands and the respective Co(II) complexes recorded in DCM (c = 0.1 mM)*

For complexes **14** and **15** (Figure **3.7**, **b** and **c** respectively), a slightly different observation was noted. Complex **14** spectrum shows a major peak at 327 nm and this peak is like the one observed in the ligand spectrum at 345 nm however it is shifted. There is an appearance of a low intensity peak at 406 nm that can be assigned to n – π^* ligand to metal charge transfer. For complex **15** almost similar behavior as in complex **14** is observed in their spectra. There is a peak at 422 nm in the spectrum of complex **15**, Figure **3.7**. This specific peak is like a peak observed at 400 nm in the spectrum of the corresponding ligand **HL3**. This peak is blue shifted in complex **15** while it is red shifted in the spectrum of complex **14**. Complex **14** and **15** both have electron donating groups on the aromatic ring however they are on different position which are ortho- and

para-positions, respectively. This seems to have influenced the direction of the shift of the $\pi - \pi^*$ transition of the C=N chromophore.

Table 3.1: UV-Vis and FTIR spectroscopy data for complexes **1 - 18**

Complex	UV-Vis (λ_{Max} /nm)		FT-IR (cm^{-1})	
	LMCT band	d -d band	ν(C=N)	ν(C-O)
1	406	591, 680, 725	1608	1300
2	400	626, 680	1608	1294
3	415	612	1609	1321
4	407	588, 679	1601	1318
5	394	566	1615	1324
6	390	574	1612	1316
7	411	652, 677, 714	1607	1298
8	403	657, 682, 711	1606	1286
9	419	690	1606	1303
10	411	651, 677, 713	1601	1300
11	402	603	1613	1321
12	394	594	1616	1332
***13**	390	-	1602	1319
14	409	517	1603	1315
***15**	422	-	1608	1319
***16**	392	-	1601	1302
****17**	-	-	1619	1291
****18**	-	-	1618	1322

*The d-d bands were not observed for these complexes, **due to poor solubility in DCM, uv-vis of this complexes was not recorded.

The d – d band transition for Co(II) Schiff base complexes is usually observed at 500 nm. This transition band just like for Cr complexes, is Laporte forbidden and have low molar absorptivity therefore is observed as broad low intensity band. The band is observed at 517 nm for complex **14** at 0.1 nM concentration however it was not observed for other Co(II) complexes **13**, **15**, and **16** at

this concentration. The peak could not be observed even when the concentration was increased to 10 M.

3.2.1.2 Characterization of Schiff base complexes 1 – 18 with cyclic voltammetry

Cyclic voltammetry was used to investigate the oxidation states of the chromium complexes (**1** – **12**). The ligands of the complexes did not show any redox activity between 0 V and -1.1 V; therefore, the curves observed in this range were attributed to the redox activity of the complexes. Figure **3.7** shows voltammograms obtained for complex **3** and **9** as representative of all the voltammograms that were obtained for the complexes. There is a clear reversible peak that is observed at $E_{1/2}$ of -0.784 V for Cr(III) complex **9** which is not observed for Cr(II) complex **3**, Figure **3.7**.

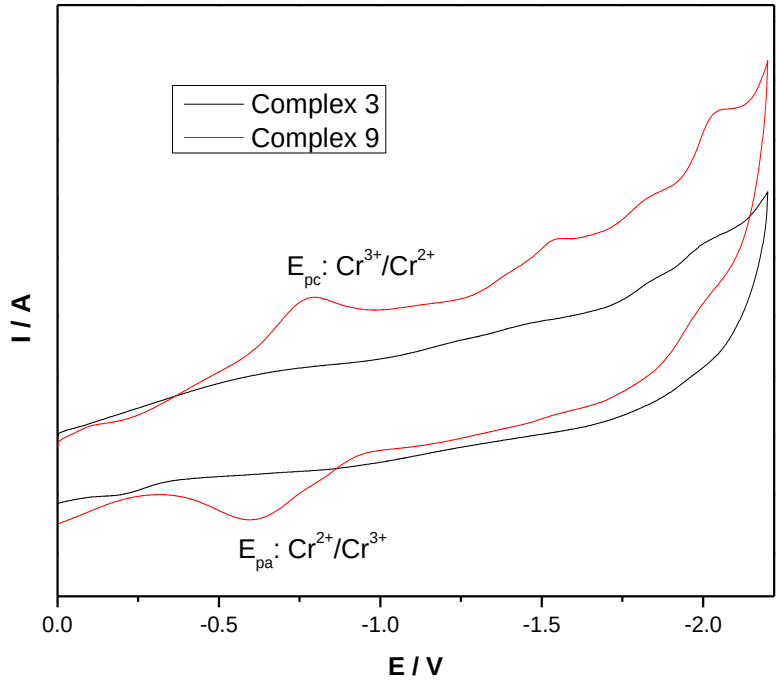


Fig. 3.7: *Overlayed CV voltammogram for 0.5 mM solution of complexes **3** and **9** in DMSO (0.1 M TBAP)*

All Cr(II) complexes (**1** – **4**) did not show any reduction peaks in their voltammogram as expected. On the other hand, all Cr(III) complexes (**7** – **12**) did show one quasi-reversible peak, Table **3.2**. The reduction peaks that are observed for these Cr(III) complexes are in agreement with peaks that were observed for Cr(III) complexes derived from Schiff base ligands reported in literature [25,

16]. This peak that is observed for the Cr(III) complexes is considered as one-electron-redox process attributed to the reduction of $[Cr(III)L_2]^+$ to $[Cr(II)L_2]$, where L = salicylaldimine ligand).

Co(II) complexes were also analyzed with cyclic voltammetry and Table **3.2** summarizes cyclic voltammogram data that was obtained for these complexes. The voltammogram of complex **14** shows a reduction wave at -1.9 V. A similar peak is also present in the ligand voltammogram, but it is found at -2.01 V. This peak is assigned to phenolate/phenoxyl radical couple [26]. The complex shows a reversible oxidative peak at 0.814 V. The ligand does not show any oxidative peak for this specific complex. Therefore, this peak is assigned to the oxidation of Co^{2+} to Co^{3+}. Complex **16** also showed an E_{pa} at 1.054 V. The reverse reduction peak could not be observed clearly for complexes **14** and **16** and that made it difficult to calculate their $E_{1/2}$. Complexes **13** and **15**, $E_{1/2}$ were recorded as 0.996 and 0.814 V, respectively.

Table 3.2: Oxidation values for Co(II) complexes DCM (0.1 M TBAP), Ag/AgCl

Cr(III) Complex	$E_{1/2}$ / V	Co(II) Complex	$E_{1/2}$ / V
7	-0.830	**13**	0.996
8	-0.761	*__14__	0.814
9	-0.783	**15**	0.816
10	-0.747	*__16__	1.054

*E_{pa} was recorded for these complexes because the E_{pc} seem to overlap with other peaks

3.2.1.3 Characterization of Schiff base complexes 1-18 with mass spectrometry thermogravimetric and elemental analysis

All complexes were also analyzed with ESI mass spectrometry. A typical mass spectrum for complex **1** is shown in Figure **3.8** as an example of the spectra that were obtained for neutral Cr(II) complexes. The parent ion of this complex is observed as M^+ at 444.0829 m/z. The predicted isotopologue pattern for complex **1**, Figure **3.8**, shows three main signals and the same pattern is observed from the spectrum obtained for complex **1**.

A signal at 369.037 m/z for complex **1** is assigned to a fragment produced due to the loss of the benzene ring from one of the ligands coordinated to the metal and the signal at 198.09 m/z is assigned to the free ligand. Table **3.3** summarizes the mass spectrometry data that was obtained for all Cr (II) complexes. From this data it can be deduced that all complexes were obtained as M^+. A similar fragmentation pattern was observed in the mass spectra of all Cr (II) complexes.

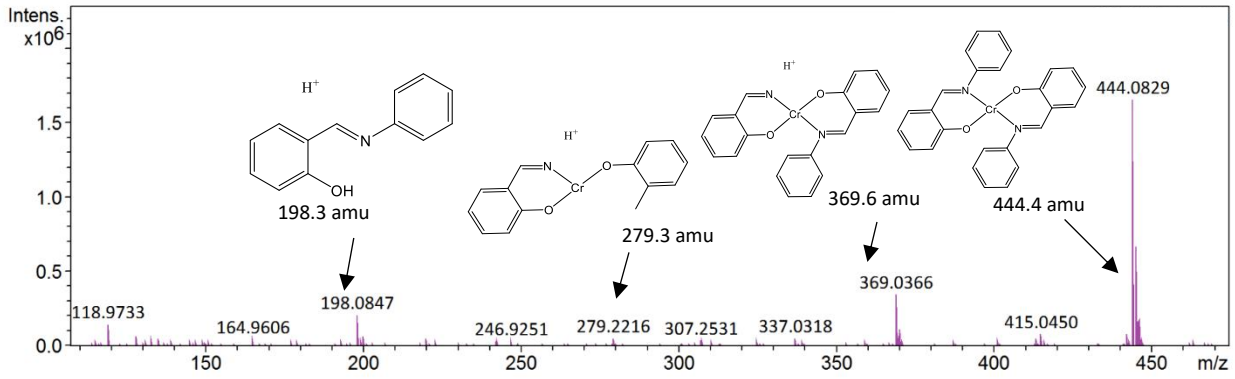


Fig. 3.8: *ESI mass spectrum obtained for complex **1***

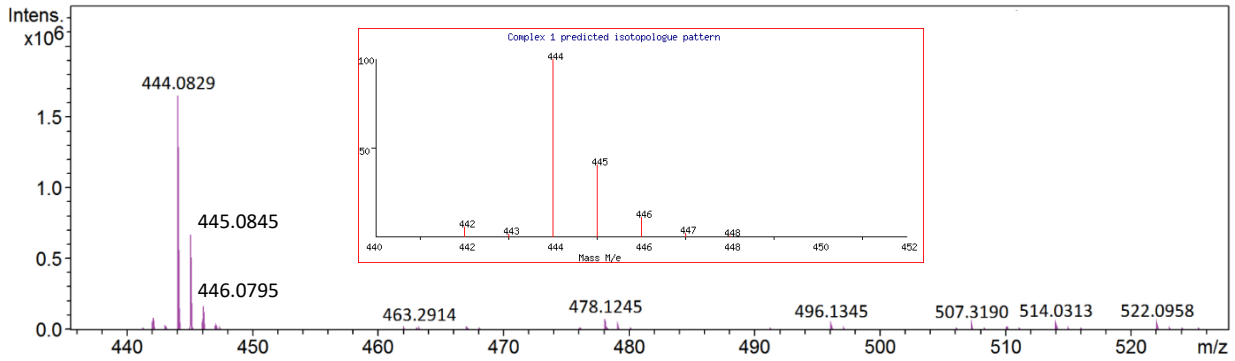


Fig. 3.9: *Isotopologue pattern for complex **1***

The mass spectrum of complex **7** is shown in Figure **3.10** as an example for the spectra that were obtained for neutral Cr(III) complexes. It can be deduced from the spectrum that complex **7** was obtained as $[M\text{-}Cl]^+$ due to the loss of the chlorine ligand. The isotopologue pattern obtained for complex **7** is like the one predicted for complex **1** (Figure **3.10**). The difference in the isotopologue pattern obtained for complex **7** from the predicted isotopologue pattern (Figure **3.11**) is attributed to the loss of the chlorine ligand. However, the isotopologue pattern observed in the spectrum of

complex **7** confirms the presence of the chromium metal. A signal at 369.042 m/z is assigned to a fragment due to the loss of the benzene ring from one of the ligands. The ligand is not observed in the spectrum of complex **7**. All Cr (III) complexes were observed as $[M\text{-}Cl]^+$ as shown in Table **3.3**. A similar fragmentation pattern is observed in the spectra of all Cr (III) complexes.

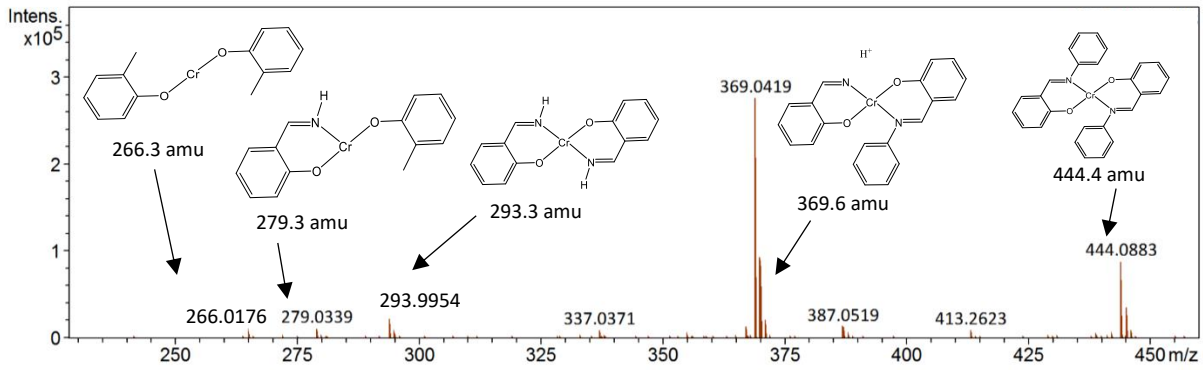


Fig. 3.10: *ESI mass spectrum obtained for complex 7.*

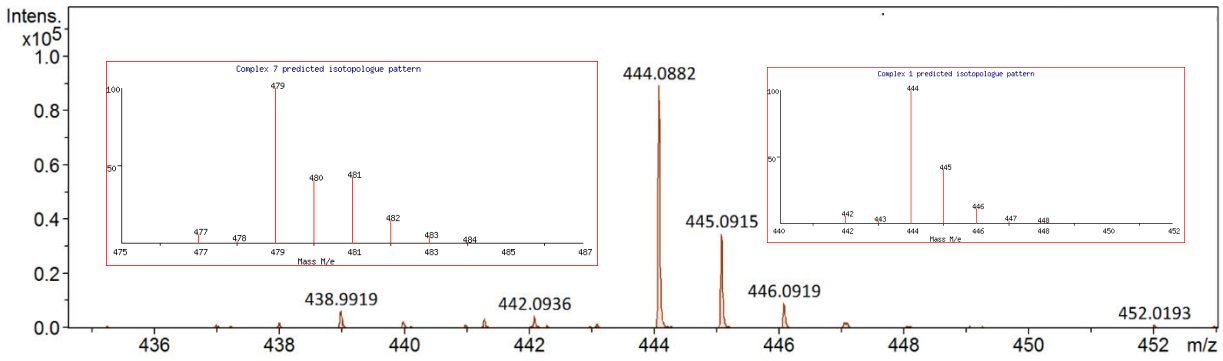


Fig. 3.11: *Isotopologue pattern for complex 7*

Neutral bis-(salicylaldminaoto)Co(II) complexes were also analyzed with mass spectroscopy. All complexes were obtained as M^+ as shown in Table **3.3.** The isotopologue pattern obtained also confirms that the obtained m/z peaks observed correspond with the theoretically expected species, for example Figure **3.12** shows mass spectrum that was obtained for complex **13**. This spectrum matches exactly the spectrum that was predicted for complex **13**.

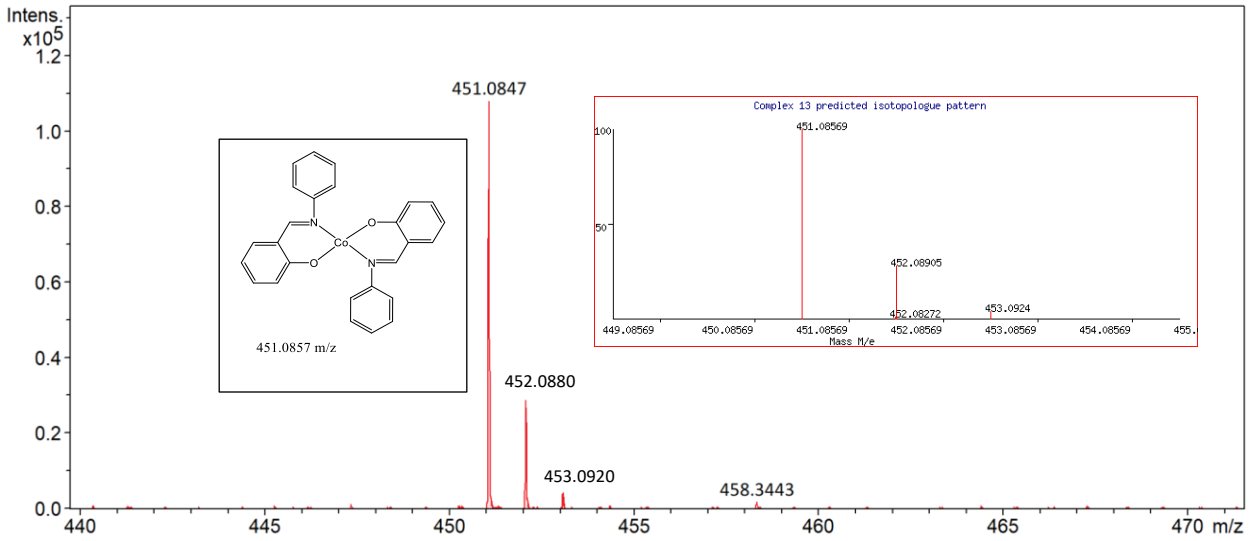


Fig. 3.12: *Isotopologue pattern for complex **13***

Elemental analysis data for the Cr(II) and Cr(III) complexes are summarized in Table **3.3.** The data confirm that for Cr (II) complexes the complexes were obtained in a 2:1 ligand to metal ratio while Cr (III) complexes were obtained in a 2:1 salicylaldimine ligand to metal ratio with chlorine as an axial ligand. According to the elemental analysis data all Cr (II) complexes (**1**, **2**, **3**, and **4**) and Cr (III) complexes (**7**, **8**, and **9**) (Scheme **3.1**) are hydrated species. This is in line with literature reports on Schiff base Cr(III) complexes [28, 29, 30, 31] and the observed hygroscopic nature of the chromium complexes. Elemental analysis for Cr(II) complexes **5** and **6** and Cr(III) complexes **11** and **12** show that these complexes were obtained with some impurities. The complexes were difficult to purify since they had poor solubility in most organic solvents. This made it difficult to remove NaCl produced as a by -product in the synthesis or other impurities.

Elemental analysis data of the Co (II) complexes **13** – **16** were also in agreement with proposed formulations shown in Scheme **3.1**. It also confirms that complexes were obtained in a 2:1 ligand to metal ratio, Table **3.4**. In this case only complex **14** and complex **16** were obtained as hydrated species. This phenomenon is also typical as it has been reported in literature that elemental analysis of cobalt complexes of this nature are observed as hydrated species [17]. Co(II) complexes **17** and **18** were not analyzed with elemental analysis also due to difficulty in purify these complexes by removing the NaOAc by product.

Table 3.3: Mass spectrometry, yield and elemental analysis data for bis-(salicylaldiminato) Cr(II) and Cr(III) complexes **1 - 12**

Complex	Formula	Yield (%)	M^+ (Calc.)	Anal. Found (Calc.)		
				C	H	N
1	$C_{26}H_{20}CrN_2O_2 \cdot 2H_2O$	80	444.08 (444.45)	64.98 (65.15)	4.52 (4.12)	5.61 (5.86)
2	$C_{38}H_{44}CrN_2O_2 \cdot 2H_2O$	66	612.27 (612.76)	69.90 (70.31)	7.63 (7.48)	4.12 (4.33)
3	$C_{34}H_{38}CrN_4O_2 \cdot 1/2H_2O$	70	586.23 (586.69)	67.54 (67.40)	6.70 (6.38)	9.11 (8.94)
4	$C_{30}H_{28}CrN_2O_4 \cdot 5/2H_2O$	77	532.13 (532.55)	62.83 (62.38)	5.47 (5.76)	4.20 (4.85)
5[#]	$C_{28}H_{42}CrN_4O_2$	71	508.23 (508.54)	61.41 (40.66)	5.55 (4.91)	10.80 (8.69)
6[#]	$C_{26}H_{28}CrN_6O_2$	85	518.26 (518.65)	64.84 (61.12)	8.16 (7.69)	16.53 (11.81)
7[*]	$C_{26}H_{20}ClCrN_2O_2 \cdot 3/2H_2O$	79	444.08 (444.45)	61.42 (61.71)	4.16 (4.38)	5.33 (5.53)
8[*]	$C_{38}H_{44}ClCrN_2O_2 \cdot 7H_2O$	80	612.35 (612.76)	59.24 (58.94)	7.42 (7.55)	3.87 (3.62)
9[*]	$C_{34}H_{38}ClCrN_4O_2 \cdot 1/2H_2O$	76	586.23 (586.69)	64.98 (64.71)	6.11 (6.23)	9.12 (8.88)
10[*]	$C_{30}H_{28}ClCrN_2O_4$	80	532.14 (532.55)	63.61 (63.45)	4.82 (5.09)	4.54 (4.91)
11[*#]	$C_{28}H_{42}ClCrN_4O_2$	82	508.16 (508.54)	57.41 (44.41)	5.19 (4.99)	15.45 (10.92)
12[*#]	$C_{26}H_{28}ClCrN_6O_2$	76	518.27 (518.65)	60.69 (43.95)	7.64 (6.89)	10.11 (6.17)

[*]obtained as $[M\text{-}Cl]^+$

[#]elemental analysis results revealed the presence of some impurities

Table 3.4: Mass spectrometry, yield and elemental analysis data for bis-(salicylaldiminato) Co(II) complexes **13 - 18**

Complex	Formula	Yield (%)	M^+ (Calc.)	Anal. Found Calc.)		
				C	H	N
13	$C_{26}H_{20}CoN_2O_2$	80	451.09(451.09)	69.18(68.92)	4.47(4.20)	6.21(6.19)
14	$C_{38}H_{44}CoN_2O_2 \cdot 2H_2O$	72	619.27 (619.27)	69.60(69.55)	7.38(7.34)	4.27(4.23)
15	$C_{34}H_{38}CoN_4O_2 \cdot 1/2H_2O$	86	593.23 (593.23)	67.95(67.76)	6.57(6.19)	9.37(9.30)
16	$C_{30}H_{28}CoN_2O_4 \cdot H_2O$	81	539.14 (539.14)	64.06(64.63)	5.40(5.42)	4.84(5.02)
17*	$C_{28}H_{42}CoN_4O_2$	90	515.16 (515.16)	ND	ND	ND
18*	$C_{26}H_{28}CoN_6O_2$	96	525.26 (525.26)	ND	ND	ND

*ND = not determined, Contain NaOAc as an impurity.

3.2.1.4 Magnetic moment calculation and determination of the number of unpaired electrons

Magnetic moments for the Cr (II) and Cr(III) complexes were calculated using the Evans method. In this method, the difference in the chemical shift of the reference solvent, caused by the presence of a paramagnetic species, was used for magnetic moment calculations [27]. The calculated magnetic moments were used to determine the number of unpaired electrons [28]. Magnetic moments of all the complexes are listed in Table **3.5**. For Cr(II) complexes magnetic moments were obtained in the range 3.15 – 4.22 BM while for Cr (III) complexes magnetic moments were obtained in the range 4.87 – 5.92 BM. Magnetic moment studies were not performed for complexes **5, 6, 11** and **12** due poor solubility of the complexes in DMSO.

The number of unpaired electrons were calculated from the magnetic moments and it was determined that Cr (II) complexes **1**, **2**, **3** and **4** have 4 unpaired electrons while all the Cr (III) complexes **7, 8, 9,** and **10** have 3 unpaired electrons which inicates that all the electrons in the d-orbitals of these complexes are unpaired. Cr (III) complexes are presumed to be in a distorted square based pyramidal [29]; elemental analysis results and magnetic moments are consistent with this formulation. The three unpaired electrons for these complexes are expected to occupy d_{xz}, d_{yz} and d_{xy} orbitals each. The geometry around the Cr (II) complexes on the other hand is presumed to be tetrahedral; elemental analysis results and magnetic moments are consistent with this formulation. The four unpaired electrons for these complexes are expected to occupy d_{xz}, d_{yz}, d_{z2} and d_{xy} orbitals each.

Magnetic moment of Co(II) complexes were investigated using a magnetic susceptibility balance and the Evan method. When magnetic moment of complexes **13**, **15** and **16** was determined with the balance, values in the range 3.79 – 4.16 B.M were obtained which agree well with tetrahedral $3d^7$ configuration for Co(II) [30, 31, 32]. Complexes in the tetrahedral configuration have magnetic moment closer to the spin only value for unpaired electrons, 3.87 B.M. [33]. All values that are higher than this value are thought to be due to spin-orbit coupling perturbation [34]. Table **3.5** shows that Co(II) complexes have 3 unpaired electrons and this was theoretically expected.

Table 3.5: Magnetic moments data and number of unpaired electrons for neutral bis-(salicylaldiminato)Co(II), Cr(II) and Cr(III) complexes **1 - 12**

Complex	Magnetic moment μ (B.M.)	Obtained unpaired e^-	Expected unpaired e^-
1	4.96	4.06	4
2	4.92	4.02	4
3	5.16	4.25	4
4	4.87	3.99	4
7	4.05	3.17	3
8	4.08	3.20	3
9	4.61	3.52	3
10	4.22	3.34	3

expected unpaired electrons are based on anticipated geometries from the experimental magnetic moment obtained.

Magnetic moment for Co(II) complexes **13**, **15** and **16** determined using the Evans method are found to be between 2.49 and 2.94 B.M. (Table **3.6**). The results obtained are in contradiction with those that were obtained from the magnetic susceptibility balance, 379 – 416 B.M. This suggest that the geometry of the complexes are most likely pseudo-square planar when they are in solution. Cobalt complexes do sometimes show this geometry and theoretically they have magnetic moments in the range of 2.1 – 2.9 B.M. [35, 36, 37, 31]. This is expected to be slightly higher than the spin only value for one unpaired electron, 1.73 B.M. Table **3.6** shows that Co(II) complexes have 1 unpaired electrons when in solution.

For complex **14**, magnetic moment performed on the balance was obtained as 2.99 B.M., Table **3.6**. This value is closer to the one obtained when the Evans method (2.46 B.M.) was used for the calculation. These two magnetic moments are suggestive that complex **14** has similar geometry when in solid state and when it is in solution or that the change in geometry could be very small.

It also suggests that complex **14** in both solid state and in solution conform to a geometry with only one unpaired electron and that is pseudo-square planar.

Table 3.6: Magnetic moment data and number of unpaired electrons for neutral bis-(salicylaldiminato)Co(II) complexes **13 - 18**

Complex	μ (B.M.)		Obtained unpaired e^-		Expected unpaired e^-	
	Balance	NMR	Balance	NMR	Balance	NMR
13	3.79	2.49	3	1.7	3	1
14	2.99	2.46	2	1.7	3	1
15	4.16	2.94	3	2.1	3	1
16	4.08	2.76	3	1.9	3	1

3.2.1.5 Crystallography

Attempts have been made to grow crystals of the synthesized Cr(II) and Cr(III) complexes however due to their hygroscopic nature these attempts failed. Another big challenge with growing crystals of the chromium complexes, was the fact that these complexes showed partial solubility in most of the organic solvents except for highly polar solvents like MeOH, DMSO, DMF etc., therefore, finding a suitable solvents combination to grow crystals was a challenge. Co(II) complexes showed good solubility in polar solvents like DCM and are not as hygroscopic as chromium complexes. It was therefore easy to grow crystals, however most of the crystal structures of the complexes investigated have been solved already except for the crystal structure for complex **15** Figure **3.16**.

The ORTEP drawing (Figure **3.13**) of the molecular structure of complex **15** shows a tetracoordinate system of two salicylaldimine ligands forming a chelate around the Co (II) metal center in a 2:1 ratio. Bond distances and bond lengths around the cobalt metal are provided in Table **3.6**. The data obtained for bond angles and bond lengths show that this complex was obtained

as a distorted tetrahedral. The distortion in the complex geometry is confirmed by the bond angels O1-Co1-N3, O2-Co1-N1, O2-Co1-O1 and N3-Co1-N1 which are found in the range 112.67 – 117.98° and are larger than 109° angle expected for a tetrahedral. The bond distances of Co-N (1.9910 and 1.9976Å) are longer than those of Co-O (1.8932 and 1.8972Å), Table **3.7**.

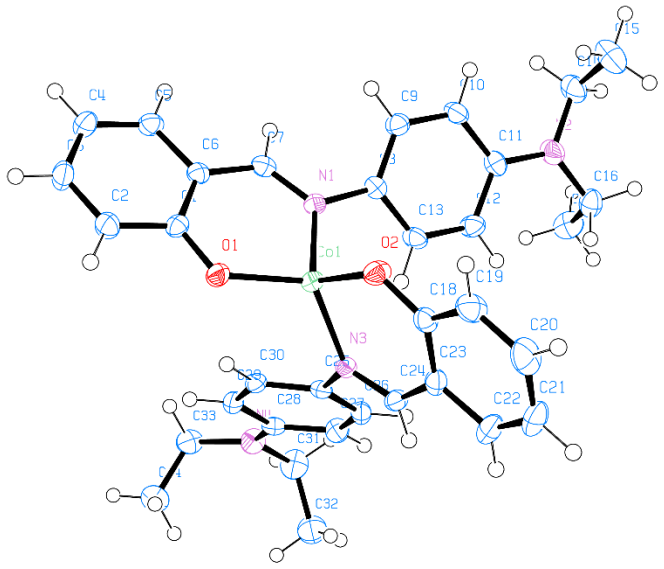


Fig. 3.13: *Ortep structure for Co(II) complex **15***

Table 3.7: Selected bond distances and bond angles for complex **15**

Co1-N1	1.9910(19)	O1-Co1-N1	96.57(7)
Co1-N3	1.9776(18)	O1-Co1-N3	117.98(7)
Co1-O1	1.8972(16)	O2-Co1-N1	112.67(7)
Co1-O2	1.8934(16)	O2-Co1-N3	97.09(7)
		O2-Co1-O1	117.05(7)
		N3-Co1-N1	116.71(8)

3.2.1.6 Attempt to synthesize bis-(salicylaldiminato)Co(III)-OAc complexes

There were several attempts that were made in order to prepare Co(III)-OAc complexes. Co(II) complex that was already prepared, complex **15**, was dissolved in methylene chloride and an equivalent amount of acetic acid was added to the mixture which was stirred at room temperature in the open atmosphere until all volatiles were evaporated. The mixture was further dried under vacuum. This method was used exactly as reported by Coats and his co-workers [38].

The solid obtained from this experiment was analyzed with FT-IR spectroscopy and the spectrum that was obtained is shown in Figure **3.14**, **a**,. From the spectra stacked in Figure **3.14**, a profile different from that of complex **15** was obtained after the reaction. It is clear that there are more peaks observed around 1600 cm^{-1} compared to the Co(II) complex **15** spectrum. Nakamoto claims that the ν(CO) of acetic acid derivatives is expected to appear around this region upon coordination to Co(III) metal. This could suggest that the additional peaks are due to the presence of coordinated acetate. The method was further modified according to Du and co-workers [39]. Complex **15** was dissolved in DCM and to the solution, acetic acid was added, and the reaction mixture was stirred in the open atmosphere for an hour. Solvent was removed and the solid was analyzed with FT-IR spectroscopy however the same spectrum as the one obtained above was observed.

The solid obtained from the first method was crystalized from methylene chloride/hexane solutions giving deep brown crystals which were similar to the Co(II) complex **15** in color and in shape. The crystals were measured and the crystal structure which confirmed that the solid was a Co(II) complex. There are two things that could be happening here; the acetate could just be free in the product as acetic acid originally added to the reaction and it is not coordinating to the metal therefore as the complex crystalized out of solution acetic acid stayed in solution. It could also suggest that the acetate falls due to the stress strain in the complex and the metal reduces back to Co(II). The FT-IR spectrum of the crystals, Figure **3.14**, **b**, is also very similar to that of a Co(II) complex.

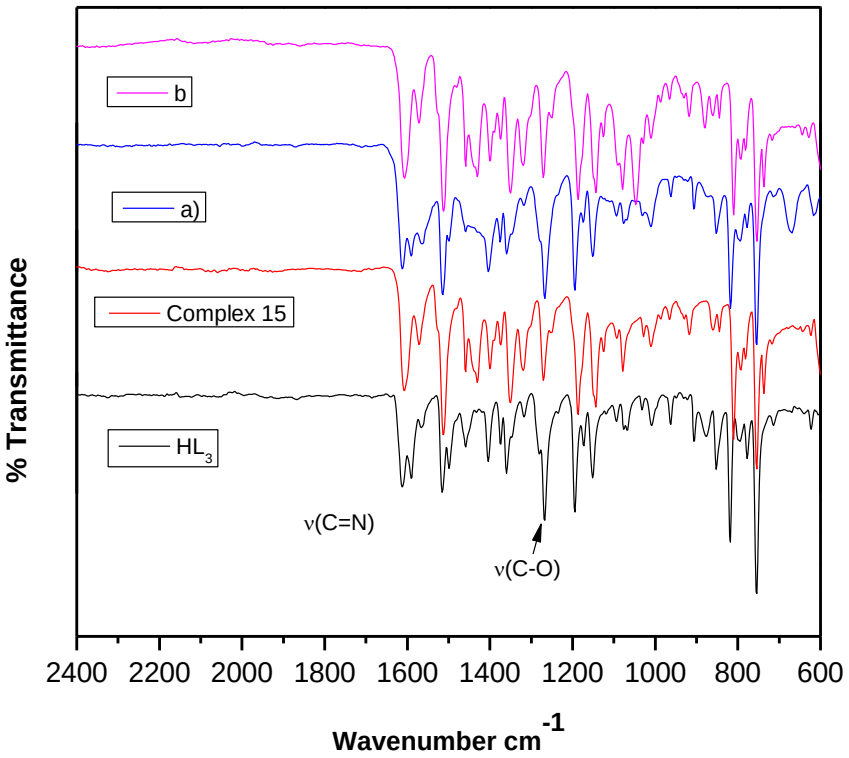


Fig. 3.14: *Stacked FT-IR spectrum for* ***HL*$_1$***, complex* ***15*** *and products* ***a*** *and* ***b*** *of attempted Co(III) reactions*

The first reaction procedure that was used in an attempt to transform Co(II) complex **15** to Co(III) was also used in an attempt to transform Co(II) complex **13** to Co(III). The reaction product which was obtained as a solid gave an FT-IR spectrum, Figure **3.15**, **a**, that is more like that of the ligand and the (C=N) stretching frequency appears just in the same position as observed in the ligand spectrum. The (C-O) is slightly shifted up. Another reaction was attempted where the solvent was changed to toluene but the FT-IR spectrum that was obtained was just like the one that was obtained for the reaction product above, Figure **3.15**, **b**.

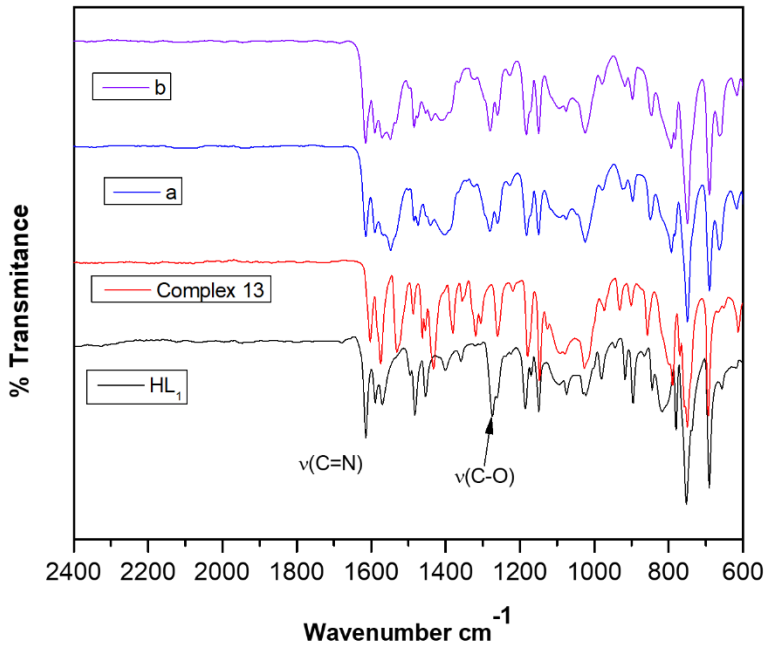
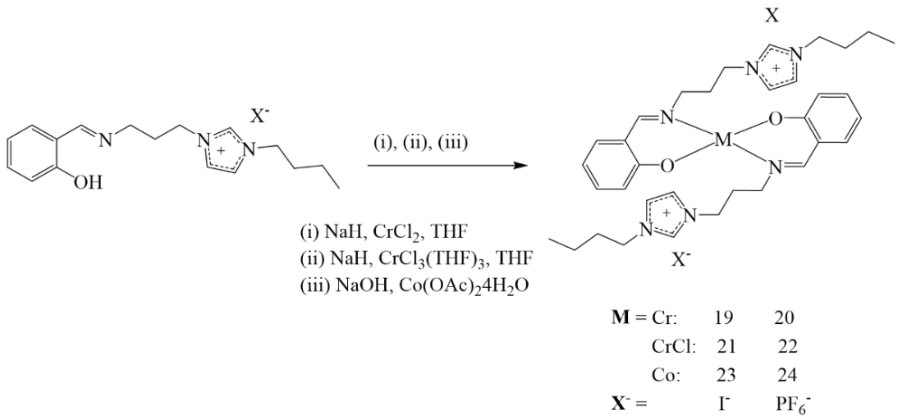


Fig. 3.15: *Stacked FT-IR spectrum for* ***HL₁****, complex* ***13*** *and products* ***a*** *and* ***b*** *of attempted Co(III) reactions*

3.2.2 Synthesis and characterization of ionic functionalized bis-(salicylaldiminato)-Cr(II), Cr(III) and Co(II) complexes

Mononuclear tetra-coordinate ionic functionalized Cr(II) complexes, **19** and **20,** and Cr(III) complexes, **21** and **22,** were prepared by adopting the same method that was used to prepare neutral chromium complexes. When this method was used a solid that did not dissolve in solvents such as THF and DCM was obtained, and this made it very difficult to remove the by-product which is NaCl. When a 98:2 percentage ratio of DCM to MeOH was used, the product dissolved while a white suspension was left not dissolved. The suspension, which is NaCl was filtered. Ionic functionalized bis-(salicylaldiminato)Co(II) complexes **23** and **24** were also prepared using the same method that was used to prepare neutral Co(II) complexes, Scheme **3.2**.



Scheme 3.2: *General procedure for the synthesis of bis-(salicylaldiminato) Cr (II), Cr (III) and Co(II) complexes **19** – **24***

3.2.2.1 Characterization of ionic functionalized bis-(salicylaldiminato) Cr (II), Cr(III) and Co(II) complexes with FT-IR and Uv-vis spectroscopy, mass spectrometry and elemental analysis

The bis-(salicylaldiminato)Cr(II), Co(II) and Cr(III) complexes were characterized using FT-IR spectroscopy and the data for these complexes is summarized in Table **3.9**. As it can be observed from the table, the ν(C=N) stretching frequency of the Cr(II) complexes appear at 1605 and 1608 cm^{-1} for **19** and **20**. There is an observable shift in these peaks compared to the ligand which appear at 1628 cm^{-1} for ligands **HL$_7$**. This stretching frequency appear at 1603 cm^{-1} and 1608 cm^{-1} for **21** and **22** respectively and it has shifted from 1630 cm^{-1} in the spectrum of ligand **HL$_8$**. The shift of this stretching frequency is also observed for Co(II) complexes where for complex **23** it appears at 1617 and it is shifted from 1628 in ligand **HL$_7$**. For Complex **24** this peak is observed at 1619 cm^{-1} and it is shifted from 1630 cm^{-1} in ligand **HL$_8$**. Figure **3.16** is an example of FT-IR spectra that were obtained for ligand **HL$_7$**, complexes **19** (Cr(II)) and **21** (Cr(III)) and the shift in the peaks is clearly demonstrated.

The ν(C-O) stretching frequency is observed at 1322 and 1319 cm^{-1} for complexes **19** and **20,** respectively. There is an observable shift in these peaks compared to the ligands which appear at 1277 cm^{-1} for ligands **HL$_7$**. The ν(C-O) stretching frequency is observed at 1300 cm^{-1} for both complexes **21** and **22**. There is an observable shift in these peaks compared to the ligands which appear at 1277 cm^{-1} for ligands **HL$_8$**. The shift of this stretching frequency is also observed for Co(II) complexes where for complex **23** it appears at 1319 cm^{-1} and it is shifted from 1277 cm^{-1} in

ligand **HL$_7$**. For complex **24** this peak is observed at 1320 cm^{-1} and it is shifted from 1277 cm^{-1} in ligand **HL$_8$**.

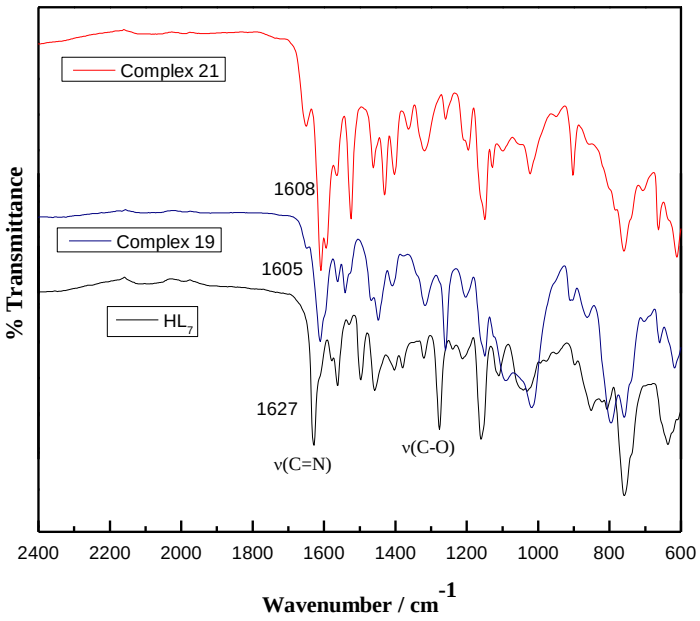


Fig. 3.16 *Overlayed FTIR spectra for ligand **HL$_7$**, Cr(II) complex **19** and Cr(III) complex **21**.*

Ionic functionalized bis-(salicylaldiminato)Cr(II) and Cr(III) complexes were also analyzed with UV-Vis spectroscopy. Table **3.8** summarizes the data that was obtained for the UV-Vis spectra of the complexes. The spectra obtained for Cr(II) complexes **19** and **20** show ligand to metal charge transfer bands at 394 nm for both complexes. This peak appears at 393 and 396 nm for Cr(III) complexes **21** and **22**. This band is observed at 400 and 389 nm for Co(II) complexes **23** and **24**.

The visible region shows peaks that can be assigned to the d-d band. The d-d transition bands of both bis-(salicylaldiminato)Cr(II) and Cr(III) complexes show two overlapped bands which could be due to Jahn Teller effect which is the distortion that occur in the geometry of the complexes. The d-d bands for Cr(III) complexes are shifted to higher wavelength with reference to Cr(II) complexes, Table **3.8**. The shift is a result of the requirement of a lower splitting energy for the d-d transition in the Cr(III) complexes compared to Cr(II) complexes. The d-d band in Co(II) complexes **23** and **24** appear at lower wavelength than that of the chromium complexes. This was expected because square planar geometry in Co(II) (proofed by magnetic moment Table 3.9) have higher crystal splitting energy than tetrahedral Cr(II) complexes.

Table 3.8: UV-Vis and FTIR spectroscopy data for ionic liquid functionalized bis-(salicylaldiminato)Co(II), Cr(II), Cr(III) complexes **13 - 24**

Complex	UV-Vis (λ_{Max} /nm)		FTIR (cm^{-1})	
	LMCT band	d -d band	ν(C=N)	ν(C-O)
19	394	650	1605	1322
20	394	635	1603	1300
21	393	683, 710, 662	1608	1320
22	396	660, 679, 712	1608	1319
23	400	582	1617	1319
24	386	595	1619	1320

These complexes were further characterized with mass spectrometry. The mass spectra of ionic functionalized bis-(salicylaldiminato)Co(II) and Cr(II) complexes show an M^{++} peaks and the data is summarized in Table **3.9**. Ionic functionalized Cr(III) complexes also show an M^{++} peak. The data confirms that the complexes still contain the counter ions as the ligands. All the ionic functionalized complexes were found very highly hygroscopic, and this was confirmed with elemental analysis results, Table **3.9**. The complexes also absorbed moisture after a couple of minutes when exposed to open atmosphere changing from powder to a sticky solid.

The magnetic moment of the complexes was performed using Evans's method and the data obtained is summarized in Table 3.9. The magnetic moment of Cr(II) complexes **1** and **2** were found as 4.81 and 4.94 B.M., respectively. These values are closer to the expected spin only magnetic moment value, 4.90 B.M. for a d^4 high spin ($t_{2g}^3\ e_g^1$). Cr(III) complexes show magnetic moment of 4.45 and 4.59 B.M.. These values are higher than the expected spin only magnetic moment for Cr(III) complexes which is 3.89 B.M. for d^3 (t_{2g}^3). This can be because of the complication in the distortion of the geometry by Jahn Teller effect. Last but not least, magnetic moment for Co(II) complexes was recorded as 1.84 and 2.17 μ for complexes 5 and 6 respectively. These values agree very well with the spin only magnetic moment, 1.73 B.M., of a d^7 low spin ($t_{2g}^6\ e_g^1$) square planner geometry.

Table 3.9: Mass spectrometry and elemental analysis data for ionic liquid functionalized bis-(salicylaldiminato)Co(II), Cr(II) and Cr(III) complexes (**19 - 24**)

Complex	Formula	Yield (%)	ESI MS $[M]^{2+}$ (Calc.)	Anal. Found (Calc.)			μ_{eff} (B.M.)
				C	H	N	
19	$C_{34}H_{50}CrI_2N_6O_2 \cdot 2H_2O$	66	311.9 (311.2)	45.10 (44.75)	5.56 (5.52)	9.33 (9.21)	4.81
20	$C_{34}H_{52}Cr(PF_6)_2N_6O_5 \cdot 3H_2O$	61	311.2 (311.2)	41.98 (42.24)	5.37 (5.42)	8.64 (8.69)	4.94
21	$C_{34}H_{60}CrClI_2N_6O_2 \cdot 7H_2O$	71	328.6 (328.6)	39.53 (39.34)	5.68 (5.83)	7.76 (8.10)	4.45
22	$C_{34}H_{51}CrCl(PF_6)_2N_6O_2 \cdot 2\frac{1}{2} H_2O$	63	328.6 (328.6)	41.51 (41.11)	5.73 (5.98)	7.99 (8.46)	4.59
23	$C_{34}H_{50}CoI_2N_6O_4 \cdot 2H_2O$	77	314.7 (314.7)	44.12 (44.41)	5.32 (5.48)	9.29 (9.14)	1.84
24	$C_{34}H_{50}Co(PF_6)_2N_6O_4 \cdot 2H_2O$	80	314.6 (314.7)	43.00 (42.73)	5.67 (5.27)	8.32 (8.79)	2.17

3.3 Conclusion

3.3.1 Neutral bis-(salicylaldiminato) complexes

Cr(II) and Cr(III) complexes bearing the synthesized neutral ligands were prepared through a reaction of the sodium salt of the ligands and chromium salts in a 2:1 ligand to metal ratio. The complexes were obtained in yields of 65.7 – 84.6 % for Cr(II) complexes and 59.9 – 81.7 % for Cr(III) complexes. The complexes were characterized with FTIR and UV-Vis spectroscopy, mass spectrometry and element analysis which all confirmed that the complexes were synthesized. Magnetic moments of the complexes were determined using the Evans method and from the magnetic moments the number of unpaired electrons of each complex were calculated. All these characterization techniques confirmed the formation of the expected coordination system on the Cr(II) and Cr(III) complexes.

Neutral bis-(salicylaldiminato) Co(II) complexes bearing the synthesized ligands were prepared through a reaction of sodium salt of the ligand and $Co(OAc)_2 \cdot 4H_2O$. The complexes were obtained in yields of 72 – 96 %. The complexes were characterized with FT-IR spectroscopy, mass spectrometry and elemental analysis. Magnetic moment of complexes **13**, **15**, and **16** in the solid state confirmed that the complexes had 3 unpaired electrons suggesting a tetrahedral geometry. Complex **14** gave one unpaired electron suggesting a distorted tetrahedral into a pseudo-square planar geometry. Evans method shows that all complexes have one unpaired electron when in solution. This could therefore suggest that the conformation of the complexes is influenced by their state.

3.3.2 Ionic functionalized bis-(salicylaldiminato) Cr(II), Co(II) and Cr(III)

Ionic functionalized complexes of Cr(II) (**19** and **20**), Cr(III) (**21** and **22**) were also prepared in this study and the yields of 65.6 and 61.2, 90.7 and 63.4 % were obtained respectively. Cr(II) and Cr(III) complexes were obtained as brown solids. These complexes were found highly hygroscopic when left in the open atmosphere. When exposed to the atmosphere they turned to a black sticky solid. They were also found only soluble in highly polar solvents such as MeOH and DMSO.

On the other hand, ionic functionalized Co(II) (**22** and **23**) complexes were obtained as black solids with the yield of 77.3 and 80.1 % respectively. These complexes were also found slightly hygroscopic in the open atmosphere but not as highly as their chromium counterparts. They stayed black in color when exposed to the atmosphere, but they went from solid to a sticky solid product

with time. These complexes were also found highly soluble in polar organic solvents such as MeOH and DMSO. In addition to that, they were also found soluble in dichloromethane, a phenomenon which was not found to be the case with chromium complexes.

The complexes were characterized with FT-IR spectroscopy and the spectra obtained confirmed coordination through the phenolic oxygen and azomethine nitrogen atoms. The complexes were further characterized with Uv-vis spectroscopy which also confirmed coordination for the complexes and the spectra obtained were used to distinguish between the oxidation states of the metals. The complexes were obtained as M^{++} on mass spectrometry and elemental analysis confirms that most of these complexes were hydrated.

3.4 Experimental

3.4.1 Material and instrumentation

All chemical reactions and manipulations were performed on a dual vacuum/nitrogen line using standard Schlenk techniques unless otherwise stated. Reagent grade chemicals were obtained from Sigma Aldrich and used as received. All solvents were dried under appropriate drying reagent and distilled prior to use. $CrCl_3(THF)_3$ was prepared according to literature procedure. FTIR spectra were recorded on Bruker TENSOR 27 spectrometer using ATR. Mass spectra were recorded on Bruker compact ultimate 3000 HR-MS. Uv-vis data was recorded from Specord 210 plus Analytik Jena Uv-ivs spectrophotometer. Elemental analyses were performed in the micro analytical laboratory of the University of Johannesburg and University of Cape Town. Magnetic moments of the complexes were determined with Evans' method using a Varian 400 MHz spectrometer and magnetic susceptibility balance provided by Sherwood scientific l.t.d.

3.4.2 Preparation of the sodium salt of salicylaldimine ligands HL_1 - HL_6 for preparation of chromium complexes

The preparation of the sodium salt of the ligands is described using conditions for ligand HL_1 as an illustrative example. A tip of a spatula of sodium hydride was added to a pre-weighted Schlenk tube and to the Schlenk tube was added distilled hexane and the mixture was stirred at room

temperature for 10 minutes under nitrogen atmosphere. Sodium hydride suspension could settle at the bottom of the Schlenk tube and hexane was decanted and NaH was dried under reduced pressure. The Schlenk tube was weight to determine the amount of NaH (0.61 mmol, 14.9 mg). THF (5 ml) was added to the Schlenk tube followed by a 1:1 molar ratio of ligand HL_1 (0.61 mmol, 122.5 mg) dissolved in THF (5 ml). Evolution of H_2 immediately followed. The mixture was stirred for 30 min under nitrogen.

3.4.3 Preparation of the sodium salt of salicylaldimine ligands HL_1 - HL_6 for the preparation of cobalt complexes

The preparation of the sodium salt of the ligands is described using conditions for ligand **HL_1** as an illustrative example. **HL_1** (0.6338 mmol, 125.0 mg) was dissolved in methanol (10 ml) and NaOH (0.6338 mmol, 25 mg) was added. The reaction mixture was then stirred for 10 min.

3.4.4 Preparation of Cr(II) complexes 1 - 6

The synthesis of Cr(II) complexes is described using conditions for complex **1** as an example. To the sodium salt of ligand **HL_1** (140.7 mg, 0.64 mmol) in THF (10 ml) was added $CrCl_2$ (0.32 mmol, 78.9 mg) and the mixture was refluxed in THF for 4 hr under a nitrogen atmosphere. The reaction mixture was cooled in an ice-water bath for approximately 15 minutes and a white solid precipitated out of the solution. The precipitate was isolated by filtration and the solvent was removed from the filtrate using a rotary evaporator. The solid residue obtained was further dried under reduced pressure.

3.4.5 Preparation of Cr(III) complexes 7 - 12

The synthesis of Cr(III) complexes is described using conditions for complex **7** as an example. To a solution of sodium salt of ligand **HL_1** (0.62 mmol, 137.4 mg) in THF (10 ml) was added $CrCl_3(THF)_3$ (117.4 mg, 0.31 mmol) and the mixture was refluxed in THF for 4 hours under a nitrogen atmosphere. The reaction mixture was cooled in an ice-water bath for approximately 15 minutes and a white solid precipitated out of the solution. The precipitate was isolated by filtration and the solvent was removed from the filtrate using a rotary evaporator. The solid was further dried under reduced pressure.

3.4.6 Preparation of Co(II) complexes 13 – 18

The preparation of the sodium salt of the ligands is described using conditions for ligand **HL_1** as an illustrative example. **HL_1** (0.6338 mmol, 125.0 mg) was dissolved in methanol (10 ml) and NaOH (0.6338 mmol, 25 mg) was added. The reaction mixture was then stirred for 10 min. To the sodium salt of the ligand in methanol was added $Co(OAc)_2 \cdot 4H_2O$ (0.1584 mmol, 39.4 mg) and the resulting reaction mixture was stirred for 4 hours under reflux. After this time, the reaction mixture was cooled in an ice-water bath for 15 minutes after which a precipitate formed. The precipitate was filtered off and dissolved in DCM (5 ml), where most of it dissolved with a white solid suspended. The white solid which is thought to be NaOAc was filtered off. The solvent of the filtrate was removed using a rotary evaporator and the solid residue obtained was dried under reduced pressure.

3.4.7 Preparation of ionic functionalized Cr(II) complexes 19 and 20

The synthesis of Cr(II) complexes is described using conditions for complex **19** as an example. To a suspension of NaH (0.521 mmol) in THF was added a solution of ligand **HL_7**(0.493 mmol, 203.9 mg) and the mixture was stirred for 5 minutes. After this time, $CrCl_2$ (0.2467 mmol, 30.3 mg) was added and the mixture was refluxed in THF for 4 hr under a nitrogen atmosphere. A solid was observed to form immediately as the metal salt was added to the sodium salt of the ligand solution. The solid was observed to stick to the walls of the flask and after the reaction the solvent was decanted. The solid that remained behind in the flask. A 98:2 percentage ratio of DCM to MeOH was used to separate the two purify the solid by precipitating out he NaCl byproduct.

3.4.8 Preparation of ionic functionalized Cr(III) complexes 21 and 22

The synthesis of Cr(III) complexes is described using conditions for complex **20** as an example. To a THF suspension of NaH (0.213 mmol) was added a solution of ligand **HL_7** (0.129 mmol, 53.1 mg) in THF (10 ml) and the mixture was stirred for 5 minutes. To the resulting solution was added $CrCl_3(THF)_3$ (0.064 mmol, 24.1 mg) and the mixture was refluxed in THF for 4 hours under nitrogen atmosphere. A solid formed immediately as the metal was added to the ligand solution. The solid sticked to the walls of the flask and after the reaction the solvent was decanted. Even in this case the solid that formed did not dissolve in DCM which is the solvent that could simply be used to separate the product from NaCl which forms as a by-product. The product however showed

very good solubility in MeOH. A 98:2 percentage ratio of DCM to MeOH was used to separate the two purify the solid by precipitating out he NaCl byproduct.

3.4.9 Preparation of ionic functionalized bis-(salicylaldiminato)Co(II) complexes 23 and 24

The preparation of ionic functionalized bis-(salicylaldiminato)Co(II) complexes is explained using complex **23** as an example. To methanol solution of the ligand (0.083 mmol, 34.3 mg) was added NaOH (0.083 mmol, 3.3 mg) and the solution was stirred for 5 minutes. To the resulting mixture was added $Co(OAc)_2 \cdot 4H_2O$ (0.0417 mmol, 10.4 mg) and the solution was stirred for roughly 4 hours under reflux. After this time, the solvent was removed using a rotary evaporator. The solid residue obtained was then dissolved in DCM, while a white solid was suspended. The white solid which was thought to be NaOAc was filtered off. The solvent of the filtrate was removed using a rotary evaporator from and the solid residue obtained was dried under reduced pressure.

3.5 References

[1] J. D. Darensbourg, M. R. Mackiewicz, L. J. Rodgers, C. C. Fang, R. D. Billodeaux and H. J. Reibenspies, *Inorg. Chem.*, vol. 43, pp. 6024 - 6034, 2004.

[2] J. D. Darensbourg and C. J. Yabrough, *J. Am. Chem. Soc.*, vol. 124, pp. 6335 - 6342, 2002.

[3] L. R. Paddock and T. B. Nguyen, *Macromolecules*, vol. 38, pp. 6251 - 6253, 2005.

[4] T. C. Cohen, T. Chu and W. G. Coates, *J. Am. Chem. Soc.*, vol. 127, pp. 10869 - 10878, 2005.

[5] J. D. Darensbourg, R. J. Anreatta, J. M. Jungman and H. J. Reibenspies, *Dalton Trans.*, pp. 8891 - 8899, 2009.

[6] E. C. Anderson, I. S. Vagin, W. Xia, H. Jin and B. Rieger, *Macromolecules*, vol. 45, pp. 6840 - 6849, 2012.

[7] J. D. Jones, C. V. Gibson, M. S. Green, J. P. Maddox, J. P. A. White and J. D. Williams, *J. Am. Chem. Soc.*, vol. 127, pp. 11037 - 11046, 2005.

[8] A. Sibaouih, P. Ryan, V. K. Axenov, R. M. Sundberg, M. Leskela and T. Repo, *J. Mol. Catal. A: Chem.*, vol. 312, pp. 87 - 91, 2009.

[9] D. Chandran, C. Hun Kwak, J. Min Oh, I. Yong Ahn, C.-S. Ha and I. Kim, *Catal. Lett.*, vol. 125, pp. 27 - 34, 2008.

[10] Y. Peng, Y. Cai, G. Song and J. Chen, Synlett, New York, 2005.

[11] W. M. Ren, X. Zhang, Y. Liu, J. F. Li, H. Wang and X. B. Lu, *Macromolecules,* vol. 43, pp. 1396 - 1402, 2010.

[12] S. Sujith, J. K. Min, J. E. Seong, S. J. Na and B. Y. Lee, *Angew. Chem., Int. Ed,* vol. 47, pp. 7306 - 7309, 2008.

[13] S. A. Abu-Surrah, A. K. Ibrahim and M. H. Abdel-Halim, *Transit. Met. Chem.,* vol. 34, pp. 803 - 808, 2009.

[14] A. P. R. Sneeden and H. H. Zeiss, *J. Organometal. Chem.,* vol. 4, pp. 355 - 359, 1965.

[15] A. G. Kohawile and S. K. Patel, *J. Chem. Soc., Dalton Trans.* , p. 1241, 1981.

[16] P. Kumar, R. Suresh, K. Giribabu, R. Manigandan, S. Munusamy, S. Muthamizh and V. Narayanan, *Spectrochemical Acta Part A: Molecular and Biomolecular Spectroscopy*, vol. 139, pp. 431 - 441, 2015.

[17] L. J. van Wyk, F. S. Mapolie, A. Lennartson, M. Hakansson and S. Jagner, *Inorg. Chem. Acta,* vol. 361, pp. 2094 - 2100, 2008.

[18] M. R. Silverstein, C. G. Bassler and C. T. Morril, New York: Wiley, 1991, pp. 110 - 111.

[19] F. Scheinmann, New York: Pergamon, 1973, p. 93.

[20] N. E. Jacobsen and P. T. Yoon, *Science,* vol. 299, pp. 1691-1693, 2003.

[21] B. Bosnich, *J. Am. Chem. Soc.* , vol. 90, p. 627, 1968.

[22] E. P. Aranha, P. M. dos Santos, S. Romera and R. E. Dockal, *Polyhedron,* vol. 26, pp. 1373 - 1382, 2007.

[23] L. Q. Chai, L. J. Tang, L. C. Chen and J. J. Huang, *Polyhedron,* vol. 122, pp. 228 - 240, 2017.

[24] Y.-R. Li, X.-X. An, L.-J. Wu, P.-Y. Zhang and K.-W. Dong, *Crystal,* vol. 9, pp. 1 - 13, 2019.

[25] K. Ghosh, P. Kumar and I. Goyal, *Inorganic Chemistry Communications,* vol. 24, pp. 81 - 86, 2012.

[26] M. Ulusoy, H. Karabiyik, R. Kihncarslan, M. Aygun, B. Cetinkaya and S. Garcia-Granda, *Struct. Chem.,* vol. 19, pp. 749 - 755, 2008.

[27] J. Loliger and R. Scheffold, *J. Chem. Educ.,* vol. 49, pp. 646 - 647, 1972.

[28] H. T. Crawford and J. Swanson, *J. Chem. Educ.,* vol. 48, pp. 382 - 386, 1971.

[29] C. V. Gibson, S. Mastroianni, C. Newton, C. Redshaw, A. G. Solan, P. J. A. White and J. D. Williams, *J. Chem. Soc., Dalton Trans.,* pp. 1969 - 1971, 2000.

[30] A. H. Bayoumi, A.-N. M.A. Alaghaz and M. S. Aljahdali, *Int. Electrochem. Sci.*, vol. 8, pp. 9399 - 9413, 2013.

[31] M. Hariharan and L. F. Urbach, *Inorg. Chem.,* vol. 8, pp. 556 - 559, 1969.

[32] S. S. Khaidir, H. Bahron, M. A. Tajuddin, K. Ramasamy and M. S. Lim, *IJET,* vol. 7, pp. 72 - 76, 2018.

[33] A. A. Soliman and W. Linert, *Thermochemica Acta,* vol. 338, pp. 67 - 75, 1999.

[34] N. S. Gill and R. S. Nyholm, *J. Chem. Soc.,* pp. 3997 - 4007, 1959.

[35] A. Earneshaw, C. P. Hewlett, A. E. King and F. L. Larkworthy, *J. Chem. Soc. (A),* pp. 241 - 246, 1968.

[36] S. K. Patel and C. J. Bairlar Jr., *J. Inorg. Nul. Chem.,* vol. 33, pp. 1399 - 1406, 1971.

[37] A. R. Ahmadi and S. Amani, *Molecule,* vol. 17, pp. 6434 - 6448, 2012.

[38] L. K. Peretti, H. Ajiri, T. C. Cohen, B. E. Lobkovsky and W. G. Coates, *J. Am. Chem. Soc.,* pp. 11566 - 11567, 2005.

[39] H. Chen, Z. Sun, S. Ye, D. Lu and P. Du, *J. Mater. Chem. A,* vol. 3, pp. 15729 - 15737, 2015.

[40] E. S. Schaus, D. B. Brandes, F. J. Larrow, M. Tokunaga, B. K. Hansen, E. A. Gould, E. M. Furrow and N. E. Jacobsen, *J. Am. Chem. Soc.,* vol. 124, pp. 1307 - 1315, 2002.

[41] H. Chen, Z. Sun, S. Ye, L. Dapeng and P. Du, *J. Mater. Chem. A,* vol. 3, pp. 15729 - 15767, 2015.

Chapter 4

Catalytic evaluation of bis(salicylaldiminato) Cr(II), Co(II) and Cr(III) complexes as catalysts for the coupling of CS_2 with PO in the absence of solvent

Contents

4.1 Introduction 122

4.2 Results and discussion 124

4.2.1 Coupling of CS_2/PO using bis-(salicylaldiminato) Cr (III) complexes as catalyst precursors 125

4.2.2 Coupling of CS_2/PO using Cr(II) complexes **1** – **4** as catalyst precursors 130

4.2.3 Effect of the chromium oxidation state in the catalytic CS_2/PO coupling reaction 134

4.2.4 Coupling of CS_2/PO using Co (II) complexes **13** – **16** as catalyst precursors 135

4.2.5 Effect of the metal center on the catalytic activity of Co(II) and Cr(II) complexes on CS_2/PO coupling reaction. 139

4.2.6 Cycloaddition mechanism 140

4.3 Conclusion 143

4.4 Experimental 144

4.4.1 Materials and instrumentation 144

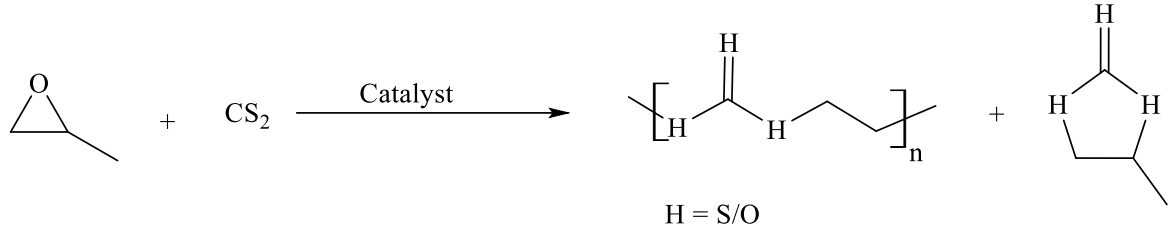
4.4.1 General procedure for the coupling of CS_2 and propylene oxide 144

4.5 References 144

4.1 Introduction

The coupling reaction of epoxides and carbon disulfide (CS_2) to form either cyclic products or a co-polymer occurs in the presence of a catalyst, Scheme **4.1**. Depending on the nature of the catalyst, different products can be obtained because of scrambling of the oxygen and sulfur atoms. Scrambling can be promoted by some catalysts and it has also been shown to depend on the reaction conditions. In most instances, scrambling products are generally produced at elevated temperatures [1, 2, 3]. For instance, when Luo and Darensbourg coupled CS_2 and oxitane they found that the ratio of cyclic product increased from 90 to >99 % when temperature was increased from 60 ^oC to 120 ^oC respectively [2].

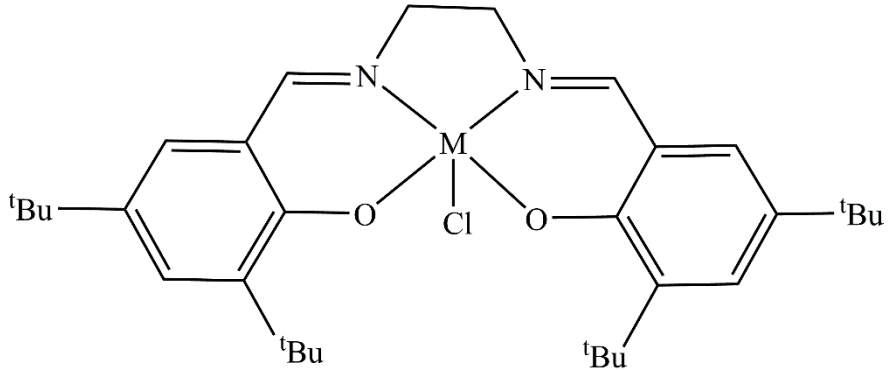
This process is currently of interest because the co-polymers prepared in this coupling reactions possess very high optical and thermal properties as well as excellent chemical resistance and can therefore be applied for use in optical instruments [4]. Cyclic products also have industrial relevance as protic solvents and precursors for polymer synthesis [5, 6, 7, 8, 9]. The cyclic compound can also be utilized for biological applications because they have radioprotective, fungicidal and antibacterial properties [10].



Scheme 4.1: *Coupling of CS_2 and propylene oxide with the H groups indicating that scrambling of the oxygen and sulfur atoms are observed for this process.*

There are different catalysts that have been reported active for the coupling of epoxides and CS_2 to produce cyclic products. Organic catalysts such as triethylamine, pyridine and *N*-methylmophorlin have been reported to be active for this coupling reaction with reaction conditions of 800 MPa, 100 ^oC and 20 hours [11]. The reaction conditions in this case had a very huge impact on the selectivity of the products produced. When the reaction was performed at atmospheric pressure, 100 ^oC for 20 hours, only one cyclic product was obtained.

Schiff base metal complexes have also been used as catalysts for the coupling reaction of epoxides and CS_2 [2, 12]. Depending on how specific they are, metal complexes were reported to either produce cyclic product or copolymers. Wang and co-workers showed that when tetradentate Schiff base complexes **4a** and **4b** (Figure **4.1)** were used in the coupling of CS_2 and propylene oxide as catalysts; very low conversions were observed with **4a** and no conversion of epoxide to any coupling products was observed with **4b**. These complexes were studied at 100 ^oC for nine hours. The poor catalytic performance observed with these two metal complexes was thought to be due to catalyst poisoning by sulfur-based compounds such as CS_2. It was also shown that electronic and steric properties of the metal complexes influence the products produced [12].



4a) Cr(III)
4b) Co(III)

Fig. 4.1: *Metal complexes used by Wang and workers for the coupling of CS_2 and epoxides [12].*

Darensbourg and his coworkers investigated the salen Cr(III)Cl, **4a** (Figure **4.1**) with [PPN]Cl as co-catalyst for the coupling of cyclohexene oxide and CS_2 at 40 ^oC for 4 hours. In their study a mixture of cyclic products and copolymer was obtained. The overall conversion of the substrates to total coupling products was recorded at 40.6 %. The reaction produced the copolymer as the main product. However, when the temperature was increased to 60 ^oC an increase in the conversion was observed and the cyclic product was found to be the main product produced [13].

In this study, bis-(salicylaldiminato) Co(II), Cr(II), and Cr(III) complexes were evaluated as catalyst precursors for the coupling of CS_2 and propylene oxide (PO). This chapter reports on studies evaluating these metal complexes as suitable catalyst precursors. Factors investigated include the influence of the oxidation state between the Cr(II) and Cr(III), effect of the nature of the metal center between Cr(II) and Co(II), the effect of the type co-catalysts used and the influence of the substituent group on the aromatic ring of the imino nitrogen of the Schiff base complex on catalytic performance.

4.2 Results and discussion

The tetra-coordinate Cr(II) (**1 - 4**) and Co(II) (**13 - 16**) complexes as well as the penta-coordinate Cr(III) (**7 - 10**) complexes shown in Figure **4.2** were investigated as catalyst precursors for the coupling of CS_2 and PO (Scheme **4.2)**. As in literature, the coupling reaction of CS_2 and PO was carried out neat at room temperature for 12 hours. All volatiles were removed under reduced pressure, and the reaction residue analyzed with ^{1}H-NMR spectroscopy in $CDCl_3$.

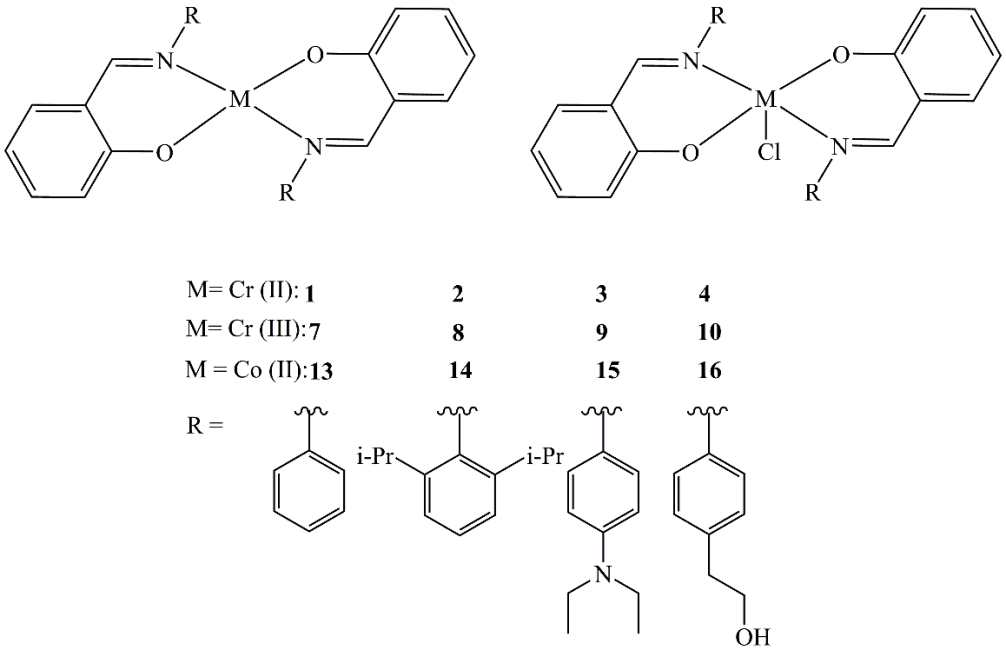
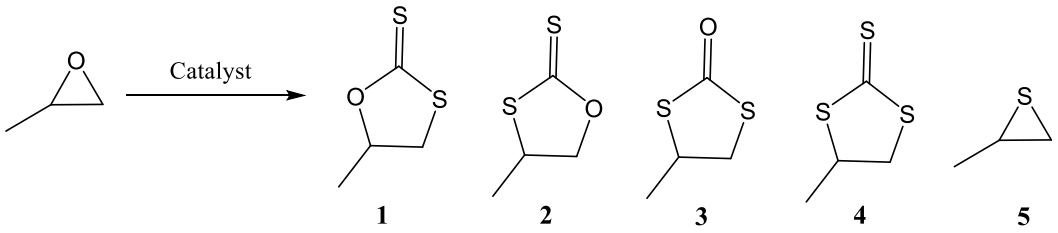


Fig. 4.2: *Bis(salicylaldiminato) Cr(II), Co(II) and Cr(III) complexes investigated as catalyst precursors in this study.*

4.2.1 Coupling of CS_2/PO using bis-(salicylaldiminato) Cr (III) complexes as catalyst precursors

The investigation was initiated by performing control reactions where Cr(III) complex **8** was evaluated as catalyst for the coupling of CS_2 and PO in the absence of a co-catalyst (Table **4.1**, entry **1**). This complex did not give any quantifiable catalytic product/s when used as a catalyst for the coupling reaction without a co-catalyst. As part of the control reactions performed in this study, [PPN]Cl, which is a co-catalyst that is mostly studied in literature, was used as catalyst in the absence of any complex for the coupling reaction. Low catalytic activity was noted for [PPN]Cl in this experiment, Table **4.1**, entry **2,** with trace amount of the cyclic product/s being produced.



Scheme. 4.2: *Coupling of CS_2 and epoxides to produce cyclic carbonate [14, 12]*

Table 4.1: CS_2/epoxide coupling using Cr (III) complexes **7** – **10** as catalysts[a]

Entry	Complex	Co-catalyst	Mass (mg)	% PO Conversion[b]	Product Ratio[c]		
					1	**3**	**4**
1	**8**	-	0	0	-	-	-
2	**-**	[PPN]Cl	Trace	Trace	100	-	-
3	**8**	[PPN]Cl	127.3	3.3	71.4	14.3	14.3
4	**8**	TBAC	93.0	2.4	71.4	7.1	21.4
5	**8**	DMAP	48.2	1.3	100	-	-
6	**8**	Melm	45.5	1.2	33.3	66.7	-
7	**7**	[PPN]Cl	86.2	2.2	23.5	17.6	58.8
8	**9**	[PPN]Cl	Trace	Trace	100	-	-
9	**10**	[PPN]Cl	51.5	1.4	66.7	6.7	26.7

[a]All reaction performed neat in PO (2.01 ml) and CS_2 (1.72 ml) at 25 °C, 12 hours, complex = cocatalyst = 0.0286 mmol, Complex:PO:CS_2 = 1:1000:1000; [b]Determined by mass difference; [c]Determined by ^{1}HNMR spectroscopy

The binary catalyst system of metal complexes and co-catalyst has been shown to perform better than the metal complex or the co-catalyst [2, 12] on their own. The same concept was observed even in this study where the binary catalyst system of complex **8** and [PPN]Cl gave a better conversion of substrates to the cyclic product/s compared to when complex **8** and [PPN]Cl were used on their own, Table **4.1**, entry **3**.

The coupling reactions were analyzed with ^{1}HNMR spectroscopy and the spectrum obtained confirmed that the reactions produced only cyclic coupling products. There was no formation of copolymer observed in the ^{1}HNMR spectra. The ^{1}HNMR spectrum of the reaction residue obtained where the binary catalyst system of [PPN]Cl and complex **8**, Table **4.1** entry **3**, was used as catalyst is shown in Figure **4.3**. The assignment of the signals of the different cyclic products produced is clearly shown in Figure **4.3**.

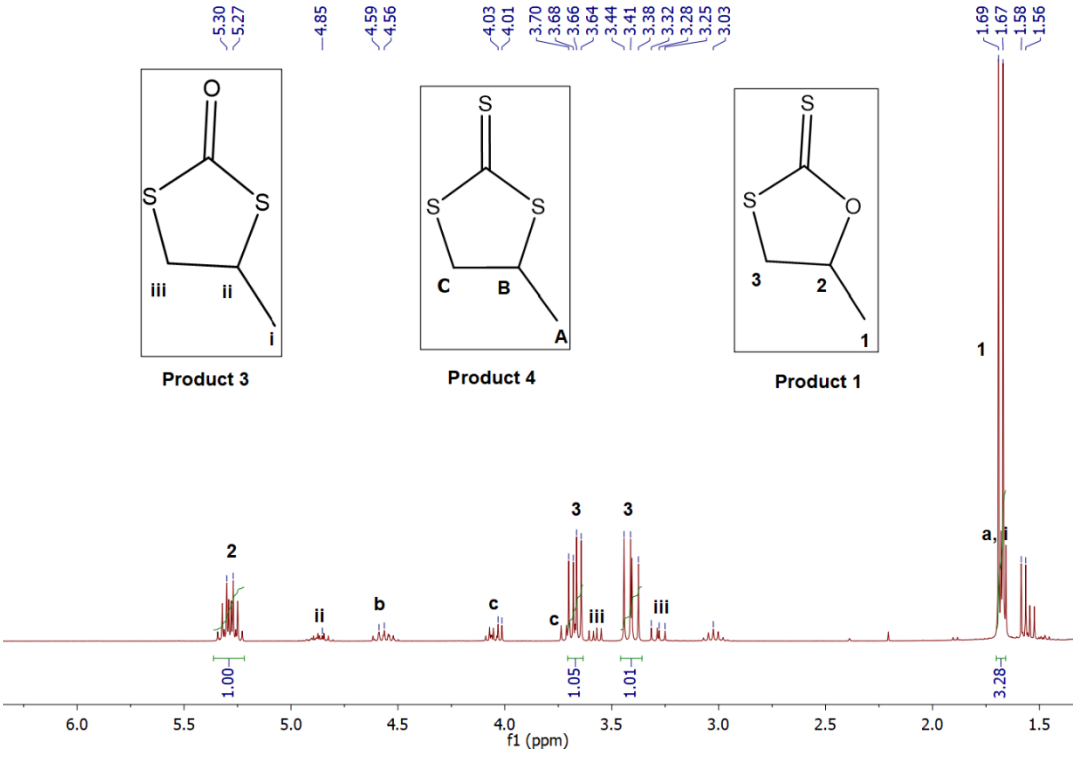


Fig. 4.3: *^{1}HNMR spectrum of the products for the CS_2 and PO coupling reaction (Table **4.1**, entry **3**) $CDCl_3$, 25 ^{o}C, products 1, 3 and 4 are shown on Scheme **4.1**.*

The full assignment of the proton's signals for cyclic product **1** (Scheme **4.2**) observed as major isomer is discussed as an example. The intense doublet signal at 1.69 (d) ppm is assigned to the protons of the methyl group, signals at 3.28 (m) and 3.68 (m) ppm are assigned to the CH_2 protons of the methylene. The protons of the methylene group are observed at different chemical shifts because of their different orientations on the planar ring of the cyclic product. One proton is oriented *cis* to the methyl group (3.28 ppm) while the other one *trans* to it (3.68 ppm). The proton at 5.27 (m) ppm is assigned to the CH proton of the methine. Proton signals for products **3** and **4** are also observed as low intensity signals and assigned in Figure 4.3. This assignment of the signals is in line with literature reports [15].

The reaction residues were also analyzed with mass spectroscopy. The mass spectrum of the crude reaction residue isolated when complex **8** and [PPN]Cl was used as catalyst system, Table **4.1** entry **3**, is shown in Figure **4.4**. In the spectrum the species observed at 134.99 m/z can be assigned to $[M+H]^+$ of the isomer products **1** and **3**. It is quite difficult to say exactly which product was produced based on the mass spectrum as these two isomers have the same theoretically m/z value. The specie observed at 149.0081 m/z was assigned to product **4** and it is clear from the mass spectrum that the reaction did not only result in one cyclic product as also confirmed with ^{1}HNMR spectroscopy.

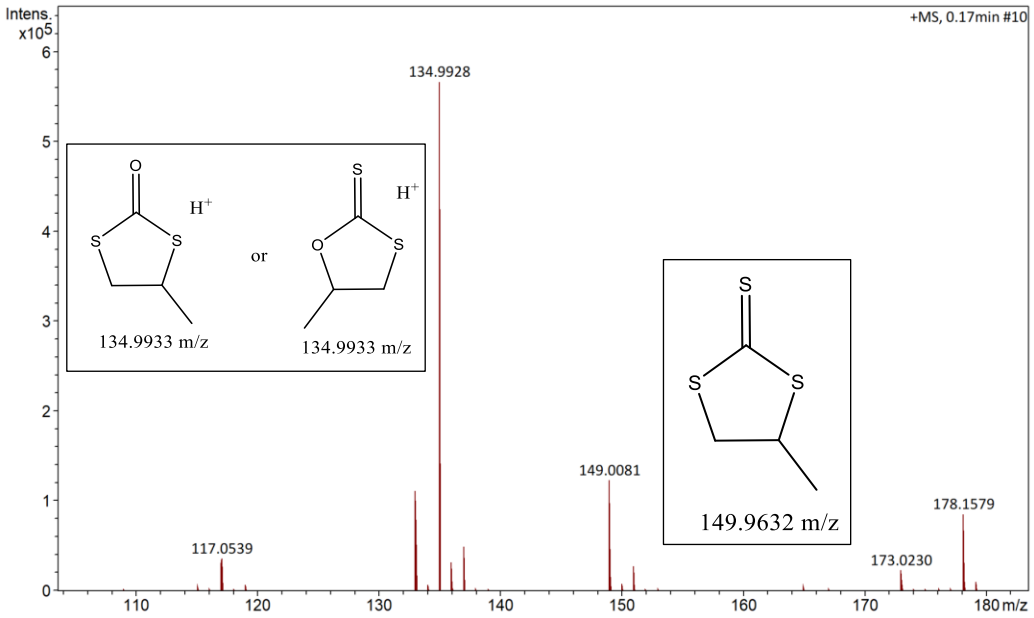


Fig. 4.4: *Mass spectrum of the reaction residue obtained for coupling reaction products (Table **4.1**, entry **3**)*

The catalytic activity of complexes for the coupling of CS_2/PO is affected by different parameters such as the nature of the co-catalyst, ligand architecture and the central metal. These parameters were investigated in this study and below are the results that were obtained. The different co-catalysts that were investigated are bis(triphenylphosphine)iminium salts ([PPN]Cl), tetra-n-butylammonium chloride (TBAC), 4-dimethylaminopyridine (DMAP) and methylimidazole (Melm). The structure of the ligands was varied as shown in Figure **4.2**. The effect of the metal center was investigated between Cr(II) and Co(II) complexes and effect of the oxidation state was investigated between Cr(II) and Cr(III) complexes.

4.2.1.1 Effect of the co-catalyst on the catalytic coupling of CS_2 and PO

In this study four co-catalysts, [PPN]Cl, TBAC, DMAP and Melm, were studied with complex **8** to investigate the effect on the catalytic performance. The highest % PO conversion of 3.0 % was obtained when [PPN]Cl (Figure **4.5**) was used as a co-catalyst. This implies that complex **8** has better activity when [PPN]Cl is used as a co-catalyst than when other co-catalysts are used. The catalyst system of complex **8** with TBAC performed second best as a catalyst with a 2.4% PO conversion being obtained.

The results obtained above agree with reports made by Darensbourg. He showed that bis(triphenylphosphine)iminium salts ($[PPN]^+X^-$) derivatives show the most activity when used as co-catalysts in the presence of transition metal complexes for CO_2/epoxide coupling reactions [16, 17]. However, the % PO conversion observed are very low compared to published data. This could be because of the poor solubility of the catalyst system in the reaction medium making it less available for catalytic activity. The catalytic could also be poor due to oversaturation of the active catalyst in the absence of an organic solvent. Catalysts poisoning by sulfur containing compounds could also result in poor activity of the catalyst system.

The product distribution seems slightly different for the various co-catalysts investigated, Table **4.1**. When [PPN]Cl and TBAC were used, three cyclic isomers were produced with product **1** being observed as a major product. When DMAP and Melm were used, one and two cyclic products were obtained, respectively. This result suggests that when complex **8** was used in the

presence of [PPN]Cl and TBAC, the scrambling process to produce other isomers of the cyclic products was more than when DMAP and Melm were used as co-catalysts.

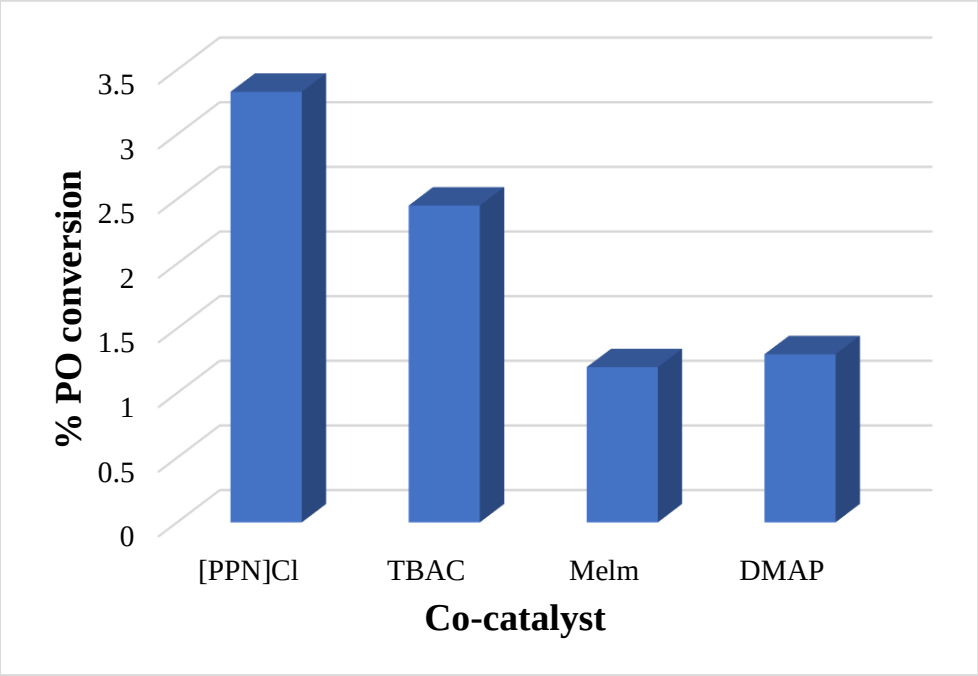


Fig. 4.5: *Comparison of the activity of complex **8** in the presence of different co-catalysts for CS_2/PO coupling.*

4.2.1.2 Effect of the ligand architecture on the catalytic activity

Substituents on the ligand's backbone have a significant impact on both the steric and electronic properties of the complexes which has an impact on the catalytic activity of the complexes [18]. Cr (III) complexes (**7, 9,** and **10**) bearing different ligands were evaluated as catalysts for the coupling of PO and CO_2 using the same reaction conditions as complex **8**. These complexes were evaluated in the presence of [PPN]Cl which is the co-catalyst that resulted in the best catalytic performance when it was used with complex **8** for the coupling reaction.

Complexes **7**, **9** and **10** also exhibited very low activity for the coupling reaction. From Figure **4.6** it can be observed that the highest % PO conversion was obtained when complex **8** was used followed by the other complexes in the order **7**>**10**>**9**. Complex **8** is more sterically hindered than complexes **7**, **9** and **10** and steric hindrance can result in less interaction between the metal and the ligand; in this context the electrophilic attack of the epoxide by the complex is reinforced and that

results in better activity. This can clearly be observed when the reactivity of complex **8** is compared to that of complex **7**. Product distribution was observed to be slightly different as different complexes were applied as catalysts for this coupling reaction, Table **4.1**. This suggests that the different complexes catalyze the scrambling process differently. For complex **7,** product **4** (58%) was observed as major isomer while for **8**, **9** and **10**, product **1** (71.4%, 100% and 66.7 % respectively) was observed as major isomer, however the selectivity was significantly different between these three complexes.

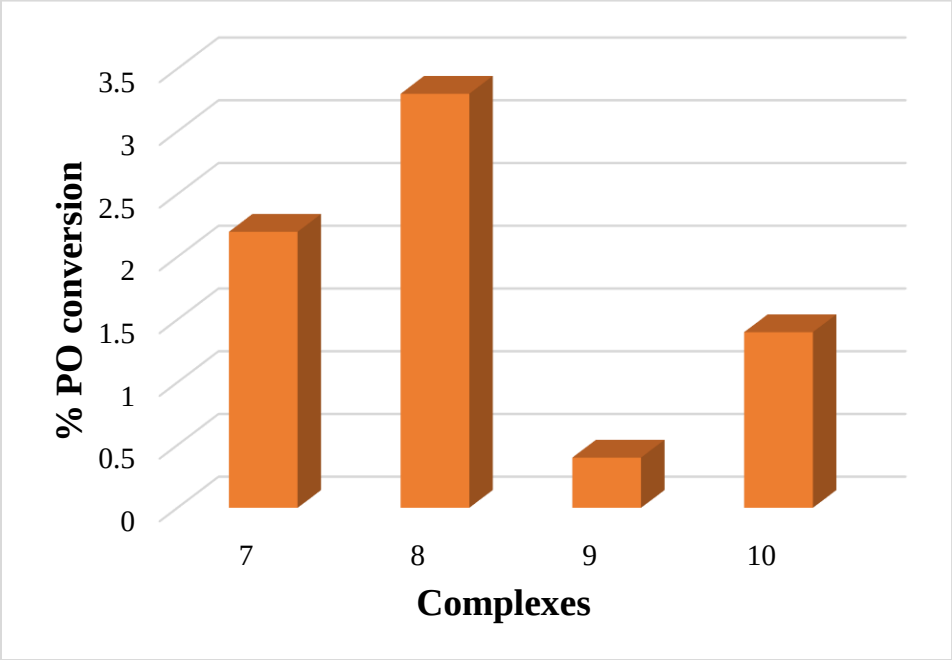


Fig. 4.6: *Comparison of the activity of Cr (III) complexes **7 - 10** towards CS_2/propylene oxide coupling*

4.2.2 Coupling of CS_2/PO using Cr(II) complexes 1 – 4 as catalyst precursors

Complexes **1 - 4** were investigated as catalysts for the coupling of CS_2 and PO. A control reaction was performed with complex **2** on its own as catalyst, Table **4.2** entry **1**. When complex **2** was used on its own as a catalyst no quantifiable amount of cyclic products was formed. The complex was then evaluated in the presence of the four co-catalyst, [PPN]Cl, DMAP, Melm and TBAC. The data obtained for these experiments are summarized in Table **4.2.**

The reaction residues were analyzed with ^{1}HNMR spectroscopy and the spectra obtained confirmed production of cyclic products for all experiments. A representative ^{1}H-NMR spectrum of the reaction residue that was obtained for the coupling reaction using complex **2** and [PPN]Cl as co-catalyst, Table **4.2** entry **2**, is shown in Figure **4.7**. The spectrum shows that the coupling reaction when Cr(II) complex **2** was used as catalyst produced the same cyclic coupling products observed for reaction performed with Cr(III) complex **8** was used as catalyst.

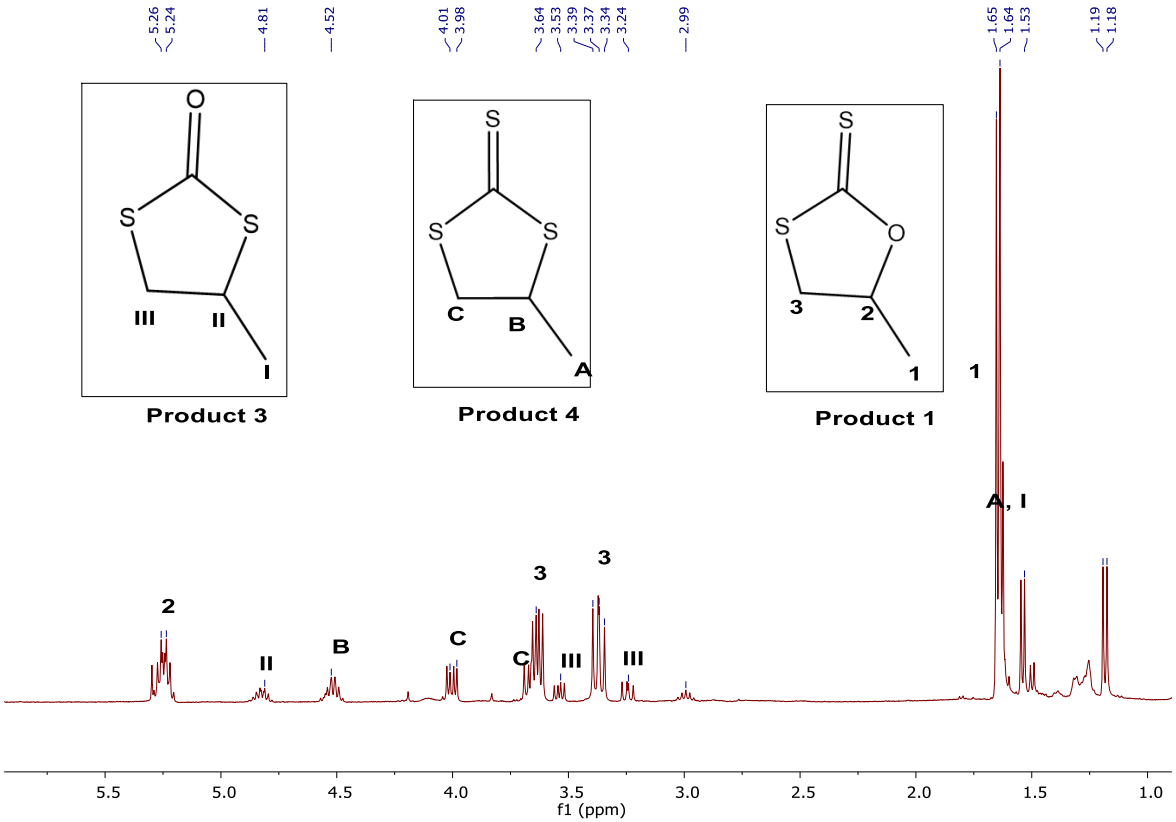


Fig. 4.7: *^{1}H-NMR spectrum of the product obtained for entry **2**, Table **4.2**, products **1**, **3** and **4** are shown on Scheme **4.1***

The binary catalyst system of complex **2** and [PPN]Cl was observed to be the best performing system amongst the co-catalyst investigated for the coupling reaction with a % PO conversion of 3.0%. The activity observed with the different co-catalyst decreased in the order TBAC>DMAP>MeIm (2.1%, 1.7% and 1.3% respectively). In the case of complex **2** the co-catalyst was also observed to influence the selectivity of the type of cyclic coupling product produced. Both [PPN]Cl and TBAC produced product **1** as major isomer, however a slightly higher

selectivity was observed with TBAC. In the reaction performed with DMAP and MeIm only two isomers (product **1** and **4**) were observed, however the distribution of the isomers were significantly different. In the reaction with DMAP a greater selectivity to product **4** (90.9 %, Table **4.2**) was observed while with Melm both isomers were produced in equal amount (50%).

Table 4.2: CS_2/epoxide coupling reactions using Cr (II) complexes **1** – **4** as catalyst precursors[a]

Entry	Complex	Co-catalyst	Mass (mg)	% PO Conversion[b]	Product Ratio[c]		
					1	**3**	**4**
1	**2**	-	0	0	-	-	-
2	**2**	[PPN]Cl	114.6	3.0	58.8	17.6	23.5
3	**2**	TBAC	78.7	2.1	66.7	6.7	26.7
4	**2**	DMAP	64.2	1.7	9.1	-	90.9
5	**2**	Melm	49.8	1.3	50	-	50
6	**1**	[PPN]Cl	72.4	2.0	66.7	13.3	20
7	**3**	[PPN]Cl	50.0	1.4	-	-	100
8	**4**	[PPN]Cl	62.0	1.8	-	-	100

[a]All reaction performed neat in PO (2.01 ml) and CS_2 (1.72 ml) at 25 °C, 12 hours, complex = cocatalyst = 0.0286 mmol, Complex:PO:CS_2 = 1:1000:1000; [b]Determined by mass difference; [c]Determined by ^{1}HNMR spectroscopy

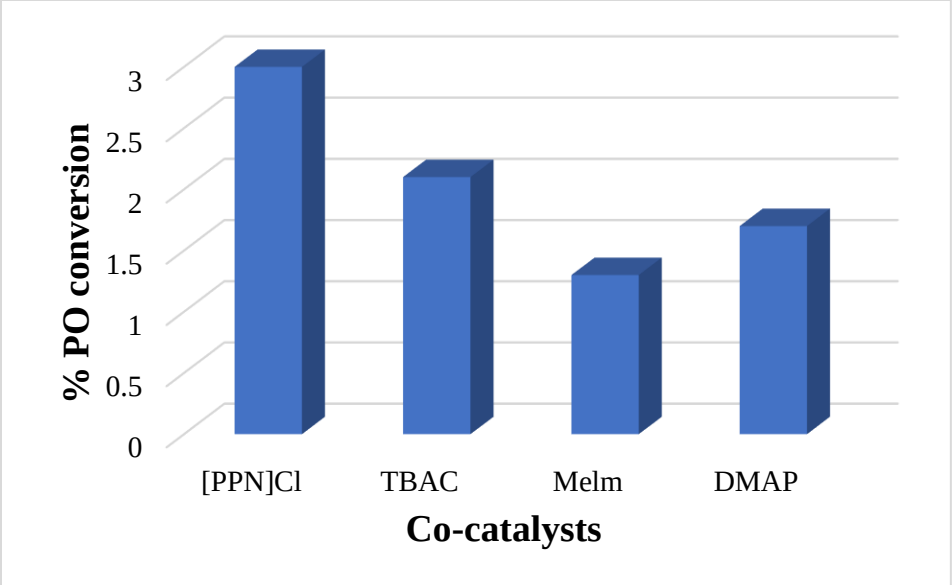


Fig. 4.8: *Comparison of the activity of complex **2** in the presence of different co-catalysts for CS_2/PO coupling reaction.*

Other Cr(II) complexes **1, 3** and **4** bearing different ligands architecture using [PPN]Cl as a co-catalyst were evaluated using the same reaction conditions used for complex **2**. From Figure **4.9** it can be observed that the activity of the Cr(II) complexes increased in the order **2**>**1**>**4**>**3**. The trend in activity observed is quite similar to the trend obtained for Cr(III) complexes where complex **8,** the Cr(III) analogue of complex **2,** was also found to have the highest activity compared to other Cr(III) complexes. The most sterically hindered complex performed better than all the less sterically hindered complexes in both cases.

Product distribution seems a bit different as different Cr(II) complexes were used as catalysts for the coupling of CS_2 and PO. When complexes **1** and **2** were used as catalysts, about three products were produced in different proportions. When complex **3** and **4** were used as catalysts one product was produced, Table **4.2**. This implies that, para substituted Cr(II) complexes **3** and **4** do not catalyze the scrambling process. While complexes **1** and **2** does. In conclusion. the nature of the ligand architecture around the Cr(II) complexes affect to some extent, the ratio of specific cyclic products product.

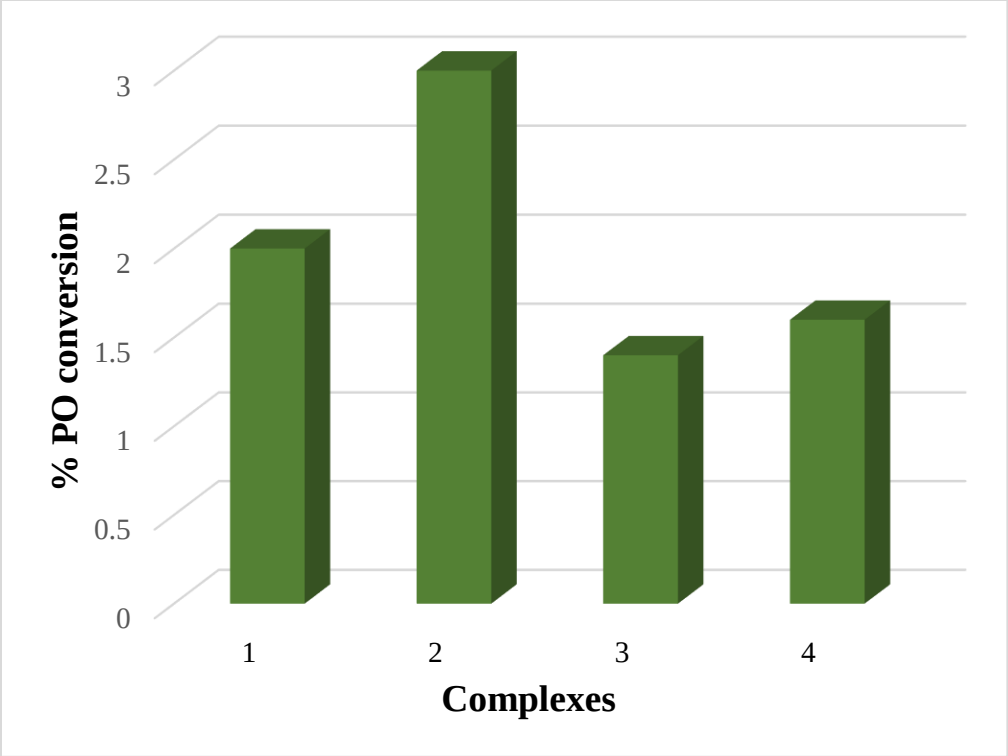


Fig. 4.9: *Comparison of the activity of different bis-salicylaldimine Cr (II) complexes towards CS_2/PO coupling*

4.2.3 Effect of the chromium oxidation state in the catalytic CS_2/PO coupling reaction.

Comparison of the activity of Cr(II) and Cr(III) complexes was made with the aim of investigating the effect of the oxidation state of the chromium metal in the presence of [PPN]Cl as a co-catalyst. Electron deficient metal is expected to increase the reaction rate due to efficient epoxide coordination which aids in its ring opening. This hypothesis is proved true in Figure **4.10**, where it is observed that Cr(III) complexes **7** and **8** performed slightly better than the corresponding Cr(II) analogues, **1** and **2**. A different case is observed for Cr(III) complexes **9** and **10** when compared to the Cr(II) complexes **3** and **4** respectively. In this case the Cr(II) complexes performed better than their corresponding Cr(III) complexes. There are many factors that can influence this, and stability of the complexes could be one of them. There is really no observable trend in the effect of the oxidation state between Cr(II) and Cr(III) on the catalytic activity of these complexes towards the coupling of CS_2 and PO.

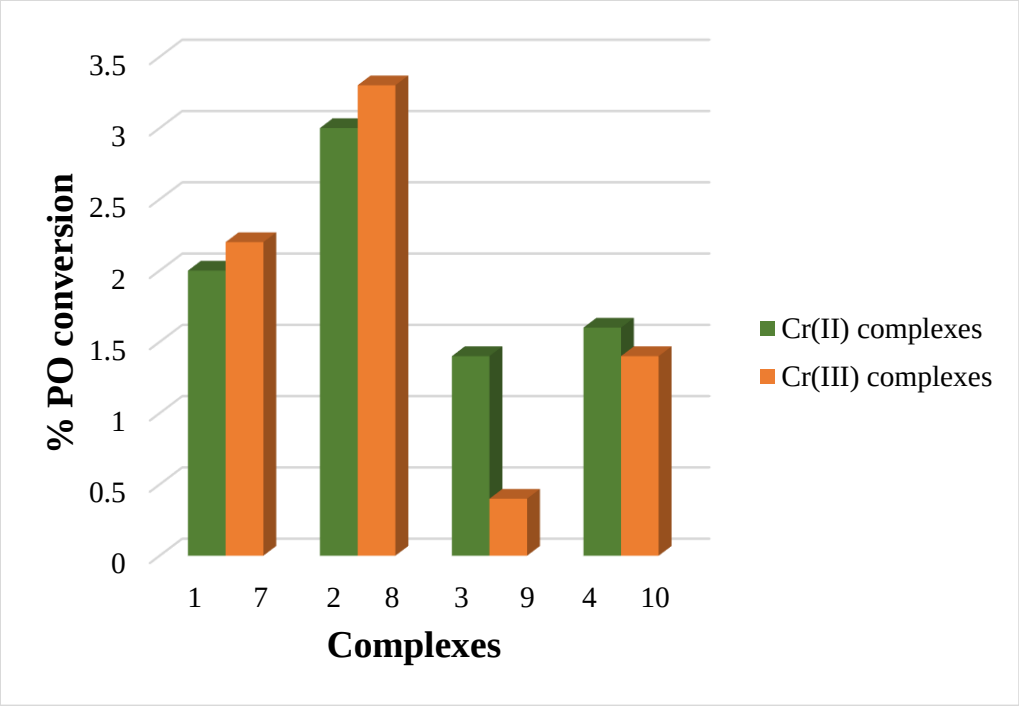


Fig. 4.10: *Comparison of the activity of bis-(salicylaldiminato) Cr (II) and Cr (III) complexes for CS_2/PO coupling in the presence of [PPN]Cl.*

4.2.4 Coupling of CS_2/PO using Co (II) complexes 13 – 16 as catalyst precursors

Cobalt complexes **13 – 16** were also evaluated as catalysts for the coupling of CS_2 and PO. The approach for investigating these complexes was similar to studies performed for Cr(II) complexes. A control experiment was first performed with complex **14** on its own. Trace amount of product was obtained when the Co(II) complex **14** was used on its own as catalyst for the coupling reaction which is inconsistent with results obtained for control experiment performed with Cr(II) complex **2** and Cr(III) complex **8** for which no cyclic products were obtained. The activity of complex **14** was also evaluated in the presence of the four co-catalysts, [PPN]Cl, TBAC, Melm and DMAP (Table **4.3)**.

Table 4.3: CS_2/epoxide coupling using Co (II) complexes **13** – **16** as catalysts

Entry	Complex	Co-catalyst	Mass/ mg	%Conversion[b]	Product ratio[c]		
					1	**3**	**4**
1	**14**	N/A	9.2	0.2	-	-	-
2	**14**	[PPN]Cl	23.1	0.6	66.7	6.7	27.7
3	**14**	TBAC	23.8	0.6	-	-	-
4	**14**	DMAP	26.5	0.7	-	-	-
5	**14**	Melm	25.7	0.7	-	-	-
6	**13**	[PPN]Cl	19.5	0.5	37.9	37.9	24.2
7	**15**	[PPN]Cl	13.6	0.4	17.6	54.0	28.4
8	**16**	[PPN]Cl	53.9	1.4	29.5	70.5	0

[a]All reaction performed in neat PO (2.01 ml) and CS_2 (1.72) at 25 °C, 6 hours, mmol complex = cocatalyst = 0.0286, Complex:PO:CS_2 = 1:1000:1000; [b]Determined by mass difference; [c]Scheme 4.1, determined by ^{1}HNMR spectroscopy

The ^{1}HNMR spectrum of the reaction residue obtained when complex **14** was used as catalyst precursor in the presence of [PPN]Cl as co-catalyst is shown in Figure **4.11**. The spectrum shows that this cobalt complex produces the same cyclic products obtained with the chromium complexes. However, in this case, product **4** was formed as a major isomer while product **1** was formed as minor isomer (Figure **4.11**).

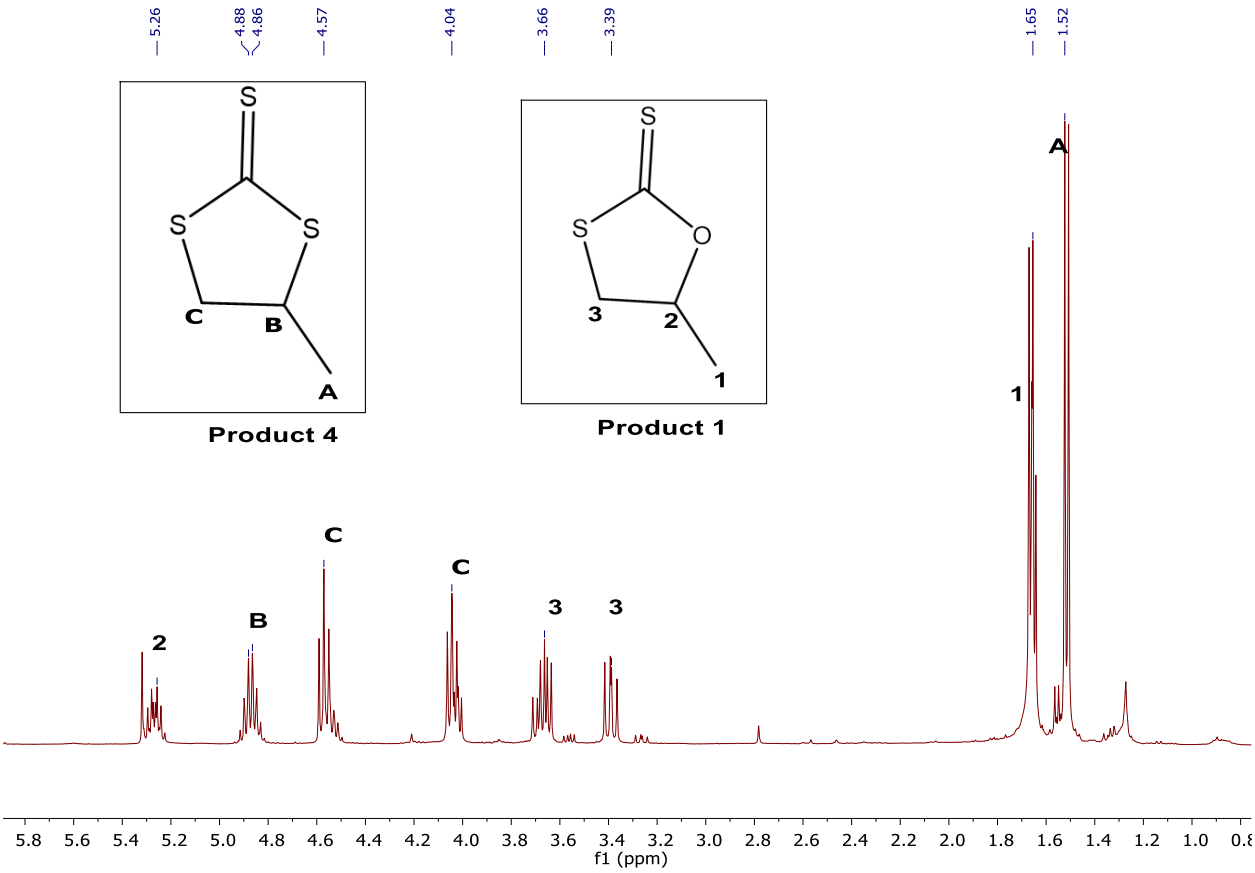


Fig. 4.11: *^{1}HNMR spectrum of the products for the coupling CS_2 and PO reaction using complex **14** and [PPNCl], entry **2** table **4.3**.*

A comparison of the activity of the binary catalyst system of complex **14** with different co-catalysts show that there was no significant difference in the amount of PO that was converted to the coupling product. However, a slightly better activity was obtained when complex **14** was used in the presence of DMAP as a co-catalyst, Figure **4.12**. This result is also different from what was obtained when the corresponding Cr(II) and Cr(III) complexes were used as catalysts, where they performed better in the presence of [PPN]Cl as co-catalysts. Product distribution was difficult to calculate for some reactions. When DMAP, Melm and TBAC were used as catalysts the NMR spectra showed broad peaks which suggests that there was some paramagnetic cobalt in the sample causing this peak broadening.

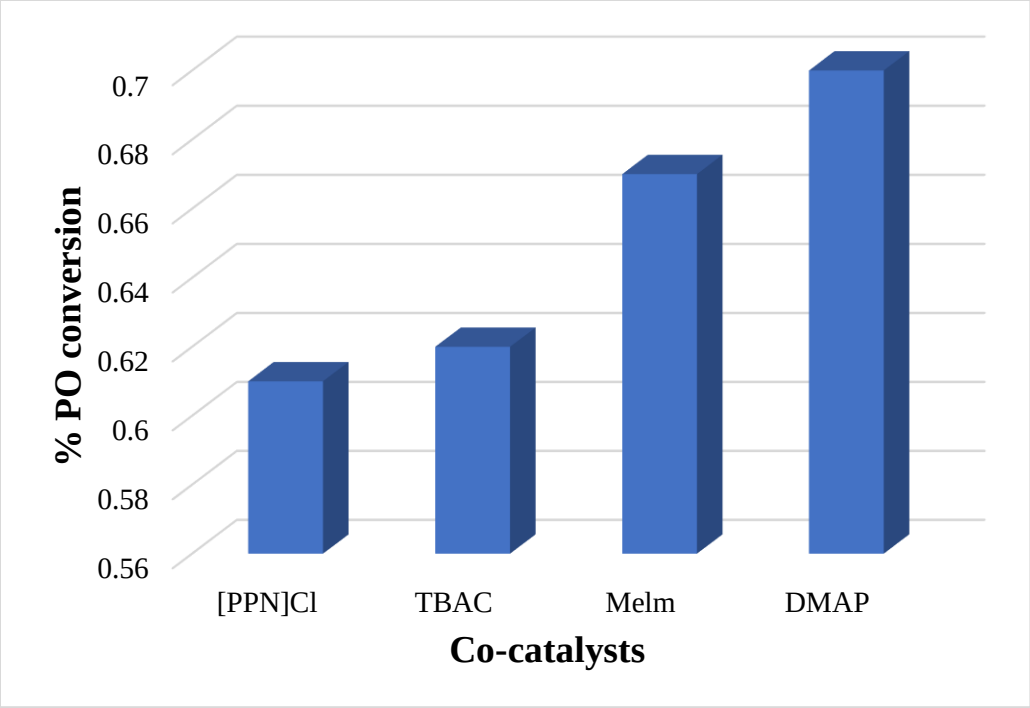


Fig. 4.12: *Comparison of the activity of different co-catalysts in the presence of complex **14** towards CS_2/epoxide*

The effect of the ligand architecture on the Co(II) complexes when they are used as catalysts for the coupling of CS_2 and PO in the presence of [PPN]Cl was also investigated. Comparison of the activity of complexes **13** – **16**, Figure **4.13**, shows that with the cobalt analogues the results are a slightly different from what was obtained for the corresponding Cr(II) and Cr(III) complexes. For Cr(II) and Cr(III) complexes **2** and **8**, bearing a ligand with isopropyl groups on the imino aromatic ring, the catalysts performed the best amongst the series studied. For Co(II) complexes, **16** was the best performing amongst the complexes evaluated, which was derived from the ligand containing an ethylacohol group as a substituent on the ligand.

Product distribution was slightly different for the series of complexes were evaluated as catalysts for this coupling reaction, Table **4.3**. When sterically hindered complex **14** was used as a catalyst there seem to less scrambling compared to other less sterically hindered complexes. This could suggest that the steric properties of the ligand play a very important role in the nature of the product produced from the coupling reaction.

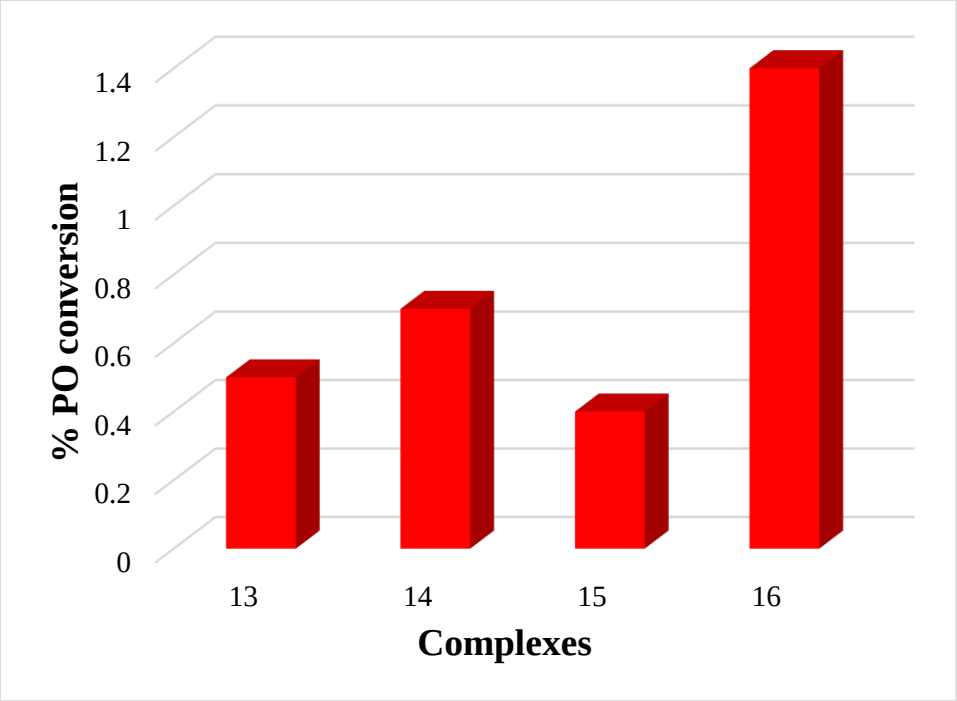


Fig. 4.13: *Comparison of the activity of different Co (II) complexes towards CS_2/epoxide coupling*

4.2.5 Effect of the metal center on the catalytic activity of Co(II) and Cr(II) complexes on CS_2/PO coupling reaction.

The effect of the metal center on the complexes that were evaluated as catalysts for the coupling of CS_2 and PO was investigated with Cr(II) (**7** – **10**, Figure **4.1**) and their corresponding Co(II) (**13** – **16** Figure **4.1**) complexes. Figure **4.14** shows that all Cr(II) complexes performed better as catalysts for the coupling of CS_2 and PO than their corresponding Co(II) complexes in the presence of [PPN]Cl as a co-catalyst. This could be first explained by the fact that Co(II) complexes showed very poor solubility in the reaction mixture. There was always a suspension that was observed when these complexes were used as catalysts indicating that the complexes could be sparingly soluble in the reaction mixture. This case could make them rarely available for the catalytic reaction compared to Cr(II) counterparts and less catalytic conversions were obtained. Secondly this was expected because even in the reactivity series of metals, chromium is slightly more reactive than cobalt. It will therefore be easier to attach an epoxide for ring opening to chromium than it will be to cobalt.

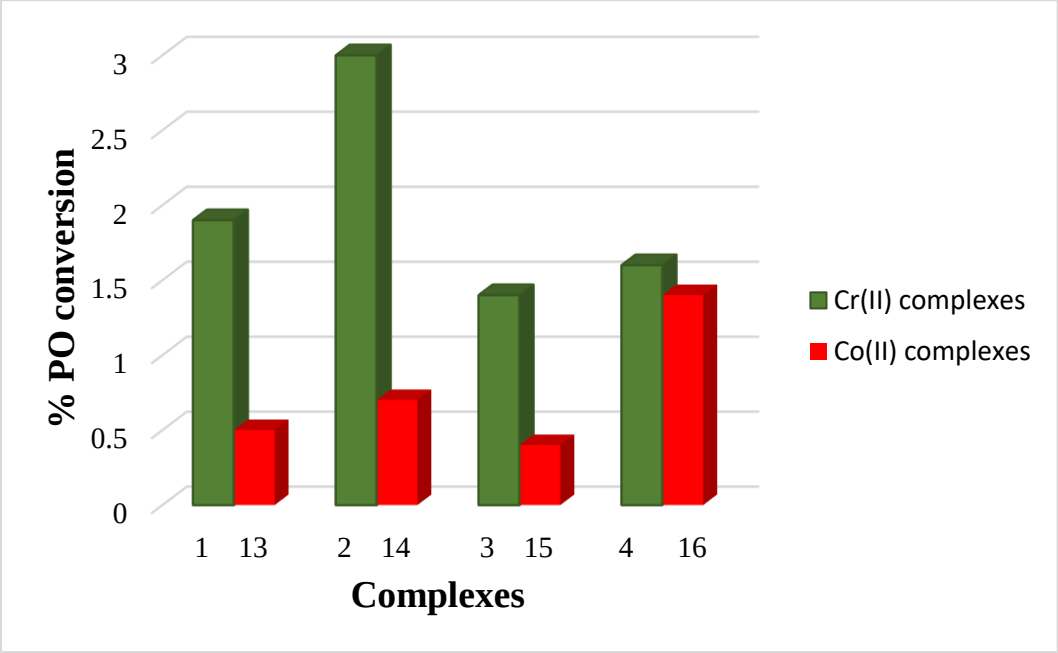


Fig. 4.14: *Comparison of the activity of Co(II) and Cr(II) complexes towards CS_2/PO coupling.*

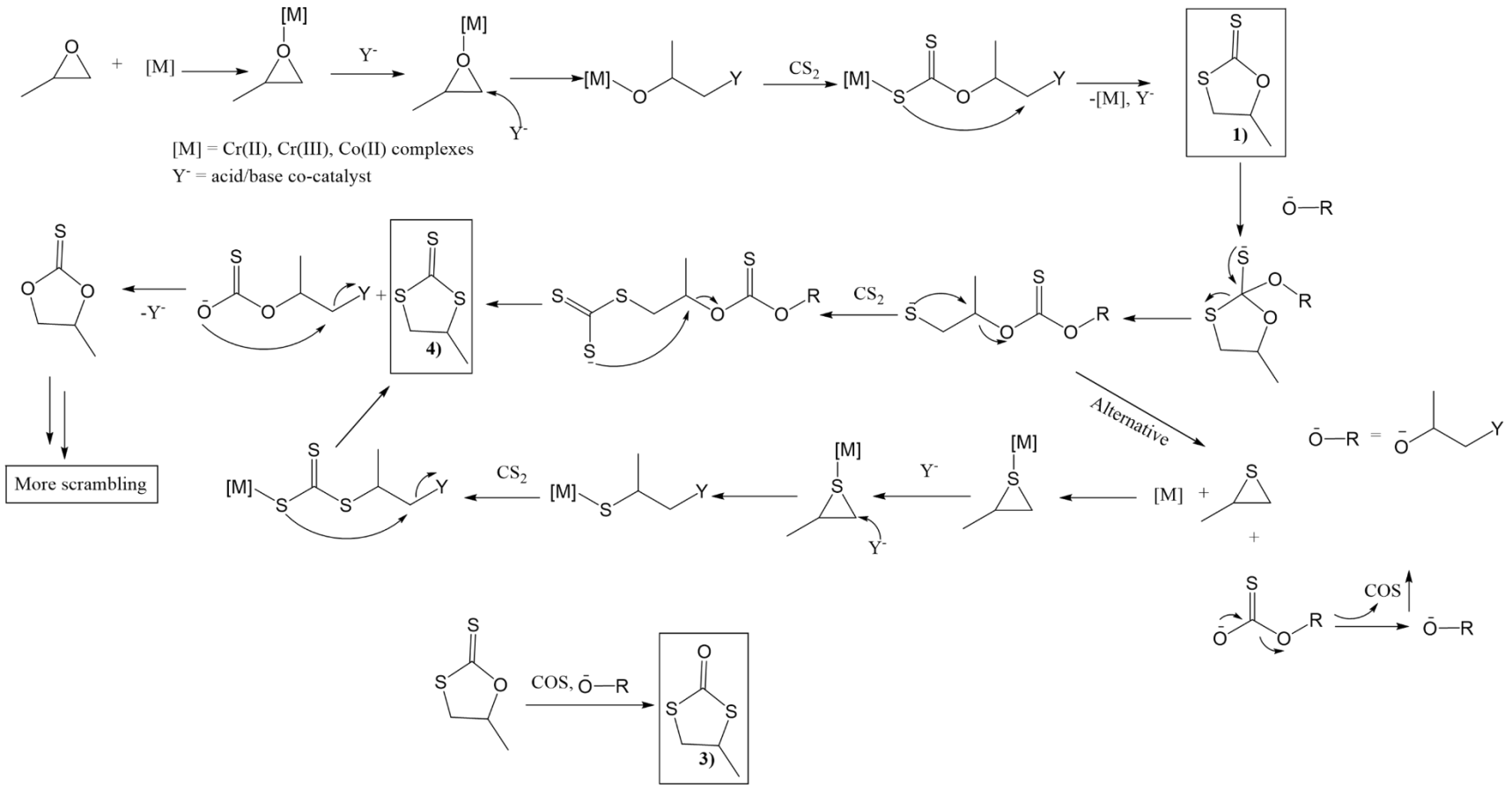
4.2.6 Cycloaddition mechanism

The mechanistic pathway has been well studied by Zhang and his coworkers [19]. It was also proposed by Wang and co-workers [12]. The reaction pathway for the catalytic coupling reaction of CS_2 and PO is proposed to occur as shown in Scheme **4.3**. The coupling reaction begins with the ring opening of the three membered ring propylene oxide at the less sterically hindered C-O or C-S bond and this is dependent on the nucleophilicity of the free Y^- (co-catalyst) and the electrophilic interaction between the mental complex and the epoxide. The coupling reaction proceeds to produce an intermediate which is a metal bound alkoxide. CS_2 can insert between the metal and the alkoxide to form an intermediate that ring closes to form a five membered ring which is product **1**, Scheme **4.2**.

A nucleophile from the ring opened epoxide can also attack product **1** and ring open it to form an intermediate that can allow insertion of anther CS_2 molecule to form another intermediate that can ring closes to form product **4**. Alternatively, after ring opening product **1**, the reaction can precede ring closure and form episulfide which can be a new source of epoxide. The episulfide just like PO can coordinate to the metal and undergo ring opening step by the co-catalyst. The ring opened

episulfide can insert CS_2 resulting in an intermediate with all sulfur atoms. This intermediate can undergo ring closure resulting in formation of product **4**.

When the episufide is formed, COS is formed as a byproduct. This can also act as feet stock material to the coupling reaction. For instance, after product **1** is ring opened by a nucleophile from ring opened PO, COS can insert into the intermediate resulting in an intermediate that ring closes to form product **3**. The presence of a Lewis acid or base easily catalyze atom exchange of 'S' and 'O' between CS_2 and PO to produce various reactive compounds such as COS and CO_2. Metal complexes and nucleophiles such as co-catalysts catalyze the coupling reaction of epoxide with either CS_2, COS, or CO_2 to produce cyclic thiocarbonates or cyclic carbonate.



Scheme 4.3: *Proposed mechanism of the CS_2 and PO coupling reaction to produce cyclic products [12, 19]*

4.3 Conclusion

Bis-(salicylaldiminato) Cr(II), Cr(III) and Co(II) metal complexes were evaluated as catalysts for the coupling of CS_2 and propylene oxide. It was found that the catalytic reactions produced generally cyclic products instead of co-polymers and this was confirmed with NMR spectroscopy and mass spectrometry. These neat reactions generally produced very low yields, less than 5 %. Even though the yields were very low, there are complexes that seemed to perform better than the others. The binary catalyst system of [PPN]Cl and complexes **2**, **8** and **16** performed better as catalysts for the CS_2/PO coupling than other Cr(II), Cr(III) and Co(II) complexes respectively giving yields of 3.0, 3.3 and 1.4 % respectively.

The effect of co-catalyst ([PPN]Cl, TBAC, DMAP, and Melm) was investigated between complexes **2**, **8** and **14**. Chromium complexes **2** and **8** performed better in the presence of [PPN]Cl with conversions of 3.0 and 3.3 % respectively while Co(II) complex **14** performed better in the presence of DMAP and Melm as catalysts with similar conversion of 0.7%. Cr(II) complex **2** and Cr(III) complex **8** did not produce quantifiable amount of coupling products when evaluated as catalysts on their own. Co(II) complex 1**4** produced trace amount of coupling product when used as a catalyst on its own. [PPN]Cl also produced trace amounts of cyclic products when used as catalyst for the coupling product on their own. Therefore, the binary catalyst system is concluded to perform better than when the metal complexes or [PPN]Cl were used as catalysts on their own.

In the investigation of the effect of the oxidation state between Cr(II) and Cr(III) complexes, some Cr(III) complexes, **7** and **8** performed better than their corresponding Cr(II) complexes, **1** and **2**. This was found to be an inverse for Cr(III) complexes **9** and **10** where their corresponding Cr(II) complexes **3** and **4** performed better than them. With this result, it is concluded that there is no observable trend in terms of the influence of the oxidation state on the catalytic process. For the investigation of the effect of metal center on the catalytic reaction, all Cr(II) complexes performed better than the corresponding Co(II) complexes. Co(II) complexes were found to perform very poor with yields of less than 1 % of the coupling products.

4.4 Experimental

4.4.1 Materials and instrumentation

Reagent grade chemicals were obtained from Sigma Aldrich and used as received. All solvents were dried under appropriate drying reagent and distilled prior to use. The coupling reactions were performed in a 12 place RADLEY's Heated Carousel Reaction Station fitted with a reflux unit as well as a gas distribution system with glass reaction vessels. Mass spectra were recorded on Bruker compact ultimate 3000 HR-MS. ^{1}HNMR and ^{13}CNMR spectra were recorded on a Varian 300 MHz spectrometer using tetramethylsilane as an internal standard. Chemical shifts are reported in (ppm) and referenced to residual proton in $CDCl_3$.

4.4.1 General procedure for the coupling of CS_2 and propylene oxide

Coupling reactions were performed in a 12 place RADLEY's Carousel Reaction Station fitted with a reflux unit as well as a gas distribution system. To the carousal reaction tubes was added the metal complex (0.028 mmol), the co-catalyst (0.028 mmol) followed by PO (28.6 mmol, 2.01 ml) and CS_2 (28.6 mmol, 1.72ml). The reaction mixture was stirred under argon for the specific time at room temperature. The reaction was stopped, and all volatiles were removed. The crude reaction residue was weighed and analyzed with ^{1}H-NMR spectroscopy in $CDCl_3$ and mass spectrometry.

4.5 References

[1] X.-X. Zang, F. Liu, K.-X. Sun, S. Chen, Y.-B. Du, R.-G. Qi and M. K. Wan, *Macromolecules,* vol. 41, pp. 1587 - 1590, 2008.

[2] M. Luo, H.-X. Zhang and J. D. Darensbourg, *Macromolecules,* vol. 48, pp. 5526 - 5532, 2015.

[3] X. -B. Lu and J. D. Darensbourg, *Chem. Soc. Rev.,* vol. 41, pp. 1462 - 1484, 2012.

[4] E. Marianucci, C. Berti, F. Pilati, P. Manararesi, M. Guaita and Chiantore, *Polymer,* vol. 35, pp. 1564 - 1566, 1994.

[5] C. Beattie and M. North, *ChemCatChem,* vol. 6, pp. 1252 - 1259, 2014.

[6] W. Choi, F. Sanda, N. Kihara and T. Endo, *J. Polym. Sci. Part A,* vol. 35, pp. 3853 - 3856, 1997.

[7] W. Choi, F. Sanda and T. Endo, *Macromolecules,* vol. 31, pp. 2454 - 2460, 1998.

[8] S. Motokucho, A. Sudo, F. Sanda and T. Endo, *Chem. Commun.,* pp. 1946 - 1947, 2002.

[9] N. Y. Belokon, I. V. Maleev, M. North and L. D. Usonov, *Chem. Commun.,* pp. 4614 - 4616, 2006.

[10] W. Choi, F. Sanda and T. Endo, *Macromolecules,* vol. 31, pp. 2454 - 2460, 1998.

[11] Y. Taguchi, K. Yanagiya, I. Shibuya and Y. Suhara, *Bull. Chem. Soc. Jpn.,* vol. 61, pp. 921 - 925, 1988.

[12] Y.-M. Wang, B. Li, H. Wang, Z.-C. Zhang and X.-B. Lu, *Appl. Organometal. Chem.,* vol. 26, pp. 614 - 618, 2012.

[13] J. D. Darnsbourg, R. J. Andreatta, J. M. Jungman and H. J. Reibenspies, *Dalton Trans.,* pp. 8891 - 8899, 2009.

[14] N. Kihara, Y. Nakawaki and T. Endo, *J. Org. Chem.,* vol. 60, pp. 473 - 475, 1995.

[15] N. Adachi, Y. Kida and K. Shikata, *J. Polym Sci,* vol. 15, pp. 937 - 944, 1977.

[16] J. D. Darensbourg and R. M. Mackiewicz, *J. Am. Chem. Soc.,* vol. 127, pp. 14026 - 14038, 2005.

[17] J. D. Darensbourg, R. M. Mackiewicz, J. L. Rodgers and A. L. Phelps, *Inorg. Chem.,* vol. 43, pp. 1831 - 1833, 2004.

[18] Y. Xu, M. Xiao, S. Wang, M. Pan and Y. Meng, *Polym. Chem.,* vol. 5, pp. 3838 - 3846, 2014.

[19] J. C. Zhang and H. X. Zhang, *Macromolecules,* vol. 53, pp. 233 - 239, 2020.

Chapter 5

Catalytic performance of bis(salicylaldiminato) Cr(II), Co(II) and Cr(III) complexes in the coupling of CS_2 with propylene oxide in the presence of organic solvent

Contents

5.1 Introduction 147

5.2 Results and discussions 148

5.2.1 Possible mechanism for the coupling of CS_2 and PO in methanol as solvent 156

5.2.2 Effect of substrate ratio on the coupling of CS_2 and PO catalytic reaction 158

5.2.3 Effect of temperature on the coupling of CS_2 and PO catalytic reaction..... 159

5.2.4 Effect of time on the coupling of CS_2 and PO catalytic reaction..... 160

5.2.5 Effect of the ligand architecture around Cr(II), Cr(II), and Co(II) metals on the catalytic activity for the coupling of CS_2 and PO at 22 and 40 ^oC 163

5.2.6 Effect of oxidation state of Cr(II) and Cr(III) metal complexes on the catalytic activity 167

5.2.7 Effect of the metal center, Cr(II) and Co(II), on the catalytic activity 168

5.3 Conclusion…… 170

5.4 Experimental 171

5.4.1 Material 171

5.4.2 General procedure for the coupling of CS_2 and propylene oxide 171

5.5 References 172

5.1 Introduction

Coupling reactions of CS_2 and epoxides have predominately been performed solventless by many researchers in the past [1 – 5]. Solventless reaction conditions are suitable for catalysts that are easily soluble in the epoxide and CS_2 [5]. Some metal complexes are not soluble or show very poor solubility in these starting materials and that makes it difficult for the metal complexes to function as catalyst since they are less available for the process. In homogeneous catalysis all the species involved in the catalytic process must be soluble so that they can participate in the reaction.

Solvents can play a very important role in catalytic reactions. Endo and his coworkers performed the coupling reaction of CS_2 and PO in the absence of any solvent and the reaction took twelve hours to completely convert the substrates to desired coupling product/s. When the same reaction was performed in the presence of $CDCl_3$ as a solvent, the same reaction only took two hours to go to completion. The use of the solvent however affected product selectivity and a percentage ratio of 2:98 cyclic product to copolymer was obtained while in the absence of solvent only a copolymer was obtained as a product [6].

Zhang and his co-workers discovered that the addition of solvents to the coupling of CS_2 ad PO can have both negative and positive impacts. When they used DMF as a solvent with a reaction ratio for PO / CS_2 / catalyst of 100 / 150 / 1 at 120 ^oC for 12 hours there was no coupling reaction observed. However, when the same reaction was performed in the presence of trichlorobenzene a copolymer and a cyclic product were obtained in the ratio 0.3:0.7 [7]. This result indicated that the catalytic reaction was better in the presence of a less polar solvent. When the same reaction was performed in toluene as a solvent, a ratio of copolymer to cyclic product was obtained as 0.8:0.2. This indicates that when toluene was used as a solvent more copolymer was produced as a product compared to the cyclic product. Therefore, using toluene as opposed to trichlorobenzene as solvent resulted in a slight improvement of selectivity of the catalytic process towards copolymer production.

The synthesized bis-(salicylaldiminato) Cr(II), Cr(III) and Co(II) complexes showed very poor catalytic activity for PO and CS_2 coupling in the neat reactions. There are many reasons why these complexes could have shown this poor catalytic behavior; poor solubility in the reaction medium which makes them less available for the catalytic reaction. These complexes showed good

solubility in some organic solvents therefore to make them as available as possible for the catalytic reaction, the complexes could be evaluated as catalysts for the coupling of CS_2 and PO in the presence of some organic solvents. Another possibility is that the active catalytic sites of the metal complexes could be blocked because of oversaturation and introducing an organic solvent will reduce the concentration of the substrate therefore improve the catalytic activity of the metal complexes. Addition of a solvent will also allow for the variation of parameters such as temperature to improve the catalytic reaction because reports have shown that it does affect the reaction. In this chapter the effect of solvents and other catalytic conditions such as time, temperature, and substrate ratio on the catalytic performance is reported for the complexes investigated for the coupling of CS_2 and PO.

5.2 Results and discussions

The metal complexes that were synthesized in this study showed very poor catalytic activity in neat reactions, chapter 4. Therefore, to improve the catalytic activity of the synthesized complexes, the coupling reactions were studied in the presence of some organic solvents. The reaction parameters were kept exactly like those of neat reactions except that 5 ml of an organic solvent was added in this case. After the reaction, solvent was removed with the volatiles and the reaction mixture was characterized with spectroscopic techniques (NMR, mass spec and FTIR). The influence of solvents on the coupling of CS_2 and PO catalytic reaction was investigated where a range of solvents from non-polar to polar were used with complex **8** as catalyst and [PPN]Cl as a co-catalyst.

Solvents seem to play a very important role in the coupling of CS_2 and PO reaction (Figure **5.1)**. It can be observed from Figure **5.1** that the highest % PO conversion (18%) was obtained when methanol was used as a solvent. No conversion of substrates was observed when dichloromethane and acetonitrile were used as solvent for the coupling reaction. This observation was also made by Jiang and Hua they studied the effect of solvent on the coupling of CO_2 and epoxides [8]. Very poor conversions were obtained, Figure **5.1**. when solvents such as acetone, toluene and diethyl ether were used. This could suggest that the complex was less available for the catalytic process

as most of it did not dissolve in the catalytic reaction when these non-polar solvents were used as solvents.

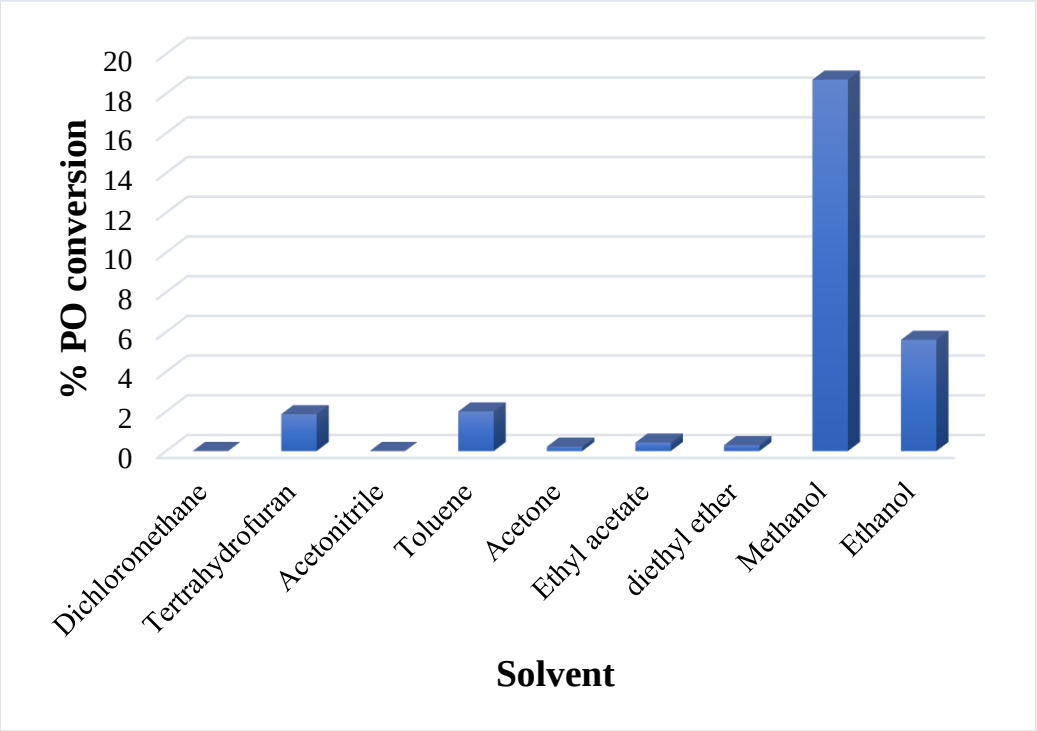
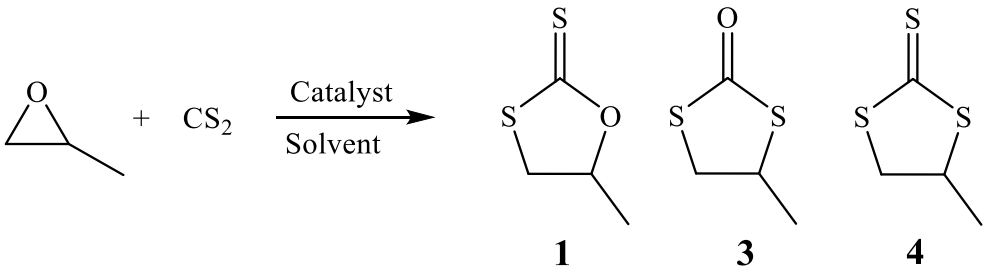


Fig. 5.1: *Effect of solvent on the coupling of CS_2 and PO when complex 8 was used as catalyst and [PPN]Cl as a co-catalyst at 24 °C and atmospheric pressure.*



Scheme 5.1: *Coupling of CS_2 and propylene oxide in the presence of organic solvents.*

The ^{1}HNMR spectra of the crude reaction residues for all the reactions conducted in different solvents showed only cyclic products with no copolymer being observed. The cyclic products **1**, **3** and **4** (Scheme **5.1**) were observed for all solvents and they are like those that were obtained in solventless reaction presented in chapter 4. An exception was observed in the case of methanol

and ethanol where the ^{1}HNMR spectra showed that different cyclic products from the ones shown in Scheme **5.1** were obtained.

In the ^{1}HNMR spectrum (Figure **5.2**) of the crude reaction mixture for the reaction performed in methanol the signals for two cyclic products (product **I** and product **II**) are observed. The assignment of the signals for the two cyclic products is shown in Figure **5.2**. The intense peaks are assigned to product **II** as follows; doublet peak observed at 1.32 ppm is assigned to the methyl group, position **1**, and the multiplets at 3.18 and 3.37 ppm are assigned to the methylene group protons at position **3**. The multiplet peak at 4.12 ppm is assigned to the methine proton, position **2**, of the cyclic product. There is a singlet peak at 4.19 ppm is assigned to the methoxy methyl protons, position **5**. There are minor peaks on the baseline which are assigned to the second product that could have been produced in this reaction because of scrambling. These peaks are assigned to methoxylated cyclic product **I**.

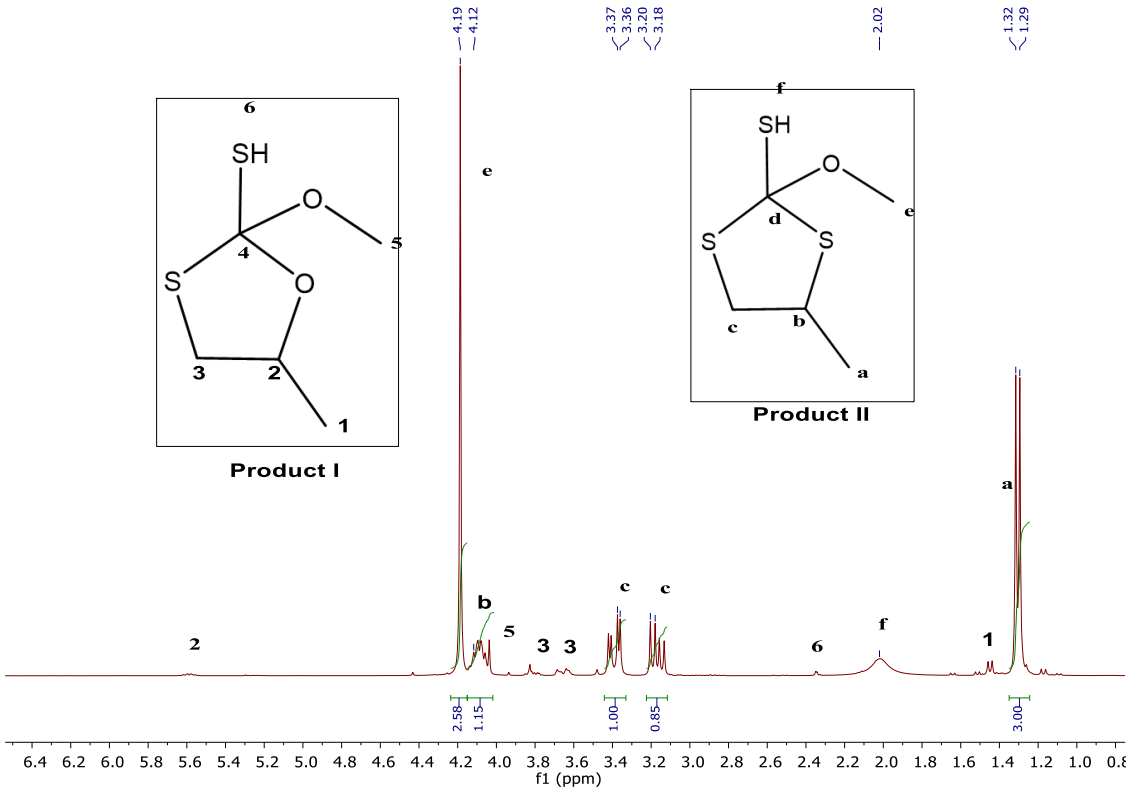


Fig. 5.2: *^{1}HNMR spectrum for the product obtained when MeOH was used as a solvent for the coupling reaction*

The spectrum of the product obtained when methanol was used as solvent seem totally different from that of the products that were obtained when the reaction was performed in other solvents, Scheme **5.1**. Figure **5.3** is a stacked spectrum of the spectra obtained when the coupling reaction of PO and CO_2 was performed in MeOH and in a neat reaction. This clearly suggest that the product that was obtained in this case is different. Surely this could also suggest that the mechanism of action in the presence of methanol compared to other solvents is totally different.

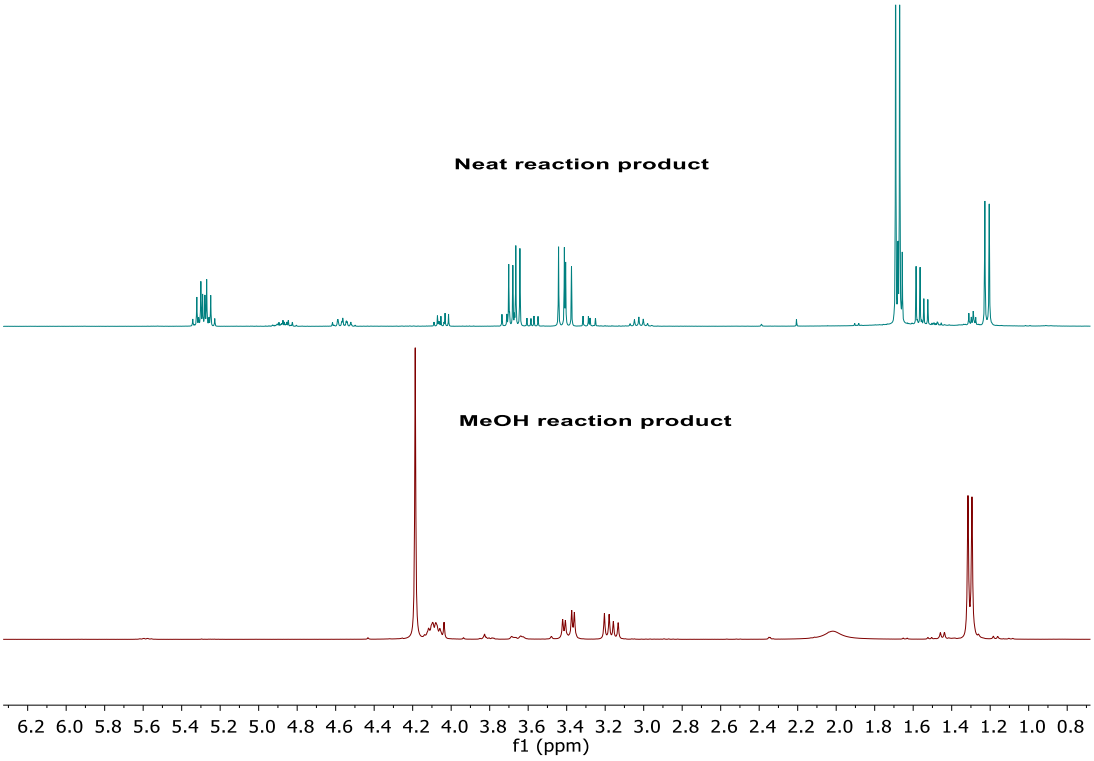


Fig. 5.3: *Staked spectrum for the spectra that was obtained when the coupling reaction was performed in MeOH and neat.*

The product that was obtained when MeOH was used as a solvent in the coupling of CO_2 and PO was analyzed with COSY NMR, ^{13}CNMR, 135DEPT, HSQC and HMBC. The COSY NMR spectrum obtained is shown in Figure **5.4**. From the spectrum it can be observed that the peak at 4.19 ppm does not correlate to any peak of the cyclic product. This peak is a result of a proton that does not have any proton three bonds away from it. This peak is assigned to a -CH_3 proton in the methoxy group attached to the cyclic product as shown in the spectrum. The broad peak at 2.02 ppm intergrades for 1 proton. This peak also does not correlate to any peak of the protons of the

cyclic product. There is correlation between peaks **a** and **b** and there is also correlation between peaks **c** and **b**. These peaks are a result of protons that are three bonds away from one another and they are assigned to the cyclic product as shown in the spectrum.

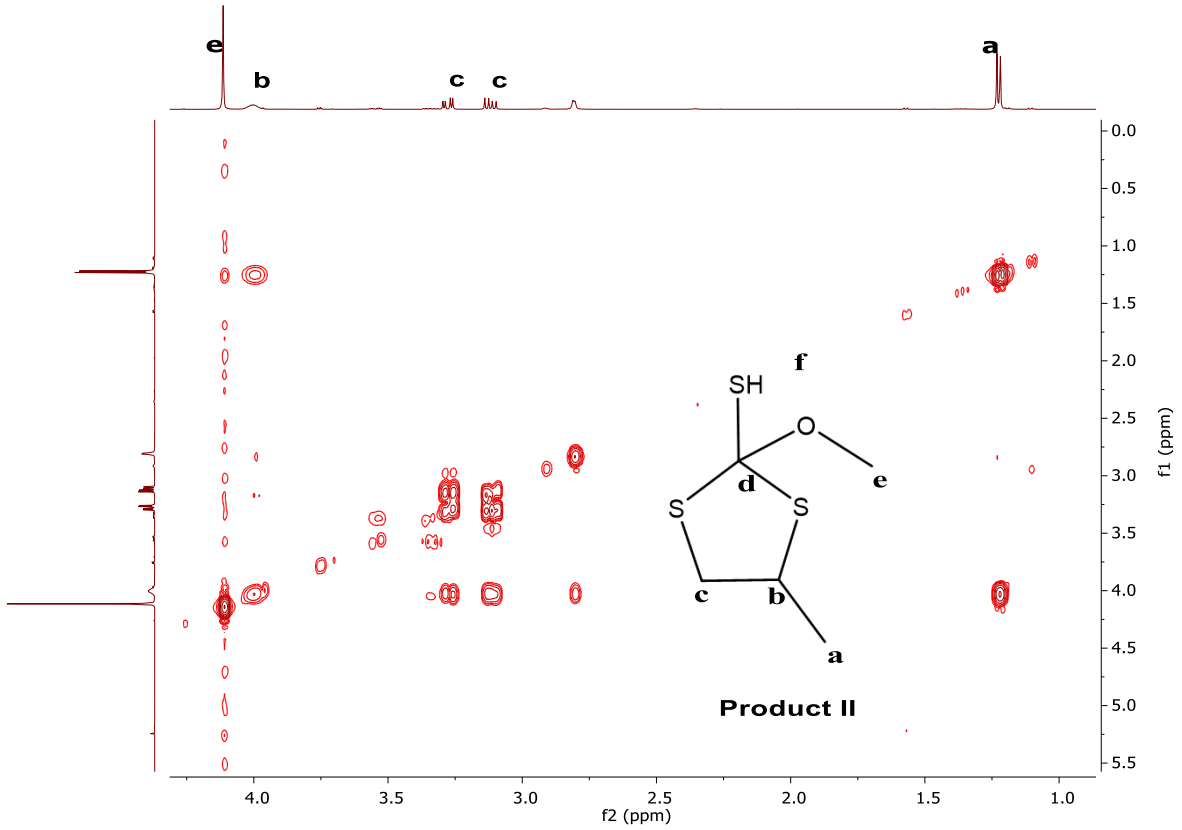


Fig. 5.4: *COSY spectrum for the product obtained when MeOH was used as a solvent for the coupling reaction*

The ^{13}CNMR spectrum of this product that was obtained for the reaction where MeOH was used as a solvent shows peaks that can be assigned to the product as shown in Figure **5.5 a**. The intense carbon peaks observed are for the major product **II** that was produced in this reaction. The peak at 60.45 ppm which could not be assigned to the carbons of a methoxy group attached to the cyclic product. 135DEPT spectrum, Figure **5.5 b**, shows that this peak may be due to a -CH_3 or a -CH group. It was assigned to a -CH_3 because ^{1}HNMR spectrum shows a singlet peak at 4.19 ppm that integrates for 3 protons. HSQC confirmed that the peak at 60.45 in the ^{13}CNMR correlate to the peak at 4.19 ppm in the ^{1}HNMR spectrum

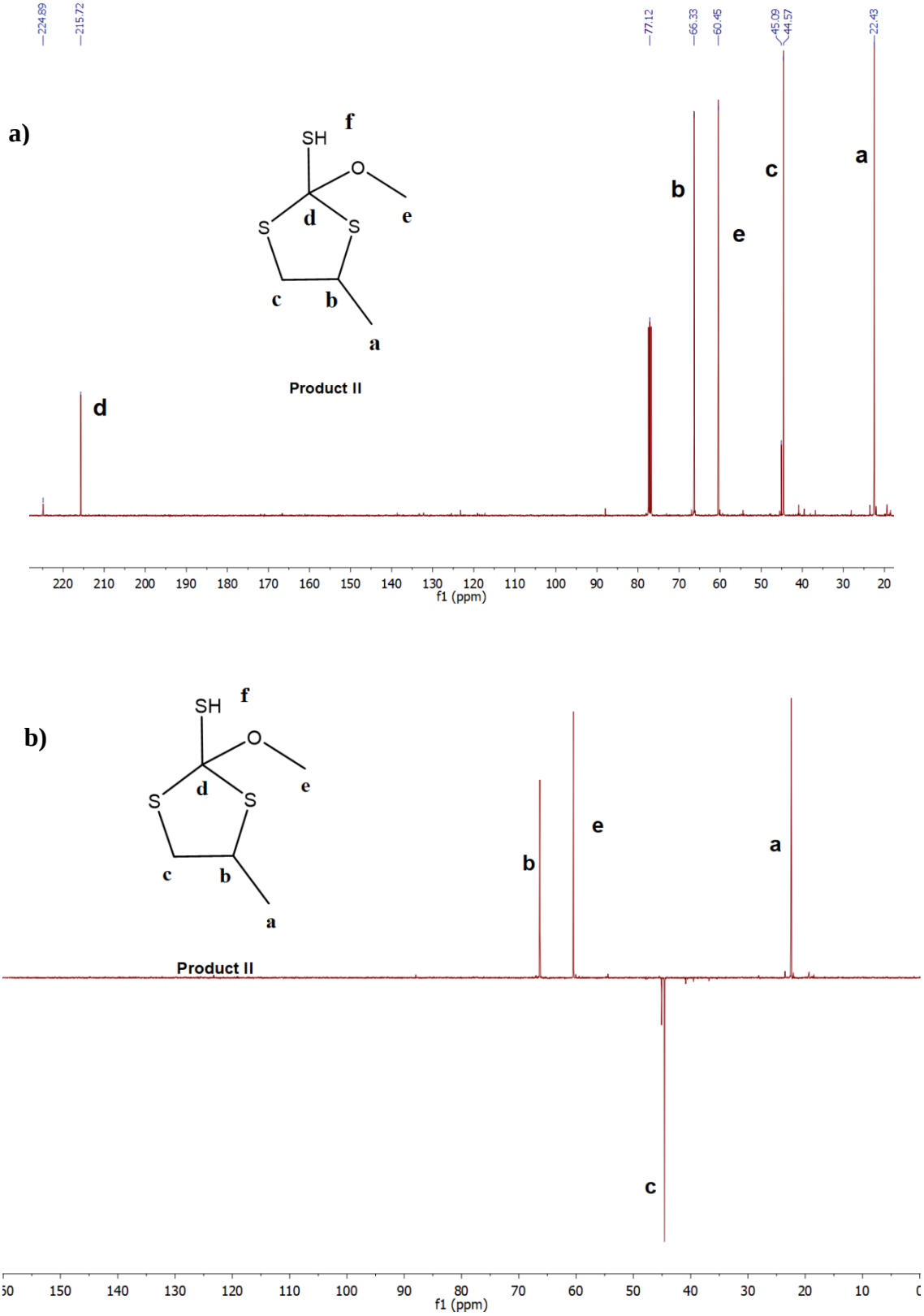


Fig. 5.5: ***a)*** *^{13}CNMR and* ***b)*** *135 DEPT spectrum when MeOH was used as a solvent for the coupling reaction*

The HMBC NMR spectrum, Figure **5.6**, that was obtained for this product shows that there is a three-bond correlation between the proton observed at 4.19 ppm and the carbon at 211 ppm in the ^{13}CNMR spectrum. This confirms that the CH_3 group is part of the cyclic product. The possibility is therefore that there is a methoxy group attached to the cyclic product as assigned in the spectrum.

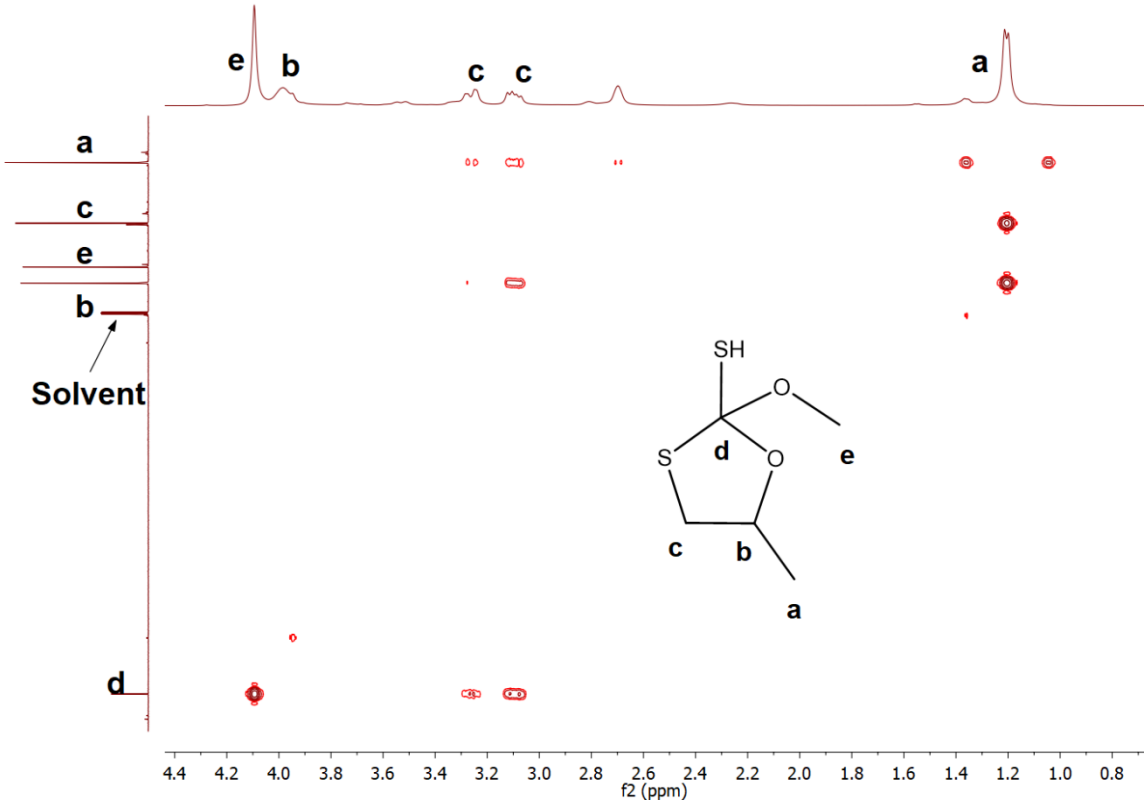


Figure 5.6: *HMBC NMR spectrum for a product formed when the coupling reaction was performed in MeOH*

FT-IR spectrum, Figure **5.7**, of the product also shows peaks that could suggest that there is some methoxy species in the product. The peak at 3300 cm^{-1} of the coupling product spectrum can be assigned to ν(S-H) and the one at 1050 cm^{-1} can be assigned to ν(C-O). There is another peak at 1250 cm^{-1} in the spectrum of the product that can be assigned to a ν(C-S) stretch.

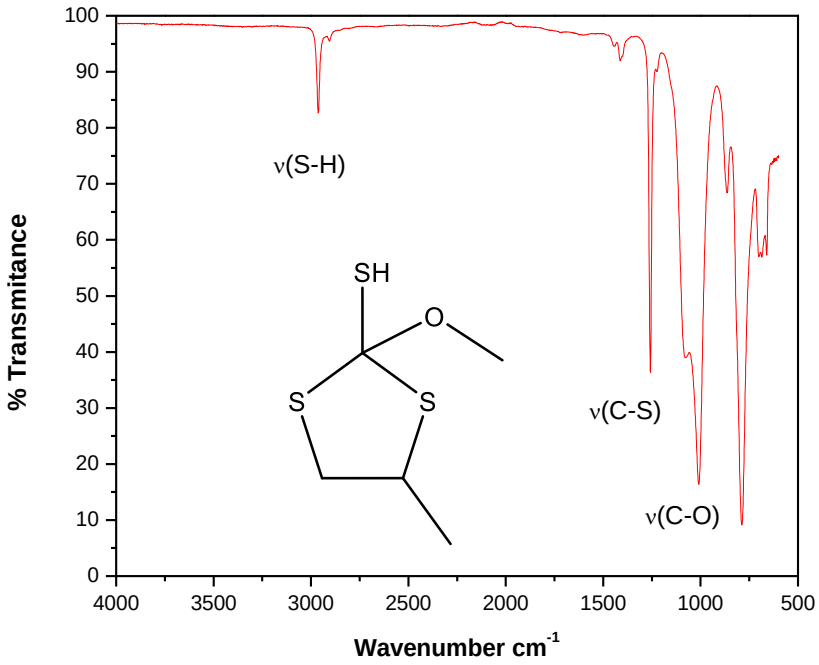


Fig. 5.7: *FT-IR spectrum of the coupling product when the reaction was performed in MeOH*

The coupling product was also analyzed with mass spectroscopy. The mass spectrum that was obtained is shown in Figure **5.8**. The spectrum shows a peak at 134.99 m/z that can be assigned to $[M+H]^+$ of the cyclic product, 5-methyl-[1,3]-oxathiolane-2-thione (product **1** Scheme **5.1)**. The peak at 149.0081 m/z was assigned to 4-methyl-[1,3]-dithiolane-2-thione (product **4** Scheme **5.1)**. There is a low intensity peak at 167.0793 m/z for the methoxylated product **I** observed in the spectrum. The spectrum is showing product **1** and **4**, Scheme **5.1**, as intense peak and this could suggest that the methoxylated products, **I** and **II**, fragment and result in these cyclic products **1** and **4** as the main stable fragments.

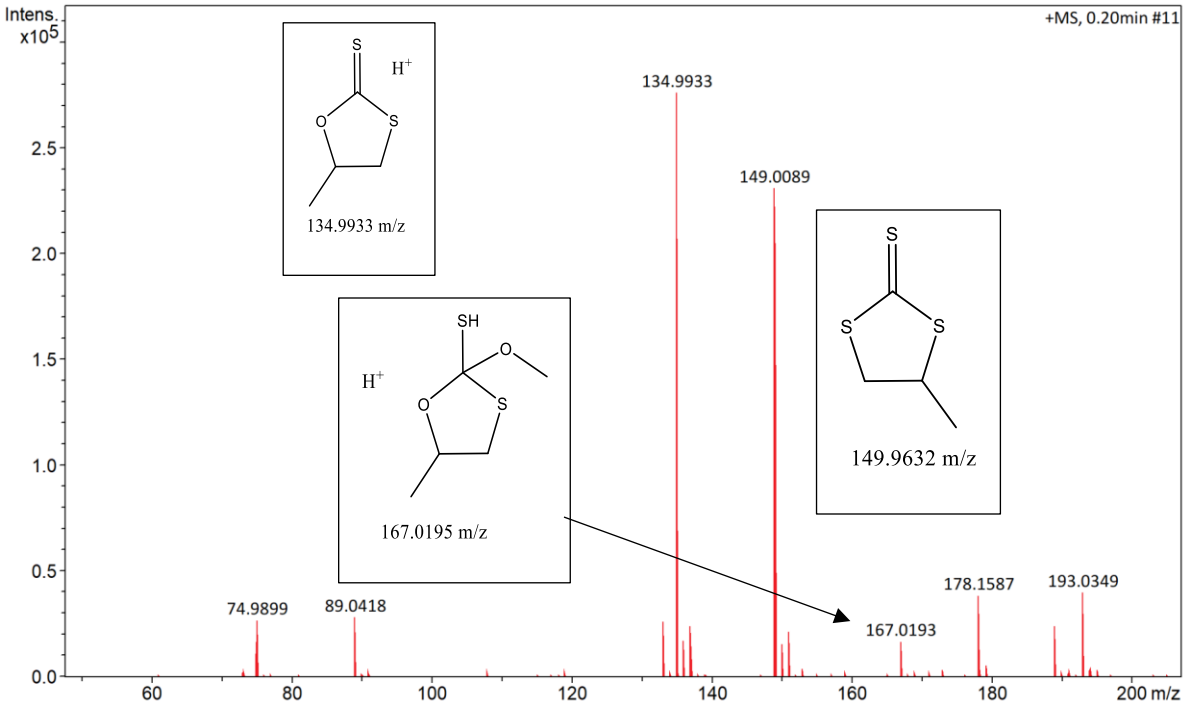
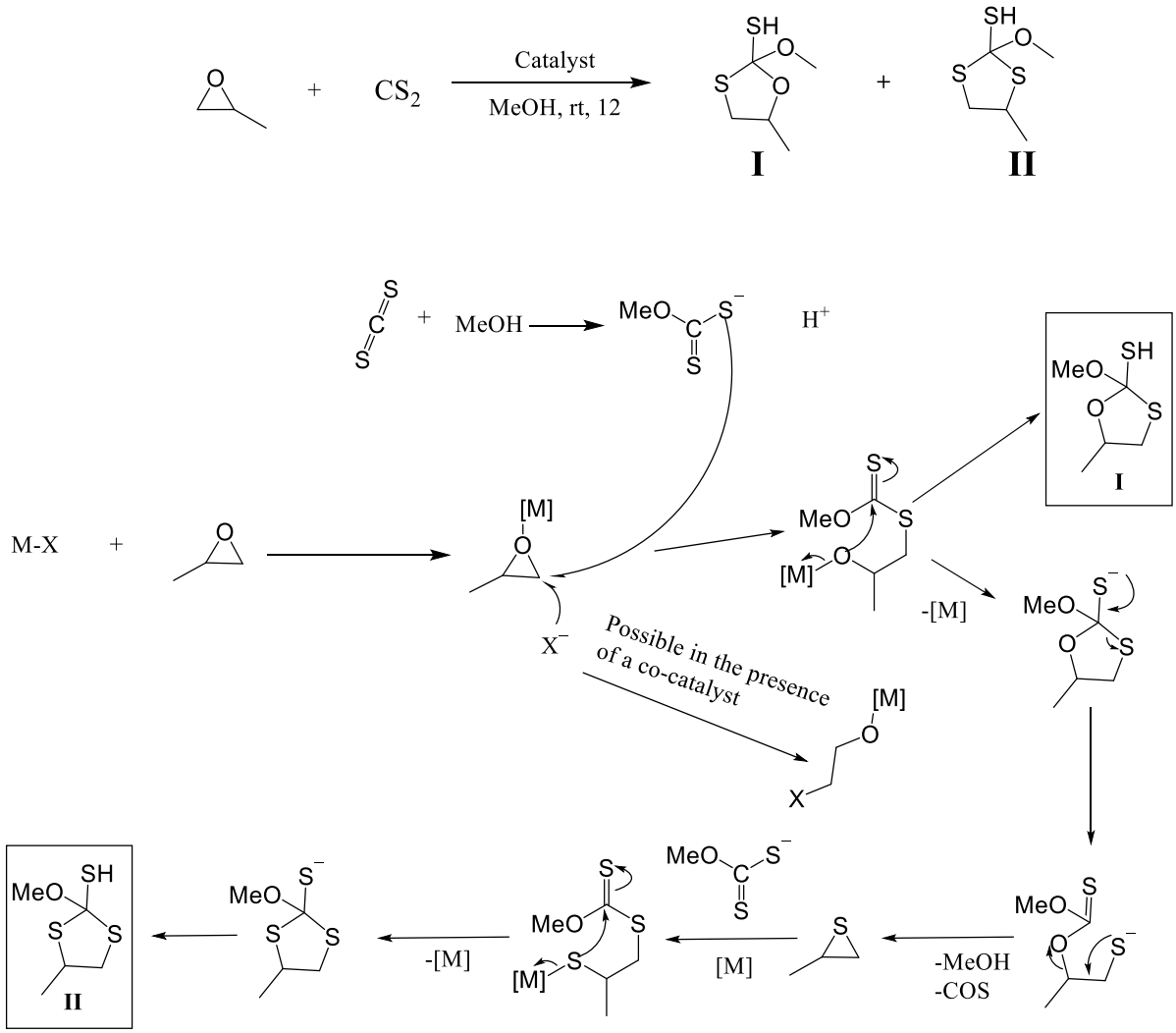


Fig. 5.8: *Mass spectrum for CS_2/PO coupling product when MeOH was used as a solvent*

For the reaction performed in ethanol an ethoxylated cyclic product was formed observed in the ^{1}HNMR spectrum (Figure **SI-24** appendix) of the crude reaction mixture with none of the cyclic products shown in Scheme **5.1** being observed. These results indicate that when the coupling reactions are performed in ethanol and methanol there is solvent activation resulting the formation of new cyclic coupling products.

5.2.1 Possible mechanism for the coupling of CS2 and PO in methanol as solvent

The mechanism of action when the reaction was performed in the presence of MeOH seem to proceed as shown in Scheme **5.2**. This mechanism is based on the ones reported by a couple of scholars before even though different catalysts were used, and the final products were the generic cyclic products similar to those that were prepared in chapter 4. In their reports, the coupling reaction was performed in the presence of alkyl halides or hydrides and MeOH [9 – 12].



Scheme 5.2: *Proposed reaction pathway for the coupling of CS_2 and PO in the presence of MeOH as solvent and Cr(II), Cr(III), and Co(II) as catalysts.*

The mechanism proceeds by the epoxide coordinating to the complex [13, 14]. The metal bound epoxide is ring opened by nucleophilic attack which can either be from the co-catalyst or the intermediated formed by the methoxy group and the CS_2. When the ring opening occurs because of the nucleophilic attack by methoxy intermediate, the reaction can proceed in two ways. One results in compound **I** (Scheme **5.2**). In the other method an episulfide is formed as an intermediate. The episulfide undergoes the same route as the epoxide to result in the formation of compound **II**. The compound that forms as the main product in this case will be determined by the pathway that requires less energy and from the NMR analysis it looks like compound **II** is formed as the major

product. This indicates that PO is isomerized to the episulfide at a much faster rate than the coupling reaction of CS_2 and PO.

5.2.2 Effect of substrate ratio on the coupling of CS_2 and PO catalytic reaction

The influence of PO/CS_2 substrate ratio on the coupling reaction of CS_2 and PO was investigated. Form Table **5.1** it seems that this ratio has an influence on the coupling reaction. The substrate ratio was also reported by Adachi to have an influence on the catalytic reaction when they used $ZnEt_2$ as a catalyst for the coupling of CS_2 and PO [15]. From Figure **5.9**, it can be observed that the best conversion was obtained when a substrate ratio of 1,5:1 PO:CS_2 was used. The least conversion was obtained when a substrate ratio of 0,5:1 PO: CS_2 was used.

Table 5.1: Effect of substrate ratio, CS_2: PO, on the coupling reaction[a]

Entry	PO:CS_2	Product/ mg	%Conversion[b]	Product ratio[c]	
				I	II
1	0.25:1	187.1	14.4	-	100
2	0.5:1	384	8.7	-	100
3	1:0.5	646.1	14.6	9.1	90.9
4	1.5:1	1562.5	30.0	9.1	90.9
5	1:2	1118.7	21.5	9.1	90.9
6	1:1	971.6	18.7	9.1	90.9

[a]All reaction performed using MeOH (5 mL) at 22 °C, 12 hours, complex **8** = cocatalyst [PPN]Cl = 0.0286 mmol, complex:PO = 1:1000; [b]Determined by mass difference; [c]Determined from ^{1}HNMR

It can also be observed that the concentration of substrate plays a very important role in the conversion of the coupling product produced. The ratios 0,5:1 and 1:2 PO:CS_2 are equal but differ in the concentration of the substrate in the total reaction mixture. It can be observed from Figure **5.9** that as the concentration of substrate increased in the 1:2 ratio more conversion was obtained. This could be attributed to the substrate being more available for the catalytic reaction as its concentration increased.

When the subtrate ratio of 0.25:1 and 0.5:1 was used, there was only one product formed in the coupling reactions, however when other ratios are used as shown in Table **5.1** two products are formed in a 1:0.1 ratio. The increase in the substrate ratio results in reduced product selectivity. When 0.5:1 PO:CO_2 ratio was used, one product was obtained but when 1:2 substrate ratio was used about two products were obtained, Table **5.1,** and this was conformed with ^{1}HNMR spectroscopy.

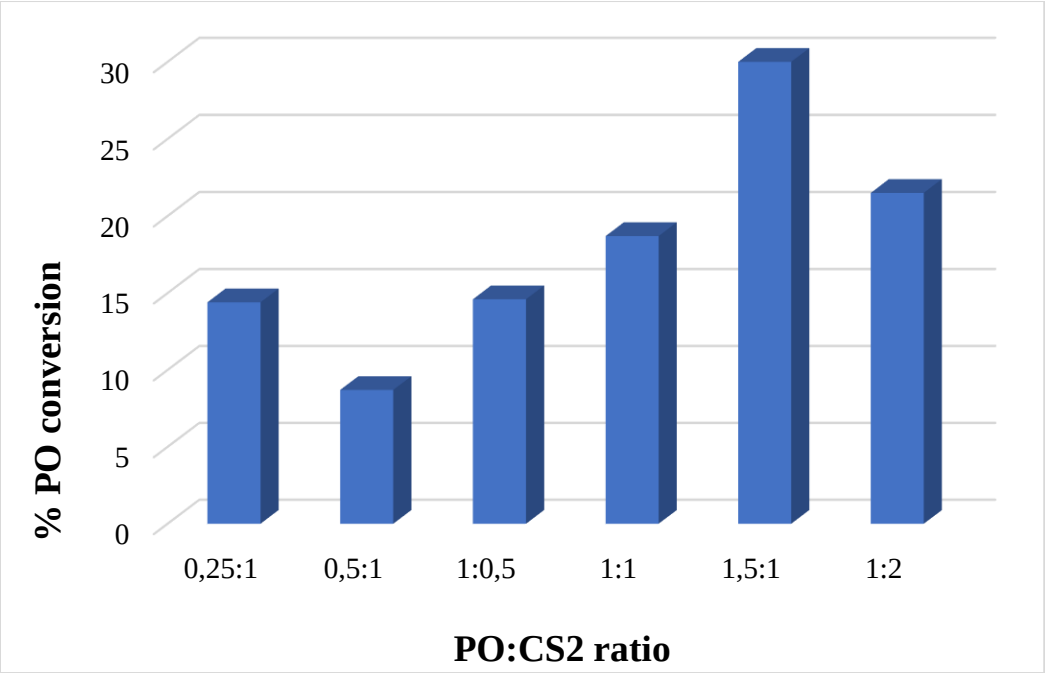


Fig. 5.9: *Effect of substrate ratio on the coupling of CS_2 and PO catalytic reaction, catalyst: complex **8**, co-catalyst: [PPN]Cl*

5.2.3 Effect of temperature on the coupling of CS2 and PO catalytic reaction

The effect of temperature was studied between 22 and 40 ^oC using methanol as solvent with complex **8** and [PPN]Cl. When the coupling reaction was performed at 22 ^oC for 12 hours, 30.0 % PO conversion was obtained. Increasing the temperature to 40 ^oC there was a drastic increase in the conversion observed to 70.1 %. When the temperature was increased to 40 ^oC and the reaction was performed for 12 hours, the ^{1}HNMR spectrum of the product obtained show appearance of more peaks compared to those in the 22 ^oC product spectrum peaks (Figure **5.8**).

This could mean that multiple products were formed due to the scrambling of the 'S' and 'O' atoms. Figure **5.10** shows stacked ^{1}HNMR spectra of the products that were obtained from coupling reactions at these different temperatures. The same observation was reported by Endo [16] and North [2] where they found that albeit the reduced conversion, there is more selectivity at lower temperatures with increase in product ratio. In conclusion, high temperature improves the conversion as well as promotes the scrambling of 'S' and 'O' atoms in the coupling products.

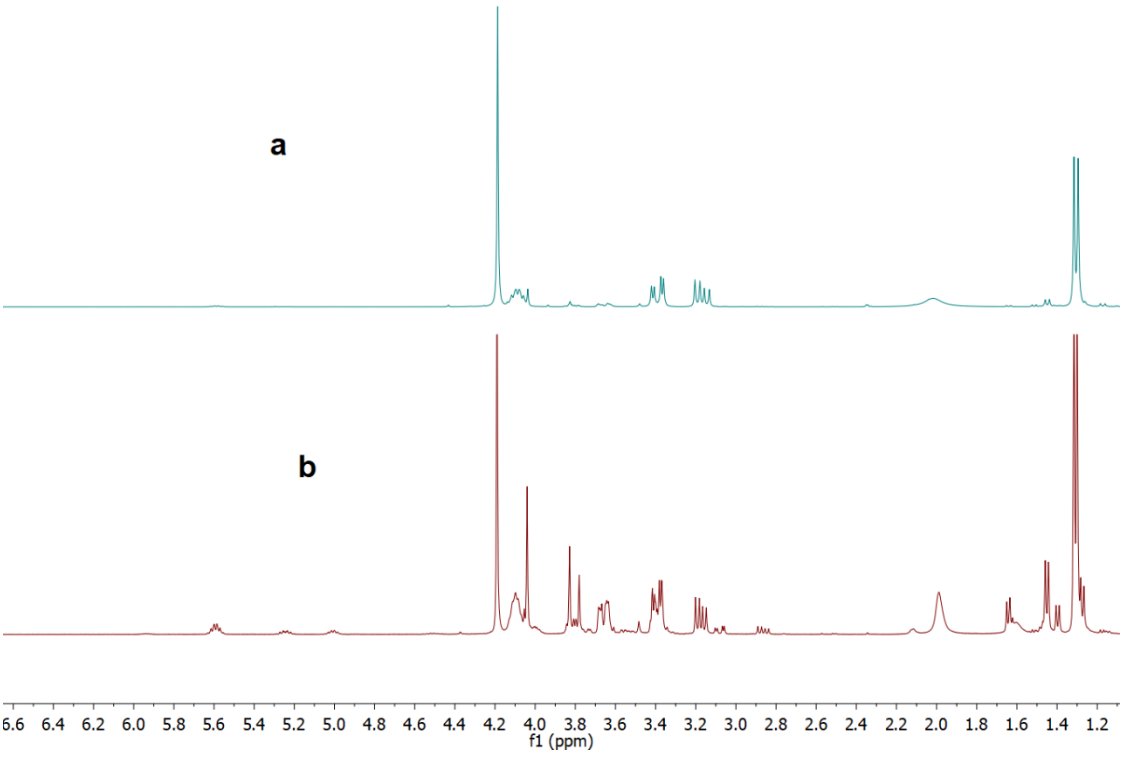


Fig. 5.10: *Stacked ^{1}HNMR spectrum for CS_2/PO coupling reaction at 22 (a), and 40 ^{o}C (b) for 6 hours*

5.2.4 Effect of time on the coupling of CS2 and PO catalytic reaction

The dependence of the coupling reaction on time was also investigated in this study, Table **S-2**. To do this investigation, a reaction was performed at 40 ^{o}C and monitored hourly for 12 hours with ^{1}HNMR spectroscopy and the conversion was calculated by mass difference. Figure **5.11** shows that there is an increase of the conversion of the coupling product/s as time was increased from 1 to 10 hours. A conversion of 8.8 % was observed for the coupling reaction after 1 hour and after

10 hours, 70.0 % conversion was observed. After ten hours, the conversion of substrate seems to be constant until the 12th hour.

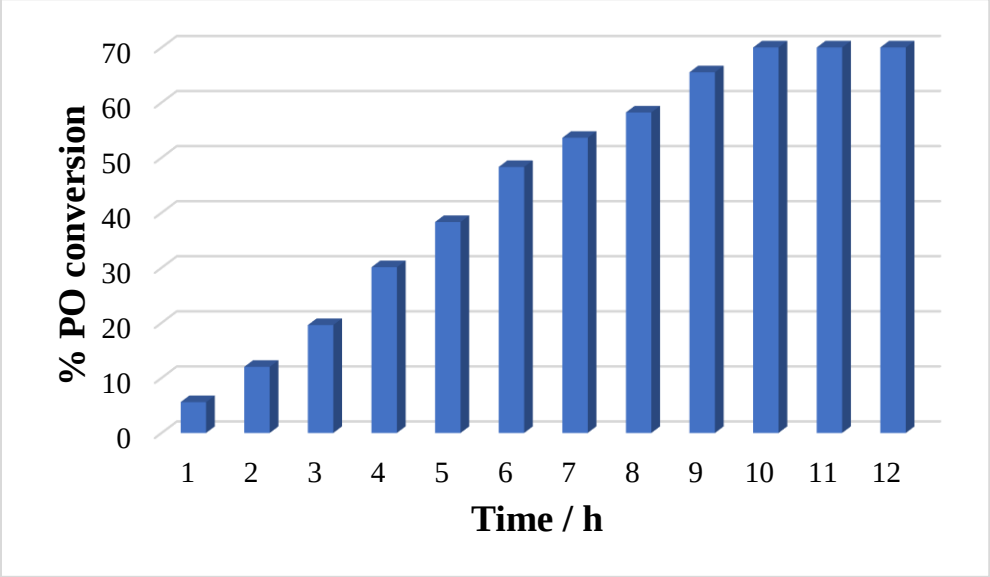


Fig. 5.11: *Effect of time on the coupling of CS_2 and PO catalytic reaction*

The crude reaction residue for these reactions was analyzed with ^{1}HNMR spectroscopy at every hour. From the stacked spectra, Figure **5.12**, it can be observed that at the first 2 hours there is predominantly one product that formed and after three hours there is another species that forms as a minor product. This could be confirmed with the low intensity peaks at 1.46 (s) ppm and others at 3.65 (m), 3.79 (m) and 5.62 (m) ppm. The peaks of the minor product grow in intensity as time goes on and they can be clearly observed after 6 hours.

The increase in the peak intensity simply means that the concentration of the product in the reaction mixture is increasing, implying that there is more of this specific product that gets produced. The concentration of this product does not seem to increase drastically as time was increased from 6 hours to 12 hours as the product distribution seem almost just the same on the ^{1}HNMR spectrum. It can therefore be concluded that time at this specific temperature, 40 ^{o}C does not only influence the conversion of the coupling cyclic products obtained but also influence the number of products produced to some extent. Scrambling of the oxygen and the sulphur atom seem to occur with time to form different cyclic coupling product/s isomers.

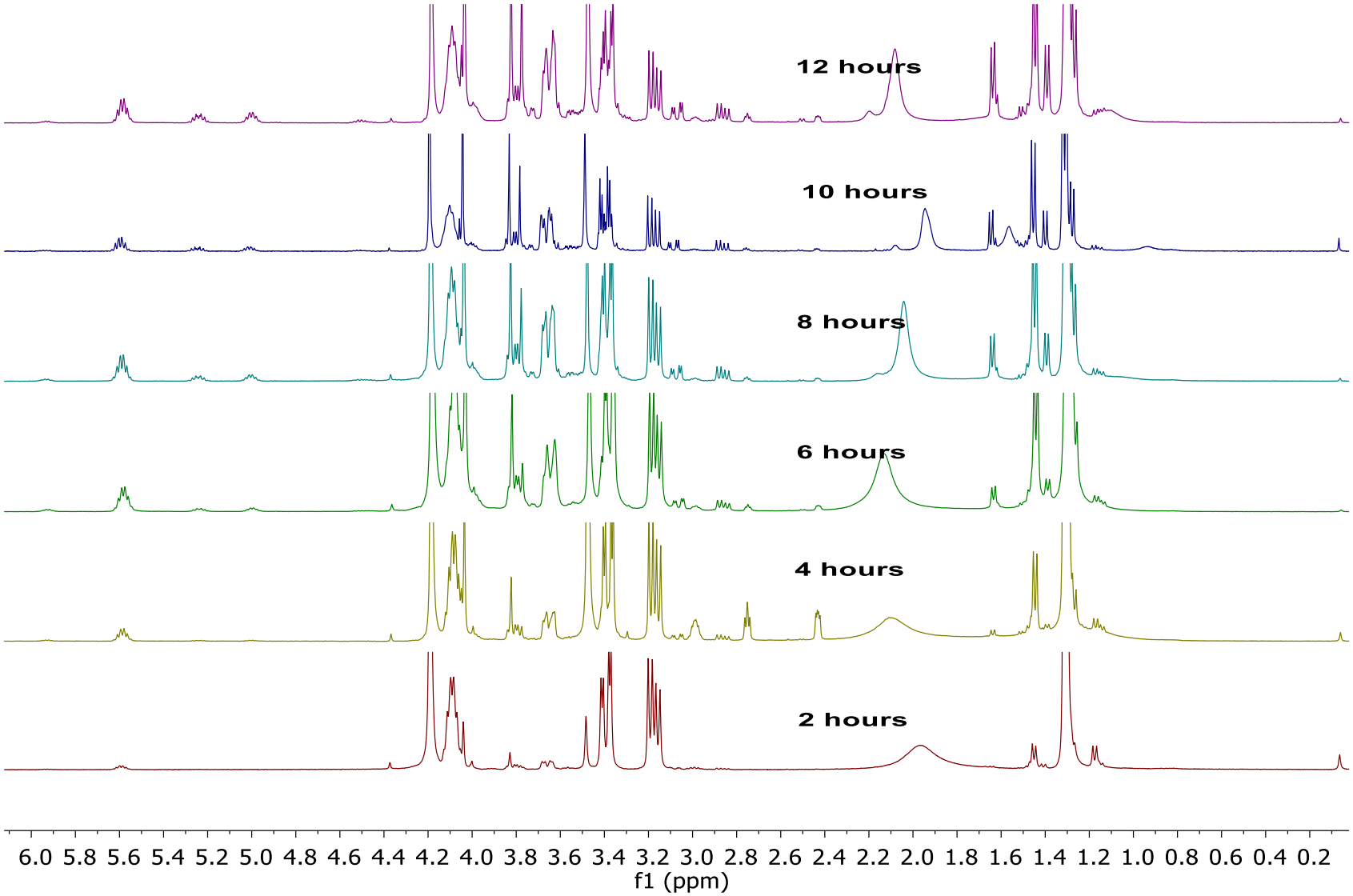


Fig. 5.12: *Stacked ^{1}HNMR spectra for the coupling of CS_2 and PO reaction product*

5.2.5 Effect of ligand architecture around Cr(II), Cr(II), and Co(II) metals on the catalytic activity for the coupling of CS_2 and PO at 22 and 40 ^oC

Substituents around the metal center influence the performance of the complexes in catalysis. Electron donating groups facilitate the insertion of CS_2 while electron withdrawing groups facilitate the binding between the metal and the epoxide making it easy for the coupling process. The substituents attached also sometimes influence the solubility properties of the complexes. Alkyl groups such as iso-propyl and tert-butyl are sometimes added to increase the solubility of the metal complexes in the coupling reactions, and this is mostly the case when the reaction medium constitutes organic solvents. The effect of the ligand architecture around the central metal on the coupling reaction was investigated.

[PPN]Cl showed, in the neat reactions, to be the best co-catalysts and it was therefore used in this case as a co-catalyst in the presence of a Cr(III) complex **8** and methanol was used as a solvent both at 22 ^oC and at 40 ^oC. A control reaction was performed where [PPN]Cl was used as catalyst on its own and about 14.1 and 34.0 % conversions of cyclic coupling product/s were obtained at 22 and 40 ^oC respectively. When complex **8** was evaluated at 22 and 40 ^oC on its own, conversions of 6.6 and 10.0 % were obtained, respectively. These results show that both complex **8** and [PPN]Cl are active as catalysts for the coupling reaction on their own in the presence of methanol as a solvent. The results also show that [PPN]Cl is more active than complex **8** as a catalyst for the coupling reaction at both temperatures.

The binary catalyst system of complex **8** and [PPN]Cl shows more activity than when these two were used as catalysts on their own at 22 and 40 ^oC as observed in Table **S-3,** entry **8** and Table **S-3,** entry **8**. Cr(III) complexes, **7**, **9**, and **10**, with [PPN]Cl as a co-catalyst were also evaluated as catalysts at 22 ^oC and 40 ^oC. It can be observed that all the binary catalyst systems are more active as catalysts than when complex **8** and [PPN]Cl were used as catalysts on their own at both temperatures. It can also be observed that the binary catalyst for complex **8** and **9** with [PPN]Cl are better catalyst than their binary catalysts of complexes **7** and **10** and [PPN]Cl at 22 and 40 ^oC, Figure **5.13**. The coupling reaction crude products were also characterized with ^{1}HNMR spectroscopy. The spectrum obtained for these reactions is like the ^{1}HNMR spectrum that was obtained when [PPN]Cl and complex **8** were used as catalysts in MeOH, Figure **5.2**. This means

that products **I** and **II** were still produced even these cases. Product distribution was also found just the same where the main product shows very intense peaks which are 1:0.1 ratio to the minor product, Table **S-3**. It can also be observed that for all complexes there is a drastic increase in the conversion of the substrates as temperature was increased from 22 to 40 ^{o}C for all binary catalyst systems.

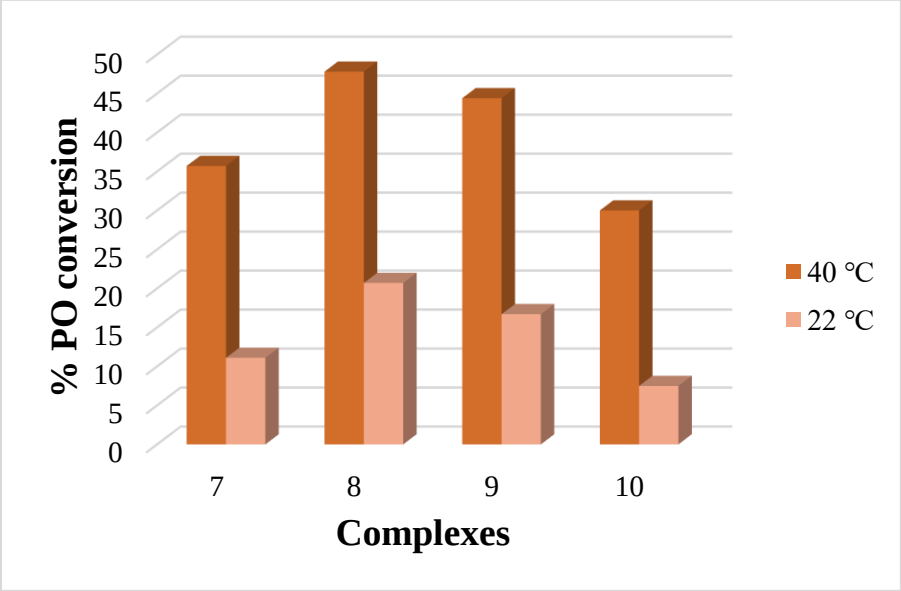


Fig. 5.13: *Effect of ligand architecture around Cr(III) complexes (**7** – **10**) on the coupling of CS_2 and PO catalytic reaction*

Cr(II) complexes bearing different ligands were also evaluated as catalysts for the coupling reaction in this study. A control reaction was also performed and when complex **2** was evaluated as catalyst on its own at 22 and 40 ^{o}C conversions of 1.3 and 6.1 % were obtained, respectively. These results are obviously all lower than the result that was obtained when the coupling reaction was performed in the presence of [PPN]Cl alone. A binary catalyst system of complex **2** and [PPN]Cl was also evaluated as catalysts for the coupling of CS_2 and PO at 22 ^{o}C, Table **S-3** entry 4, and 40 ^{o}C, Table **S-4** entry 4. This binary catalyst system performed better than when either complex **2** or [PPN]Cl were used as catalysts on their own.

Different Cr(II) complexes were also evaluated as catalysts in the presence of [PPN]Cl as a co-catalyst at 22 and 40 ^{o}C. It can be observed that all the binary catalyst systems performed better as catalysts than when complex **2** and [PPN]Cl were used as catalysts on their own at both temperatures**,** Table **S-2,** and Table **S-3**. The only exception was observed with complex **3**/[PPN]Cl which shows slightly poorer activity than when [PPN]Cl was used alone as catalyst at 22 ^{o}C. This phenomenon was not observed at 40 ^{o}C. The binary catalysts system performed better than [PPN]Cl at this temperature.

It can be observed from Figure **5.14** that when complex **2** was used as a catalyst in the presence of [PPN]Cl at 22 ^{o}C it gave the best conversion compared to other Cr(II) catalysts followed by complex **4**/[PPN]Cl. When complex **4**/[PPN]Cl was used as catalyst, slightly better conversion of the coupling reaction was obtained than when complex **2** and other Cr(II) complexes were used as a catalyst at 40 ^{o}C. This result is clearly an inverse of what was obtained at 22 ^{o}C. The ^{1}HNMR spectra of the crude reaction residues confirmed that cyclic products **I** and **II** were also produced for the Cr(II) analogues.

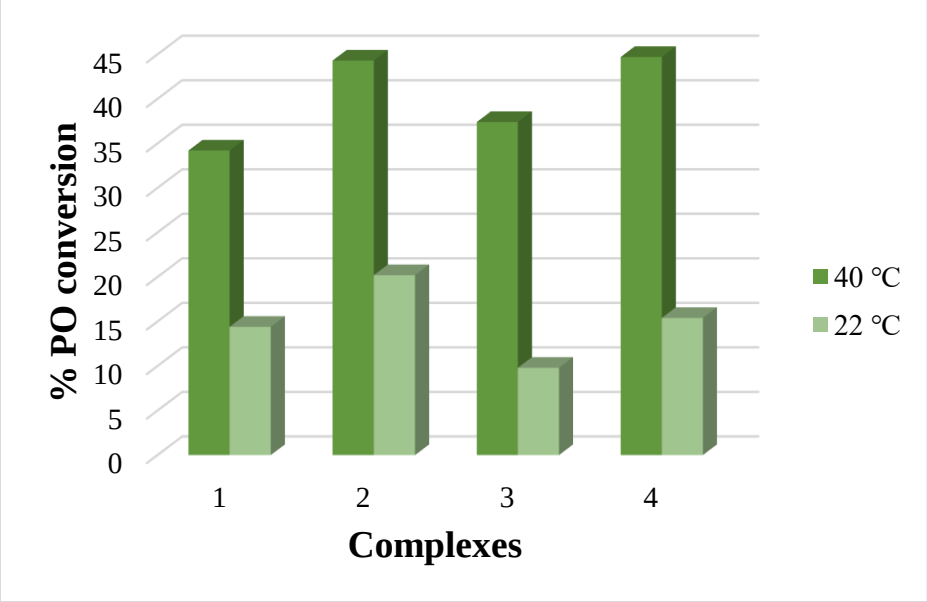


Fig. 5.14: *Effect of ligand architecture around Cr(II) complexes (**1** – **4**) on the coupling of CS_2 and PO catalytic reaction*

Cobalt complexes were also evaluated as catalyst for the coupling process at 22 ^{o}C, Table **S-3** and 40 ^{o}C, Table **S-4**. A control reaction was performed with Co (II) complex **14** as a catalyst on its own at 22 ^{o}C and 40 ^{o}C using methanol as a solvent. At both temperatures, it was found that the cobalt complex **14** performed poorer than [PPN]Cl as a catalyst. The binary catalyst system of [PPN]Cl and complex **14** evaluated in the presence of MeOH at 22 and 40 ^{o}C performed better than when complex **14** was used as catalyst.

Co(II) complexes, **13**, **15**, and **16**, with [PPN]Cl all performed better than complex **14** as catalysts but poorer than [PPN]Cl as catalysts both at 22 ^{o}C Table **S-3** and 40 ^{o}C **S-4** appendix. It therefore means that the Co(II) complexes retard the activity of the [PPN]Cl and on the other hand the [PPN]Cl does not improve the activity of the Co(II) complexes. Binary catalyst system of complex **14**/[PPN]Cl performed better than other systems at 22 ^{o}C while that of complex **15**/[PPN]Cl performed better than others at 40 ^{o}C. Even in this case, the catalytic reaction still produced products **I** and **II** and this was also confirmed with ^{1}HNMR spectroscopy.

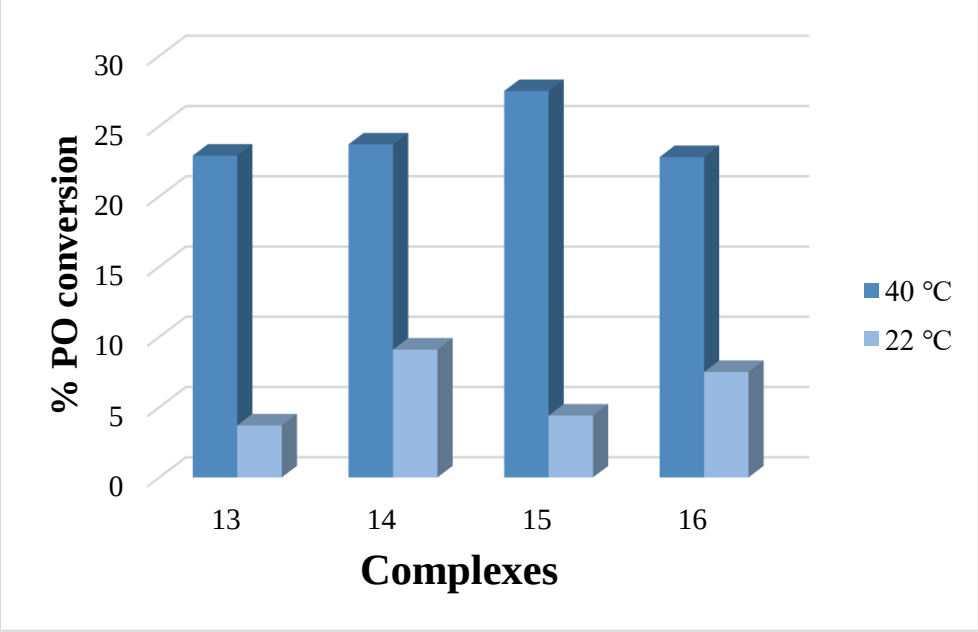


Fig. 5.15: *Effect of ligand architecture around Co(II) complexes, **13** – **16**, on the coupling of CS_2 and PO catalytic reaction*

5.2.6 Effect of oxidation state of Cr(II) and Cr(III) metal complexes on the catalytic activity

The catalytic activity of the Cr(II) and Cr(III) complexes investigated at 22 ^{o}C, Tables **S-3** and 40 ^{o}C, Table **S-4** was compared to determine if the oxidation state of the central metal has an effect on the coupling reaction, however there is no noticeable trend. Cr(III) complexes **8** and **9** have slightly higher activity than corresponding Cr(II) complexes **2** and **3** (Figure **5.16)**, when the coupling reaction was performed at 22 ^{o}C. The inverse seem to be the case for some of the Cr(II) complexes (**1** and **4**). This complexes have higher catalytic activity than their corresponding Cr(III) complexes (**7** and **10**), Figure **5.16**, when the same reaction was performed at 22 ^{o}C.

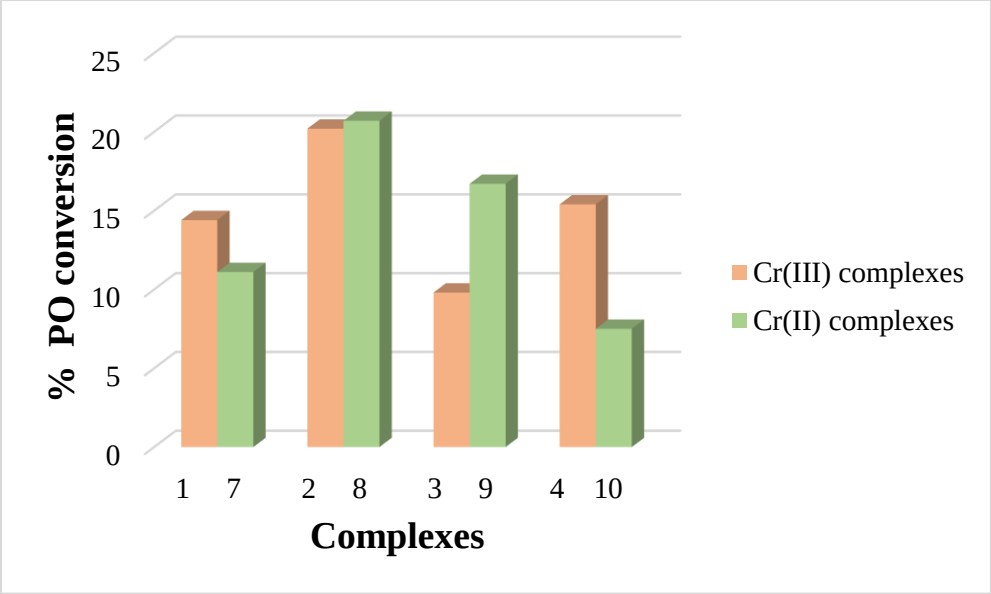


Fig. 5.16: *Effect of Cr metal oxidation state on the coupling of CS_2 and PO catalytic reaction at 22 ^{o}C.*

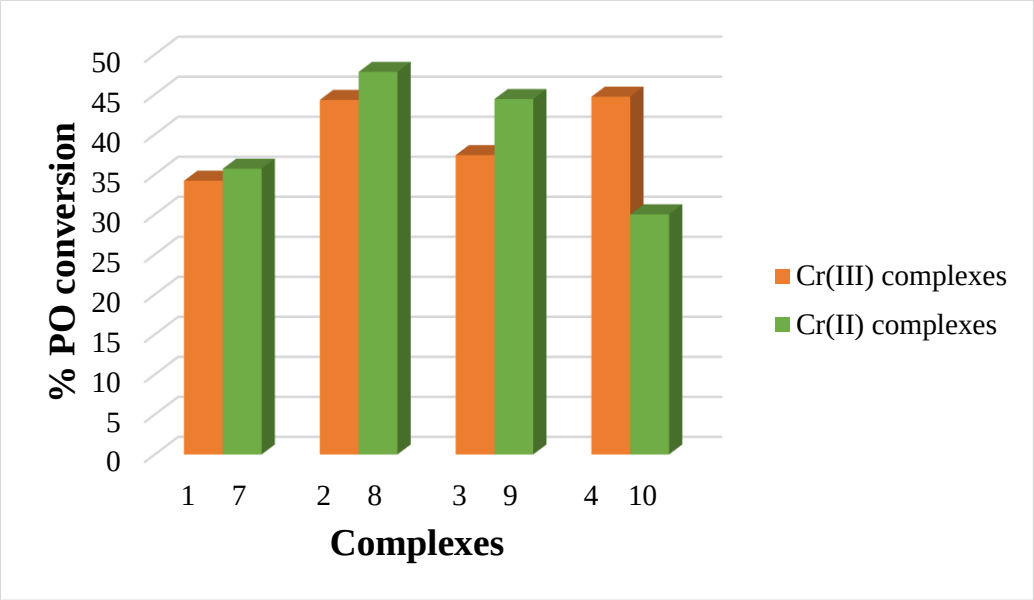


Fig. 5.17: *Effect of Cr metal oxidation state on the coupling of CS_2 and PO catalytic reaction at 40 ^oC.*

The same observation was observed at 40 ^oC for Cr(III) complexes (**8** and **9**) which still performed better than corresponding Cr(II) complexes (**2** and **3**) even in this case, Figure **5.17**. There is a slight difference that is observed where a Cr(II) complex **1** performed slightly poorer than its corresponding Cr(III) complex **4** at 40 ^oC and the inverse of this was observed at 22 ^oC. Complex **10** which showed lower catalytic activity than the corresponding Cr(II) complex **2** when the reaction was performed at 22 ^oC still showed the same observation even at 40 ^oC.

5.2.7 Effect of the metal center, Cr(II) and Co(II), on the catalytic activity

The influence of the metal center on the coupling reaction was compared between studies performed for Cr(II) and Co(II) complexes at 22 ^oC, Table **S-3,** and at 40 ^oC, Table **S-4**. The metal center of the complexes seems to play a very important role in the catalytic coupling reaction of CS_2 and PO. All Cr(II) complexes are better as catalysts for the coupling of CS_2 and PO than their corresponding Co(II) complexes when the reactions were performed at 22 and 40 ^oC Figure **5.18** and **5.19**.

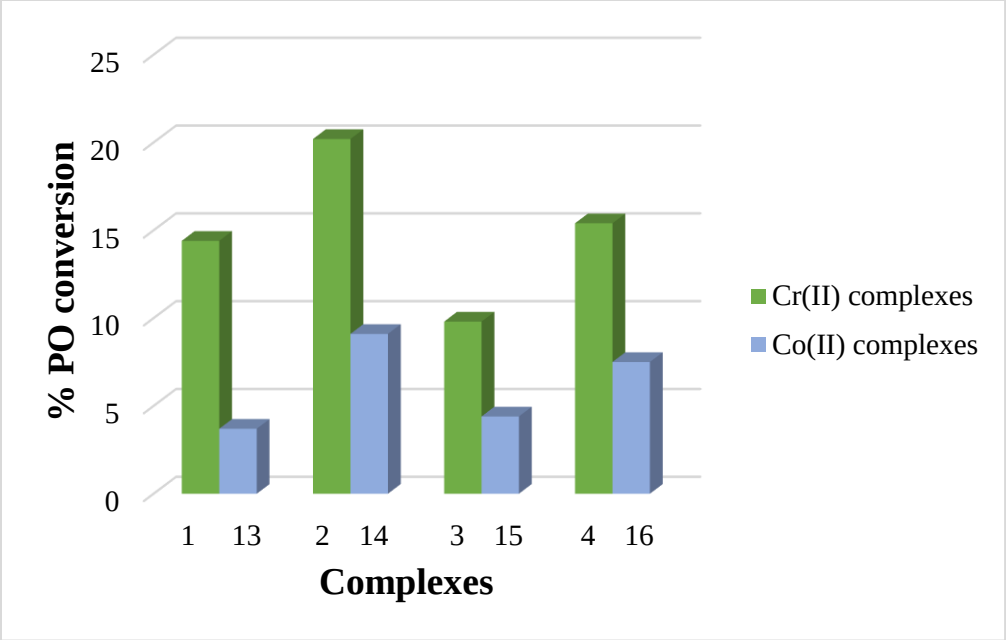


Fig. 5.18: *Effect of metal center on the coupling of CS_2 and PO catalytic reaction at 22 °C*

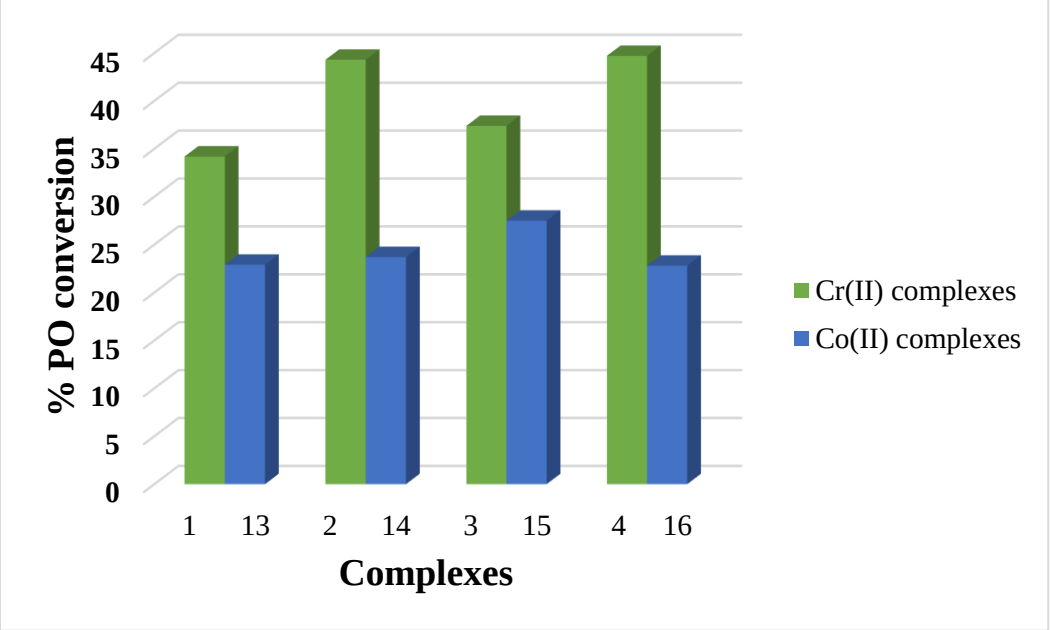


Fig. 5.19: *Effect of metal center on the coupling of CS_2 and PO catalytic reaction at 40 °C*

5.3 Conclusion

Solvents were found to play very important role in the coupling reaction of CS_2 and PO. Protic solvent like, MeOH and EtOH produced more coupling cyclic products than non-protic solvents with DCM and acetonitrile producing none. In the presence of MeOH, all complexes showed a very huge improvement in the conversion of cyclic product. The reactions that were performed in MeOH however gave a product totally different form the product that was obtained either in the neat reactions or in the presence of other organic solvents and this was confirmed with ^{1}HNMR spectroscopy. This is suggestive that the reactions pathway between neat reactions and the reactions that were done in MeOH is different.

Substrate ratio was found to have an influence on the conversion of the PO to cyclic products. The best conversion was obtained when a ratio of 1,5:1 PO:CS_2 was used. The least conversion was obtained when a substrate ratio of 0,5:1 PO: CS_2 was used. It can also be observed that the concentration of substrates plays a very important role in the catalytic reaction. The ratios 0,5:1 and 1:2 PO:CS_2 are equal but differ in the concentration of the substrates. When the concentration of substrates increased in the 1:2 ratio more conversion was obtained.

Temperature and time seem to have a very huge influence on the coupling reaction especially those that were performed in MeOH. When complex **8** was used to investigate the effect of temperature on the coupling reactions it was observed that not only the conversion increases as temperature was increased from 22 to 40 ^{o}C but also the number of cyclic products that were formed seem to be more than one and this was confirmed with ^{1}HNMR spectroscopy. The conversion of the coupling products seems to also increase with time with the highest conversion obtained after about 10 hours.

Ligands around the central metal seem to have some impact of the coupling reaction. When Cr(III) complexes were used as catalysts, complex **8** produced greater conversion than other Cr(III)complexes. The corresponding Cr(II) complex of complex **8** which is complex **2** also performed better than other Cr(II) complexes as catalysts for the coupling reactions both at room temperature and while complex **4** performed better at 40 ^{o}C. On the other hand, complex **14**

performed better than other Co(II) complexes at room temperature while complex **15** performed better than other Co(II) complexes at 40 ^{o}C.

The oxidation state of chromium complexes has a slight effect on their catalytic activity. At room temperature complexes **8** and **9** performed better than their corresponding Cr(II) complexes **2** and **3**. On the other hand Cr(II) complexes **1** and **4** performed better than their corresponding Cr(III) complexes **7** and **10**. The nature of the central metal also has an impact on the catalytic reaction. The influence of the oxidation state was investigated between Co(II) and Cr(II). Cr(II) complexes performed way better than their corresponding Co(II) complexes at both temperatures that were investigated in this study.

5.4 Experimental

5.4.1 Material

Reagent grade chemicals were obtained from Sigma Aldrich and used as received. All solvents were dried under appropriate drying reagent and distilled prior to use. The coupling reactions were performed in a 12 place RADLEY's Heated Carousel Reaction Station fitted with a reflux unit as well as a gas distribution system with glass reaction vessels. ^{1}HNMR and ^{13}CNMR spectra were recorded on a Varian 300 MHz spectrometer using tetramethylsilane as an internal standard. Chemical shifts are reported in (ppm) and referenced to residual proton in $CDCl_3$. FTIR spectra were recorded on Bruker TENSOR 27 spectrometer using ATR. Mass spectra were recorded on Bruker compact ultimate 3000 HR-MS.

5.4.2 General procedure for the coupling of CS_2 and propylene oxide

Coupling reactions were performed in a 12 place RADLEY's Heated Carousel Reaction Station fitted with a reflux unit as well as a gas distribution system. To the carousel reaction tubes was added the catalyst, co-catalyst followed by solvent. The mixture was stirred for 5 minutes and to resulting solution was added PO followed by CS_2. The reaction mixture was stirred under argon for the specific time and at the specific temperature as required. When the temperature was increased to 40 ^{o}C, the carousel was cooled using an ice water bath. The reaction was stopped,

and all volatiles were removed under vacuum. The resulting crude reaction residue was weighed, and the 1H-NMR spectrum obtained in $CDCl_3$.

5.5 References

[1] C. Beattie and M. Norht, *ChemCatChem*, vol. 6, pp. 1252 - 1259, 2014.

[2] W. Clegg, W. R. Harrington, M. Norht and P. Villuendas, *J. Org. Chem.*, vol. 75, pp. 6201 - 6207, 2010.

[3] M. North and P. Villuendas, *SYNLETT*, vol. 4, pp. 623 - 627, 2010.

[4] J. D. Darensbourg, R. J. Andreatta, J. M. Jungman and H. J. Reibenspies, *Dalton Trans.*, pp. 8891 - 8899, 2009.

[5] M.-M. Wang, B. Li, H. Wang, Z.-C. Zhang and X.-B. Lu, *Appl. Organometal. Chem.*, vol. 26, pp. 614 - 618, 2012.

[6] W. Choi, F. Sanda and T. Endo, *Macromolecule*, vol. 31, pp. 2454 - 2460, 1998.

[7] J.-C. Zhang and H.-X. Zhang, *Macromolecule*, vol. 53, pp. 233 - 239, 2020.

[8] L.-J. Jiang and R. Hua, *Synth. Commun.*, vol. 36, pp. 3141 - 3148, 2006.

[9] S. Hayashi, M. Furukawa, Y. Fujino, T. Nakao and K. Nagato, *Chem. Pharm. Bull.*, vol. 19, pp. 1594 - 1597, 1971.

[10] I. A. Dotsenko, Q. Zhao, A. H. Franz, B. Patrick, N. M. Samoshina and V. V. Samoshin, *ARKIVOC*, pp. 16 - 41, 2014.

[11] A. M. Creighton and L. N. Owen, *J. Chem. Soc.*, pp. 1024 - 1029, 1960.

[12] I. Yavarid, M. Ghazanfarpour-Darjani, Z. Hossaini, M. Sabbaghan and N. Hosseini, *SYNLETT*, vol. 6, pp. 889 - 891, 2007.

[13] G. Trott, K. P. Saini and C. Williams, *Phil. Trans. R. Soc.*, p. 2015, 1 - 19.

[14] J. D. Darensbourg, M. R. Mackiewicz, L. J. Rodgers and L. A. Phelps, *Inorg. Cem.*, vol. 43, pp. 1831 - 1833, 2004.

[15] N. Adachi, Y. Kida and K. Shikata, *J. Polym. Sci.: Polym. Chem. Ed.*, vol. 15, pp. 937 - 944, 1977.

[16] N. Kihara, Y. Nakawaki and T. Endo, *J. Org. Chem.*, vol. 60, pp. 473 - 475, 1995.

Chapter 6

Catalytic evaluation of ionic functionalized Cr(II), Co(II) and Cr(III) salicylaldiminato complexes as catalysts for the coupling of CS_2 with PO

Contents

6.1. Introduction 175

6.2. Results and discussion 177

6.2.1 Evaluation of ionic tagged complexes in solventless reactions 178

6.2.2 Evaluation of ionic tagged complexes in the presence of MeOH as a solvent 182

6.3. Conclusion 185

6.3.1. Coupling of CS_2 and PO in neat reactions 185

6.3.2 Coupling of CS_2 and PO in neat reactions 186

6.4 Experimental 187

6.4.1 Materials and instrumentation 187

6.4.2 Evaluation ionic functionalized complexes for catalytic activity for the coupling of CS_2 and PO in the absence of a cocatalyst. 187

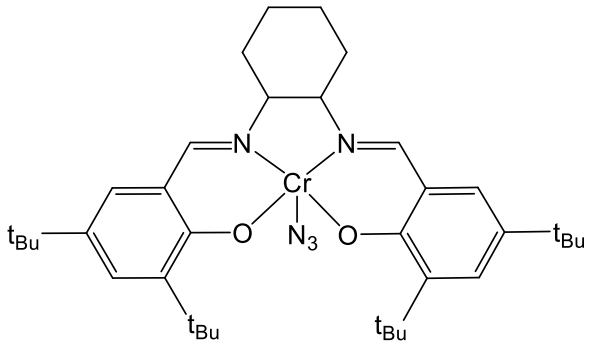
6.4.3 Evaluation of the binary catalyst system of ionic functionalized complexes and [PPN]Cl for catalytic activity for the coupling of CS_2 and PO 187

6.4.4 Evaluation ionic functionalized complexes for catalytic activity for the coupling of CS_2 and PO in the absence of a cocatalyst using MeOH as solvent. 188

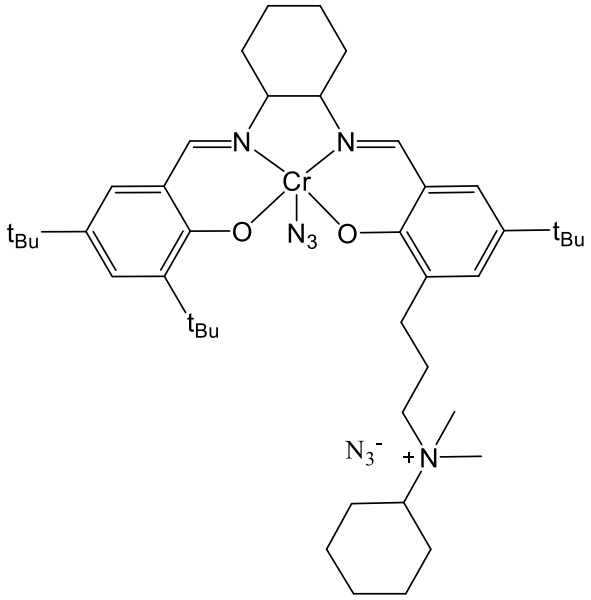
6.5 References 188

6.1 Introduction

The incorporation of ionic functionalities into metal complexes has attracted a lot of attention recently in many fields such as catalysis [1 – 4] and biological activity [5, 6, 7]. In catalysis there are many reasons why these catalysts have attracted so much attention. In the catalytic coupling reaction of CO_2 and epoxide, these classes of compounds turn to improve some selectivity for the coupling reaction products. Darensbourg and his co-workers discovered that when binary catalyst system of complex **6a** (Figure **6.1**) and $PPNN_3$ was used as catalyst for the coupling of cyclopentane oxide (CPO) and CO_2, the reaction produced 99% of cyclopentene carbonate cyclic product. When the same reaction was performed with the bifunctional catalyst complex **6b (**Figure **6.1**) the reaction produced copolymer as the main product [8, 9]. Therefore, depending on the targeted product the nucleophilic groups can be incorporated in the complex backbone or used from co-catalysts.



6a)

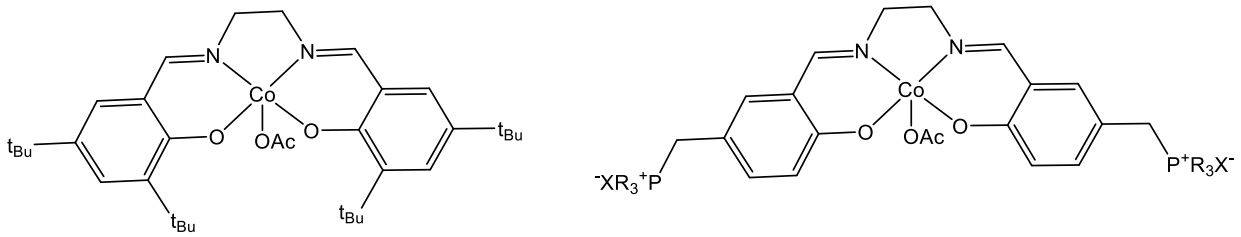


6b)

Fig. 6.1: *Asymmetric single functional, 6a* [9]*, and bifunctional, 6b, salenCrN_3 [8] reported by Darensbourg and co-woekers for the coupling of CPO and CO_2.*

The bifunctional catalysts also play a pivotal role in providing both the metal for catalytic sites and the nucleophilic site that is highly needed for ring opening of the epoxides in CO_2 and epoxide coupling reactions. The nucleophilic group incorporated in the complexes can act in place of the co-catalyst of the binary catalyst systems therefore there could be no need to use co-catalysts. These types of catalysts are therefore termed multi-functional catalysts due to the presence of Lewis acid (metal center) and an anion X^- (nucleophile) [10].

Multi-functional catalyst systems have not been applied as catalysts for the coupling of CS_2 and epoxides before, but they have however been applied as catalysts for the coupling of CO_2 and epoxides. When He and his co-workers applied complex **6c**, Figure **6.2**, (Yield 23 %) as a catalyst for the coupling of CO_2 and PO, it performed way poorer than when **6d** and **6e**, Figure **6.2**, (Yield 88 and 71 % respectively) were applied as catalysts [11]. The bifunctional catalysts showed very good catalytic activity compared to the neutral catalyst. These bifunctional catalysts also showed less poisoning/ contamination of the products and good recyclability.



6 c)

6 d) R = Ph, X = Br
6 e) R = Ph, X = Cl
6 f) R = Ph, X = OAc

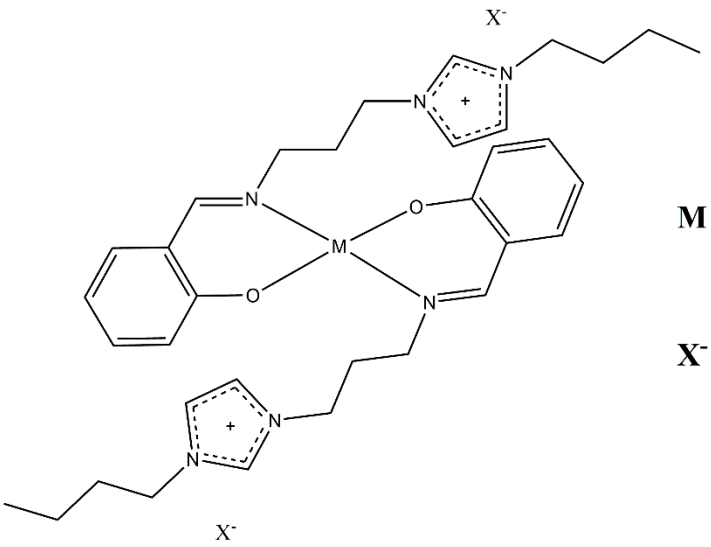
Fig 6.2: *Co(III) complexes that were used as catalysts for the coupling of CO_2 and PO by He and his co-workers* [11]

Among the bifunctional catalysts, the counter ion seems to play a very important role in the catalytic activity of the complexes. When the nucleophile was changed from a halogen to an acetate, there seem to be a drastic drop in the yield of the coupling product that was obtained. Complex **6f** gave yield of 41 % and this value is twice less than the yield that was obtained when

complex **6d** and **6e**, Figure **6.2**, were used as catalysts for the coupling process [11]. This chapter reports on the evaluation of ionic tagged complexes successfully prepared in this investigation as catalyst for the coupling of CS_2 and PO.

6.2 Results and discussion

Ionic functionalized bis-(salicylaldiminato) Cr(II) (**19** and **20**), Cr(III) (**21** and **22**)and Co(II) (**23** and **24**) complexes, Figure **6.3**, were evaluated as catalysts for the coupling of CS_2 and PO, Scheme **6.1**. The evaluation of these metal complexes was performed in two ways. The complexes were evaluated as catalysts in the presence and in the absence of MeOH as solvent. The presence of the ionic functionalities in the complexes is believed to introduce nucleophile groups that could have been introduced by a co-catalyst, therefore these catalysts were evaluated in the presence and in the absence of a co-catalyst in the solventless reactions to investigate the effect of the co-catalyst on the catalytic reaction. With motivation from the results obtained in these reactions, the complexes were further evaluated without a co-catalyst in the presence of MeOH as a solvent.



M =	Cr:	**19**	**20**
	CrCl:	**21**	**22**
	Co:	**23**	**24**
X⁻ =		I^-	PF_6^-

Figure 6.3: *Ionic functionalized complexes used as catalysts for the coupling of CS_2 and PO*

6.2.1 Evaluation of ionic tagged complexes in solventless reactions

6.2.1.1 Evaluation of ionic tagged complexes in the absence of a co-catalyst

All complexes were evaluated as catalysts for the coupling of CS_2 and PO in the absence of a co-catalyst, Table **6.1**. The coupling reactions produced only cyclic products with no copolymer being observed in the ^{1}HNMR spectra of the crude reaction residues. From the spectra obtained it is evident that **1**, **3** and **4**, were obtained as products and they are similar to when the neutral complexes were evaluated as catalyst in solventless reaction in chapter 4. Figure **6.4** below is an example of ^{1}HNMR spectrum that was obtained and it is for when Cr(II) complex **19** was used as a catalyst (entry **1**, Table **6.1**). It is clear from the spectrum that three coupling products were obtained as products as assigned with 5-methyl-1,3-oxathiolane-2-thione, product **1** (85%) as the major product and **3** (7%) and **4** (8%) as minor products (Scheme **6.1**). The product selectivity was determined from the ^{1}HNMR spectrum.

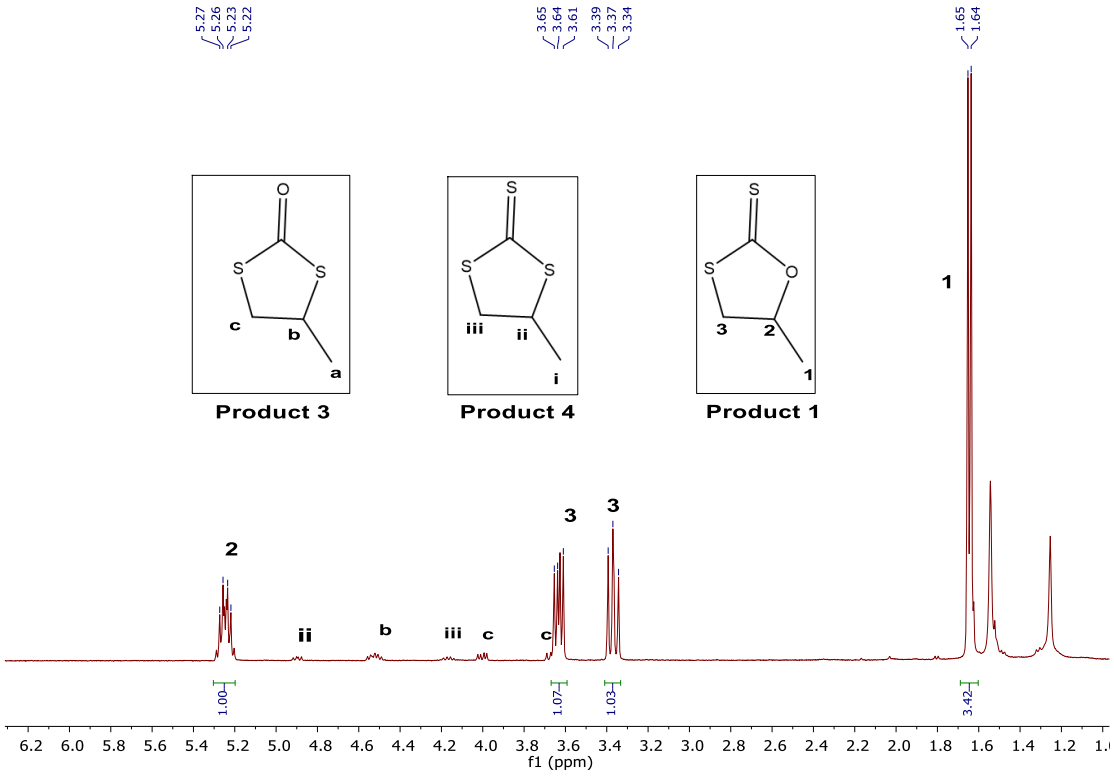
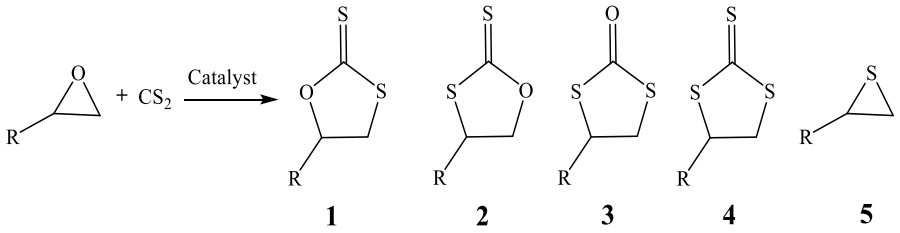


Figure 6.4: *^{1}HNMR spectrum of product that was obtained when complex **19** was used as catalysts for CS_2 and PO coupling reaction (entry **1**, Table **6.1**)*



Scheme. 6.1: *Coupling of CS_2 and epoxides to produce cyclic carbonates*

Table 6.1: Evaluation of ionic functionalized complexes for CS_2 and PO catalytic activity in absence of a co-catalyst.

[a]Entry	Complex	Product /mg	%Conversion[b]	Product Ratio[c]		
				1	**3**	**4**
1	**19**	38.9	1.01	85.2	6.8	8.0
2	**20**	24.2	0.63	82.5	6.5	11.0
3	**21**	30.5	0.79	86.5	5.1	8.4
4	**22**	16.0	0.42	85.2	7.4	7.4
5	**23**	19.4	0.51	75.5	13.3	13.3
6	**24**	5.2	0.13	71.6	14.3	14.3

[a]All reaction performed in neat PO (2.01 ml) at 25 °C, 12 hours, mmol complex = 0.0286, cocatalyst = 0, Complex:PO:CS_2 = 1:1000:1000; [b]Determined by mass difference; [c]Scheme 6.1, determined by ^{1}HNMR spectroscopy

It can be observed form Table **6.1** that overall, very low catalytic conversions were obtained. The main observation from the reaction was that ionic functionalized complexes were poorly soluble in the reaction mixture with a sticky solid suspended throughout the experiment. A very interesting observation from this reactions is that Cr(II) complexes seem to perform better than their corresponding Cr(III) counterparts as catalysts for the coupling reaction. For instance, Cr(II)

complex **19** (entry **1**, Table **6.1**) performed slightly better than Cr(III) complex **21** (entry **3**, Table **6.1**). In terms of product distribution, Cr(III) complexes are slightly more selective than their corresponding Cr(II) analogues favoring production of product **1**, Scheme **6.1**.

On the other hand Cr(II) complexes still performed better than their corresponding Co(II) complexes same as the neutral complexes. For instance Cr(II) complex **19** (entry **1**, Table **6.1**) performed better than Co(II) complex **23** (entry **5**, Table **6.1**). Cr(II) complexes are more selective than their corresponding product Co(II) complexes, Table **6.1**.

The counter ion of the complexes seems to have an impact on the coupling reaction. It can be observed from Table **6.1** that more conversions were obtained for complexes containing I^- as counter ion compared to corresponding complexes that contain PF_6^- as counter. This is observed for all Cr(II), Cr(III) and Co(II) complexes studied. For instance, Cr(II) complex **19** that contain I^- as a counter ion (entry **1**, Table **6.1**) performed better than Cr(II) complex **20** that contain PF_6^- as a counter ion (entry **2**, Table **6.1**). This result could mean that I^- is more nucleophilic than PF_6^- in this case. The complexes that contain I^- as a counter ion seem to be more selective and they produced product **1** as the main product than their corresponding complexes that contain PF_6^- as a counter ion. As an example, this can be observed between Cr(II) complexes **19** (entry **1**, Table **6.1**) and **20** (entry **2**, Table **6.1**).

6.2.1.2 Evaluation of ionic tagged complexes in the presence of [PPN]Cl as a co-catalyst

All complexes were also evaluated as catalysts for the coupling of CS_2 and PO in the presence of [PPN]Cl as a co-catalyst. Products **1**, **3** and **4** were once again observed to be the only coupling products produced and this was confirmed with ^{1}HNMR spectroscopy. There was a slight improvement in the conversion that was obtained when the complexes were used as catalyst for the coupling reaction in the presence of a co-catalyst compared to when they were used in the absence of a co-catalyst. For instance, when complex **19** was used as a catalyst without a co-catalyst (entry 1, Table **6.1**), 1.01 % PO conversion was obtained but when it was used in the presence of [PPN]Cl as a co-catalyst (entry 1, Table **6.2**) the conversion of PO was slightly increased to 1.23 %. It can be observed that the conversion was still however practically very low

even in this case. Product selectivity was found to be more when the complexes were used as catalysts in the absence of a co-catalyst compared to when they were used as catalysts in the presence of a co-catalyst. A clear example can be observed from when complex **19** was used as a catalyst on its own, (entry 1, Table **6.1**), compared to when it was used in the presence of [PPN]Cl, (entry 1, Table **6.2**).

Table 6.2: Evaluation of ionic functionalized complexes for CS_2 and PO catalytic activity in the presence of [PPN]Cl as a co-catalyst.

[a]Entry	Complex	Product /mg	%Conversion[b]	Product Ratio[c]		
				1	**3**	**4**
1	**19**	46.2	1.23	61.1	4.9	34.0
2	**20**	48.3	1.26	69.4	6.5	24.1
3	**21**	106.9	1.66	74.0	4.6	21.4
4	**22**	36.9	0.96	76.3	4.7	19.0
5	**23**	23.4	0.61	65.1	12.6	22.3
6	**24**	15.5	0.41	72.0	6.5	21.5

[a]All reaction performed in neat PO (2.01 ml) at 25 °C, 12 hours, mmol complex = cocatalyst [PPN]Cl = 0.0286, Complex:PO:CS_2 = 1:1000:1000; [b]Determined by mass difference; [c]Scheme 6.1, determined by ^{1}HNMR spectroscopy

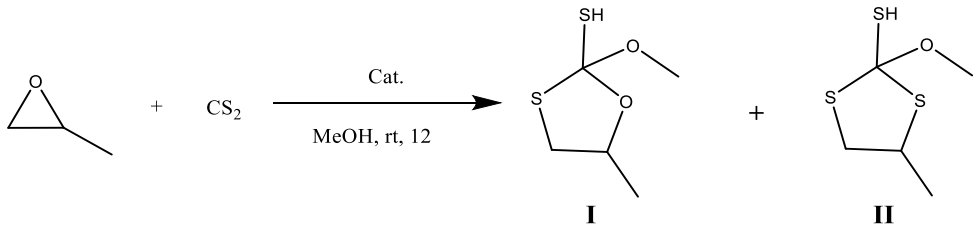
The investigation of the influence of the counter ion on the catalytic activity of these ionic functionalized complexes show that comparable activity was observed for complexes **19** and **20** which contains I^- and PF^-_6 as counter ions, respectively. When Cr(II) and Co(II) complexes were evaluated as catalysts in the presence of [PPN]Cl the same trend was observed as when they were used as catalysts without [PPN]Cl. Where the complexes that contain I^- as a counter ion performed better than their corresponding complexes that contain PF_6^-. In terms of product distribution, all

complexes that contain PF_6^- as a counter ion seem to be more selective than the complexes bearing I^- as a counter ion. This is also different from the result that was obtained when these complexes were evaluated as catalysts in the absence of [PPN]Cl. In this case the complexes with I^- gave more selectivity than their corresponding complexes that contain PF_6^- as a counter ion.

6.2.2 Evaluation of ionic tagged complexes in the presence of MeOH as a solvent

The ionic functionalized complexes were also evaluated as catalysts in the presence of MeOH as a solvent. The complexes were evaluated in the absence of [PPN]Cl as a co-catalyst. This was motivated by the fact that they showed better selectivity for product **1** in the neat reactions discussed above. The reaction conditions such as temperature and time were kept exactly like those of neat reactions except that MeOH was now used as a solvent in this case. The product obtained when the coupling reaction was performed in the presence of ionic functionalized complexes and MeOH as solvent was also characterized with ^{1}HNMR spectroscopy. Figure **6.5** is an example of the spectrum that was obtained for these reactions, and it is the spectrum that was obtained when complex **19** was used as a catalyst, (entry **1**, Table **6.3**).

The spectrum shows that when MeOH was used as a solvent, products (Scheme **6.2**) different from the ones that was obtained when the coupling reaction was performed neat were obtained. The same product was obtained when neutral complexes were evaluated in the presence of MeOH as a solvent in chapter 5. This product was assigned as shown in the spectrum. MeOH, therefore, seem to have a very big influence on the catalytic reaction in terms of product and the conversion of PO to the cyclic products.



Scheme 6.2: *Coupling of CS_2 and PO using ionic functionalized complexes as catalysts in the presence of MeOH as solvent.*

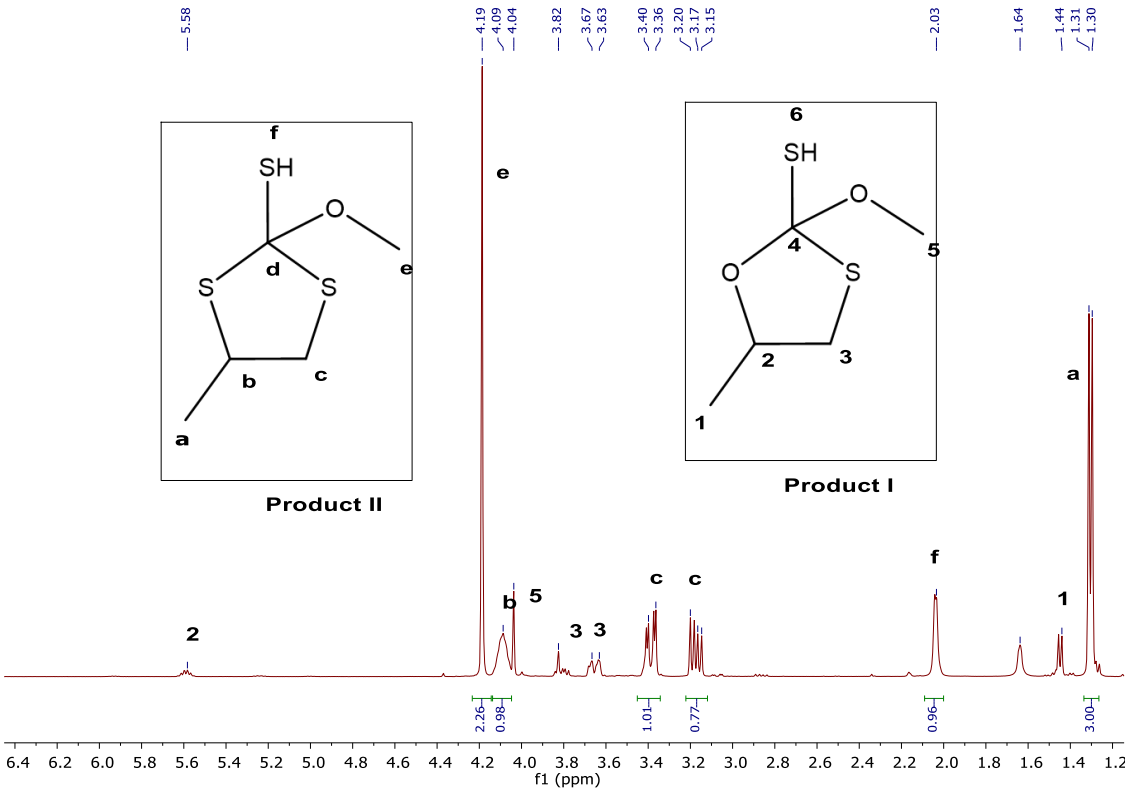


Fig. 6.5: *^{1}HNMR spectrum of the products for the CS_2 and PO coupling reaction in the presence of MeOH as a solvent (Table **6.3**, entry **1**) $CDCl_3$, 25 ^{o}C.*

The influence of the solvent on the catalytic reaction was also observed on the conversion of the coupling products obtained. For all the ionic functionalized complexes evaluated as catalysts for the coupling reaction, significantly higher conversions were obtained when the catalytic reactions were performed in the presence of MeOH compared to when the catalytic reactions were performed neat.

When the effect of the oxidation state was investigated it was observed that Cr(II) complexes performed better than corresponding Cr(III) complexes. For instance, Cr(II) complex **19**, entry 1, Table **6.3**, performed better than Cr(III) complex **21**, entry 3, Table **6.3**, as a catalyst giving 34 and 29 % PO conversions respectively. This result is different from what was expected. The expectation was that Cr(III) complexes will perform better than their corresponding Cr(II)

complexes due to high nucleophilicity. Cr(III) complexes however seem to be slightly more selective for product **1**, Scheme **6.2**, than their corresponding Cr(II) complexes.

Ionic functionalized Co(II) complexes gave higher catalytic conversion than their corresponding Cr(II) complexes. For instance, Co(II) complex **23**, entry 5, Table **6.3**, performed better than its corresponding Cr(II) complex **19** , entry 1, Table **6.3**, as a catalyst giving 37 and 34 % PO conversion respectively. This is the inverse of what was obtained before when the catalytic reaction was performed neat. Co(II) complexes have always showed lower conversions than Cr(II) complexes.

The counter ion of the ionic functionalized complexes even in this case seem to have an impact on the coupling reactions. For Cr(II) and Cr(III) complexes, the complexes bearing I^- as a counter ion still performed better than the corresponding complexes bearing PF_6^- as a counter ion. For instance, for Cr(II) complexes **19** and **20** PO conversions of 34 and 30 % were obtained respectively (entries 1 and 2 Table **6.3**). Complexes bearing PF_6^- as a counter ion seem more selective than those bearing I^- as a counter ion. This could mean that I^- is a better nucleophile than PF_6^-. The capacity of hydrogen bonding increase with an increase in basicity therefore in the presence of methanol I^- is expected to have less hydrogen bonding compared to PF_6^- therefore it becomes a better nucleophile. A different case was observed for Co(II) complexes. In this case, complex **24**, with PF_6^- as a counter ion performed better than complex **23** with I^- as a counter ion with PO conversions of 39 and 37 % obtained, respectively. Product distribution amongst the Co(II) complexes, **23** and **24**, seem more or less the same.

Table 6.3: Evaluation of ionic functionalized complexes for CS_2 and PO catalytic activity in the absence of [PPN]Cl as a co-catalyst and in the presence of MeOH a s a solvent.

[a]Entry	Complex	Product /mg	%Conversion[b]	Product Ratio[c]	
				I	II
1	**19**	1745.8	33.5	10.4	89.6
2	**20**	1569.7	30.1	7.7	92.3
3	**21**	1511.7	29.1	8	92
4	**22**	804.1	15.4	3.8	96.2
5	**23**	1912.0	36.7	13.1	86.9
6	**24**	2025.3	38.9	13.4	86.6

[a]All reaction performed in MeOH (5 mL), PO (2.01 ml) at 25 °C, 12 hours, mmol complex = 0.0286 cocatalyst = 0, Complex:PO:CS_2 = 1:1500:1000; [b]Determined by mass difference; [c]Scheme 6.2, determined by ^{1}HNMR spectroscopy

6.3 Conclusion

6.3.1 Coupling of CS_2 and PO in neat reactions

The coupling reaction of CS_2 and PO in the presence of ionic functionalized complexes also produced cyclic products instead of a copolymer and this was conformed with ^{1}HNMR spectroscopy. This result was obtained when the ionic functionalized complexes were evaluated as catalysts for the coupling CS_2 and PO in the presence and in the absence of [PPN]Cl as a co-catalyst. The spectrum confirmed that about three cyclic products (**1**, **3,** and **4**, Scheme **6.1**) were produced in all the reactions with 5-methyl-1,3-oxathiolane-2-thione, **1**, as the main product.

The oxidation state of the metal still affected the catalytic reaction even in this case. When the complexes were used as catalysts in the presence and in the absence of a co-catalyst, Cr(II) complexes performed better than their corresponding Cr(III) complexes in most cases. Cr(II) complexes also performed better than their corresponding Co(II) complexes in all cases. The

catalytic reactions in the presence of a complex as catalyst and [PPN]Cl as co-catalyst gave slightly higher conversion than when only the complex was used as catalyst. The binary catalyst system of complexes and [PPN]Cl was found less selective than when the complexes were used as catalysts in the absence of a co-catalyst.

The counter ion on the ionic functionalized complexes seems to have a major influence on the catalytic reaction. When CR(II), Cr(III) and Co(II) complexes containing I^- as a counter ion were used as a catalyst in the absence of a co-catalyst, slightly higher conversions were obtained than when the ones with PF_6^- were used as catalysts for all complexes. The complexes with I^- are also more specific as they have low product distribution compared to the ones with PF_6^- as a counter ion when the complexes were used in the absence of a co-catalyst. When the complexes were evaluated in the presence of a cocatalyst. Similar results were obtained except for Cr(II) complexes **19** and **20** which showed similar activity in this case giving activity of 1.2 and 1.3 % respectively.

6.3.2 Coupling of CS_2 and PO in neat reactions

The solvent seems to have a very big impact on the catalytic reaction. ^{1}HNMR spectroscopy was used as characterization method and it confirmed that the products obtained in the presence of MeOH as a solvent was totally different from the products that was obtained in neat reactions. Products **I** and **II**, Scheme **6.2**, were obtained as products in this case instead of products **1**, **2** and **3**, Scheme **6.1**, that were obtained as in neat reactions. When MeOH was used as solvent, Cr(II) complexes still performed better than their corresponding Cr(III) complexes as catalysts. Product selectivity for product **II** was found better in Cr(III) complexes than in Cr(II) complexes. On the other hand, Co(II) complexes in this case performed better than Cr(II) complexes as catalysts. The counter ion of the complexes still had an effect even in this case where Cr(II) and Cr(III) complexes with I^- as a counter ion performed better than their corresponding complexes with PF_6^- as a counter ion. Co(II) complex **24** with PF_6^- as a counter ion performed better than complex **23** with I^- as a counter ion. Product selectivity for product **II** was found better when Cr(II) and Cr(III) complexes with PF^-_6 as counter ion than for complexes with I^- as a counter ion.

6.4 Experimental

6.4.1 Materials and instrumentation

Reagent grade chemicals were obtained from Sigma Aldrich and used as received. All solvents were dried under appropriate drying reagent and distilled prior to use. The coupling reactions were performed in a 12 place RADLEY's Heated Carousel Reaction Station fitted with a reflux unit as well as a gas distribution system with glass reaction vessels. Mass spectra were recorded on Bruker compact ultimate 3000 HR-MS. ^{1}HNMR and ^{13}CNMR spectra were recorded on a Varian 300, 400 and 500 MHz spectrometer using tetramethylsilane as an internal standard. Chemical shifts are reported in (ppm) and referenced to residual proton in $CDCl_3$.

6.4.2 Evaluation ionic functionalized complexes for catalytic activity for the coupling of CS_2 and PO in the absence of a cocatalyst.

To the 12-tube reaction carousal was added complexes (0.0286 mmol) followed by PO (28.6 mmol) and CS_2 (28.6 mmol). The reactions were performed under argon at room temperature for 12 hours. After this time volatiles were removed under reduced pressure and the crude reaction residue weighed and analyzed with ^{1}H-NMR in $CDCl_3$. The catalysts were removed from the reaction products by dissolving the products in either methylene chloride/ chloroform and then passed the solution through a short silica column.

6.4.3 Evaluation of the binary catalyst system of ionic functionalized complexes and [PPN]Cl for catalytic activity for the coupling of CS_2 and PO

To the 12-tube reaction carousal was added complexes (0.0286 mmol) and [PPN]Cl (0.0286 mmol) followed by PO (28.6 mmol) and CS_2 (28.6 mmol). The reactions were performed under argon at room temperature for 12 hours. After this time volatiles were removed under reduced pressure and the crude reaction residue was weighed and analyzed with ^{1}H-NMR in $CDCl_3$. The catalysts were removed from the reaction products by dissolving the products in either methylene chloride/ chloroform and then passed the solution through a short silica column

6.4.4 Evaluation ionic functionalized complexes for catalytic activity for the coupling of CS_2 and PO in the absence of a cocatalyst using MeOH as solvent.

To the 12-tube reaction carousal was added complexes (0.0286 mmol) followed by MeOH (4 ml) PO (42.9 mmol, 3.01 ml) and CS_2 (28.6 mmol, 1.7 ml). The reactions were performed under argon at room temperature for 12 hours. After this time volatiles were removed under reduced pressure and crude reaction residue was weighed and analyzed with ^{1}H-NMR in $CDCl_3$. The catalysts were removed from the reaction products by dissolving the products in either methylene chloride/ chloroform and then passed the solution through a short silica column

6.5 References

[1] Y. Ren, O. Jiang, H. Zeng, Q. Mao and H. Jiang, *RSC Adv.*, vol. 6, pp. 3243 - 3249, 2016.

[2] M. W. Ren, X. Zhang, Y. Liu, F. J. Li, H. Wang and B. X. Lu, *Macromolecules*, vol. 43, pp. 1396 - 1402, 2010.

[3] J. S. Na, A. Cyriac, E. B. Kim, J. Yoo, K. Y. Kang, J. S. Han and C. Lee, *Inorg. Chem.*, vol. 48, pp. 10455 - 10465, 2009.

[4] W. Wu, X. Sheng, Y. Qin, L. Qiao, Y. Miao, X. Wang and F. Wang, *J. Polym. Sci.*, vol. 52, pp. 2346 - 2355, 2014.

[5] S. Saha, D. Brahman and B. Sinha, *J. Serb. Chem.*, vol. 80, pp. 35 - 43, 2015.

[6] S. Saha, *Int. J. Appl. Eng. Res.*, vol. 4, pp. 257 - 262, 2017.

[7] S. Saha, A. Das, K. Acharjee and B. Sinha, *J. Serb. CHem. Soc.*, vol. 81, pp. 1151 - 1159, 2016.

[8] J. D. Darensbourg, C. W. Chung and J. S. Wilson, *ACS Catal.*, vol. 3, pp. 3050 - 3057, 2013.

[9] J. D. Darensbourg and I. A. Moncada, *Inorg. Chem.*, vol. 47, pp. 10000 - 10008, 2008.

[10] R. Luo, X. Zhou, S. Chen, Y. Li, L. Zhou and H. Ji, *Green Chem.*, vol. 16, pp. 1496 -1502, 2014.

[11] X. C. Miao, Q. J. Wang, Y. Wu, Y. Du and N. L. He, *ChemSusChem*, vol. 1, pp. 236 - 241, 2008.

Chapter 7

Catalytic evaluation of neutral and multifunctional Cr(II), Co(II) and Cr(III) complexes as catalysts for the coupling of CO_2 with PO

Contents

7.1. Introduction 191

7.2. Results and discussions 195

7.2.1. Preliminary catalytic reactions 196

7.2.2. Effect of ligand architecture around metal on CO_2 and PO coupling reaction 200

7.2.3. Effect of oxidation state of the central Cr metal on CO_2 and PO coupling reaction 201

7.2.4. Effect of metal center between Cr(II) and Co(II) complexes on CO_2 and PO coupling reaction 202

7.2.5. Evaluation of ionic functionalized Cr(II), Cr(III) and Co(II) complexes as catalysts for the coupling CO_2 and PO 204

7.3. Conclusion 206

7.4. Experimental 207

7.4.1. Material 207

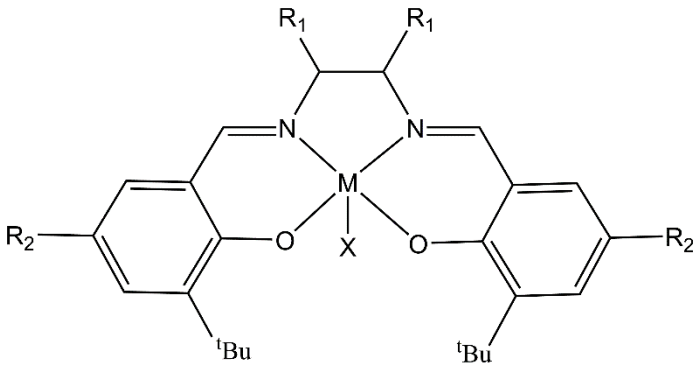
7.4.2. General procedure for the coupling of CO_2 and propylene oxide 208

7.5. References 208

7.1. Introduction

A range of transition metal complexes derived from tetradentate Schiff base ligands, Co(III) [1, 2], Cr(III) [3, 4, 5], Mn(III) [6], have been shown to be active as catalysts for the coupling of CO_2 and epoxide producing either co-polymers or cyclic carbonates. There are many parameters that have been reported to play a role in this catalytic process and those are the pressure, time, temperature, monomer ratio to mention but just a few [7 – 10].

Darensbourg and co-workers investigated the effect of pressure on the coupling of CO_2 and cyclohexene oxide using SalenCr(III)Cl complex, Figure **7.1**. They discovered that when the reaction was performed at 6.90 bar at 80 ^oC for 10 hours, a turnover frequency of 23 h^{-1} was obtained and when the pressure was increased to 13.8 bar, there was an increase in the TOF to 46.7 h^{-1}. Further increase in CO_2 pressure to 34.5 bar resulted in TOF of 67 h^{-1}. A drop in the TOF to 44.4 h^{-1} was observed when the CO_2 pressure was increased further to 55.2 bar [11].



a: R_1 = H, R_2 = ^{t}Bu, M= Cr(III), X = N_3
b: R_1 = -$(CH_2)_4$; R_2 = ^{t}Bu, M = Co(III), X = OTs
c: R_1 = -$(CH)_4$, R_2 = ^{t}Bu, M = Cr(III), X = Cl

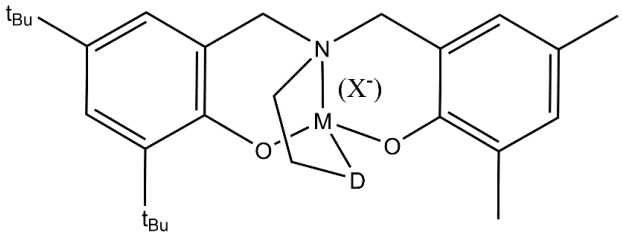
Fig. 7.1: *SalenCr(III) and Co(III) complexes reported by Darensbourg as catalysts for the coupling of CO_2 and cyclohexene oxide*

There are two phases that exist in the catalytic reaction of CO_2 and epoxides: a CO_2-rich phase and a cyclohexene oxide-rich phase. Most catalysts are insoluble in CO_2 and therefore they reside in

cyclohexene oxide-rich phase. When the pressure is increased beyond 34.5 bar, this results in a volumetric expansion of the cyclohexene oxide-phase where the catalyst resides. This is known as catalyst/epoxide dilution effect on the reaction rate, and it negatively affects the reaction.

When Darensbourg evaluated Salen-Cr(III)Cl complex, **c** Figure **7.1,** at constant 4.8 MPa CO_2 pressure for the coupling of PO and CO_2 it was found that temperature affected product distribution. When the reaction was performed at 303 and 323 K, only a polymer was produced but when the temperature was increased to 338 and 353 K a mixture of polymer and cyclic products was obtained. Only a cyclic product was obtained when the reaction was performed at 373 K [12].

The effect of the oxidation state was investigated between Co(II) and Co(III) complexes (**a** and **b** Figure **7.2**) by Saunders and coworkers. This investigation was performed for the coupling CO_2 and PO at 25 ^oC and 3.5 MPa CO_2 pressure for 12 hours. When these complexes were evaluated as catalysts on their own, Co(II) complexes did not show any catalytic activity but Co(III) complex did show some catalytic activity producing cyclic product (TON of 65). The observed activity was concluded to be due to the presence of the axial ligand of the Co(III) complex which can act as a nucleophile in the ring opening of the epoxide which is usually the function of the co-catalysts.



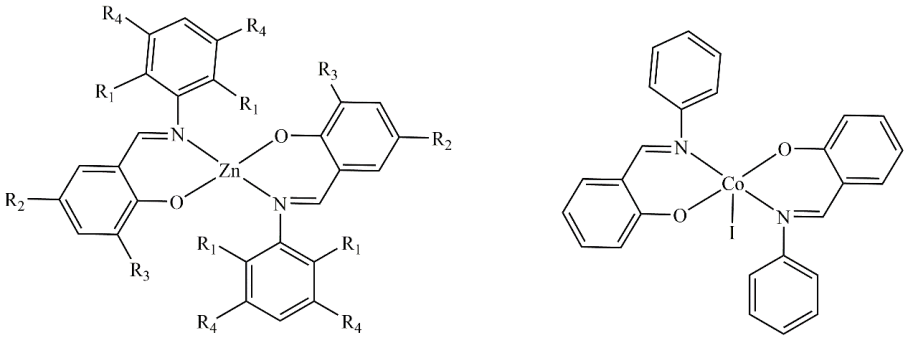
a) M = Co(II), D = C_5H_4N
b) M = Co(III), D = NMe_2, X^- = NO_3^-

Fig. 7.2: *Aminebisphenolato cobalt(II) complexes reported by Saunders as catalysts for the coupling of PO and CO_2*

CO-catalyst showed a very significant effect on the catalytic reaction when Co(II) complex, Figure **7.2**, was used as catalysts. The binary catalyst system of Co(II) complex and TBAB performed

better than the binary catalysts system of Co(II) complex and $PPNN_3$ with TON of 950 and 800 respectively. These results were different from the one that was obtained when this complex was used as catalysts on its own without a cocatalyst where no conversion of PO was observed. The influence of the co-catalysts can be noted. [13].

There have not been many reports on the application of complexes derived from bidentate Schiff base ligands such as salicylaldimies, as catalysts for this coupling process. Salicylaldimine ligands are attractive because of their ease in preparation, which readily allows for varying of their steric and electronic properties [7]. Among the few complexes that were reported as catalysts for CO_2/epoxide coupling reaction that were reported, Darensbourg group used some mono nuclear bis-(salicylaldimonato) Zn(II) complexes (Figure 6.1) as catalysts for the coupling of CO_2 and cyclohexene oxide at 80 °C and 55 bar. These complexes produced a copolymer and the catalytic activity of the complexes was reported to degrees in the order **a** > **b** > **c** with TOF of 15 > 5.0 > 1.2 g·polym·/g·Zn/hr [14]. Sibaouih's group also reported Co(III) complex, **d** Figure **7.3**, for the coupling of PO and CO_2. This catalyst was active and produced, selectively, cyclic product in the presence of DMAP as a co-catalyst, at 10 bar CO_2 pressure and 145 ^oC for one hour [15].



a) R_1 = iPr, R_3 = Me, R_2 = R_4 = H
b) R_1 = iPr, R_2 = R_3 = tBu, R_4 = H
c) R_1 = iPr, R_2 = OMe, R_3 = R_4 = H

d)

Figure 7.3: *Bis-(salicylaldiminato)Zn(II) complexes reported by Darensbourg and co-workers*

Recent research work in this area has focused on synthesizing multifunctional complexes which incorporate both the metal center and the ionic functionalities that can act as nucleophilic groups

that could be obtained from the co-catalysts. There are examples where ionic functionalized complexes were prepared and an example is the Co(III), **b** Figure **7.4**, complexes in tetradentate salen complexes that was prepared by Lu. This complex was applied as multifunctional catalysts for the coupling of CO_2 and PO. Lu reported that ionic functionalized complex, **b** Figure **7.4**, performed better as a catalyst than the binary catalyst system of complex, **a** Figure **7.4**, and $^{n}Bu_4NX$ [16]. The catalytic reaction produced a copolymer with a TOF of 170 h^{-1} in 6 hours when complex **b** was used as a catalyst. A lower TOF of 87 h^{-1} was obtained in 8 hours when the binary catalyst system of complex **a**, and $^{n}Bu_4NX$ was used as catalyst. The addition of the ionic functionality seems to have a very big influence on the catalyst activity on the coupling reaction.

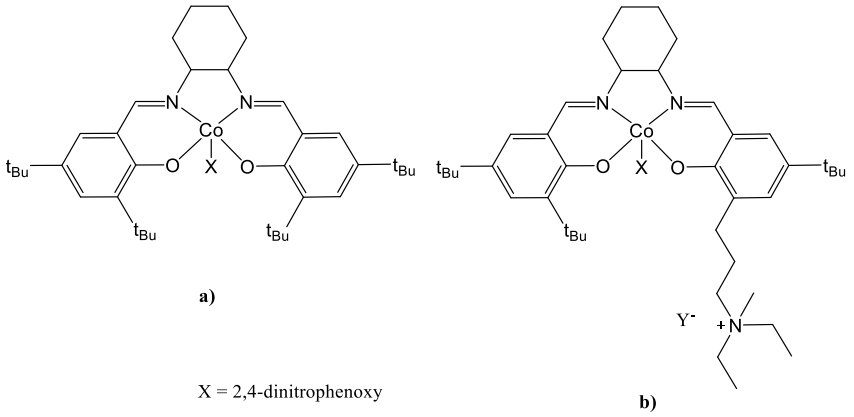
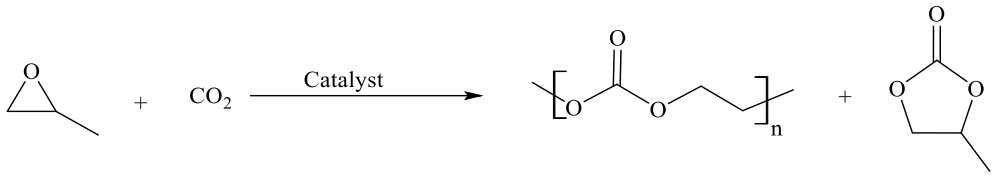


Fig. 7.4: *Single functional, a, and bifunctional salen Co(III) metal complexes reported by Darensbourg as catalysts for the coupling of CO_2 and PO.*

This chapter reports on preliminary catalytic studies on the evaluation of single and multifunctional bis-(salicylaldiminato) Co(II), Cr(II) and Cr(III) complexes as catalyst precursors for CO_2 and PO coupling reaction. The effect of reaction parameters such as solvent, temperature and pressure on the catalytic performance of these complexes was investigated in this study. The effect of the metal center between (Cr(II) vs Co(II)), oxidation state (Cr(II) vs Cr(III)) as well as the multifunctional nature of metal complexes on catalytic performance was also investigated.

7.2. Results and discussions

The metal complexes investigated as catalysts for the coupling of CO_2 and PO, Scheme **7.1**, were neutral Cr(II) (**1** – **4**), Cr(III) (7 – **10**) and Co(II) (**13** – **16**) complexes, Figure **7.5**, as well as ionic functionalized complexes Cr(II) (**19** and **20**), Cr(III) (**21** and **22**) and Co(II) (**23** and **24**) , Figure **7.6**. These reactions were performed under solventless conditions as well as using methanol as solvent in a bottom stirred Berghof 150 mL stainless steel reactor. The effect of reaction conditions such as temperature, pressure and time were investigated.



Scheme 7.1: *Coupling of CO_2 and propylene oxide.*

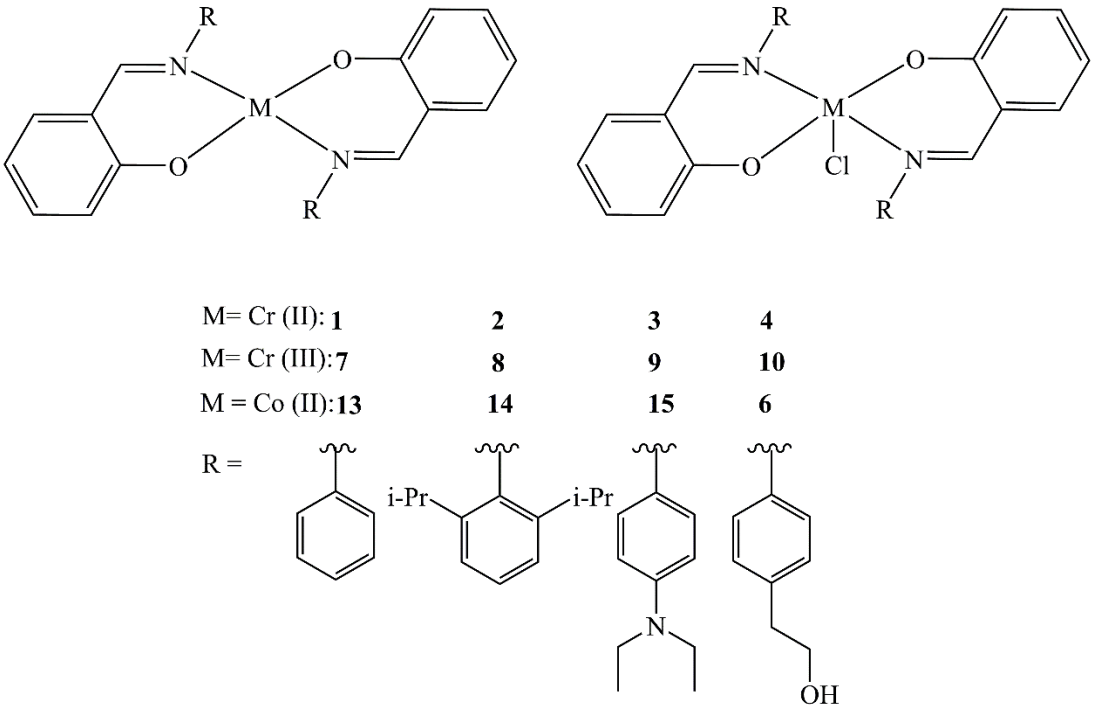
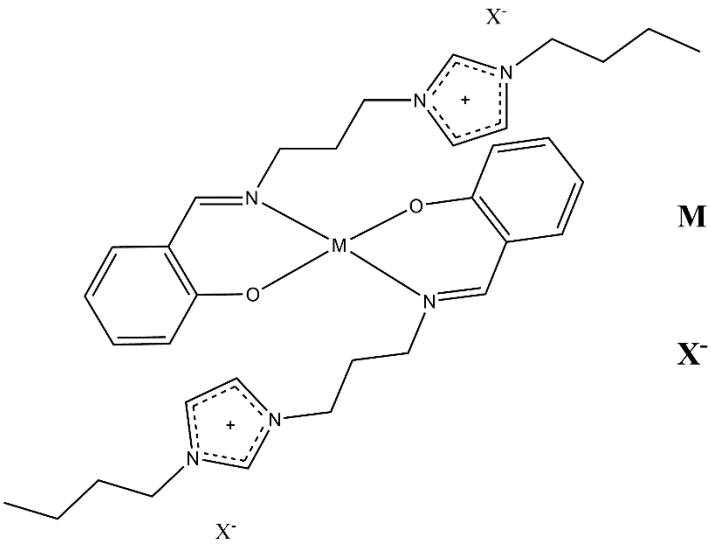


Fig. 7.5: *Neutral complexes used as catalysts for the coupling of CO_2 and PO*



M = Cr:	**19**	**20**
CrCl:	**21**	**22**
Co:	**23**	**24**
X$^-$ =	I^-	PF_6^-

Fig. 7.6: *Ionic functionalized complexes used as catalysts for the coupling of CS_2 and PO*

7.2.1. Preliminary catalytic reactions

Cr(III) complex, **8**, was used to screen reaction conditions that could be suitable for the catalytic reaction. This complex was first evaluated as catalyst on its own using 1 MPa CO_2 pressure, solvent less and at room temperature for 12 hours (Table **7.1**, entry **1**). Analysis of the crude reaction mixture for these experiments with ^{1}HNMR in $CDCl_3$ showed that no coupling products were obtained under these conditions. The big challenge here was that the complex did not show any solubility in PO and this could have made it unavailable for the homogeneous catalytic process.

[PPN]Cl was observed to be the co-catalyst that resulted in the best binary catalyst system for the coupling of CS_2 and PO and was therefore also investigated as co-catalyst for the coupling of CO_2 and PO. A control experiment using only [PPN]Cl without metal complex was first performed using 1 MPa CO_2, solventless at room temperature for 12. Analysis of this crude reaction mixture with ^{1}HNMR spectroscopy also revealed that no coupling products were obtained (Table **7.1**, entry **2**). The binary catalyst system of complex **8** and [PPN]Cl was then investigated (Table **7.1**, entry **3**) and it was confirmed with ^{1}HNMR spectroscopy that only propylene carbonate (PC) was obtained as a coupling product, however only 1.8 % PO conversion was observed.

7.2.1.1. Effect of reaction conditions such as temperature, pressure, and time

The effect of temperature on the coupling of CO_2 and epoxide was evaluated using three different temperatures: 25 ^oC, 60 ^oC and 80 ^oC (Table **7.1**, entries **3, 4** and **5** respectively). At all these temperatures the coupling process produced the cyclic product PC only with no copolymer formation being observed. Increasing the temperature resulted with an increase in % PO conversion with conversions of 1.8, 12.7 and 27.0 %, being observed at 25 ^oC, 60 ^oC and 80 ^oC respectively. The increase in the formation of PC, as temperature increases is a result of the high activation barrier for CO_2 and PO cyclization [17]. Darensbourg and coworkers also observed that as temperature was increased from 30 to 60 ^oC, there was an increase in the formation of PC [10]. The formation of PC as only coupling products was confirmed with ^{1}HNMR spectroscopy with a typical spectrum obtained shown in Figure **7.7**. The signal at 1.40 ppm is assigned to the methyl carbon and those at 3.96 and 4.50 ppm are assigned to methine protons of propylene carbonate. Lastly, the signal at 4.79 ppm is assigned to the methylene proton of the cyclic product.

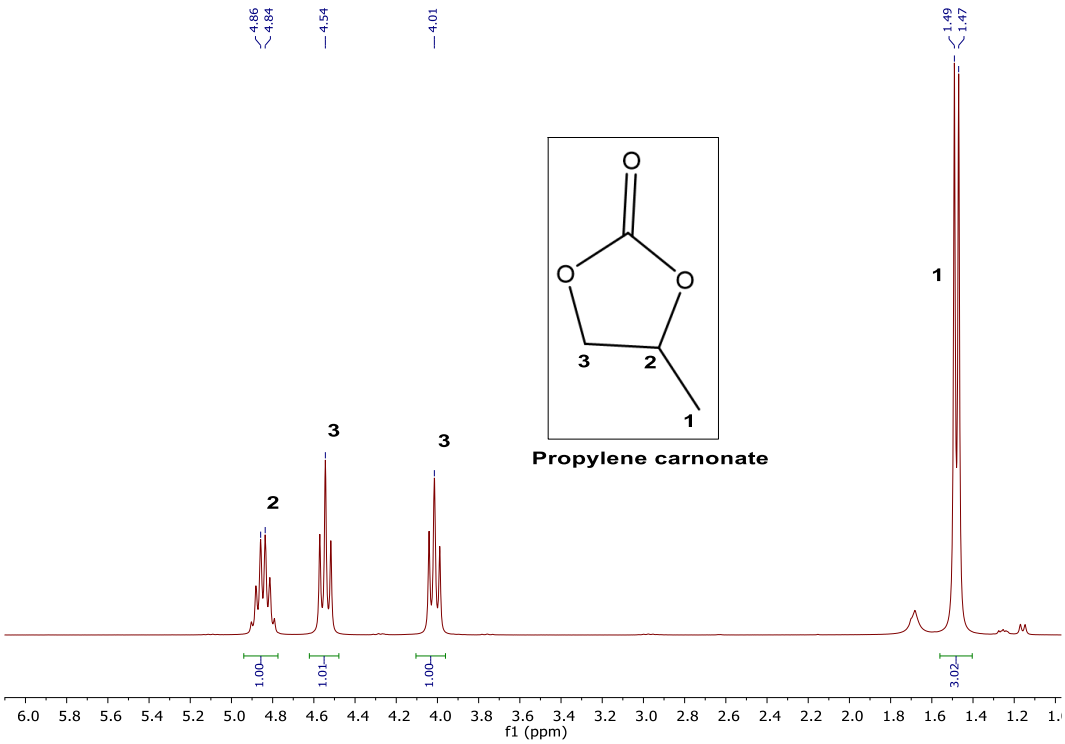


Fig. 7.7: *^{1}HNMR spectrum for the product obtained at 80 ^oC, Table **7.1**, entry **5***

Table 7.1: CO_2/epoxide coupling using bis-salicylaldiminato complex **8** as catalysts[a]

Entry	Temp/ °C	Time/ h	Pressure/ MPa	Solvent	Mass/ g	%Conversion[b]	TOF[c]
1	25	12	1	-	0	0	0
2[*]	25	12	1	-	0	0	0
3	25	12	1	-	0.052	1.8	1.5
4	60	12	1	-	0.371	12.7	10.6
5	80	12	1	-	0.787	27.0	22.5
6	80	12	5	-	0.660	22.6	18.8
7	80	6	1	-	0.401	13.8	11.5
8	25	12	1	MeOH	0	0	0
9	80	12	1	MeOH	0.055	1.9	1.6
10	80	12	1	DCM	0.951	32.6	27.1
11	80	12	1	Tol	0.861	29.5	24.6

[a]All reaction performed; PO (28.6 mmol, 2.01 ml), 12 hours, mol Co-catalyst ([PPN]Cl) = mol catalyst = 0.0286 mmol, Complex:PO:CS_2 = 1:1000:1000; [b]Determined by mass difference, [c]TOF = mmol substrate (PO) converted per mmol complex per hour. [*]Without complex **8** as a catalyst

The coupling of CO_2 and PO occur in a gas-liquid two phase reaction and CO_2 pressure is important because it determines the molar ration of CO_2 in the catalytic reaction [18]. It is therefore important to investigate the effect of pressure on the catalytic process. Darenbourg and co-workers found that pressure does affect the catalytic activity of Cr(III) salen complex when they applied it as a catalyst for the coupling of cyclohexene oxide and CO_2 at 80 ^oC for 10 hours [19]. They found that when pressure was increased from 6.90 to 34.5 bar the catalytic activity increased from 23 to 67 h^{-1} TOF. However, when the pressure was increase further to 55.2 bar there was a drop-in activity of the catalyst and 44.4 h^{-1} TOF was observed.

In this study the effect of pressure was investigated at 1 MPa (Table **7.1**, entry **6**) and 5 MPa (Table **6.1**, entry **7**). These two pressures were chosen as they are the commonly used in literature. It can be observed from Table **7.1** that as pressure was increased from 1 MPa to 5 MPa conversions of 27.0 and 22.6 % were obtained, respectively. When the effect of pressure was also studied by Darensbourg and co-workers, they found that when pressure was increase from 3.1 to 5.5 MPa there was a drop in the turnover frequency from 1150 to 760 h^{-1}, respectively [20]. The rate of

reaction sometimes drops in the CO_2 coupling reactions because of CO_2-induced diluting effect in the solvent-free conditions [21, 22, 20]. ^{1}HNMR spectrum confirmed that at these two pressures the coupling reaction still produced only propylene carbonate as coupling product.

The influence of time was investigated by performing the coupling experiments for 6 and 12 hours. When the reaction was performed for 6 hours 13.8 % conversion of PO to the cyclic product was observed. When the same reaction conditions were used for the coupling reaction and time increased to 12 hours, 27.0% conversion was obtained.

7.2.1.2. Effect of solvents on CO_2 and PO coupling reaction

The effect of solvent on the coupling reaction was investigated by performing the catalytic experiments in MeOH, DCM and toluene at room temperature and 1 MPa CO_2 pressure. For the rection performed in methanol there was no conversion of PO observed at 25 ^{o}C compared to the solventless reaction where 1.8 % PO conversion was observed. However, increasing the reaction temperature to 80 ^{o}C for the reaction using methanol as solvent a conversion of 1.9% was observed. The % PO conversion is still significantly lower than the conversion observed for the coupling reaction performed solventless (27%) under the same reaction conditions indicating that the presence of methanol retards the coupling reaction quite significantly.

When dichloromethane (Table **7.1** entry **10**) and toluene (Table **7.1** entry **11**) were used as solvents for the coupling reaction at 80 ^{o}C and 1 MPa, conversions of 32.6 and 29.5 % were obtained, respectively. These conversions which are comparable, are better than conversion observed in MeOH and solventless at the same reaction conditions. It can therefore be concluded that, DCM is a better solvent followed by toluene and MeOH is the worst solvent for the coupling process. CO_2 does not have a net dipole moment therefore it is non-polar. It means therefore that it will have the poorest solubility in methanol and that can result in lower catalytic conversion than when DCM and toluene are used as solvents.

7.2.2. Evaluation neutral Cr(II), Cr(III) and Co(II) complexes as catalysts for the coupling CO_2 and PO

Following the preliminary studies performed with complex **8** the other neutral metal complexes were also studied using [PPN]Cl as cocatalyst. The data obtained for these studies are summarized in Table **7.2**. All the complexes exhibited very low activity under the conditions studied. ^{1}HNMR analysis of the crude reaction mixtures obtained in $CDCl_3$ showed that for all experiments only PC was produced as coupling product.

Table 7.2: CO_2/epoxide coupling using neutral bis-salicylaldiminato Cr (1 – 4 and 6 – 10) and Co (13 – 16) complexes as catalysts[a]

Entry	Complex	Pressure MPa	Mass /g	%Conversion[b]	TOF[c]
1	**1**	1	1.000	33.9	28.5
2	**2**	1	0.819	28.1	23.3
3	**3**	1	0.477	16.4	13.6
4	**4**	1	0.864	29.6	24.7
5	**5**	1	0.957	32.8	27.3
6	**6**	1	0.787	27.0	22.4
7	**7**	1	0.829	28.5	23.7
8	**8**	1	0.722	24.8	20.6
9	**9**	1	0.290	9.9	8.3
10	**10**	1	0.395	13.6	11.3
11	**11**	1	0.314	11.4	9.0
12	**12**	1	0.213	7.4	6.1

[a]All reaction performed in neat PO (28.6 mmol, 2.01 ml), 12 hours, mol Co-catalyst([PPN]Cl) = mol catalyst = 0.0286; Complex:PO:CS_2 = 1:1000:1000, Temperature 80 ^oC , [b]Determined by mass difference, [c]TOF = mmol substrate (PO) converted per mmol complex per hou

7.2.3. Effect of ligand architecture on activity

Ligand architectures affect the activity of the metal complexes for the coupling processes depending on their electronic and steric properties [23, 24]. A comparison of the catalytic activity of the metal complexes derived from the same ligand is shown in Figure **7.8.** It is evident from the

graph that there is no clear trend in terms of ligand architecture that can be observed when comparing the series of metal complexes derived from the same ligands. However, complexes **1** and **7**, which are the Cr(II) and Cr(III) analogues derived from the unsubstituted salicylaldimine ligand, are observed to be the best performing complexes amongst the series of complexes investigated. Whereas complex **14,** which is derived from the 2,6-diispropyl substituted salicylaldimine ligand, is the best performing cobalt complex. When observing metal complexes derived from similar metal center and different ligand architecture, the activity is observed in this order **1**>**4**>**2**>**3**, **7**>**9**>**8**>**10** and **14**>**15**>**13**>**16** for Cr(II), Cr(III) and Co(II) respectively.

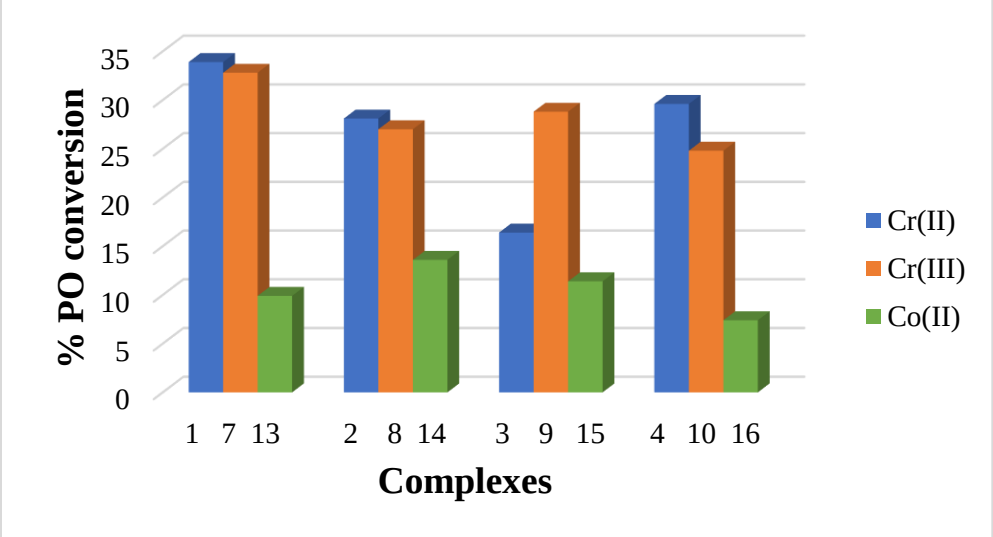


Figure 7.8: *Comparison of the activity of Cr(II), Cr(III) and Co(II) complexes derived from the same ligand for CO_2 and PO coupling.*

7.2.4. Effect of oxidation state of the central metal on catalytic performance

The electronic properties of the metal complexes can also be affected by the oxidation state of the metals. All Cr(II) complexes seem to perform just slightly better than their corresponding Cr(III) complexes for the coupling of CO_2 and PO reaction. This result is against the idea that metals with higher oxidation state should perform better because the metal is more available for ring opening process than those that have lower oxidation states. The dissociation of the product from the metal

also counts. It could be that after the product is formed, it dissociates quicker in Cr(II) complexes to allow for a continuous catalytic process than in Cr(III) complexes. The only exception is observed for Cr(III) complex **9** which shows better activity than its corresponding Cr(II) complex **3**. The effect of oxidation state was also confirmed by Saunders and coworkers between Co(II) and Co(III) complexes [13]. They found that the oxidation state of the central metal did have an impact on the catalytic reaction of CO_2 and epoxide. When they used a Co(II) complex in the presence of either TBAB of $[PPN]N_3$, they found that it performed better than its corresponding Co(III) complex.

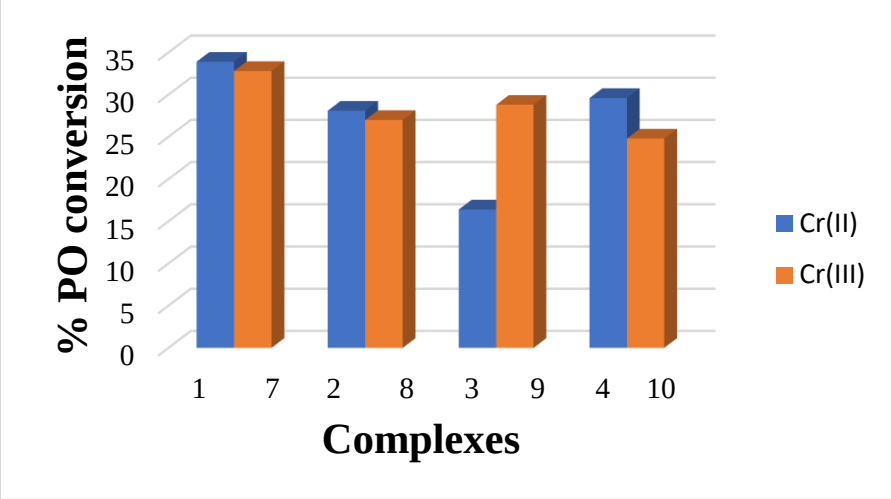


Figure 7.9: *Comparison of the effect of oxidation state of Cr complexes for CO_2 and PO coupling reaction.*

7.2.5. Effect of the nature of the metal center on catalytic performance

The coupling reaction of CO_2 and epoxides go through a couple of steps and the binding of the epoxide to the metal center for the ring opening of the epoxide is one of them. This step is crucial because it can influence the rate of the reaction. The nature of the metal involved can therefore influence the coupling reaction [25, 26, 27]. The polarity of the ($M^{\delta+}$ - $O^{\delta-}$) in the metal epoxide bond play a very important role and when the effect of metal center was investigated between Cr(III), Al(III) and Co(III) the reactivity was recorded in the order Cr > Al ~ Co. This trend was

expected between Cr(III) and Co(III). They are group four elements and the electronegativity increases from left to right making Co(III) more oxidizing than Cr(III) [25, 28].

The effect of the metal center on the coupling reaction in this study was investigated between Cr(II), **1** – **14**, and Co(II), **13** – **16**, complexes (Table **7.2**) in this study. It was highlighted before that all these complexes produced a cyclic product, PC, instead of a co-polymer and this was confirmed with ^{1}HNMR spectroscopy. Therefore, the metal center of the complex did not seem to influence the nature of the product produced by the coupling process. This could suggest that the pathway of the catalytic process is the same resulting in similar product.

The metal center however influenced the quantity of the product produced. For instance, a Cr(II) complex **2** produced 28.1 % of PC while a corresponding Co(II) complex, **14**, produced 14.3 % of the cyclic product. This significant difference in percentage conversion was observed for all Cr(II) and Co(II) complexes investigated in this study with all Cr(II) complexes performing way better than their corresponding Co(II) complexes, Figure **7.10**. The difference in percentage conversion shows that Cr(II) complexes are better as catalysts than Co(II) complexes. This justifies that the nature of the central metal does influences the catalytic activity of the metal complex in terms of conversion. This could mean Cr(II) metal is more reactive than Co(II) metal as it is indicated in the reactivity series.

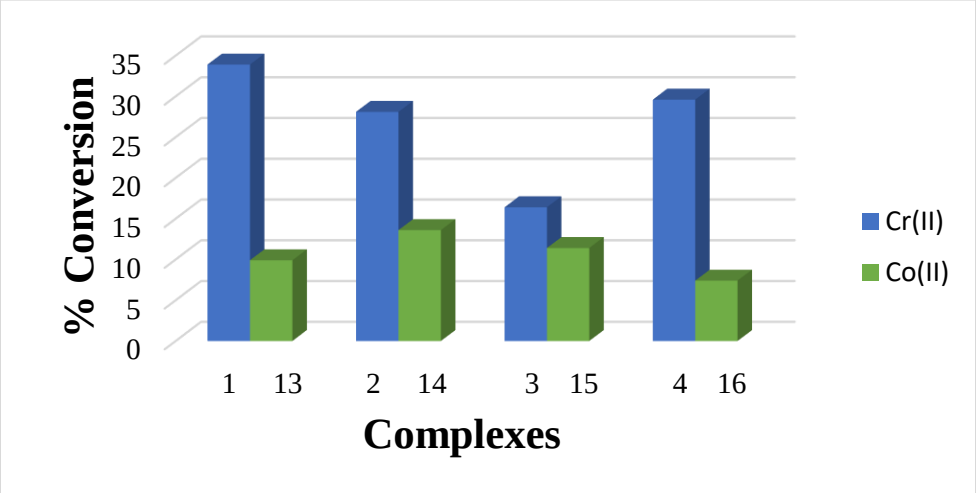


Figure 7.10: *Influence of metal center between Cr(II) and Co(II) complexes for CO_2 and PO coupling reaction.*

7.2.6. Evaluation of ionic functionalized Cr(II), Cr(III) and Co(II) complexes as catalysts for the coupling CO_2 and PO

Ionic functionalized metal complexes, Figure **7.6**, prepared in this study were also evaluated as catalyst for the coupling of CO_2 and PO. The data obtained for the catalytic experiments performed with the ionic tagged complexes is summarized in Table **7.3**. Complex **21** was evaluated firstly as a catalyst on its own at 25 ^oC and 1 MPa CO_2 pressure for 12 hours. For this experiment 0.4% PO conversion was obtained, however by performing this reaction at 80 ^oC a significant increase in PO conversion was observed to be 19.4%. The complex showed activity in the absence of a co-catalyst and that could be because the ionic functionality incorporated in the complex provided the anion that could have been provided by the co-catalyst.

The binary catalyst system of complex **21**/[PPN]Cl was also used at 25 ^oC, 1 MPa CO_2 for 12 hours, which resulted in a slightly improved PO conversion of 2.4%. Addition of PPNCl to the catalytic reaction increase the anion in the catalyst system therefore this can increase ring opening rate of the epoxide and therefore improve the percentage conversion of PO to the cyclic product. The other ionic functionalized metal complexes were then evaluated at 80 ^oC, 1 MPa CO_2 pressure for 12 hours. All the complexes exhibit some activity in the absence of a co-catalyst for the coupling reaction.

7.2.6.1 Effect of metal oxidation state and nature of metal center on catalytic performance

The effect of the oxidation state between bifunctional Cr(II) and Cr(III) shows that Cr(III) complexes show better catalytic activity than their corresponding Cr(II) complexes. For instance Cr(III) complex **21** performed better than its corresponding Cr(II) complex **19**. Conversions of 19.4 and 13.2 % were obtained for Cr(III) complex **21** and Cr(II) complexes **19** respectively. The effect of the metal center between Cr(II) and Co(II) complexes show that bifunctional Co(II) complexes are more active than their corresponding Cr(II) complexes. For instance Co(II) complex gave 37.1 % conversion of PO while Cr(II) complex gave 13.2 %. Darensbourg showed that metal center of the complexes does influence the catalytic reaction when bifunctional complexes are used as catalyst. When bifunctional salen-Cr(III) and Co(III) complexes were used as catalysts for

the coupling of cyclopentene oxide and CO_2 at 70 ^oC and 2 Mpa conversions of 1.1 and 28.2 % were obtained respectively [29].

7.2.6.2 Effect of the type of counter ion on catalytic performance

From this study it can be observed from Table **7.3** that all complexes containing I^- as a counter ion performed slightly better than their corresponding complexes that have PF_6^- as counter ions. This was observed for all complexes studied. For example, Cr(II) complex **19** has I^- as counter ion and it gave conversion of PO to cyclic product of 13.2 % while complex **20** that has PF_6^- as a counter ion gave 12.6 % conversion. The investigation of the effect of the counterion was investigated by Jing and co-workers for the copolymerization of propylene oxide and CO_2. The catalytic reaction was performed at 0.6 MPa and 20 ^oC with bifunctional salen-Co(III) catalysts bearing I^-, Br^-, Cl^-, F^- as counter ions. The order of activity with respect to the counter ions was observed as $I^->Br^->Cl^->F^-$ with % conversions of 53.5, 44.8, 29.5 and 14.9 % respectively [30].

Table 7.3: CO_2/epoxide co-polymerization using ionic functionalized bis-salicylaldiminato Cr (19 – 22) and Co (23 – 24) complexes as catalysts[a]

Entry	Complex	Temp(°C)	Mass PC[b] (mg)	%PO Conversion	TOF[c]
1	**19**	80	386.7	13.2	11.0
2	**20**	80	367.6	12.6	10.5
3	**21**	25	12.6	0.4	0.3
4[d]	**21**	25	70.9	2.4	2.0
5	**21**	80	566.0	19.4	16.2
6	**22**	80	500.9	17.2	14.3
7	**23**	80	1080.1	37.1	30.9
8	**24**	80	886.4	30.4	25.3

[a]All reaction performed in neat PO (2.01 ml), complex = 0.028 mmol, 12 hours, 1MPa CO_2; Complex:PO = 1:1000,; [b]mass propylene carbonate (PC) produced determined by mass difference, [c]TOF = mmol substrate (PO) converted per mmol complex per hour. [d][PPN]Cl (0.028 mmol) used as co-catalyst.

7.3. Conclusion

7.3.1. Neutral metal complexes as catalysts for the coupling of CO_2 and PO

All neutral complexes were found active as catalysts for the coupling of PO and CO_2 process in the presence of a co-catalyst. The catalytic process produced propylene carbonate with no copolymer formation being observed for any of the metal complexes studied. The binary catalyst system of complex **8**/[PPN]Cl exhibited some activity at 25 ^oC, which significantly improved when the reaction temperature was increased to 80 ^oC. The CO_2 pressure was found to have small effect on the activity of complex **8** at 80 ^oC. Conversions of 27.0 and 22.6 % were obtained using 1 MPa and 5 MPa, respectively and this reaction was performed neat. Solvents influenced the coupling reaction. When MeOH, DCM and Toluene were used as solvents at 1 MPa for 12 hours, 1.9, 32.6 and 29.5 % conversions of PC were obtained, respectively.

A clear trend on catalytic performance could not be observed when considering the ligand architecture for the series of complexes studied. It was however observed that complexes **1** and **7**, which are the Cr(II) and Cr(III) complexes (giving 33.9 and 32.8 % conversions respectively) derived from the same ligand were the best performing amongst the series of Cr(II) and Cr(III) complexes investigated. Whereas for the series of Co(II) complexes the best performing complex was complex **14** derived from the 2,6-diispropyl substituted ligand.

The effect of the oxidation state was investigated between Cr(II) and Cr(III) complexes. Cr(II) complexes **1**, **2** and **4** show slightly better conversion than their corresponding Cr(II) complexes **7**, **8** and **10**. Cr(II) complex **3** show significantly lower conversion than the corresponding Cr(III) complex **9**. The effect of the oxidation state was also investigated between Cr(II) and Co(II) complexes in this study. All Cr(III) complexes show better activity compared to their corresponding Co(II) complexes.

7.3.2. Ionic functionalized metal complexes as catalysts for the coupling of CO_2 and PO

Ionic functionalized metal complexes synthesized in this study were also evaluated as catalysts. These metal complexes also produced propylene carbonate as the coupling product, and this was

also confirmed with ^{1}HNMR. A preliminary study was carried out where complex **21** was investigated as a catalyst individually and in the presence of [PPN]Cl at 25 ^{o}C, 1 MPa and neat and a conversion of 0.4% was obtained. These complexes showed better catalytic activity when a co-catalyst was added and a conversion of 2.4 % was obtained. This shows that the co-catalyst influenced the catalytic reaction. When the catalytic reaction was performed at 80 ^{o}C and complex **21** was used as catalyst the conversion of PO to cyclic products increased from 2.4 % to 19.4 %.

When Cr(II) and Cr(III) complexes were evaluated as catalysts in the absence of a co-catalyst they also showed that the oxidation state has some effect on the coupling reaction with Cr(III) complexes performing better than their corresponding Cr(II) complexes. This investigation was done at 80 ^{o}C, 1 MPa and 12 hours. For instance complex, complex **21** gave a conversion of 19.4 % while Cr(II) complex **19** gave 13.2 %. This result is a bit different from the one that was obtained for neutral complexes where some Cr(II) complexes performed slightly better than their corresponding Cr(III) complexes. The metal center also still proved to have an influence on the catalytic reaction. In this case Co(II) complexes performed better than their corresponding Cr(II) complexes. The counter ion of the metal complex did influence the catalytic reaction for Cr(II) and Cr(III) complexes. Cr(II) complex **19** that contains I^{-} as a counter ion gave a conversion of 13.2 % while Cr(II) complex **20** that contains PF_6^{-} as counter ion gave a conversion of 12.6 %. For Cr(III) complexes, Cr(III) complex **21** that has I^{-} as a counter ion gave a catalytic conversion of 19.4 % while complex **22** that contains PF_6^{-} as a counter ion gave a conversion of 17.2 %. In the case of Co(II) complexes, complex **23** that has I^{-} as a counter ion performed better that its corresponding Co(II) complex, **24**, bearing PF_6^{-} as a counter ion.

7.4. Experimental

7.4.1. Material and Instrumentation

Reagent grade chemicals were obtained from Sigma Aldrich and used as received. All solvents were dried under appropriate drying reagent and distilled prior to use. The coupling reactions were performed in a bottom stirred Berghof 150 mL stainless steel reactor. ^{1}HNMR spectra were recorded on a Varian 300, 400 and 500 MHz spectrometer in $CDCl_3$ using tetramethylsilane as an

internal standard. Chemical shifts are reported in (ppm) and referenced to residual proton in $CDCl_3$.

7.4.2. General procedure for the coupling of CO_2 and propylene oxide

The method used for this coupling reaction is described using conditions for complex **8**, Table **7.1** entry **3** as an example. A stirrer bar and metal complex (0.0286 mmol) was added to the reactor followed by PO (28.6 mmol). The reactor was sealed, purged with CO_2, and then pressured to 1MPa CO_2. This reaction mixture was then stirred at room temperature for 12 hours. The reactor was vented, and the reaction residue transferred to a round bottom flask. All volatiles were removed under vacuum and the crude reaction residue was weighed and the ^{1}HNMR spectrum obtained in $CDCl_3$. The reaction using [PPN]Cl) as co-catalyst was performed in a similar manner by adding [PPN]Cl (0.0286 mmol) to the reactor. Reaction at 80 ^oC was performed by heating the reactor in an oil bath to the desired temperature while monitoring the internal reactor temperature with a thermocouple.

7.5. References

[1] T. C. Cohen, T. Chu and W. G. Coates, *J. Am. Chem. Soc.*, vol. 127, pp. 10869 - 10878, 2005.

[2] L. R. Paddock and T. S. Nguyen, *Macromolecule*, vol. 38, pp. 6251 - 6253, 2005.

[3] J. D. Darensbourg, M. R. Mackiewicz, L. J. Rodgers, C. C. Fang, R. D. Billodeaux and H. J. Reibenspies, *Inorg. Chem.*, vol. 43, pp. 6024 - 6034, 2004.

[4] J. D. Darensbourg, M. R. Mackiewick, L. J. Rodgers and L. A. Phelps, *Inorg. Chem.*, vol. 43, pp. 1831 - 1833, 2004.

[5] L. Guo, C. Wang, W. Zhao, H. Li, W. Sun and Z. Shen, *Dalton Trans.*, pp. 5406 - 5410, 2009.

[6] F. Jutz, D.-J. Grunwaldt and A. Baiker, *J. Mol. Catal. A-Chem.* , vol. 279, pp. 94 - 103, 2008.

[7] S. Narang, R. Mehta, D. Berek and N. S. Upadhyay, *Journal of Molecular Science, Part A; Pure and applied Chemistry,* vol. 53, pp. 297 - 300, 2016.

[8] Y. Niu and H. Li, *Colloid Polym. Sci.*, vol. 291, pp. 2181 - 2189, 2013.

[9] "Li, H.; Niu, Y.," vol. 43, pp. 121 - 125, 2011.

[10] D. J. Darensbourg, J. C. Yarbrough, C. Ortiz and C. C. Fang, *J. Am. Chem. Soc.*, vol. 125, pp. 7586 - 7591, 2003.

[11] J. D. Darensbourg, M. R. Mackiewicz and R. D. Billodeaux, *Organometallics*, vol. 24, pp. 144 - 148, 2005.

[12] J. D. Darensbourg, C. J. Yarbough, C. Ortiz and C. C. Fang, *J. Am. Chem. Soc.*, vol. 125, pp. 7586 - 7591, 2003.

[13] N. L. Saunders, N. Ikpo, F. C. Petten, K. U. Das, N. L. Dawe, M. C. Kozak and M. F. Kerton, "Cat," *Catal. Commun.*, vol. 18, pp. 165 - 167, 2012.

[14] D. J. Darensbourg, R. P. and J. Yarbrough, *Inorg. Chem.,* vol. 40, pp. 986 - 993, 2001.

[15] A. Sibaouih, P. Ryan, V. K. Axenov, R. M. Sundberg, M. Leskela and T. Repo, *J. Mol. Catal. A Chem.*, vol. 312, pp. 87 - 91, 2009.

[16] M.-W. Ren, X. Zhang, Y. Liu, F.-J. Li, H. Wang and B.-X. Lu, *Macromolecules*, vol. 43, pp. 1396 - 1402, 2010.

[17] D. J. Darensbourg and A. D. Yeung, *Polym. Chem.,* vol. 6, pp. 1103 - 1117, 2015.

[18] D. Jintang, W. Jiajun, F. Lianfang, W. Long and G. Xueping, *J. Appl. Polym. Sci.,* vol. 118, pp. 366 - 371, 2010.

[19] J. D. Darensbourg, M. R. Mackiewicz and R. D. Billodeaux, *Organometallics*, vol. 24, pp. 144 - 148, 2005.

[20] J. D. Darensbourg, M. R. Mackiewicz, L. A. Phelps and R. D. Billodeaux, *Acc. Chem. Res.,* vol. 37, pp. 836 - 844, 2004.

[21] F. Jutz, A. Buchard, R. M. Kember, B. S. Fredriksen and K. C. Williams, *J. Am. Chem. Soc.,* vol. 133, pp. 17395 - 17405, 2011.

[22] W. G. Yang, Y. Y. Zhang, R. Xie and P. G. Wu, *J. Am. Chem. Soc.,* vol. 142, pp. 12245 - 12255, 2020.

[23] T. C. Cohen, M. C. Thomas, L. K. Peretti, B. E. Lobkovsky and W. G. Coates, *Dalton Trans.,* pp. 237 - 249, 2006.

[24] L. R. Paddock and T. S. Nguyen, *Macromolecule,* vol. 38, pp. 6251 - 6253, 2005.

[25] P. Chen, H. M. Chrisholm, C. J. Gallucci, X. Zhang and Z. Zhou, *Inorg. Chem.,* vol. 44, pp. 2588 - 2595, 2005.

[26] A. G. Luinstra, R. G. Haas, F. Molnar, V. Bernhart, R. Eberhardt and B. Rieger, *Chem. Eur. J.,* vol. 11, pp. 6298 - 6314, 2005.

[27] C. Chatterjee and H. M. Chrisholm, *Inorg. Chem.,* vol. 50, pp. 4481 - 4492, 2011.

[28] C. Chatterjee, H. M. Chisholm, A. El-Khaldy, D. R. Mclntosh, T. J. Miller and T. Wu, *Inorg. Cem.,* vol. 52, pp. 4547 - 4553, 2013.

[29] J. D. Darensbourg, C.-W. Chung and J. Wilson, *ACS Catal.,* vol. 3, pp. 3050 - 3057, 2013.

[30] T. Chang, L. Jin and H. Jing, *ChemCatChem,* vol. 1, pp. 379 - 383, 2009.

Chapter 8

Summary

Chapter one of this thesis provides a brief literature survey on the coupling of CS_2 and CO_2 with epoxides. Several metal complexes that have been reported as active catalysts for these coupling reactions are summarized in this chapter. Specifically, metal complexes based on porphyrins and tetradentate Schiff base ligands, salens, have been extensively discussed in this chapter. In addition, this chapter provides a problem statement and the main objective of this study which is to prepare both neutral and ionic functionalized chromium and cobalt metal complexes and evaluate them as catalysts for the coupling of CO_2/ CS_2 with propylene oxide.

Chapter two of this thesis is focused on the synthesis of neutral salicylaldimine ligands that contain groups that can be easily ionic functionalized. Some of the neutral ligands were transformed to ionic functionalized ligands. Attempts were made to use quaternization to prepare ionic functionalized ligands. This method was successful for transforming ligand **HL_5** and **HL_6** to ionic functionalized ligands **HL_7** and **HL_9**, respectively. The quaternization method was not successful to transform ligand **HL_3** into an ionic functionalized ligand. An attempt to prepare ionic functionalized ligand from **HL_4** through sulfonation was not successful. All the ligands were characterized with analytical techniques.

Chapter three is focused on the preparation of neutral and ionic functionalized Cr(II), C(III), and Co(II) complexes from the successfully synthesized ligands. $CrCl_2$, $CrCl_3(THF)_3$ and $Co(OAc)_4{\bullet}4H_2O$ were employed as metal sources respectively. The complexes were characterized with analytical techniques such as FT-IR and Uv-vis spectroscopy, mass spectrometry and elemental analysis. Attempts to prepare Co(III) complexes from neutral ligands was not successful and because of this failure no attempts were further made to prepare Co(III) complexes from ionic functionalized ligands.

Chapter four reports on the catalytic evaluation of the synthesized neutral complexes as catalysts for the coupling of CS_2 and PO reaction in a neat reaction condition. The complexes all produced cyclic products instead of a copolymer and this was confirmed with NMR spectroscopy. These

complexes showed no catalytic activity towards CS_2/PO coupling reactions in the absence of a co-catalysts. When complexes **2**, **8** and **14** were evaluated as catalysts in the presence of Melm, TBAC, DMAP and [PPN]Cl these complexes showed some activity for CS_2/PO coupling reaction with chromium complexes **8** and **2** showing better conversion in the presence of [PPN]Cl. Co(II) complex **14** showed better conversion of PO to cyclic products in the presence of DMAP instead of [PPN]Cl.

Chapter five describes the evaluation of the neutral complexes as catalysts for the coupling of CS_2 and PO in the presence of organic solvents. Different solvents do have an impact on the catalytic activity of the complexes toward the coupling reaction. Protic polar solvents such as MeOH and EtOH produced different cyclic products compared to when non-polar solvents such as toluene was used. These non-polar solvents produced cyclic products that are like when the reactions were performed neat. No coupling reaction products were obtained when dichloromethane was used as a solvent.

Chapter six details evaluation of ionic functionalized complexes as catalysts for the coupling of CS_2 and PO both neat and in the presence of MeOH as an organic solvent. MeOH had so much influence in the catalytic reaction even in this case. The cyclic products that were obtained in its presence are different from those that were obtained when the reactions were performed neat. When the coupling reaction was performed in MeOH, there was also an improvement in the conversion of PO to the coupling product.

Chapter seven describes the evaluation of both neutral and ionic functionalized complexes as catalysts for the coupling of CO_2 and PO. NMR spectroscopy also showed that all the complexes that were investigated as catalysts produced cyclic products instead of a copolymer. Reaction conditions such as temperature and pressure influenced the coupling rection of CO_2 and PO.

Future work should be focused on, firstly, optimization of reaction conditions to prepare more ionic functionalized ligands that contain different substituents. Secondly, optimization of the reaction conditions in order to achieve successful synthesis of Co(III) complexes. Thirdly, optimization of reaction conditions for these coupling reactions to favor formation of co-polymers instead of cyclic products. Finally, kinetics as well as mechanistic studies should also be carried

out to study the role of the catalysts and co-catalysts as well as reaction conditions in CS_2/PO and CO_2/PO coupling reactions.

APPENDIX

Figure S-1: HL_2 FT-IR spectrum

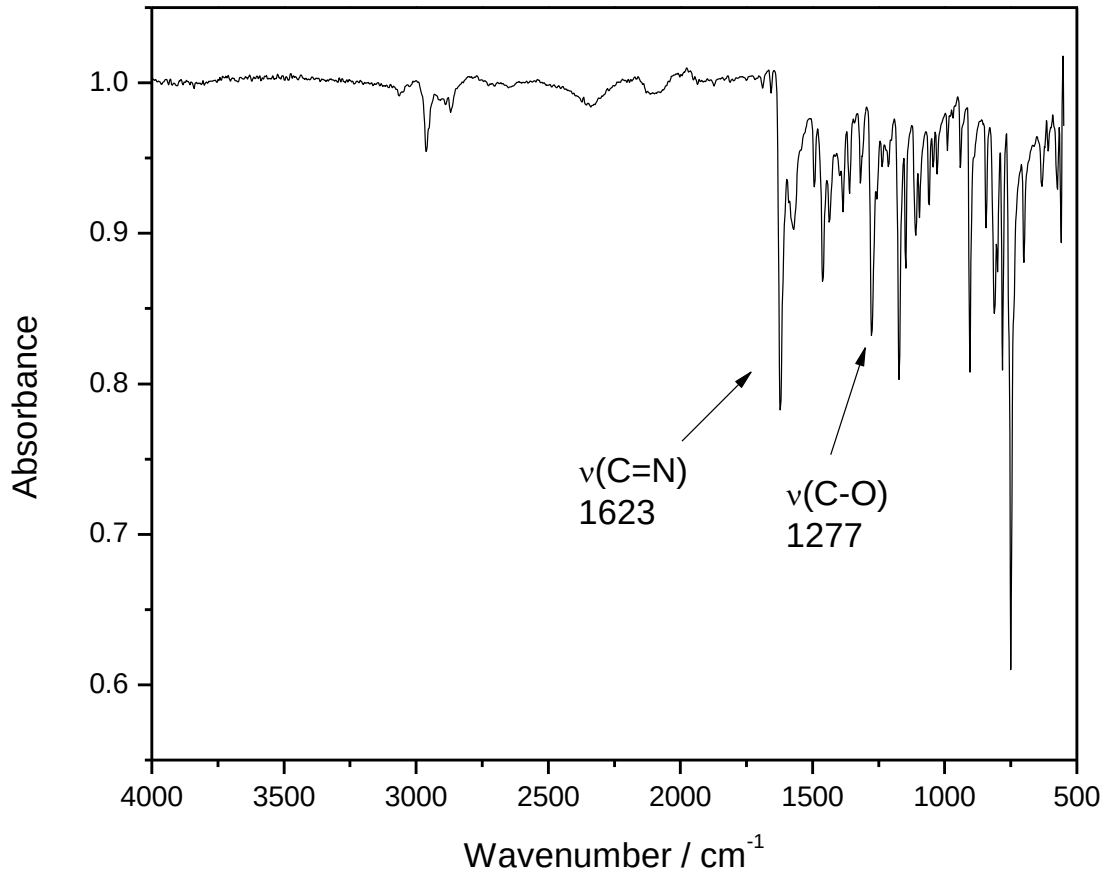


Figure S-2: HL_2 ^{1}HNMR spectrum

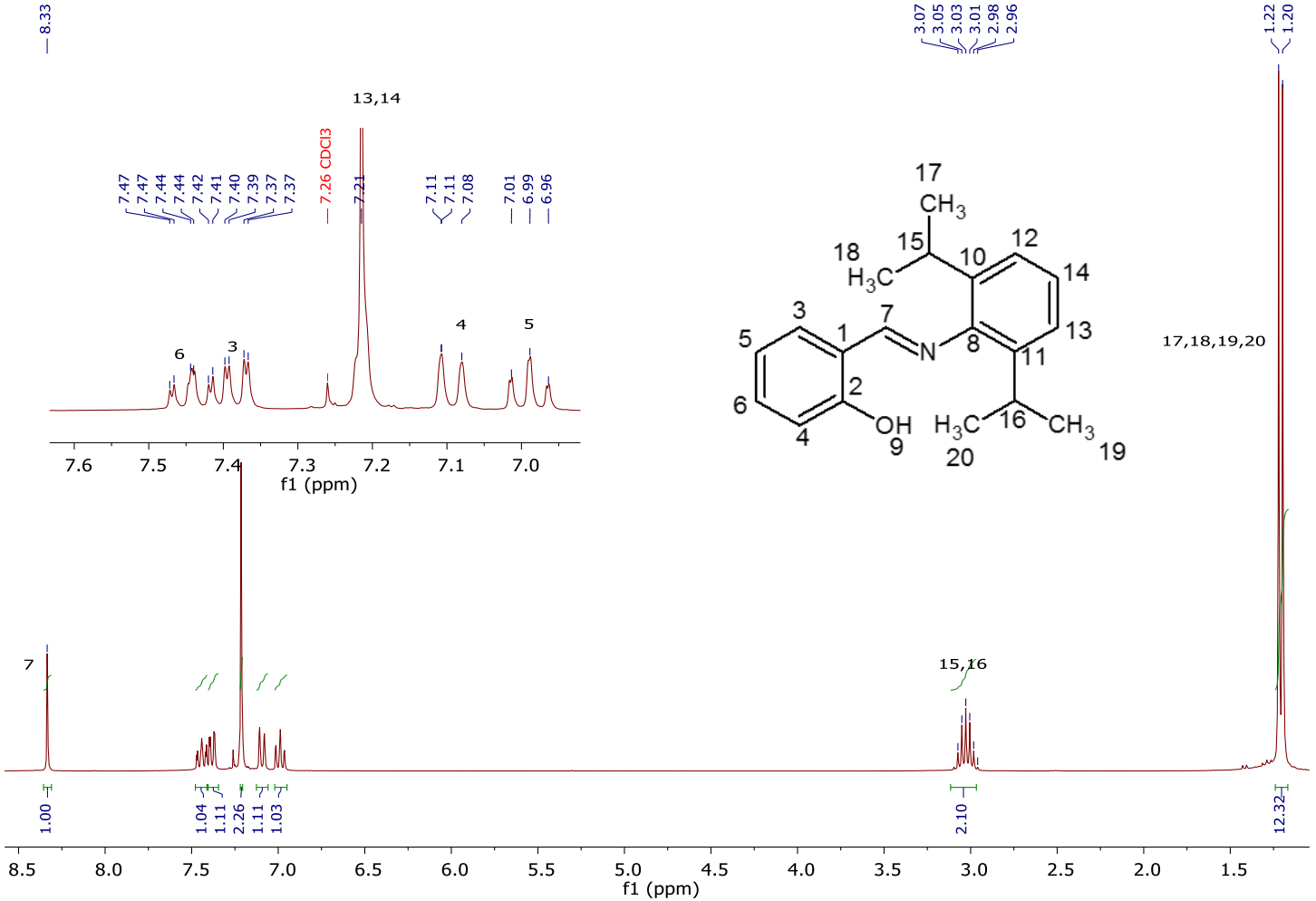


Figure S-3: HL_2 ^{13}CNMR spectrum

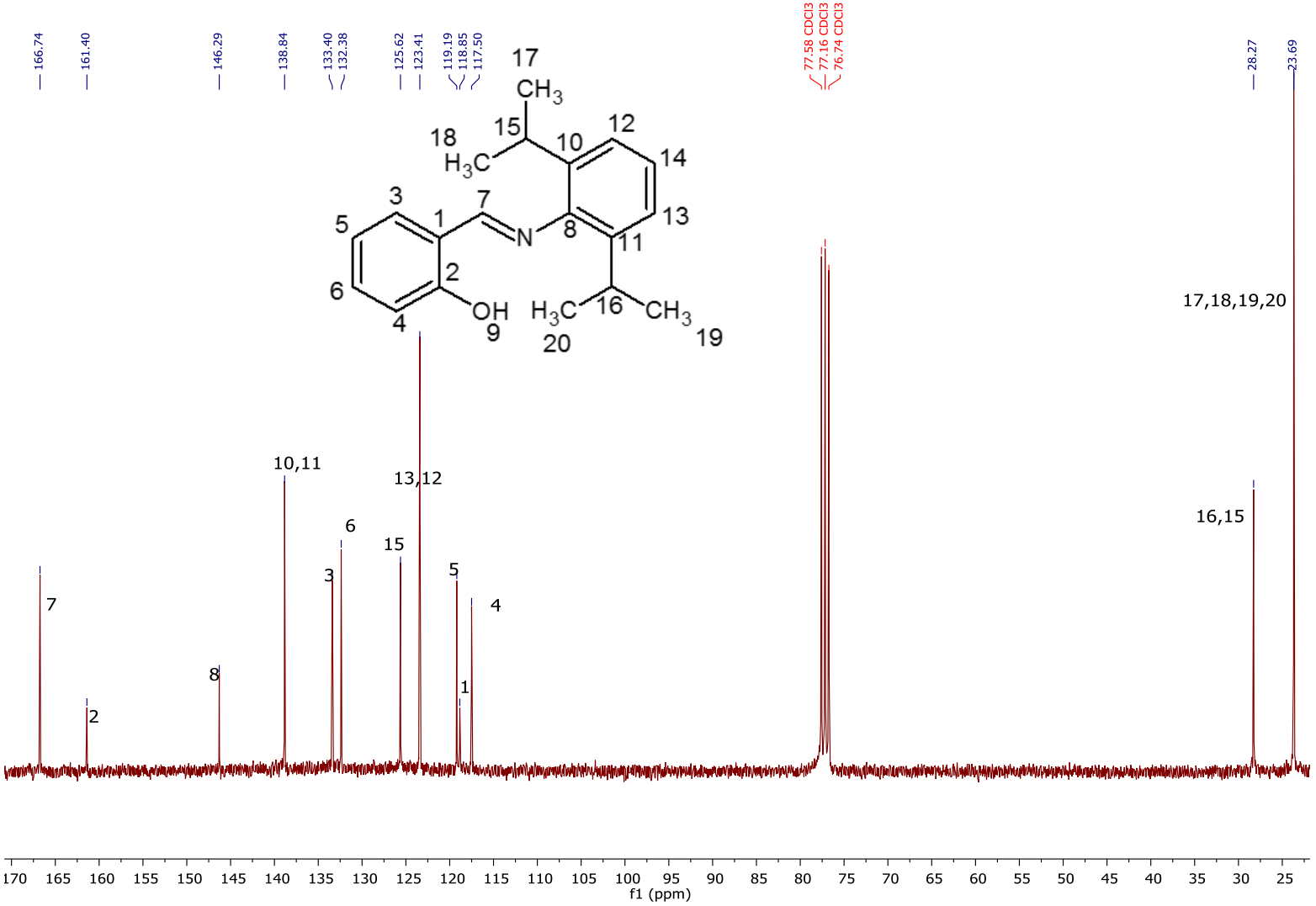


Figure S-4: HL_2 COSY NMR spectrum

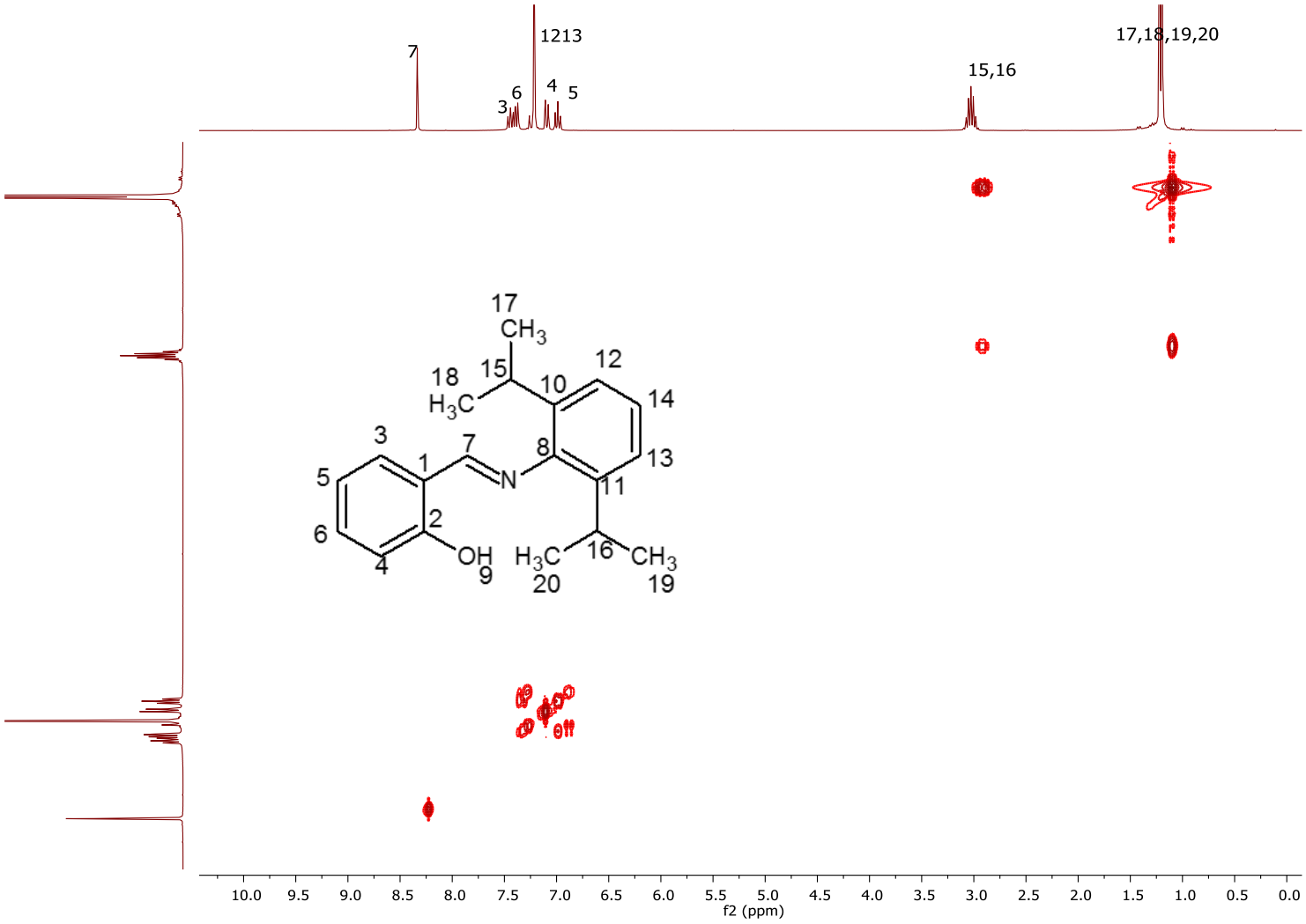


Figure S-5: HL_2 HSQC NMR spectrum

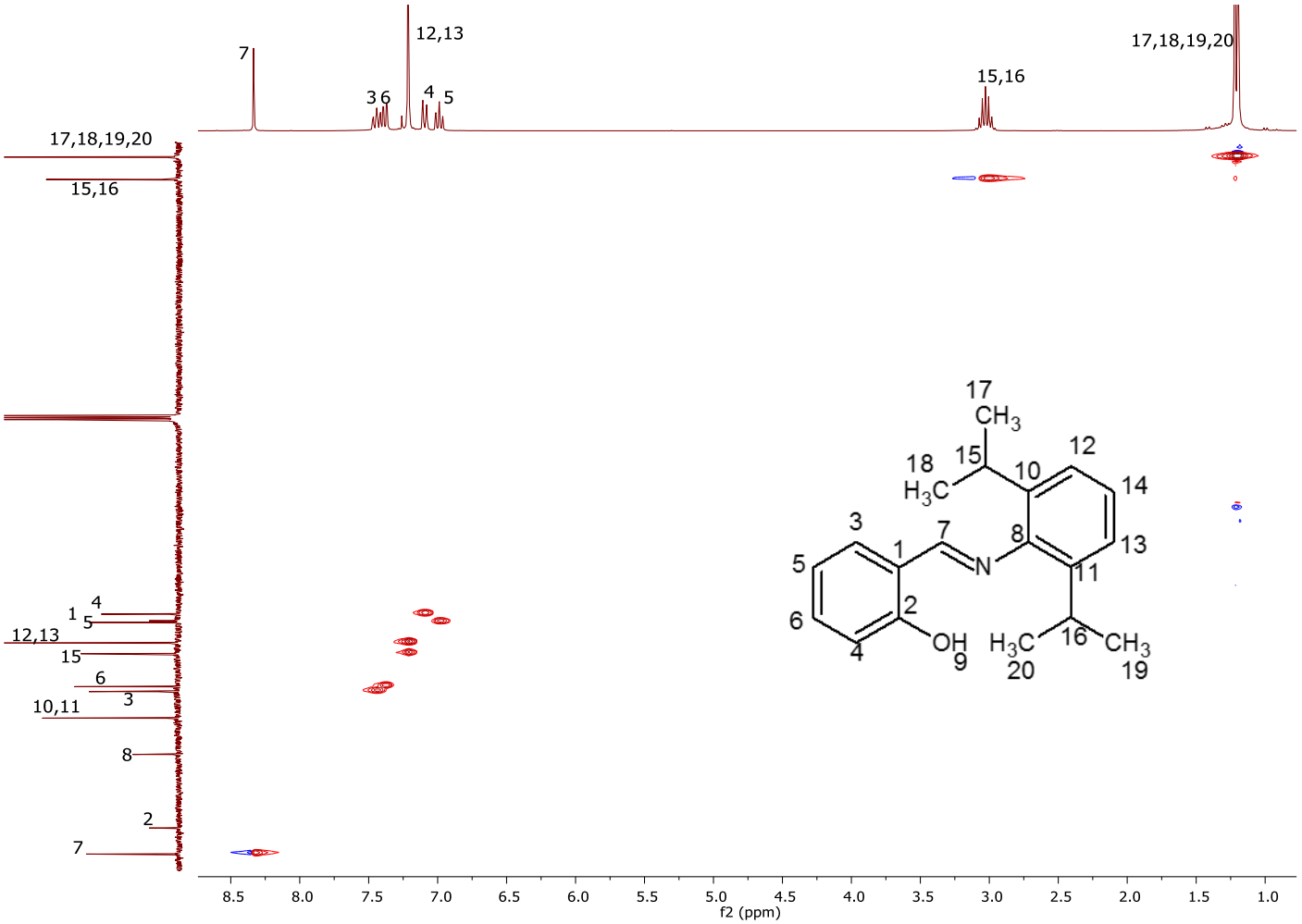


Figure S-6: HL$_7$ ^{1}HNMR spectrum

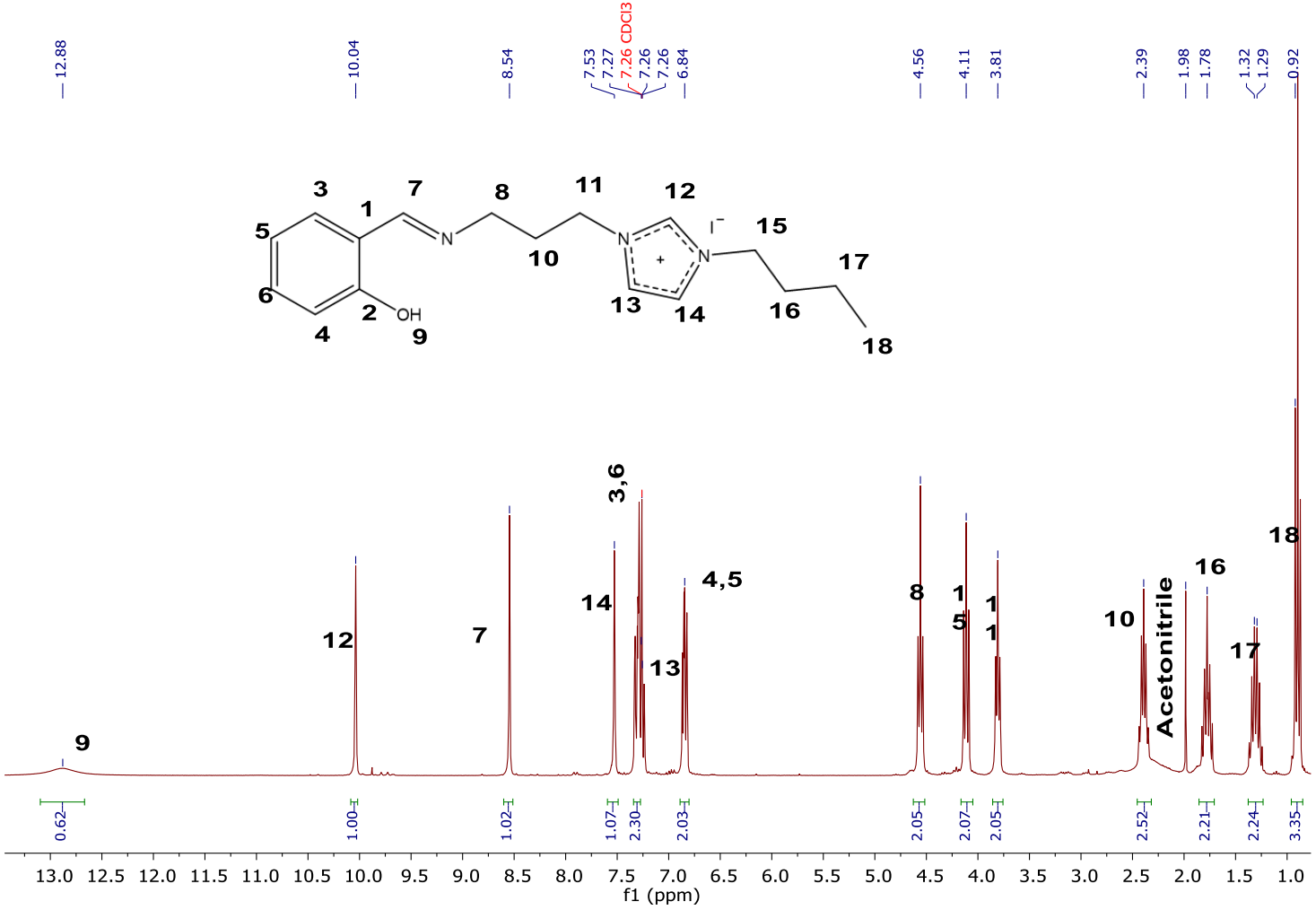


Figure S-7: HL_{10} ^{13}CNMR spectroscopy

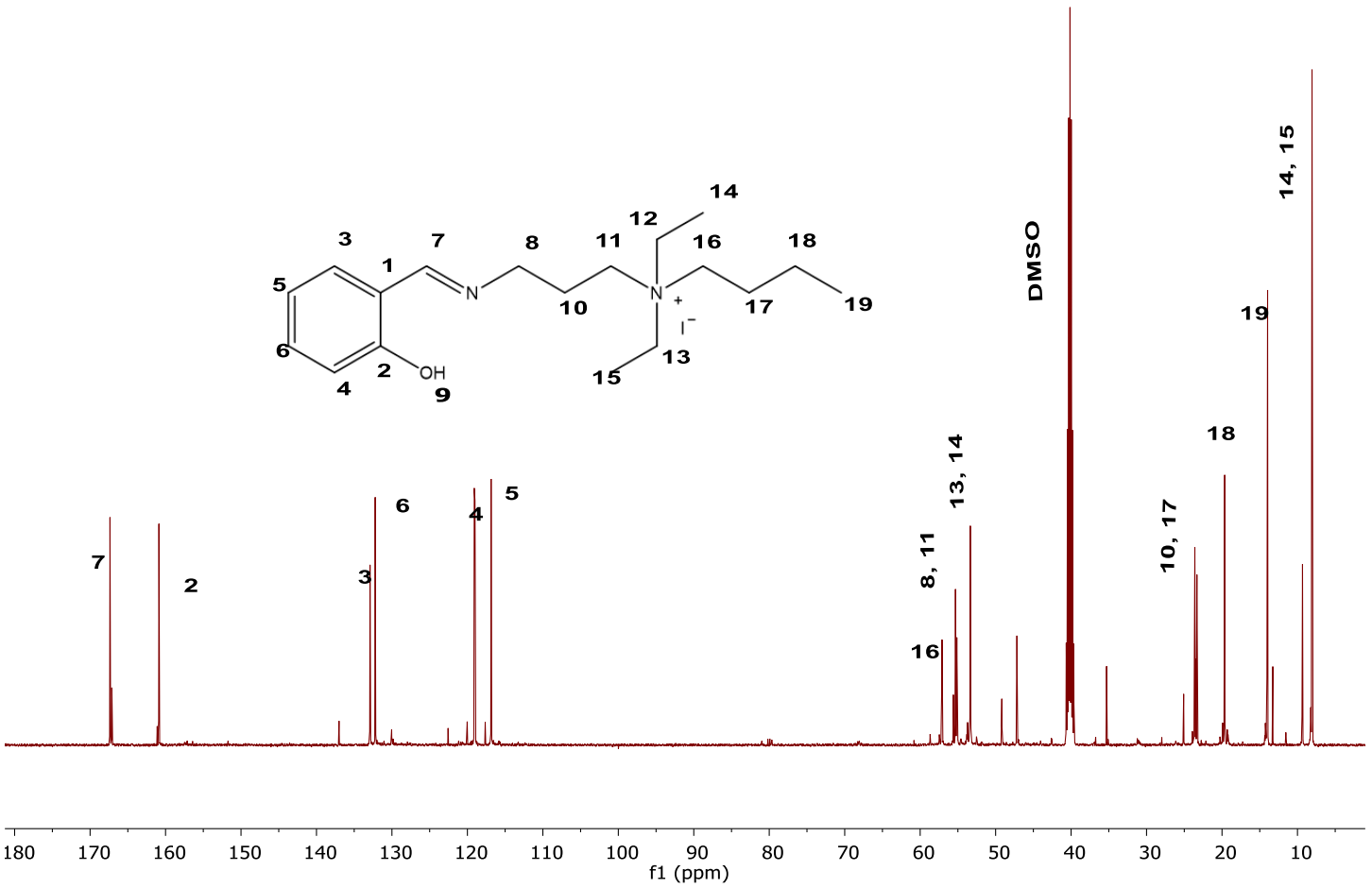


Figure S-8: HL_{10} COSY NMR spectroscopy

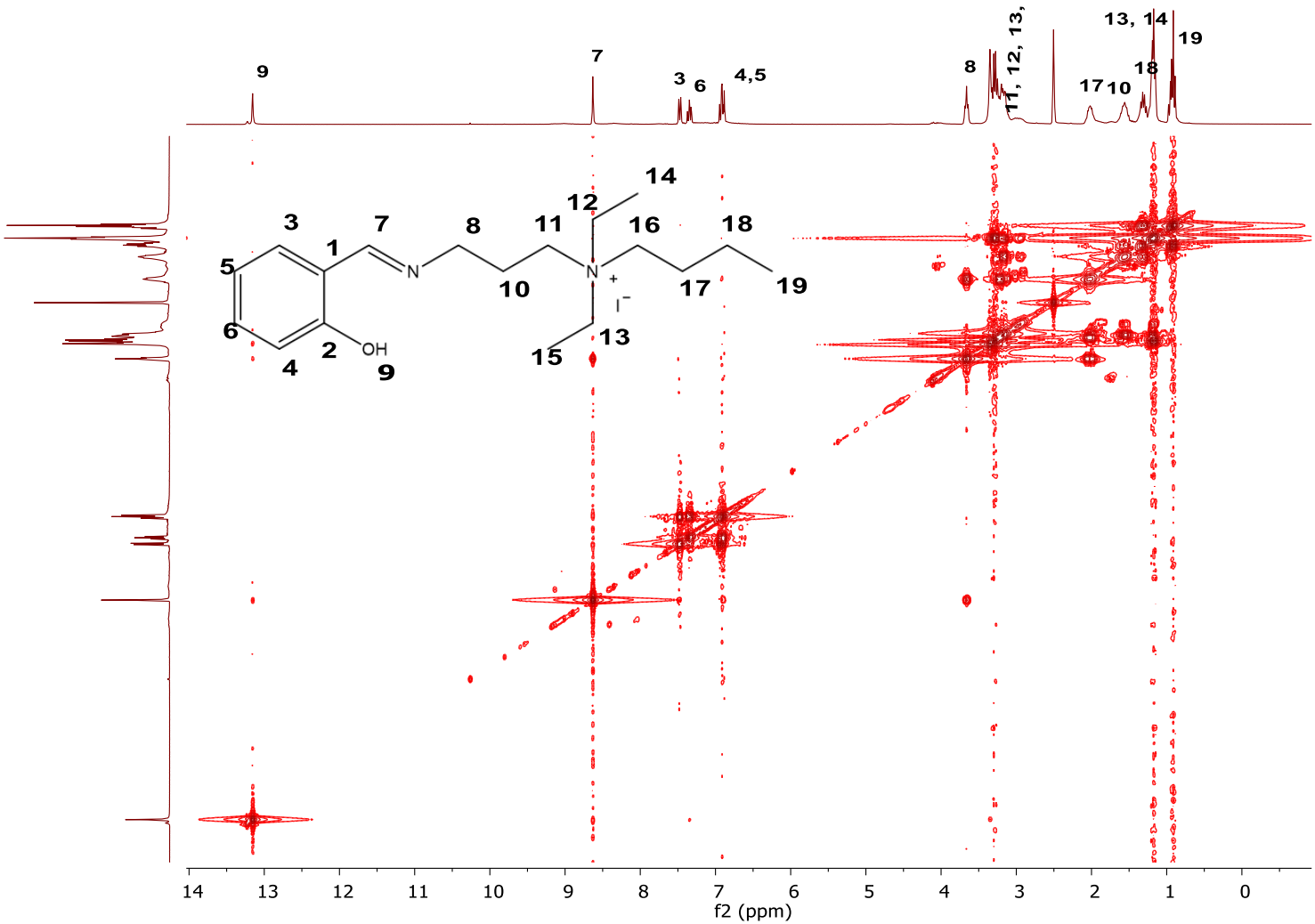


Figure S-9: HL_{10} Mass spectrum

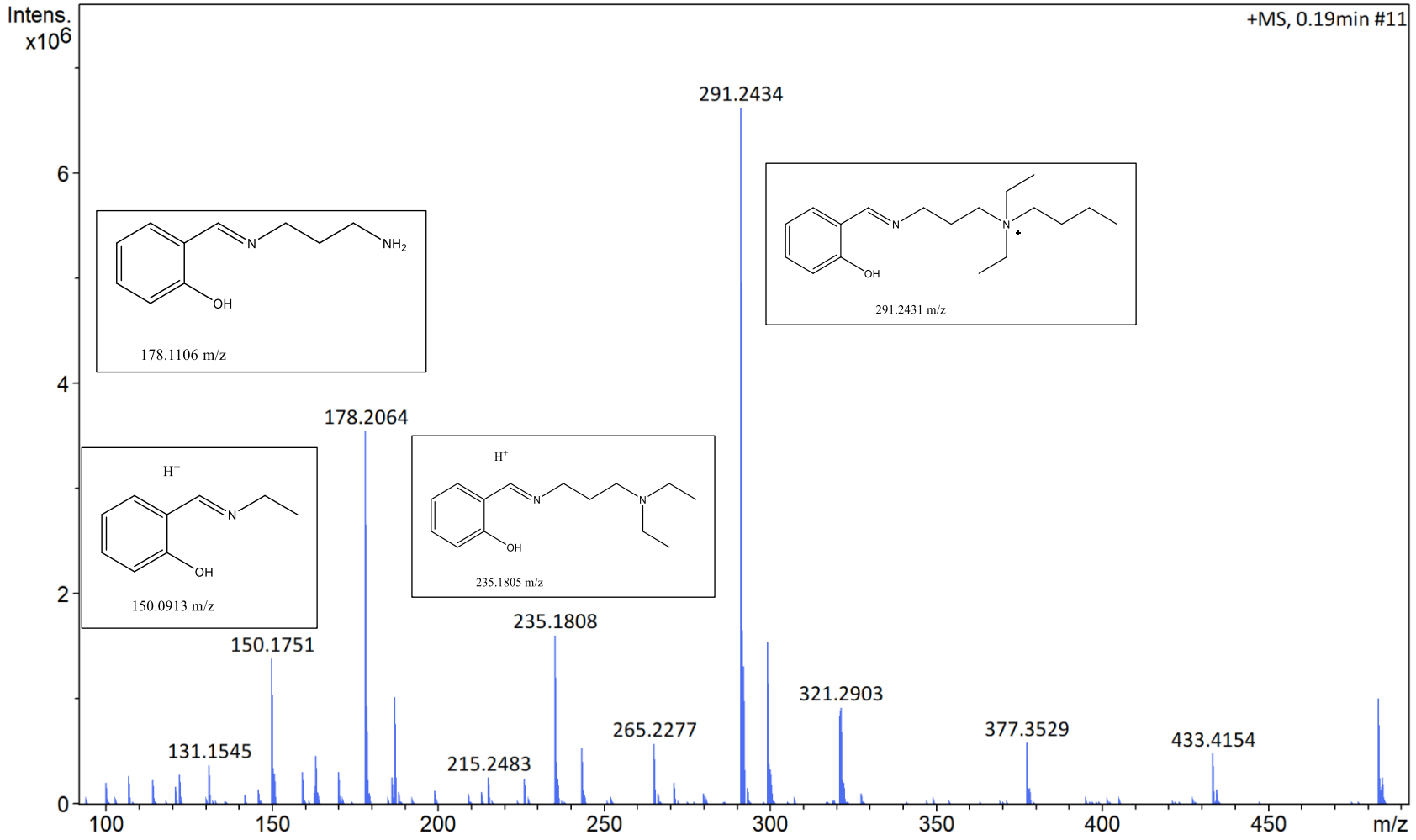


Figure S-10: [1]HNMR spectrum product of intermediate, **a**, Scheme 2.5, DMSO

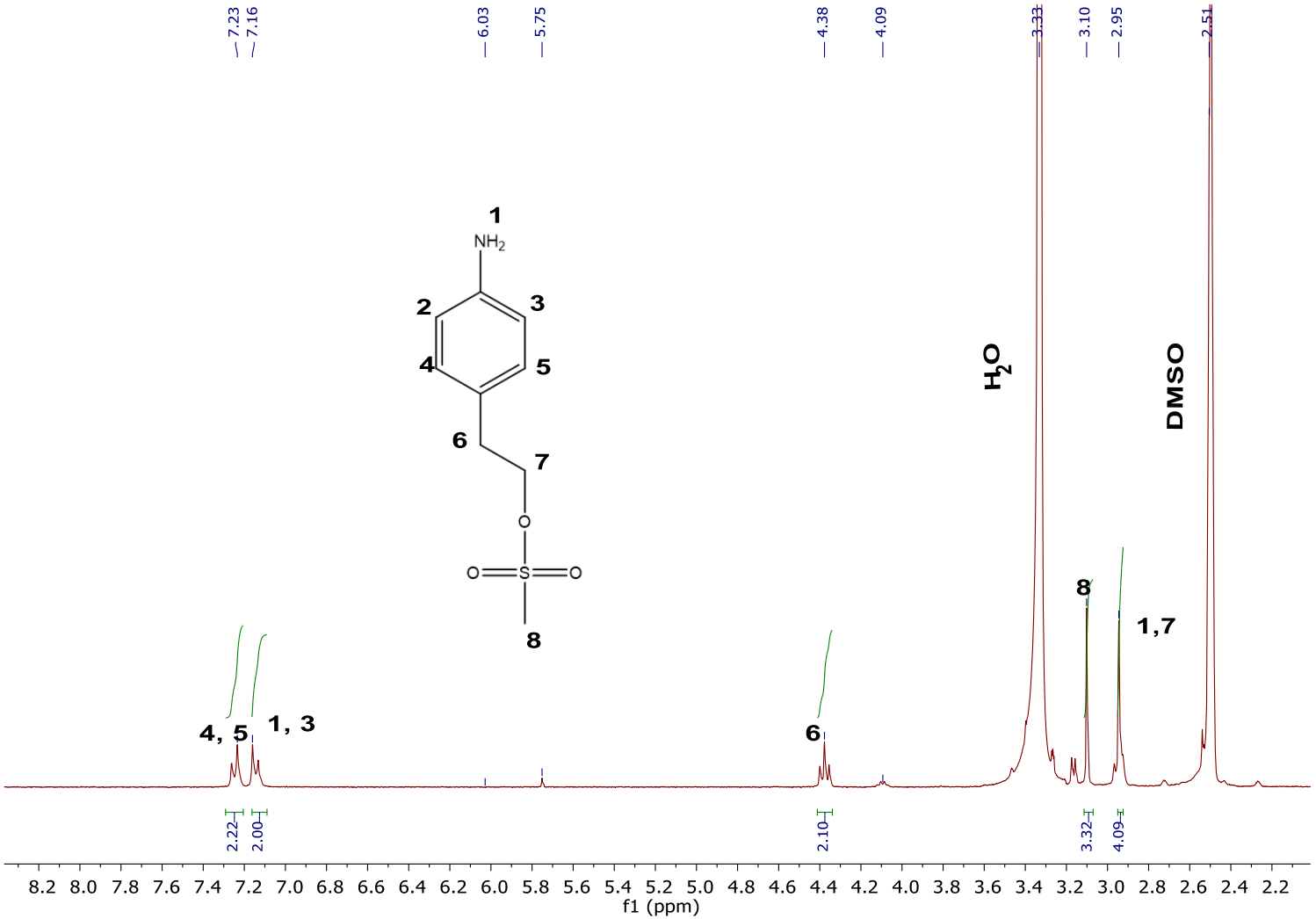


Figure S-11: FTIR spectra for **HL_2,** complex **2** and complex **8**

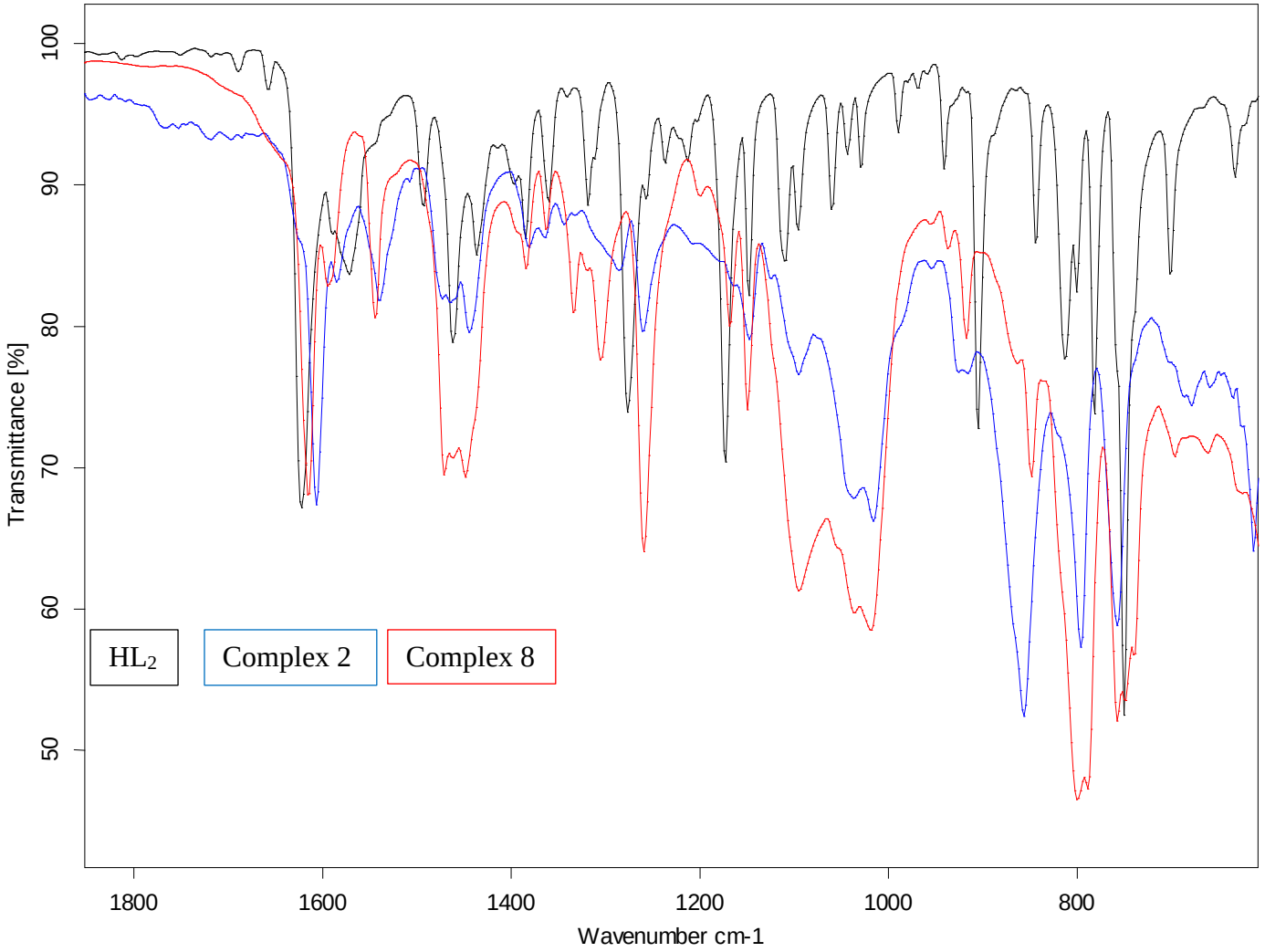


Figure S-12: UV-Vis spectra for **HL_2,** complex **2** and complex **8** (0.1 mM, 250 – 600 nm)

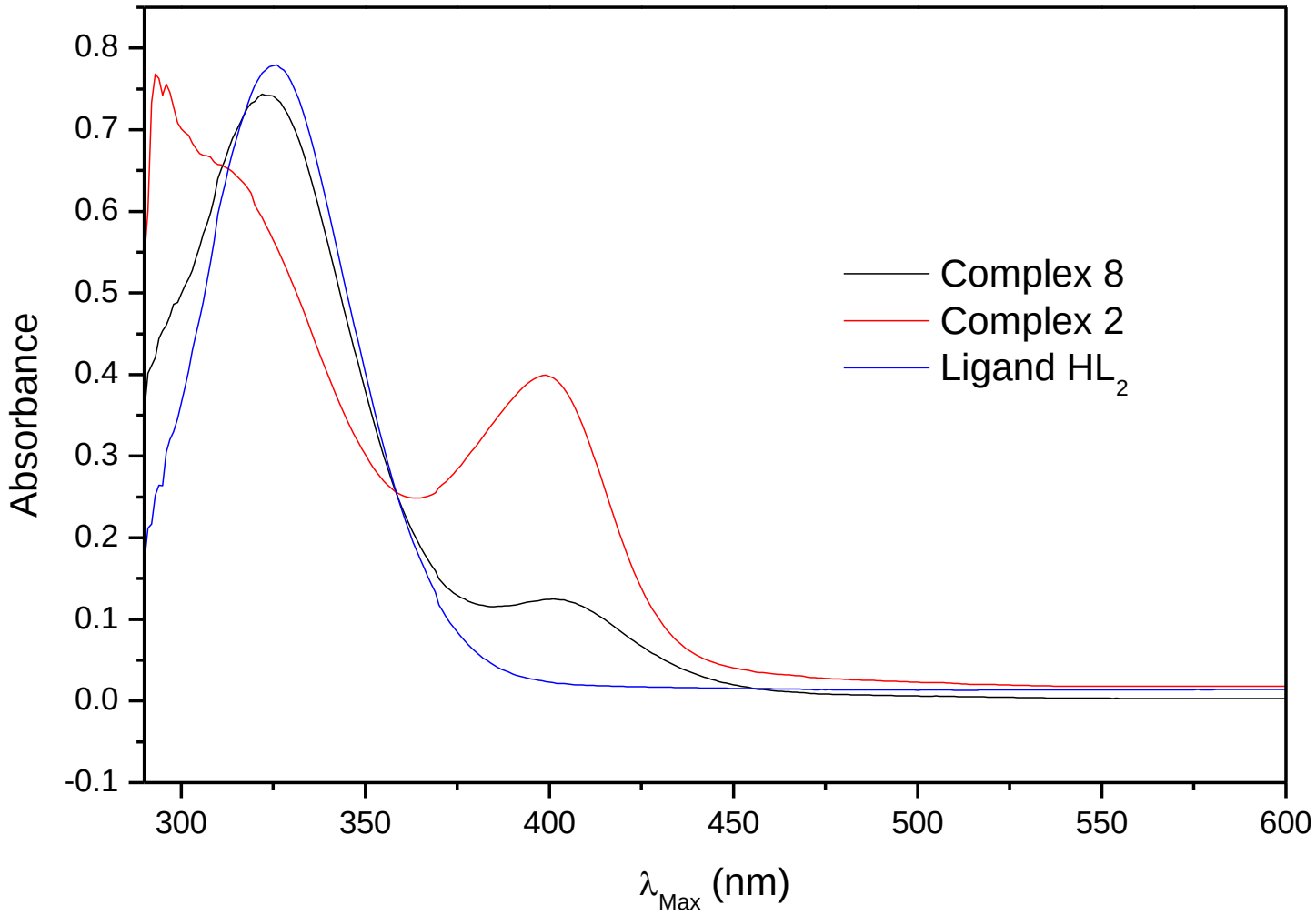


Figure S-13: UV-Vis spectra for **HL_2,** complex **2** and complex **8** (0.1 M, 500 – 100 nm)

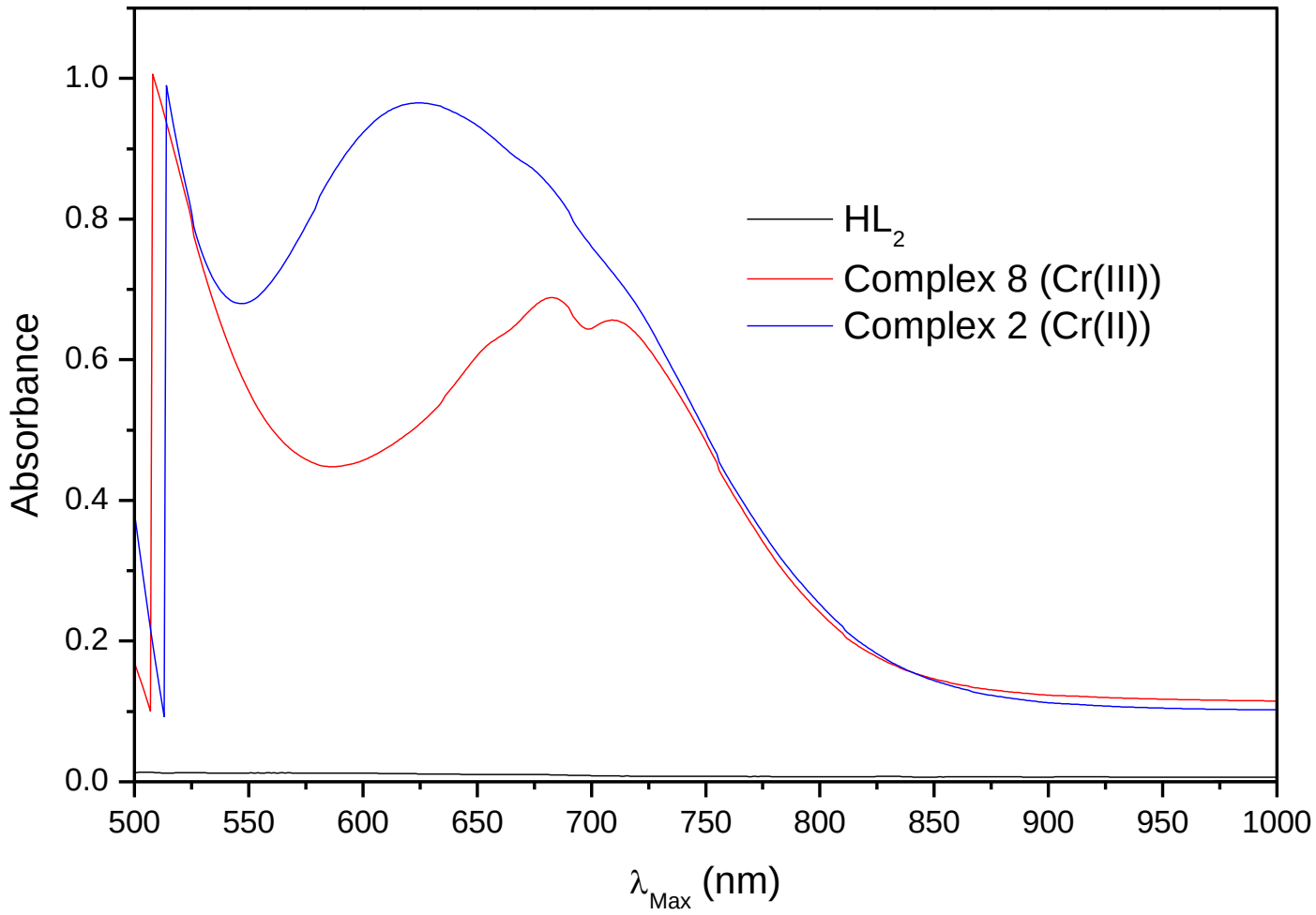


Figure S-14: Cyclic voltammogram for complex **15**

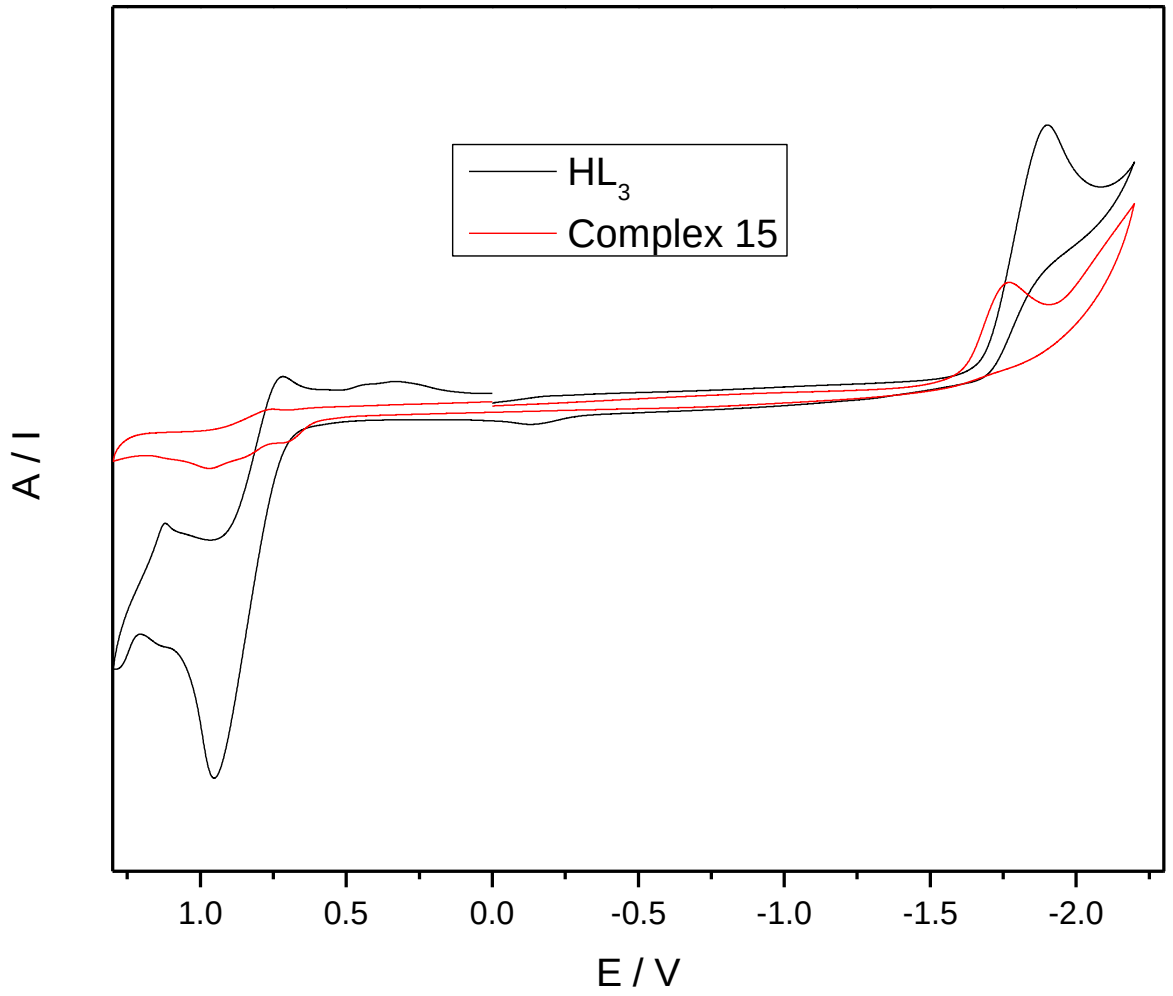


Figure S-15: Cyclic voltammogram for complex **13**

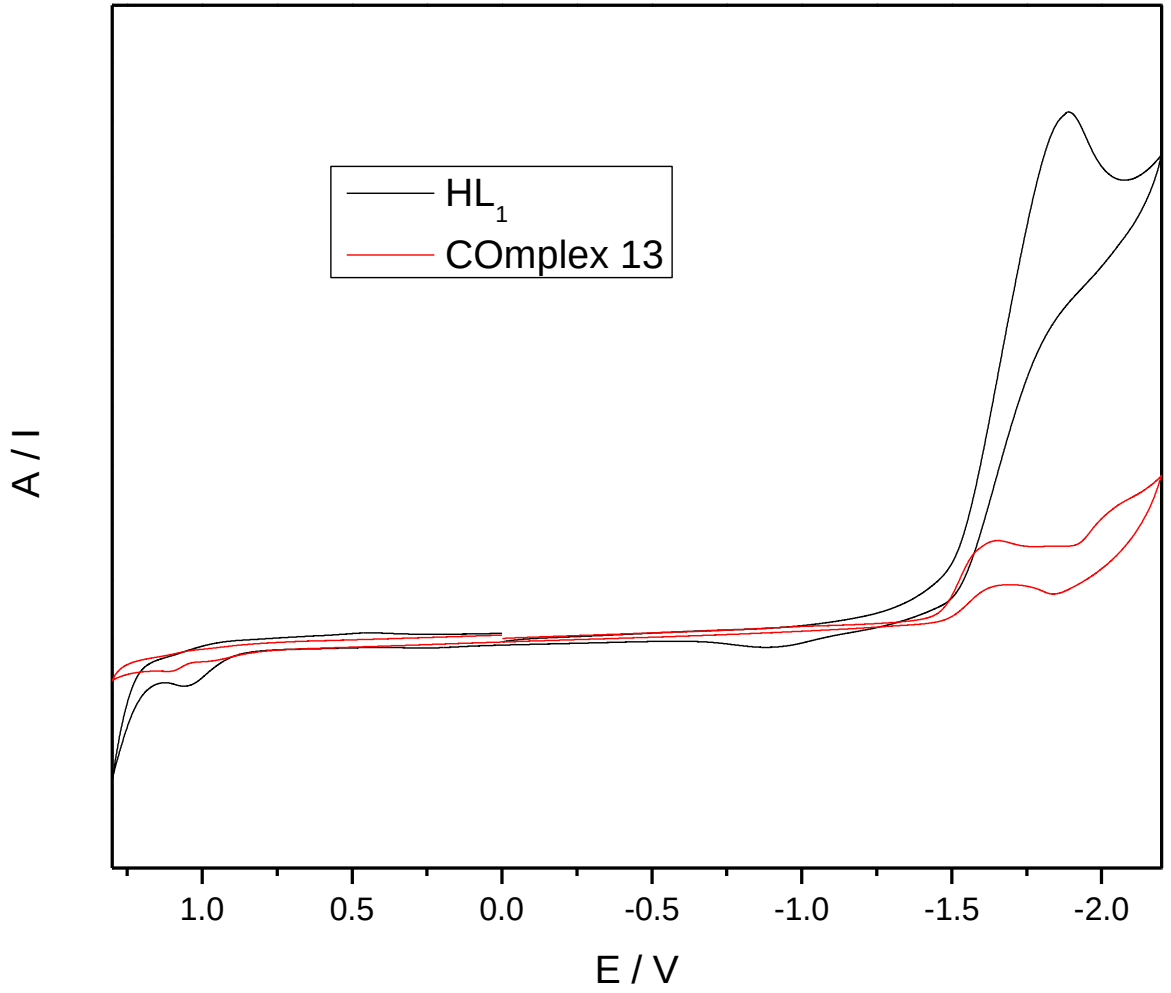


Figure S-16: Cyclic voltammogram for complex **16**

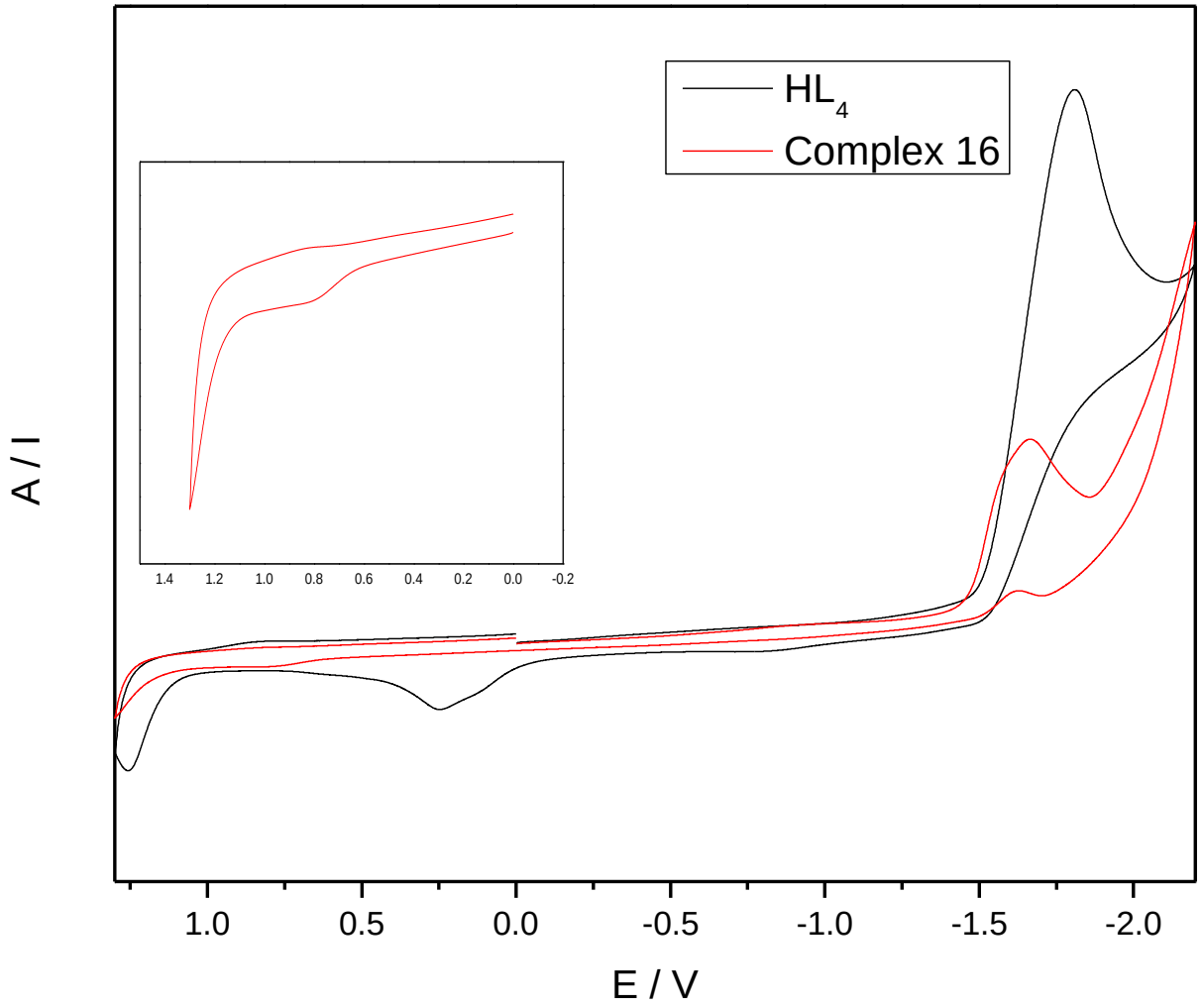


Figure S-17: Mass spectrum for complex **2**

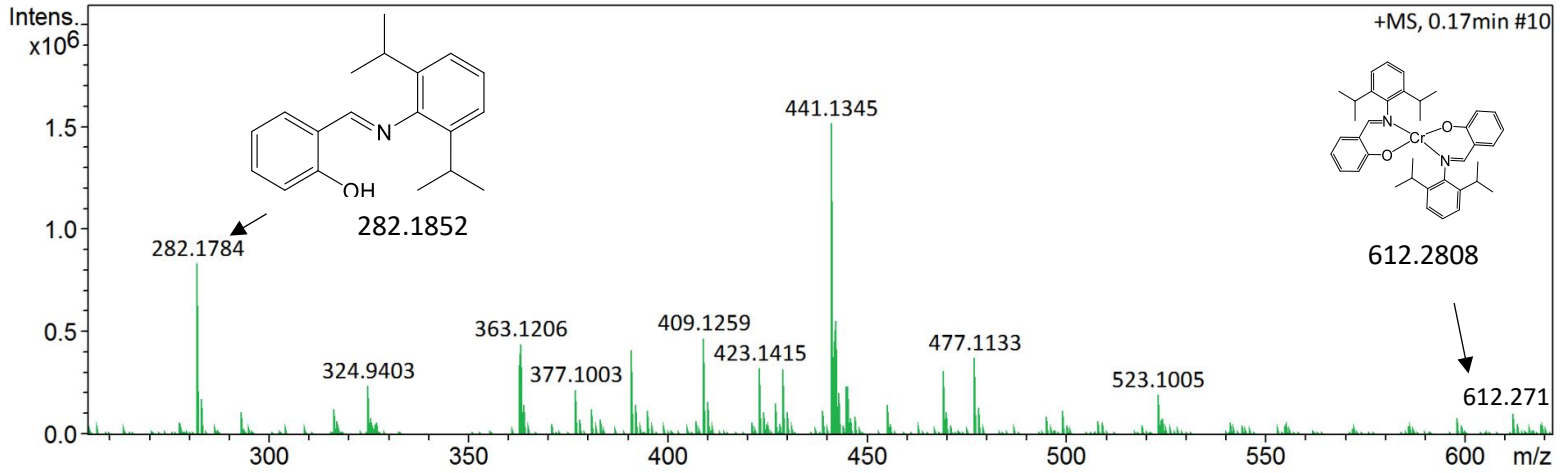


Figure S-18: Isotopologue pattern for complex **2**

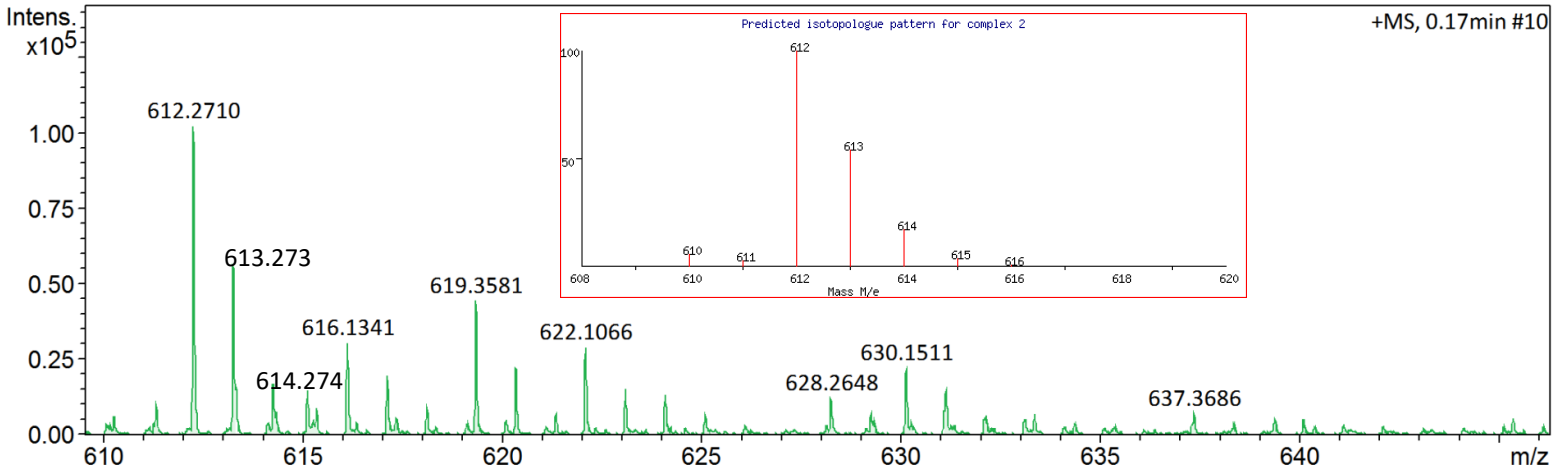


Figure S-19: Mass spectrum for complex **8**

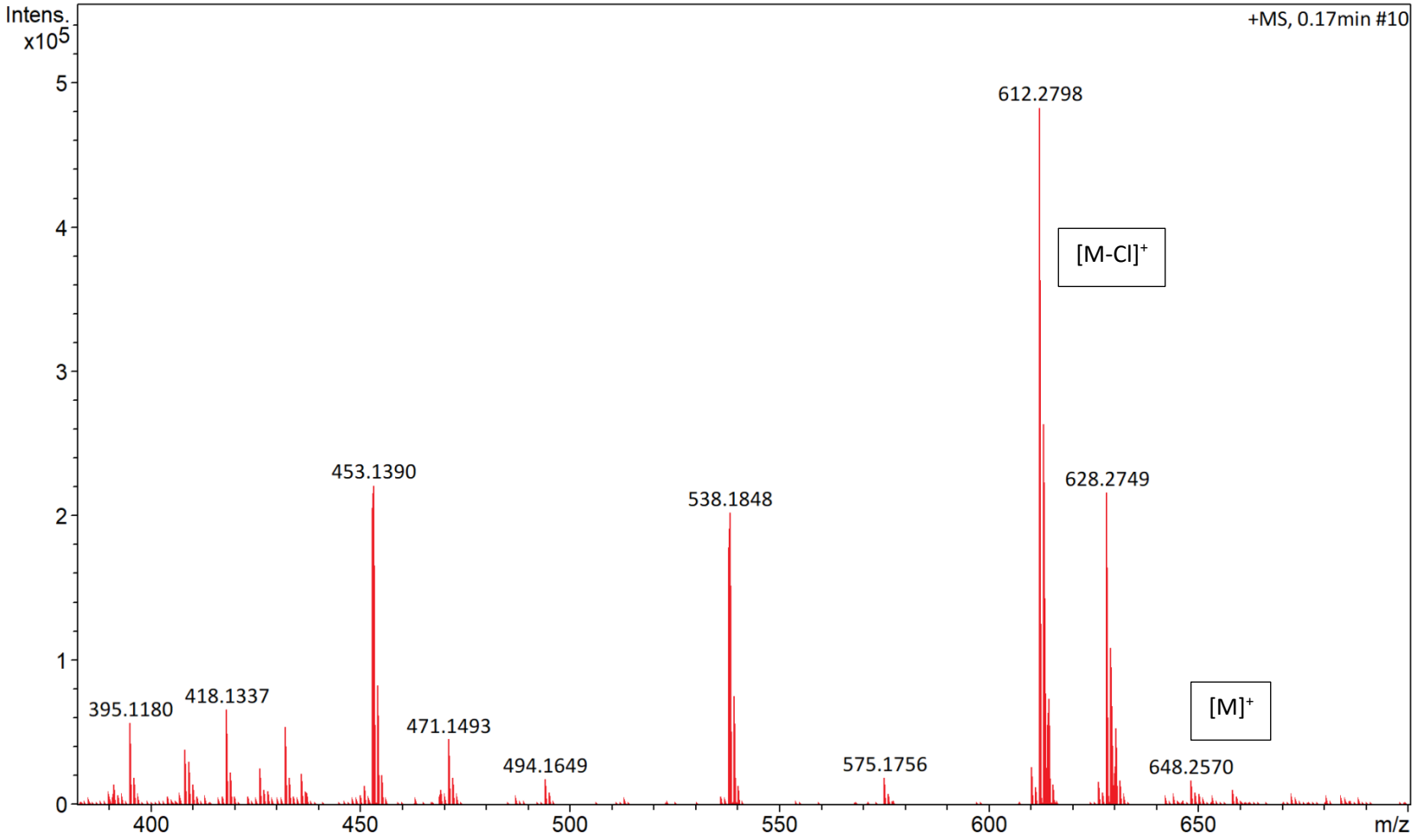


Figure S-20: Isotopologue pattern for complex **8**

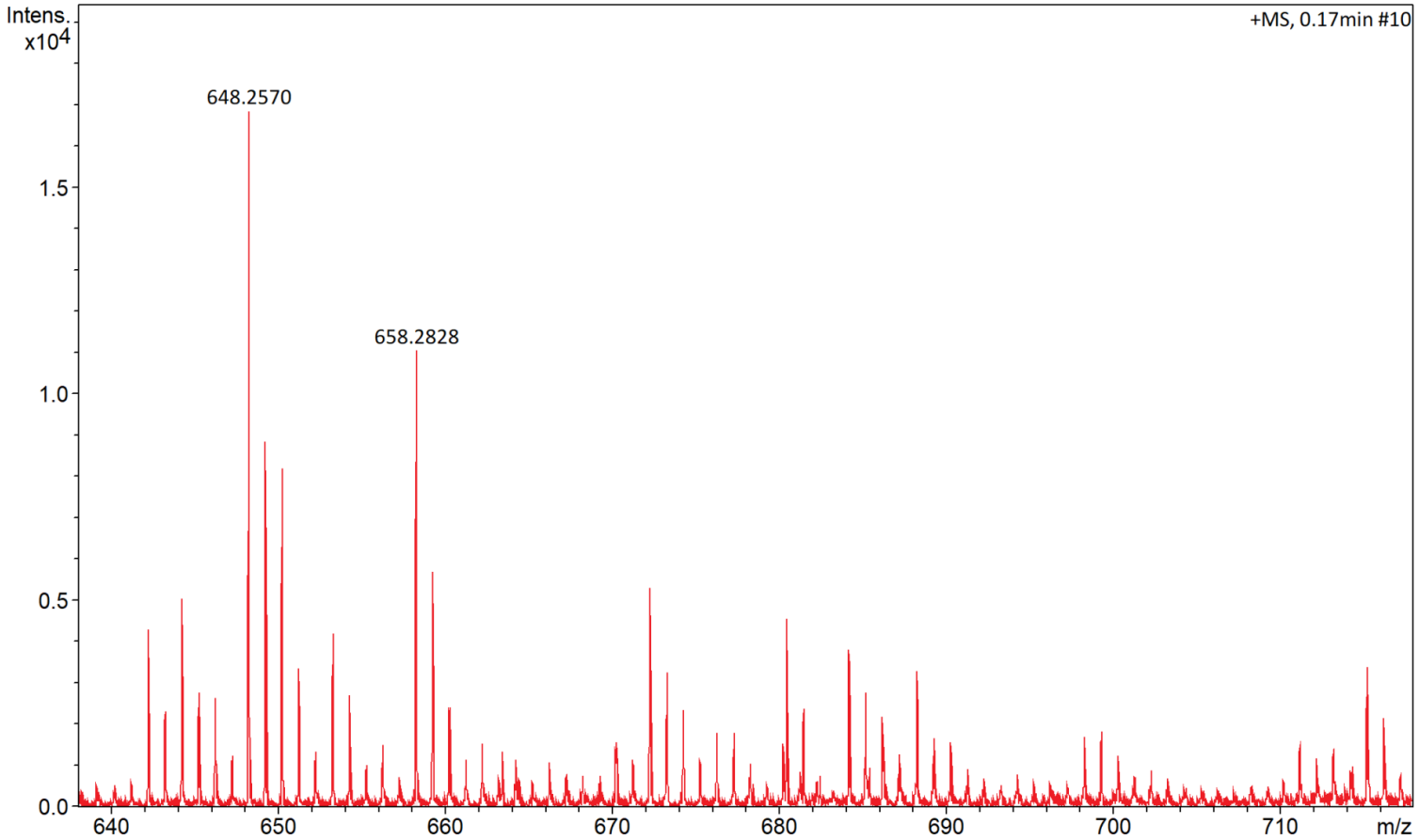


Figure S-21: Mass spectrum for Complex **13**

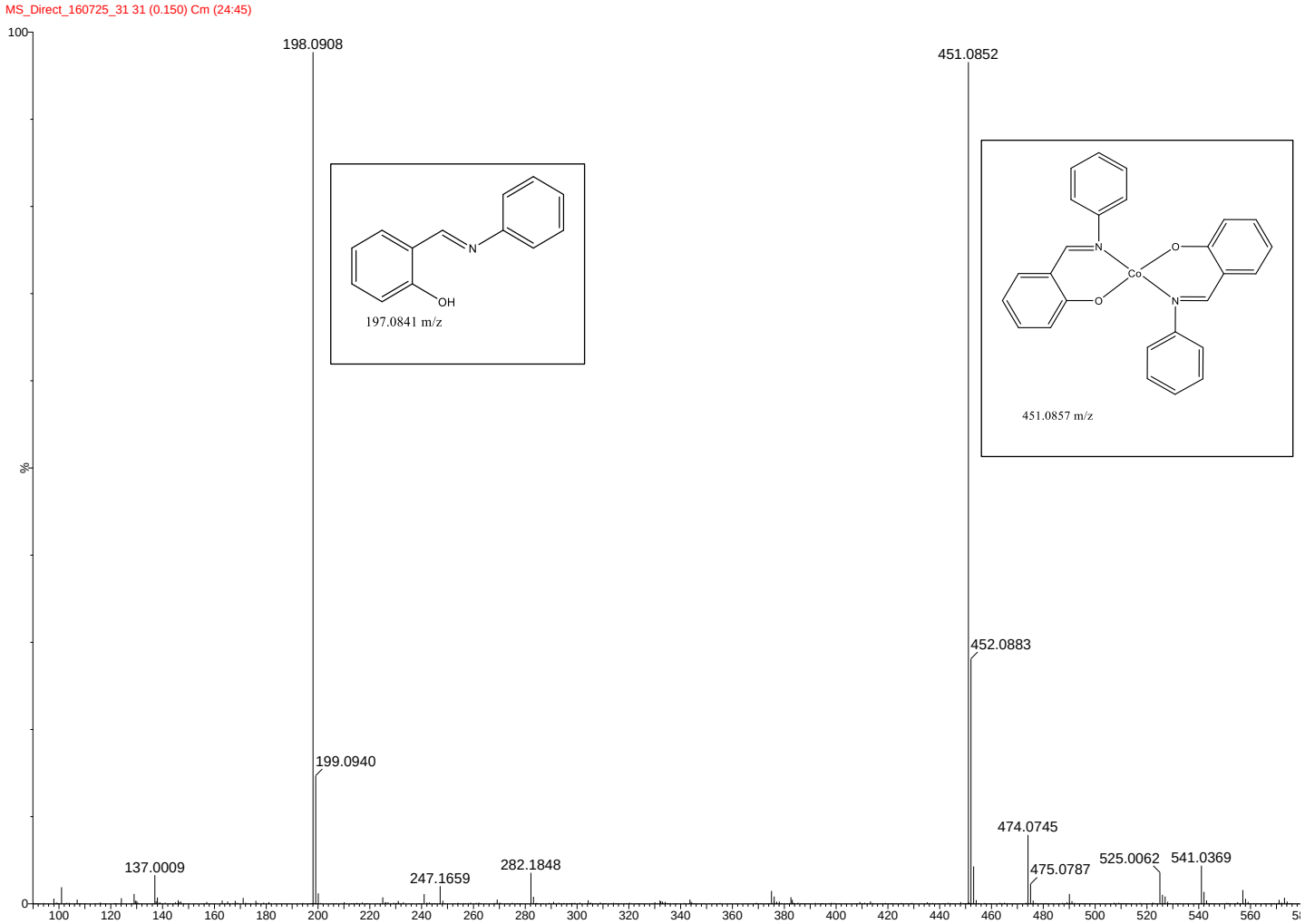


Figure S-22: UV-Vis spectrum for ionic functionalized Co(II) complexes

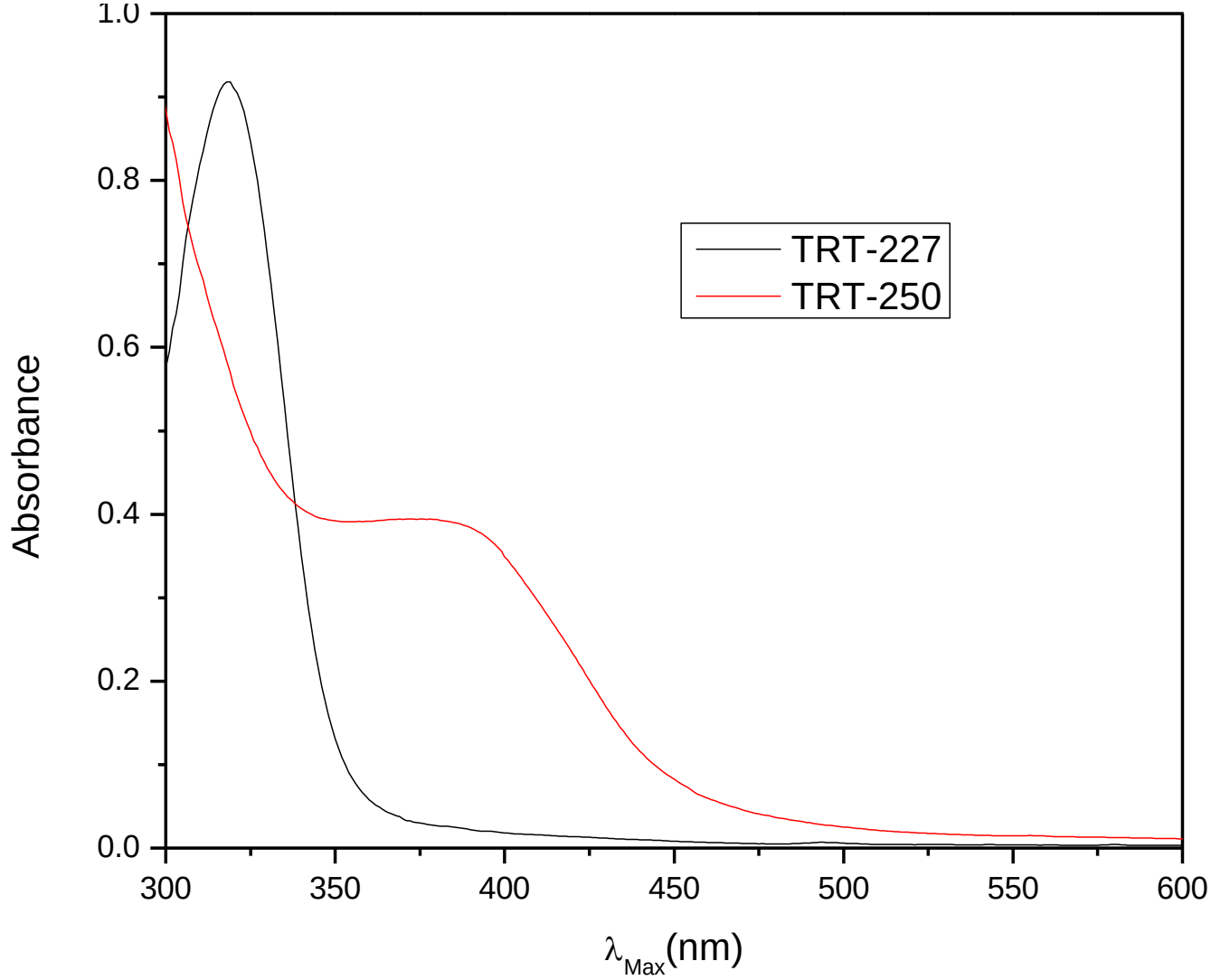


Figure S-23: UV-Vis spectrum for ionic functionalized Co(II) complexes

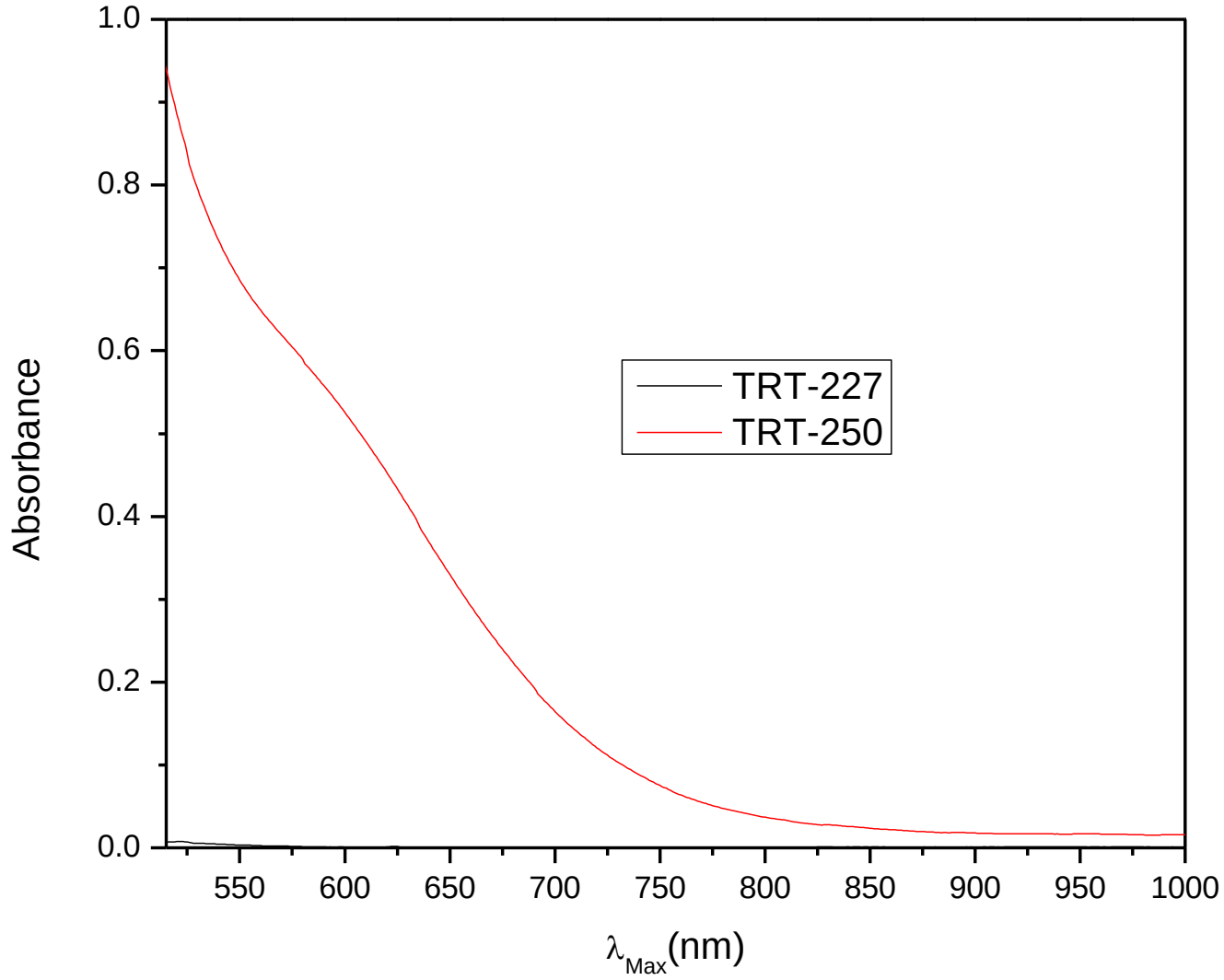


Table S-1: Crystallography data for complex **15**

Empirical formula	$C_{34}H_{38}CoN_4O_2$
Formula weight	593.61
Temperature/K	173.15
Crystal system	monoclinic
Space group	$P2_1/n$
a/Å	12.6153(9)
b/Å	21.0339(15)
c/Å	12.6399(9)
α/°	90
β/°	117.5826(14)
γ/°	90
Volume/Å^3	2972.8(4)
Z	4
ρ_{calc}g/cm^3	1.326
μ/mm^{-1}	0.615
F(000)	1252.0
Crystal size/mm^3	0.199 × 0.151 × 0.071
Radiation	MoKα (λ = 0.71073)
2Θ range for data collection/°	3.772 to 56.838
Index ranges	$-16 \leq h \leq 16$, $-28 \leq k \leq 27$, $-16 \leq l \leq 16$
Reflections collected	26623
Independent reflections	7427 [R_{int} = 0.0763, R_{sigma} = 0.0798]
Data/restraints/parameters	7427/0/374
Goodness-of-fit on F^2	0.997
Final R indexes [I>=2σ (I)]	R_1 = 0.0463, wR_2 = 0.0830
Final R indexes [all data]	R_1 = 0.0958, wR_2 = 0.0978

Table S-2: Effect of time on the coupling of CS_2/PO reactions

Entry	Complex	Co-catalyst	Solvent	Time/ hr	Mass/mg	%Conversion[b]
1	**8**	[PPN]Cl	MeOH	1	304.9	5.6
2	**8**	[PPN]Cl	MeOH	2	626.1	12.0
3	**8**	[PPN]Cl	MeOH	3	1022	19.6
4	**8**	[PPN]Cl	MeOH	4	1565.5	30.1
5	**8**	[PPN]Cl	MeOH	5	1994.3	38.6
6	**8**	[PPN]Cl	MeOH	6	2513.5	48.3
7	**8**	[PPN]Cl	MeOH	7	2792.3	53.6
8	**8**	[PPN]Cl	MeOH	8	3031.4	58.2
9	**8**	[PPN]Cl	MeOH	9	3408.3	65.5
10	**8**	[PPN]Cl	MeOH	10	3643.3	70.0
11	**8**	[PPN]Cl	MeOH	11	3646.5	70.0
12	**8**	[PPN]Cl	MeOH	12	3599.7	70.1

[a]All reaction performed in MeOH 40 °C, 12 hours, Complex:PO:CS_2 = 1:1500:1000; [b]Determined by mass difference

Table S-3: Effect of oxidation state of Cr metal and different metal center of the complex on the coupling of CS_2/PO reactions[a]

Entry	Complex	complexco-catalyst	Mass/ mg	%COnversion[b]	Product ratio[c]	
					I	II
1*	**2**	1:0	68.8	1.3	Trace	>99
2*	**8**	1:0	344.4	6.6	Trace	>99
3*	**14**	1:0	10.7	0.2	Trace	>99
4	**1**	1:1	748.7	14.4	28.6	71.4
5	**2**	1:1	1048.7	20.2	9.1	90.9
6	**3**	1:1	510.2	9.8	16.7	83.3
7	**4**	1:1	800.5	15.4	9.1	90.9
8	**7**	1:1	576.6	11.1	16.7	83.3
9	**8**	1:1	1078.9	20.7	16.7	83.3
10	**9**	1:1	875.5	16.7	9.1	90.9
11	**10**	1:1	392.1	7.5	9.1	90.9
12	**13**	1:1	191.6	3.7	9.1	90.9
13	**14**	1:1	473.6	9.1	9.1	90.9
14	**15**	1:1	226.6	4.4	9.1	90.9
15	**16**	1:1	392.1	7.5	9.1	90.9

[a]All reaction performed in MeOH, 22 °C, 6 hours, cocatalyst: [PPN]Cl, Complex:PO:CS_2 = 1:1500:1000; [b]Determined by mass difference; [c]Scheme 5.2, calculated from ^{1}HNMR. *no co-catalyst used

Table S-4: Effect of oxidation state of Cr metal and different metal center of the complex on the coupling of CS_2/PO reactions

Entry	Complex	complexco-catalyst	Mass/ mg	%Conversion[b]	Product ratio[c]	
					I	II
1*	**2**	1:0	317.8	6.1	trace	>99
2*	**8**	1:0	522.3	10.0	trace	>99
3*	**14**	1:0	trace	Trace	trace	>99
4	**1**	1:1	1781.8	34.2	28.6	71.4
5	**2**	1:1	2303.6	44.3	9.1	90.9
6	**3**	1:1	1947.2	37.4	9.1	90.9
7	**4**	1:1	2325.8	44.7	9.1	90.9
8	**7**	1:1	1860.5	35.7	9.1	90.9
9	**8**	1:1	2489.0	47.8	16.7	83.3
10	**9**	1:1	2311.8	44.4	9.1	90.9
11	**10**	1:1	1559.6	30.0	9.1	90.9
12	**13**	1:1	1189.9	22.9	9.1	90.9
13	**14**	1:1	1232.4	23.7	16.7	83.3
14	**15**	1:1	1429.4	27.5	23.1	76.9
15	**16**	1:1	1188.2	22.8	16.7	83.3

[a]All reaction performed in MeOH, co-catalyst: [PPN]Cl, 40 °C, 6 hours, Complex:PO:CS_2 = 1:1500:1000; [b]Determined by mass difference; [c]Scheme 5.2, calculated from ^{1}HNMR, *no co-catalyst used

Figure S-24: [1]HNMR spectrum for the product obtained when the reaction was performed in ethanol

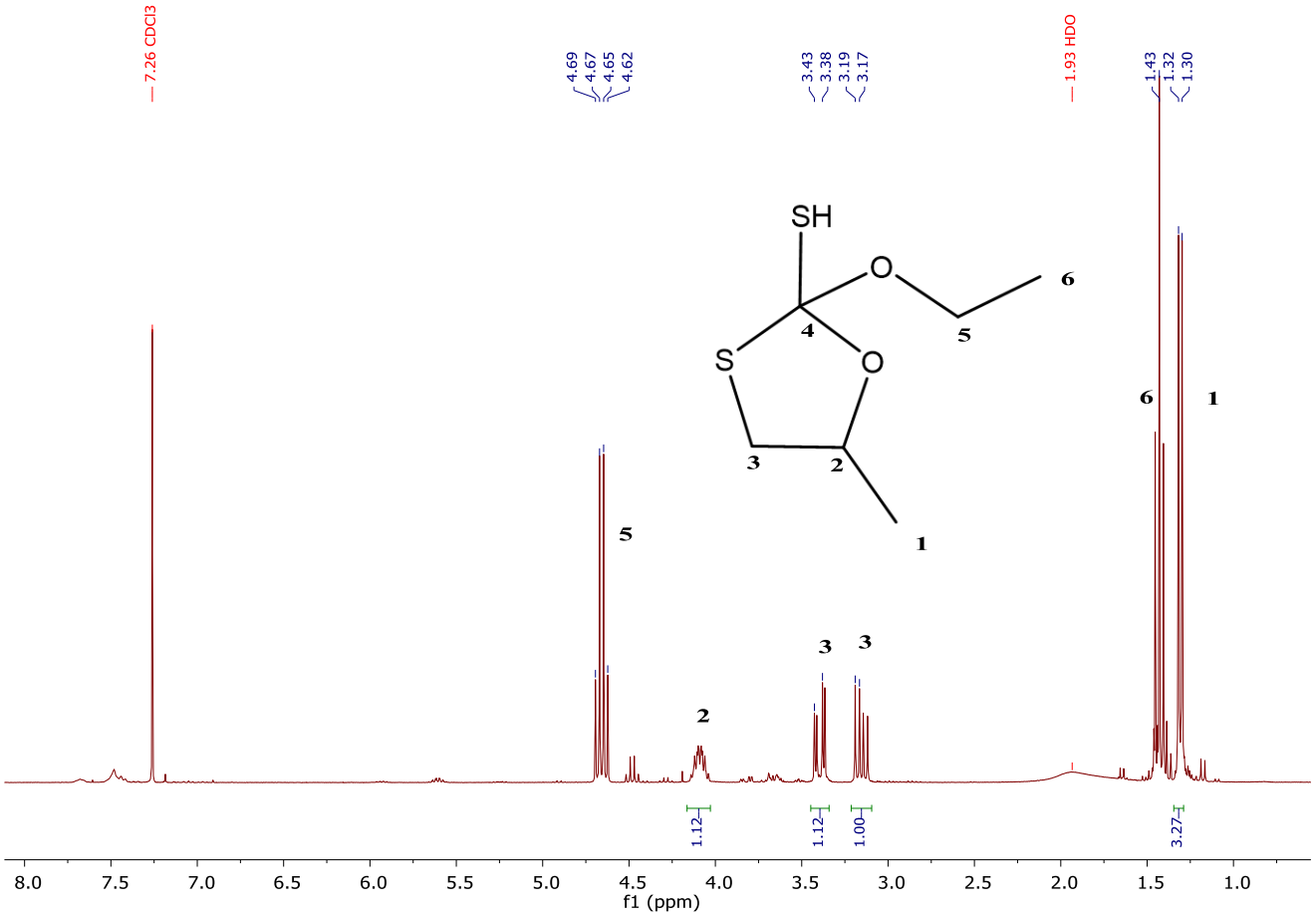


Figure S-25: ^{1}HNMR spectrum for ligand **HL_{10}** in $CDCl_3$

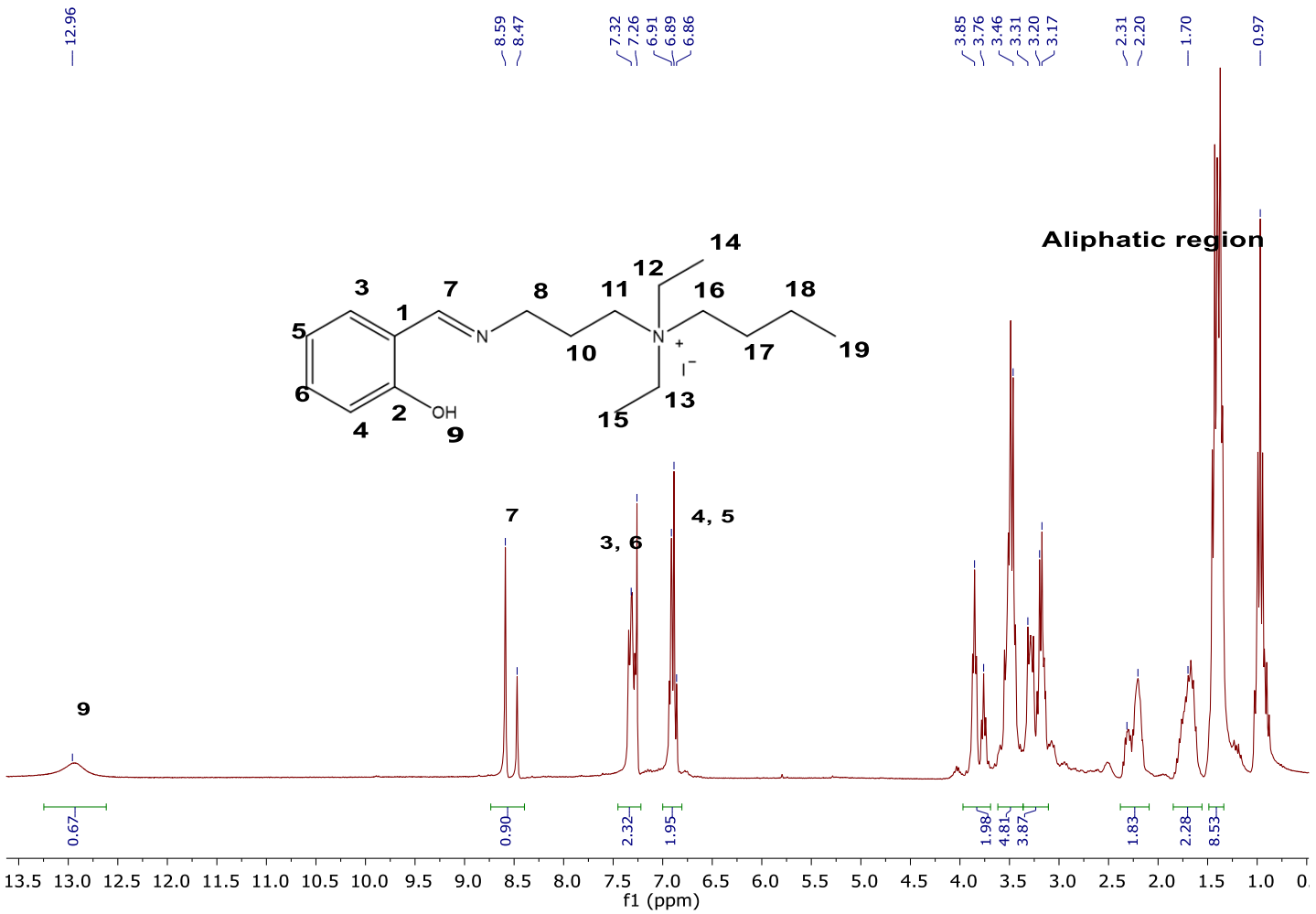


Figure S-26: ^{1}HNMR spectrum for **HL_{10}** in DMSO

